Methods in Molecular Biology 1789

Springer Protocols

Cláudia Pereira *Editor*

Plant Vacuolar Trafficking

Methods and Protocols

Humana Press

METHODS IN MOLECULAR BIOLOGY

Series Editor
John M. Walker
School of Life and Medical Sciences
University of Hertfordshire
Hatfield, Hertfordshire, AL10 9AB, UK

For further volumes:
http://www.springer.com/series/7651

Plant Vacuolar Trafficking

Methods and Protocols

Edited by

Cláudia Pereira

Faculty of Sciences, University of Porto, Porto, Portugal

Humana Press

Editor
Cláudia Pereira
Faculty of Sciences
University of Porto
Porto, Portugal

ISSN 1064-3745 ISSN 1940-6029 (electronic)
Methods in Molecular Biology
ISBN 978-1-4939-7855-7 ISBN 978-1-4939-7856-4 (eBook)
https://doi.org/10.1007/978-1-4939-7856-4

Library of Congress Control Number: 2018942329

Printed on acid-free paper

This Humana Press imprint is published by the registered company Springer Science+Business Media, LLC part of Springer Nature.
The registered company address is: 233 Spring Street, New York, NY 10013, U.S.A.

Preface

Vacuoles occupy a large volume in a plant cell and have important storage, homeostatic, and regulatory functions. Given the status of this organelle in the cell, it is crucial to understand not only its biogenesis but also how proteins reach and accumulate in the plant vacuole. Indeed, protein vacuolar trafficking is a major topic in the study of protein sorting in plants, being the issue of several studies for several years. This volume of the Methods in Molecular Biology series aims to provide the scientific community in this subject with a collection of a significant number of state-of-the-art protocols, ranging from the design and preparation of fusion proteins and expression vectors to a more detailed analysis involving different microscopy techniques. *Plant Vacuolar Trafficking: Methods and Protocols* will guide researchers along the different chapters, including introductions to their respective topics, lists of the necessary materials and reagents, and step-by-step and readily reproducible laboratory protocols. Cutting edge and comprehensive, *Plant Vacuolar Trafficking: Methods and Protocols* is a highly valuable resource for researchers interested in learning more about this field.

Porto, Portugal ***Cláudia Pereira***

Contents

Contributors

Lucia Atehortùa · *Laboratorio de Biotecnología, Sede de Investigación Universitaria, Universidad de Antioquia, Medellin, Colombia*

Margaret R. Baker · *Department of Molecular Biosciences and Bioengineering, University of Hawaii at Manoa, Honolulu, HI, USA*

Thomas Dugé de Bernonville · *EA2106 "Biomolécules et Biotechnologies Végétales", UFR Sciences et Techniques, Université François-Rabelais de Tours, Tours, France*

Sébastien Besseau · *EA2106 "Biomolécules et Biotechnologies Végétales", UFR Sciences et Techniques, Université François-Rabelais de Tours, Tours, France*

Sara Bettencourt · *CIBIO/InBIO—Centro de Investigação em Biodiversidade e Recursos Genéticos, Universidade do Porto, Vairão, Portugal*

Federica Brandizzi · *MSU-DOE Plant Research Lab, Plant Biology Department, Michigan State University, East Lansing, MI, USA; Department of Plant Biology, Michigan State University, East Lansing, MI, USA*

Brian Burkel · *Laboratory for Optical and Computational Instrumentation (LOCI), University of Wisconsin-Madison, Madison, WI, USA*

Inês Carqueijeiro · *EA2106 Biomolécules et Biotechnologies Végétales, Département de Biologie et Physiologie Végétales, UFR Pharmacologie, Université François-Rabelais de Tours, Tours, France*

Alexandra Chanoca · *Department of Botany, University of Wisconsin-Madison, Madison, WI, USA; Laboratory of Molecular and Cellular Biology, University of Wisconsin-Madison, Madison, WI, USA*

Travers Ching · *Department of Molecular Biosciences and Bioengineering, University of Hawaii at Manoa, Honolulu, HI, USA*

Marc Clastre · *EA2106 "Biomolécules et Biotechnologies Végétales", UFR Sciences et Techniques, Université François-Rabelais de Tours, Tours, France*

Cyrielle Corbin · *EA2106 "Biomolécules et Biotechnologies Végétales", UFR Sciences et Techniques, Université François-Rabelais de Tours, Tours, France*

Manuela Côrte-Real · *Centre of Molecular and Environmental Biology, CBMA, University of Minho, Braga, Portugal*

Vincent Courdavault · *EA2106 "Biomolécules et Biotechnologies Végétales", UFR Sciences et Techniques, Université François-Rabelais de Tours, Tours, France*

Patrícia Duarte · *CIBIO/InBIO—Centro de Investigação em Biodiversidade e Recursos Genéticos, Universidade do Porto, Vairão, Portugal*

Kevin W. Eliceiri · *Laboratory of Molecular and Cellular Biology, University of Wisconsin-Madison, Madison, WI, USA; Laboratory for Optical and Computational Instrumentation (LOCI), University of Wisconsin-Madison, Madison, WI, USA*

Natacha Fontes · *Sogrape Vinhos, S.A., Research and Development Department, Aldeia Nova, Avintes, Portugal*

Kentaro Fuji · *Graduate School of Science, Kyoto University, Kyoto, Japan*

Hernâni Gerós · *Centre of Molecular and Environmental Biology, CBMA, University of Minho, Braga, Portugal; Centre of Biological Engineering, CEB, University of Minho, Braga, Portugal; Centre for the Research and Technology of Agro-environmental and Biological Sciences, CITAB—UMinho Pole, University of Minho, Braga, Portugal*

Nathalie Giglioli-Guivarc'h · *EA2106 "Biomolécules et Biotechnologies Végétales", UFR Sciences et Techniques, Université François-Rabelais de Tours, Tours, France*

Gaëlle Glévarec · *EA2106 "Biomolécules et Biotechnologies Végétales", UFR Sciences et Techniques, Université François-Rabelais de Tours, Tours, France*

Erich Grotewold · *Department of Biochemistry and Molecular Biology, Michigan State University, East Lansing, MI, USA*

Joana G. Guedes · *CIBIO/InBIO—Centro de Investigação em Biodiversidade e Recursos Genéticos, Universidade do Porto, Vairão, Portugal; Departamento de Biologia, Faculdade de Ciências da, Universidade do Porto, Porto, Portugal; Instituto de Ciências Biomédicas Abel Salazar, Porto, Portugal*

Ikuko Hara-Nishimura · *Graduate School of Science, Kyoto University, Kyoto, Japan; Faculty of Science and Engineering, Konan University, Kobe, Japan*

Lei Huang · *Department of Botany and Pathology, Purdue University, West Lafayette, IN, USA*

Takuji Ichino · *Graduate School of Science, Kyoto University, Kyoto, Japan*

Kiersun Jones · *Department of Plant Biology, University of Georgia, Athens, GA, USA*

Eszter Kapusi · *Department of Applied Genetics and Cell Biology, University of Natural Resources and Life Sciences, Vienna, Austria*

Chang Hyun Khang · *Department of Plant Biology, University of Georgia, Athens, GA, USA*

Yasuko Koumoto · *Graduate School of Science, Kyoto University, Kyoto, Japan*

Arnaud Lanoue · *EA2106 "Biomolécules et Biotechnologies Végétales", UFR Sciences et Techniques, Université François-Rabelais de Tours, Tours, France*

Qing X. Li · *Department of Molecular Biosciences and Bioengineering, University of Hawaii at Manoa, Honolulu, HI, USA*

Angela Mosquera · *EA2106 "Biomolécules et Biotechnologies Végétales", UFR Sciences et Techniques, Université François-Rabelais de Tours, Tours, France; Laboratorio de Biotecnología, Sede de Investigación Universitaria, Universidad de Antioquia, Medellin, Colombia*

Lorena Norambuena · *Department of Biology, Faculty of Sciences, Plant Molecular Biology Centre, Universidad de Chile, Santiago, Chile*

Henrique Noronha · *Centro de Investigação e de Tecnologias Agro-Ambientais e Biológicas, Vila Real, Portugal; Centro de Biologia Molecular e Ambiental (CBMA), Departamento de Biologia, Universidade do Minho, Braga, Portugal*

Carolina Gabriela Ocampo · *CIDCA-CCT-La Plata CONICET, Facultad de Ciencias Exactas, Universidad Nacional de La Plata (UNLP), La Plata, Argentina*

Alessandro Occhialini · *Department of Food Science, University of Tennessee, Food Safety and Processing Building, Knoxville, TN, USA*

Sarah E. O'Connor · *Department of Biological Chemistry, The John Innes Centre, Norwich Research Park, Norwich, UK*

Claudio Osorio-Navarro · *Department of Biology, Faculty of Sciences, Plant Molecular Biology Centre, Universidad de Chile, Santiago, Chile*

Marisa S. Otegui · *Department of Botany, University of Wisconsin-Madison, Madison, WI, USA; Laboratory of Molecular and Cellular Biology, University of Wisconsin-Madison, Madison, WI, USA; Department of Genetics, University of Wisconsin-Madison, Madison, WI, USA*

Audrey Oudin · *EA2106 "Biomolécules et Biotechnologies Végétales", UFR Sciences et Techniques, Université François-Rabelais de Tours, Tours, France*

Nicolas Papon · *EA3142 "Groupe d'Etude des Interactions Hôte-Pathogène", Université d'Angers, Angers, France*

Richard Payne · *Department of Biological Chemistry, The John Innes Centre, Norwich, UK*

Bruno Peixoto · *Department of Biology, Faculty of Sciences, BioISI—Biosystems and Integrative Sciences Institute, University of Porto, Porto, Portugal*

Cátia S. Pereira · *Centre of Molecular and Environmental Biology, CBMA, University of Minho, Braga, Portugal; Centre of Biological Engineering, CEB, University of Minho, Braga, Portugal*

Cláudia Pereira · *Faculty of Sciences, University of Porto, Porto, Portugal*

Susana Pereira · *Department of Biology, Faculty of Sciences, BioISI—Biosystems and Integrative Sciences Institute, University of Porto, Porto, Portugal*

Silvana Petruccelli · *CIDCA-CCT-La Plata CONICET, Facultad de Ciencias Exactas, Universidad Nacional de La Plata (UNLP), La Plata, Argentina*

José Pissarra · *Department of Biology, Faculty of Sciences, BioISI—Biosystems and Integrative Sciences Institute, University of Porto, Porto, Portugal*

Luciana Renna · *MSU-DOE Plant Research Lab, Plant Biology Department, Michigan State University, East Lansing, MI, USA; Department of Plant Biology, Michigan State University, East Lansing, MI, USA*

Jorge M. P. Rodrigues · *Centre of Molecular and Environmental Biology, CBMA, University of Minho, Braga, Portugal*

Liuda J. Sepúlveda · *EA2106 "Biomolécules et Biotechnologies Végétales", UFR Sciences et Techniques, Université François-Rabelais de Tours, Tours, France; Laboratorio de Biotecnología, Sede de Investigación Universitaria, Universidad de Antioquia, Medellin, Colombia*

Tomoo Shimada · *Graduate School of Science, Kyoto University, Kyoto, Japan*

Mariana Sottomayor · *CIBIO/InBIO—Centro de Investigação em Biodiversidade e Recursos Genéticos, Universidade do Porto, Vairão, Portugal; Departamento de Biologia, Faculdade de Ciências da, Universidade do Porto, Porto, Portugal*

Giovanni Stefano · *MSU-DOE Plant Research Lab, Michigan State University, East Lansing, MI, USA; Department of Plant Biology, Michigan State University, East Lansing, MI, USA*

Eva Stöger · *Department of Applied Genetics and Cell Biology, University of Natural Resources and Life Sciences, Vienna, Austria*

Benoit St-Pierre · *EA2106 "Biomolécules et Biotechnologies Végétales", UFR Sciences et Techniques, Université François-Rabelais de Tours, Tours, France*

David L. Tabb · *Division of Molecular Biology and Human Genetics, Faculty of Medicine and Health Sciences, SA MRC Centre for TB Research, DST/NRF Centre of Excellence for Biomedical TB Research, Stellenbosch University, Cape Town, South Africa*

Junpei Takagi · *Department of Biological Sciences, Graduate School of Science, The University of Tokyo, Tokyo, Japan*
Ooi-Kock Teh · *Graduate School of Science, Kyoto University, Kyoto, Japan*
Ricardo Tejos · *Facultad de Recursos Naturales Renovables, Universidad Arturo Prat, Iquique, Chile*
Tomohiro Uemura · *Department of Biological Sciences, Graduate School of Science, The University of Tokyo, Tokyo, Japan*
Chunhua Zhang · *Department of Botany and Pathology, Purdue University, West Lafayette, IN, USA*

Chapter 1

GREEN FLUORESCENT SEED, to Evaluate Vacuolar Trafficking in *Arabidopsis* Seeds

Tomoo Shimada, Kentaro Fuji, Takuji Ichino, Ooi-Kock Teh, Yasuko Koumoto, and Ikuko Hara-Nishimura

Abstract

Vacuolar trafficking plays a vital role in plant growth and development. In this chapter, we describe a powerful technique for the evaluation of vacuolar protein trafficking, which is designated as GREEN FLUORESCENT SEED. Based on vacuole-targeted green fluorescent protein in *Arabidopsis* seeds, this method enables the nondestructive isolation of mutant seeds defective in vacuolar trafficking and their visual characterization.

Key words *Arabidopsis thaliana*, Green fluorescent protein (GFP), GREEN FLUORESCENT SEED (GFS), Vacuolar sorting receptor 1 (VSR1), Vacuolar trafficking, Vacuole

1 Introduction

Plant vacuoles are dynamic organelles involved in diverse cellular functions, such as the maintenance of turgor pressure, storage of various materials, and programmed cell death. The vacuolar functions depend on the specific proteins that are sequestered in the vacuole. Most vacuolar proteins that are synthesized on the rough endoplasmic reticulum are transported to vacuoles through the Golgi apparatus [1, 2]. To properly deliver soluble vacuolar proteins, VACUOLAR SORTING RECEPTOR (VSR) family proteins play a critical role in recognizing the vacuole-targeting signals of the vacuolar proteins. In *Arabidopsis vsr1* mutant seeds, vacuolar storage proteins are secreted out of the cells [3].

We previously developed a nondestructive and high-throughput screening method, GREEN FLUORESCENT SEED (GFS), to isolate *Arabidopsis* mutants deficient in vacuolar protein sorting [4]. The GFS method is based on a vacuolar-targeted reporter, SP-GFP-CT24, that is composed of a signal peptide (SP) and green fluorescent protein (GFP), followed by the CT24 peptide,

Cláudia Pereira (ed.), *Plant Vacuolar Trafficking: Methods and Protocols*, Methods in Molecular Biology, vol. 1789,
https://doi.org/10.1007/978-1-4939-7856-4_1,

which corresponds to the C-terminal 24 amino acids of the soybean storage protein β-conglycinin [5]. In the wild-type seeds, the GFP-CT24 molecules transported to protein storage vacuoles are partially degraded owing to their lower level of stability in the vacuole [6] (Fig. 1). However, in *vsr1* seeds, most of the GFP-CT24 molecules are mis-sorted to secrete out of the cells and accumulate in the extracellular space, resulting in the fluoresced seeds (Fig. 1). This means that a deficiency in vacuolar trafficking allows the seeds to fluoresce. Conversely, fluoresced seeds might be defective in vacuolar trafficking. The fluorescent seed phenotype makes it possible to instantly isolate a number of vacuolar trafficking mutants. We designated the mutants as *green-fluorescent seed* (*gfs*) [4].

To date, we have isolated and characterized several *gfs* mutants. *gfs2* [4] is allelic to *gravitropism defective 2* (*grv2*) [7] and *katamari 2* (*kam2*) [8]. GRV2/KAM2 is an ortholog of the DnaJ domain-containing Receptor-Mediated Endocytosis 8 (RME8) of *Caenorhabditis elegans*, which is required for endocytosis and endosome organization [9]. In plants, GFS2/GRV2/KAM2 is required for vacuolar protein trafficking [8] and vacuolar membrane flow [10]. *GFS3* and *GFS12* are allelic to each other and GFS3/GFS12 is a Beige and Chediak–Higashi (BEACH) domain-containing protein [11]. BEACH domain-containing proteins are highly conserved in eukaryotes and thought to act as scaffolds to facilitate membrane events, such as vesicle fusion or fission, to regulate trafficking,

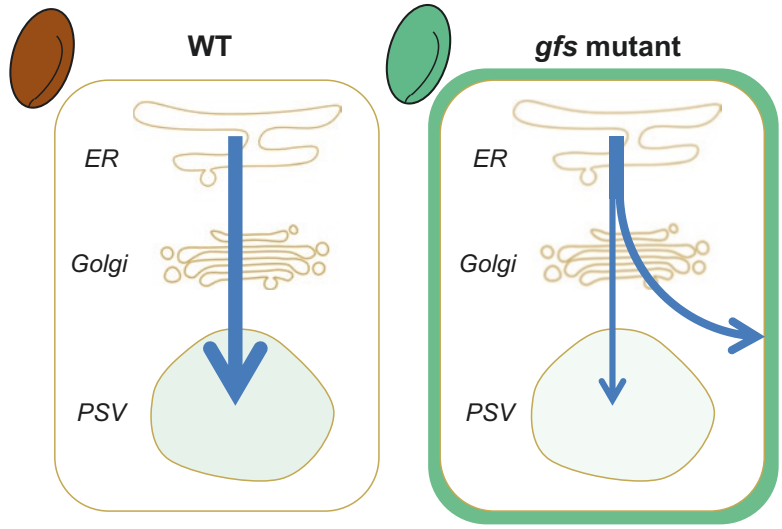

Fig. 1 Schematic model of enhanced GFP fluorescence in *gfs* seeds. In the wild-type (WT) seeds, GFP-CT24 molecules that are transported to protein storage vacuoles (PSVs) are partially degraded because of their lower stability level in the vacuole. Thus, WT seeds do not exhibit strong GFP fluorescence. In *gfs* mutant seeds, some GFP-CT24 molecules are mis-sorted to secrete out of the cells and accumulate in the extracellular space. This enhances GFP fluorescence of *gfs* seeds. Arrows indicate the trafficking pathways of GFP-CT24. *ER* endoplasmic reticulum, *Golgi* Golgi apparatus

although direct evidence for their mechanistic actions remains elusive [12]. In *Arabidopsis thaliana*, members of the BEACH family act together in a cascade to mediate vacuolar trafficking and plant immunity [11]. GFS4, GFS5, and GFS6 are β-, μ-, and σ-subunits of the adaptor protein (AP)-4 complex, respectively [13]. The AP-4 μ-subunit has the ability to bind to the tyrosine-based motif of VSR1. AP-4 localizes at the *trans*-Golgi network and mediates the VSR1-dependent vacuolar protein sorting. *gfs9* is allelic to unidentified *transparent testa 9* (*tt9*) [14]. Both *gfs9* and *tt9* have abnormal pale tan-colored seeds because of the low flavonoid levels in the seeds coats. GFS9/TT9 is a membrane-trafficking factor that contains the region that is conserved among eukaryotes, such as Endosomal Maturation defective (Ema) of *Drosophila melanogaster* [15]. Furthermore, the GFS method can be used to evaluate the efficiency of vacuolar trafficking in various mutants by introducing GFP-CT24 [4, 16–22]. The GFS method is an easy and versatile technique to monitor vacuolar trafficking in plant cells.

2 Materials

Prepare all solutions using ultrapure water (prepared by purifying deionized water to attain a sensitivity of 18 MΩ/cm) and analytical grade reagents. Prepare and store all reagents at room temperature (unless indicated otherwise). Diligently follow all waste disposal regulations when disposing of waste materials.

2.1 Plant Materials and Growth Conditions

1. *Arabidopsis thaliana* accession Columbia-0 (Col-0).
2. *Arabidopsis thaliana* transgenic line, GFP-CT24, harboring SP-GFP-CT24, which is composed of signal peptide (SP) and green fluorescent protein (GFP), followed by the CT24 peptide of soybean β-conglycinin under the control of the β-conglycinin promoter [5].
3. Murashige and Skoog basal salt mixture.
4. Gellan gum.
5. Sucrose.
6. 70% (v/v) and 99.5% (v/v) ethanol.
7. Sterile disposable petri dishes.
8. Pots (6-cm diameter).
9. Vermiculite.

2.2 Mutagenesis of Arabidopsis Seeds with Ethyl Methanesulfonate

1. Methanesulfonic acid, ethyl ester (EMS, Sigma-Aldrich) (*see* **Note 1**): 0.2% (v/v) or 0.25% (v/v) solution (*see* **Note 2**).
2. Fine bags, such as tea bags.

2.3 Crossing Arabidopsis Mutants

1. Fine forceps.
2. Colored sewing thread.
3. 99.5% (v/v) ethanol.
4. Binoculars, if necessary.

2.4 Isolation of Mutants by Monitoring GFP Fluorescence

1. Black paper.
2. Wooden toothpicks.
3. Fluorescence stereomicroscope (MZ-APO; Leica Micro-systems).

2.5 Confocal Laser Scanning Microscopy

1. Glass slides and cover glasses.
2. Glycerol.
3. Confocal laser scanning microscope (Zeiss LSM 780; Carl Zeiss) with filter sets for GFP and red fluorescent protein.
4. Image analysis software.

3 Methods

3.1 Preparation of Arabidopsis GFP-CT24 Seeds

1. Sterilize seeds in 70% (v/v) ethanol with shaking for 5 min.
2. Remove the 70% (v/v) ethanol and add 99.5% (v/v) ethanol.
3. Remove the 99.5% (v/v) ethanol and dry seeds.
4. Sow onto a plate of 0.5% (w/v) Gellan Gum containing 1/2 Murashige and Skoog medium supplemented with 1% (w/v) sucrose and grow at 22 °C under continuous light.
5. Transfer to soil after 2 weeks and grow at 22 °C with a 16–h light/8–h dark cycle.
6. Collect seeds when their siliques are dry.

3.2 Mutagenesis of Arabidopsis Seeds with EMS

1. Put *Arabidopsis* GFP-CT24 seeds (~1000 grains) in a tea bag.
2. Soak seeds in 0.2 or 0.25% (v/v) EMS solution for 16 h with stirring.
3. Wash for 3 h in running water. The washed seeds are called M1 seeds.
4. Sow and grow the M1 seeds in soil pots (~14 seeds/pot).
5. Collect the seeds after self-fertilization. These are the M2 seed populations.

3.3 Cross the GFP-CT24 Line with Potential Vacuolar-Trafficking Mutants

1. Sterilize forceps with ethanol.
2. Select a young flower bud at the top of an inflorescence as the female parent.
3. Carefully remove all the flower organs except the pistil with forceps.
4. Select a newly opened flower containing fresh pollen as the male parent.

5. Remove the flower from the flower stalk.
6. Pollinate the pistil with the flower by tapping the anthers on the stigma.
7. Mark the pollinated bud with colored thread.

3.4 Isolation of GFS Lines by Monitoring Seed Fluorescence

1. Put ~1000 M2 seeds on a sheet of black paper.
2. Spread them without overlapping.
3. Inspect with a fluorescence stereomicroscope (MZ-APO; Leica Micro-systems).
4. Pick up the seeds with strong fluorescence using a wooden toothpick and transfer them into collecting tubes (*see* **Note 3**).
5. Acquire fluorescent images using a digital camera (Fig. 2).

3.5 Observing GFP Fluorescence with a Confocal Laser Scanning Microscope

1. Put dry seeds in glycerol between a glass slide and a cover glass.
2. Press the cover glass to spread the embryos.
3. Inspect cotyledons or embryo axes with a confocal laser scanning microscope (Zeiss LSM 780).
4. Obtain fluorescent images using multitrack mode and analyze using ImageJ software (National Institutes of Health) (Fig. 3).

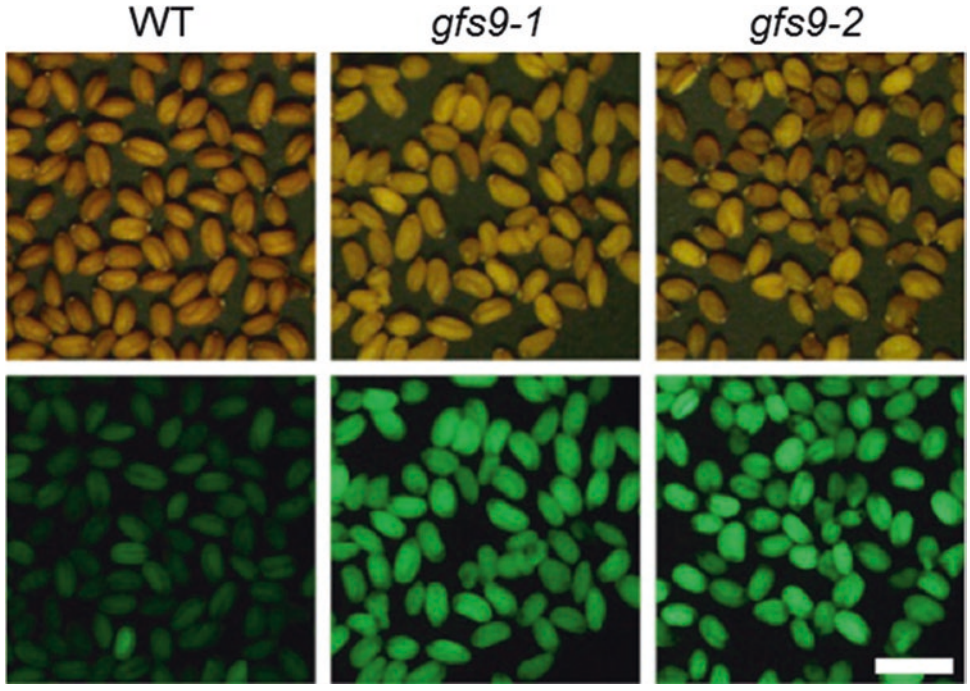

Fig. 2 *Arabidopsis gfs* seeds have strong GFP fluorescence. Stereomicroscopic (upper panels) and fluorescence microscopic (lower panels) images of wild-type (WT), *gfs9-1*, and *gfs9-2* seeds. *gfs9* seeds display strong GFP fluorescence, whereas WT seeds do not. Bar, 1 mm. Panels are reproduced from ref. 14. Copyright John Wiley & Sons Limited

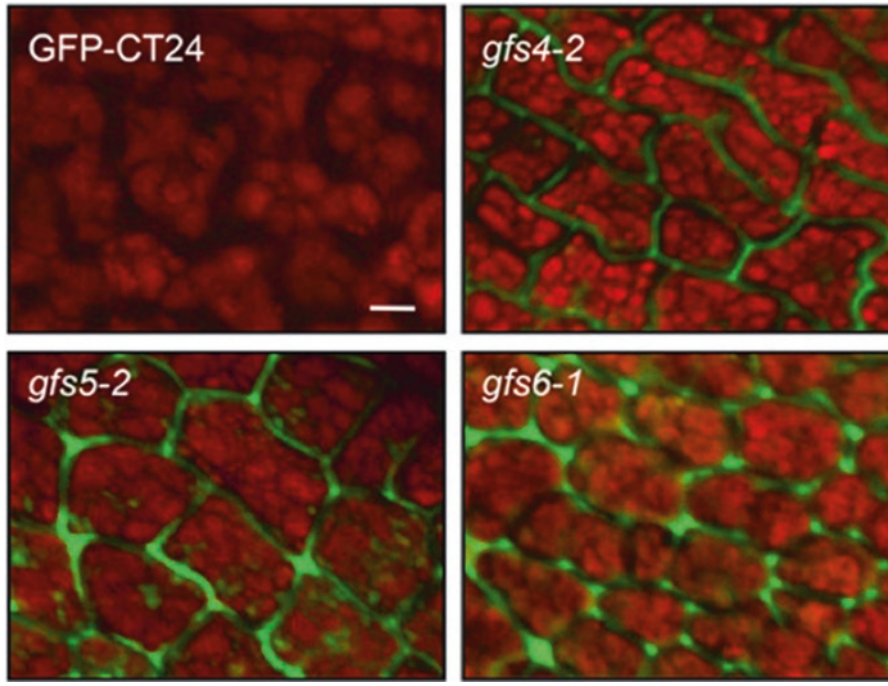

Fig. 3 Mis-sorting of GFP-CT24 out of the cells in *gfs* seeds. Confocal images of *gfs4-2*, *gfs5-2*, and *gfs6-1* seed cells, and the parental line GFP-CT24. GFP fluorescence is detected outside the cells of these mutants. The autofluorescence of protein storage vacuoles is shown in red. Bar, 5 μm. Panels are reproduced from ref. 13. Copyright American Society of Plant Biologists

4 Notes

1. EMS is carcinogenic in mammals. Follow the manufacturer's safety precautions.
2. We use two different EMS concentrations to obtain a suitable result.
3. The toothpick should be wetted in water to easily pick up seeds. The selected seeds should be dried again for long-term storage.

Acknowledgment

This work was supported by a Grant-in-Aid for Scientific Research to I.H.-N. (15H05776) from the Japan Society for the Promotion of Science.

References

1. De Marcos Lousa C, Denecke J (2016) Lysosomal and vacuolar sorting: not so different after all! Biochem Soc Trans 44:891–897
2. Robinson DG, Neuhaus JM (2016) Receptor-mediated sorting of soluble vacuolar proteins: myths, facts, and a new model. J Exp Bot 67:4435–4449
3. Shimada T, Fuji K, Tamura K et al (2003) Vacuolar sorting receptor for seed storage proteins in Arabidopsis thaliana. Proc Natl Acad Sci U S A 100:16095–16100
4. Fuji K, Shimada T, Takahashi H et al (2007) Arabidopsis vacuolar sorting mutants (green fluorescent seed) can be identified efficiently by secretion of vacuole-targeted green fluorescent protein in their seeds. Plant Cell 19:597–609
5. Nishizawa K, Maruyama N, Satoh R et al (2003) A C-terminal sequence of soybean β-conglycinin α' subunit acts as a vacuolar sorting determinant in seed cells. Plant J 34:647–659
6. Tamura K, Shimada T, Ono E et al (2003) Why green fluorescent fusion proteins have not been observed in the vacuoles of higher plants. Plant J 35:545–555
7. Silady RA, Kato T, Lukowitz W et al (2004) The gravitropism defective 2 mutants of Arabidopsis are deficient in a protein implicated in endocytosis in Caenorhabditis elegans. Plant Physiol 136:3095–3103.
8. Tamura K, Takahashi H, Kunieda T et al (2007) Arabidopsis KAM2/GRV2 is required for proper endosome formation and functions in vacuolar sorting and determination of the embryo growth axis. Plant Cell 19:320–332
9. Zhang Y, Grant BHirsh D (2001) RME-8, a conserved J-domain protein, is required for endocytosis in Caenorhabditis elegans. Mol Biol Cell 12:2011–2021
10. Silady RA, Ehrhardt DW, Jackson K et al (2008) The GRV2/RME-8 protein of Arabidopsis functions in the late endocytic pathway and is required for vacuolar membrane flow. Plant J 53:29–41
11. Teh OK, Hatsugai N, Tamura K et al (2015) BEACH-domain proteins act together in a cascade to mediate vacuolar protein trafficking and disease resistance in Arabidopsis. Mol Plant 8:389–398
12. Cullinane AR, Schaffer AAHuizing M (2013) The BEACH is hot: a LYST of emerging roles for BEACH-domain containing proteins in human disease. Traffic 14:749–766
13. Fuji K, Shirakawa M, Shimono Y et al (2016) The adaptor complex AP-4 regulates vacuolar protein sorting at the trans-Golgi network by interacting with VACUOLAR SORTING RECEPTOR1. Plant Physiol 170:211–219
14. Ichino T, Fuji K, Ueda H et al (2014) GFS9/TT9 contributes to intracellular membrane trafficking and flavonoid accumulation in Arabidopsis thaliana. Plant J 80:410–423
15. Kim S, Wairkar YP, Daniels RW et al (2010) The novel endosomal membrane protein Ema interacts with the class C Vps-HOPS complex to promote endosomal maturation. J Cell Biol 188:717–734
16. Ebine K, Okatani Y, Uemura T et al (2008) A SNARE complex unique to seed plants is required for protein storage vacuole biogenesis and seed development of Arabidopsis thaliana. Plant Cell 20:3006–3021
17. Ebine K, Inoue T, Ito J et al (2014) Plant vacuolar trafficking occurs through distinctly regulated pathways. Curr Biol 24:1375–1382
18. Gao C, Zhuang X, Cui Y et al (2015) Dual roles of an Arabidopsis ESCRT component FREE1 in regulating vacuolar protein transport and autophagic degradation. Proc Natl Acad Sci U S A 112:1886–1891
19. Isono E, Katsiarimpa A, Muller IK et al (2010) The deubiquitinating enzyme AMSH3 is required for intracellular trafficking and vacuole biogenesis in Arabidopsis thaliana. Plant Cell 22:1826–1837
20. Kolb C, Nagel MK, Kalinowska K et al (2015) FYVE1 is essential for vacuole biogenesis and intracellular trafficking in Arabidopsis. Plant Physiol 167:1361–1373
21. Singh MK, Kruger F, Beckmann H et al (2014) Protein delivery to vacuole requires SAND protein-dependent Rab GTPase conversion for MVB-vacuole fusion. Curr Biol 24:1383–1389
22. Wu X, Ebine K, Ueda T et al (2016) AtNHX5 and AtNHX6 Are Required for the Subcellular Localization of the SNARE Complex That Mediates the Trafficking of Seed Storage Proteins in Arabidopsis. PLoS One 11:e0151658

Chapter 2

Detection of CRISPR/Cas9-Induced Genomic Fragment Deletions in Barley and Generation of Homozygous Edited Lines via Embryogenic Pollen Culture

Eszter Kapusi and Eva Stöger

Abstract

The CRISPR/Cas9 system from *Streptococcus pyogenes* is an increasingly popular tool for genome editing due to its ease of application. Here we demonstrate genomic DNA fragment removal using RNA directed Cas9 nuclease in barley. The high mutation frequency confirms the exceptional efficiency of the system and its suitability for generating loss-of-function mutant lines that may be used in functional genetics approaches to study endomembrane trafficking pathways and posttranslational protein modifications. The generation of doubled haploids from genome edited plants allows the recovery of true breeding lines that are instantly homozygous for the edited alleles.

Key words CRISPR/Cas9, Induced mutation frequency, Cereals, *Hordeum vulgare* cv. "Golden Promise", Genome editing, GC rich sequence, Doubled haploid

1 Introduction

Precision genome modification in model and crop plants provides an important platform for the design of targeted mutations to study gene function and to engineer novel traits [1, 2]. The rapid progress in genome editing reflects the development of reprogrammable site-directed nucleases that introduce double-stranded breaks (DSBs) at preselected positions. Among them, the CRISPR/Cas9 system from *Streptococcus pyogenes* has been successfully used in various organisms including microbes, animals and plants [3]. Its greatest advantage is the ease of reprogramming, which is achieved by changing the sequence of the synthetic single guide RNA (sgRNA) that binds Cas9 and directs the ribonucleoprotein complex to its genomic target where DSBs are induced. The chromosome breaks are mended via the cell repair mechanisms, mostly nonhomologous end joining (NHEJ), which results in mutations, typically small deletions or insertions [4].

Cláudia Pereira (ed.), *Plant Vacuolar Trafficking: Methods and Protocols*, Methods in Molecular Biology, vol. 1789,
https://doi.org/10.1007/978-1-4939-7856-4_2,

The only prerequisite for the binding of the nuclease is the presence of an 5′-NGG-3′ protospacer adjacent motif (PAM) downstream of the 20 nt genomic target. Cas9-triggered cleavage of DNA occurs typically three nucleotides upstream of the PAM.

The versatility of the system allows for fast generation of knockout mutants in model and crop plants that may be used to identify and confirm gene functions involved in trafficking and modification of endomembrane-resident proteins. Here we provide a detailed protocol for the generation of loss-of-function mutations to study the barley (*Hordeum vulgare* cv. "Golden promise") machinery for N-glycan modification and removal [5–8]. We selected the putative endogenous barley ENGase (endo-*N*-acetyl-β-D-glucosaminidase) gene (MLOC_10039.2) as a candidate for genome editing. This single copy gene has high GC content and produces two alternatively spliced mRNAs. Five single guide RNAs (sgRNAs) were designed for different target sites in the upstream part of the ENGase coding region close to the ATG start codon. Targeted fragment deletions were induced by introducing pairwise combinations of sgRNAs via co-infection with separate *Agrobacterium tumefaciens* cultures [8]. The removal of chromosomal segments offers several advantages over simple frameshift mutations via small indels. It allows the deletion of exons, protein domains, promoters or even entire genes preventing cells from synthesizing truncated, nonfunctional polypeptides. The loss of genomic DNA sequences between selected targets and site-specific small indels were identified via genotype screening of the primary transformants. Cas9-triggered mutation frequency reached 78%, and fragment deletions were identified in 18.8% of the plants producing active sgRNA-directed Cas9 [8]. The induced indels and fragment deletions were transmitted to the T1 generation, and with the help of the doubled haploid technique [9] we were able to generate lines instantly homozygous for the edited allele.

2 Materials

Protocols used for *Agrobacterium*-mediated immature barley embryo transformation and regeneration of the primary transgenic plants, are based on the publications by Tingay et al. and Hensel and Kumlehn [10, 11]. The tissue culture and preparation of respective solutions must be carried out under sterile conditions. Prepare solutions using ultrapure water and analytical grade reagents. Waste disposal of genetically modified organisms must follow local regulations.

2.1 Cloning of the Vector Constructs

1. pENTRY vector (DNA Cloning Service, Hamburg, Germany), containing the wild-type cas9 from *Streptococcus pyogenes* under the control of the maize ubiquitin promoter, sgRNA scaffold and hygromycin phosphotransferase gene (*hpt*) as a selectable marker.

2. BsmBI restriction enzyme and corresponding buffer.
3. Sense and antisense oligonucleotides representing the selected sgRNA sequence and containing complementary ends with the pENTRY vector after digestion with BsmBI.
4. T4 ligase and corresponding buffer.
5. T4 polynucleotide kinase (PNK).
6. EcoRI and EcoRV restriction enzymes for test digest.

2.2 Plant Donor Material

1. Diploid wildtype spring barley cv. "Golden Promise" plants.
2. Osmocote (4.0 g/7.5 L), a long-term fertilizer.
3. 0.3% Hakaphos Blau.
4. Chamber with a 18/16 °C day–night regime, 16-h photoperiod, min. 25,000 lux, and 70% humidity.
5. Wheat cv. "Bobwhite."

2.3 Barley Genetic Transformation and Tissue Culture Conditions

1. MG/L medium [12]: 5 g/L mannitol, 1 g/L L-glutamic acid, 250 mg/L KH_2PO_4, 100 mg/L NaCl, 100 mg/L $MgSO_4$, 1 μg/L biotin, 5 g/L trypton, 2.5 g/L yeast extract. For solid medium add 1.2% agar. Set pH at 7, and sterilize by autoclaving. Store at room temperature.
2. *Agrobacterium tumefaciens* strain AGL1.
3. 70% ethanol.
4. 3.7% NaOCl–Tween solution: measure 10 mL 37 m/m% NaOCl solution and add water to a final volume of 100 mL and a drop of Tween.
5. Autoclaved double distilled water.
6. 6-well plate.
7. CCM (co-culture medium) medium: 0.86 g Murashige and Skoog medium including vitamins, 0.2 g casein hydrolysate, 0.2 g L-proline, 0.2 mg thiamine–HCl (200 μL from 1 mg/mL stock solution), 0.05 g myo-inosytol, 6.0 g maltose monohydrate, 0.5 mg dicamba (200 μL from 2.5 mg/mL stock solution), add water to a final volume of 200 mL. Adjust pH to 5.8, add 160 mg L-cysteine (*see* **Note 1**) and 0.05 mM acetosyringone (100 μL of 1 M stock solution). Sterilize the solution by filtration through 0.2 μm pores into an autoclaved bottle (*see* **Note 2**) and store at 4 °C until use (*see* **Note 3**).
8. CIM (callus induction) medium: measure 1.72 g Murashige and Skoog basal salt mixture medium, 12.0 g maltose monohydrate, 0.4 mg thiamine–HCl (400 μL from 1 mg/mL stock solution), 0.276 g L-proline, 0.4 g casein hydrolysate, 0.1 g myo-inositol, 1.0 mg dicamba (400 μL from 2.5 mg/mL stock solution), 0.02 mg CuSO4 (200 μL from 0.01 M stock solution) and

60.0 mg ticarcillin disodium/clavulanate potassium, water to a total volume of 100 mL. Adjust pH to 5.8, pass through a sterile filter into an autoclaved bottle, and add antibiotics for plant selection (e.g., 50 mg/L hygromycin). Add 1.2 g Phytagel to 300 mL water, autoclave and cool down to 60 °C. Add the filter-sterilized solution (100 mL) to the autoclaved water–Phytagel mixture under constant stirring. Prepare ca. 20 medium plates, store them at 4 °C until use (*see* **Note 4**).

9. RM (regeneration medium): measure 20 mL K-macro (*see* **Note 5**) 20× salt solution (6.4 g/L NH_4NO_3, 72.80 g/L KNO_3, 6.8 g/L KH_2PO_4, 8.82 g/L $CaCl_2{\cdot}2H_2O$, 4.92 g/L $MgSO_4{\cdot}7H_2O$ $MgSO_4$), 0.4 mL K-micro 1000x (8.4 g/L $MnSO_4{\cdot}H_2O$, 3.1 g/L H_3BO_3, 7.2 g/L $ZnSO_4{\cdot}7H_2O$, 120 mg/L $Na_2MoO_4{\cdot}2H_2O$, 25 mg/L $CuSO_4{\cdot}5H_2O$, 24 mg/L $CoCl_2{\cdot}6H_2O$, 170 mg/L KI), 0.4 mL 75 mM NaFeEDTA, 0.4 mL Gamborg B5 vitamin mixture (1000×), 1.6 mL 0.25 M L-glutamine, 40.0 mL 1 M maltose monohydrate, 0.4 mL 1 mM 6-Benzylaminopurine (6-BAP), 0.2 mL 0.01 M $CuSO_4$, 0.4 mL 150 mg/L ticarcillin disodium and add water to a final volume of 100 mL. Adjust pH to 5.8, and add antibiotics for plant selection (e.g., 25 mg/L hygromycin) to the sterile solution. Add 1.2 g Phytagel to 300 mL water, autoclave and cool down to 60 °C. Add the filter-sterilized solution (100 mL) to the autoclaved water–Phytagel mixture under constant stirring. Prepare ca. 20 medium plates, store them at 4 °C until use (*see* **Note 4**).
10. Transgenic plant selection agent, e.g., hygromycin B.

2.4 Plant Genomic DNA Isolation

1. DNA extraction buffer: 1 g *N*-lauryl-sarcosine sodium salt, 10 mL 100 mM Tris–HCl (pH 8.0), 2 mL 10 mM EDTA (pH 8.0), 2.5 mL 100 mM NaCl. Add double distilled water to a final volume of 100 mL and store at room temperature.
2. Phenol–chloroform–isoamyl alcohol.
3. Retsch mill.
4. 3 M Na-acetate, pH 5.2.
5. 2-propanol.
6. 70% etanol.
7. TE-buffer with RNAse: 1 mL 1 M Tris–HCl (pH 8.0), 200 µL 10 mM EDTA (pH 8.0), double distilled water to a final volume of 100 mL. Add RNAse to a final concentration of 40 µg/mL, and store at −20 °C.

2.5 PCR and Sanger Sequencing

1. Taq DNA polymerase and corresponding buffer.
2. Q5 HiFi high-fidelity DNA polymerase and corresponding buffer (New England Biolabs, Ipswich, MA, USA).

3. Primers CAS-F 5′-CTGACGTCGATAAGTTGTTCA-3′, and CAS-R 5′-TGATGAACTTGTAGAACTCCT-3′.
4. Primers: ENG-F 5′-GTCTCATCCGCGAGCTCAT-3′, and ENG-R 5′-TCCTGTGTTGCAAACATCTCC-3′.

2.6 Embryogenic Pollen Culture

1. 5 mL/12 mL sterile pipette.
2. 100 μm nylon mesh sieve.
3. Sterile 50 mL Falcon tubes.
4. Sterile 12 mL screw cap tube.
5. 0.4 M D-mannitol. Sterilize by autoclaving and store at 4 °C.
6. 0.55 M maltose. Sterile filter solution and store at 4 °C.
7. Starvation medium (SM): 20 mL 1 M maltose, 50 μL 1 M NH_4Cl, 50 μL K-micro 1000×, 100 μL 1 M 2-morpholinoethanesulfonic acid (MES, pH 5.5), 50 μL 1 M $CaCl_2$, 200 μL 1 mM 6-benzylaminopurine (BAP) and 62.5 μL 200 mg/mL cefotaxime (*see* **Note 6**). Add water to a final volume of 50 mL. Adjust pH to 5.5 and sterilize by filtration. Store solution at 4 °C until use.
8. Pollen medium (PM): 25 mL 1 M maltose, 5 mL K-macro (20×) salt solution, 100 μL K-micro (1000×) solution, 100 μL 75 mM NaFeEDTA, 1 mL Kao and Michayluk (100×) medium (Duchefa, K0214), 1.2 mL 0.25 M L-glutamine, 400 μL 1 mM BAP and 125 μL 200mg/mL cefotaxime. Add water to a volume of 100 mL, adjust pH to 5.9, and store solution at 4 °C until use.
9. Solid pollen medium: 100 mL 1 M maltose, 20 mL K-macro (20), 0.4 mL K-micro (1000×), 0.4 mL 75 mM NaFeEDTA, 4.0 mL Kao and Michayluk (100×) medium, 4.8 mL 0.25 M L-glutamine, 400 μL 1 mM BAP and 100 μL 200 mg/mL cefotaxime. Add water to a final volume of 250 mL, adjust pH to 5.8 and sterilize by filtration. Add 1.2 g Phytagel to 150 mL water, autoclave and cool down solution to 60 °C. Add the filter-sterilized solution (250 mL) to the autoclaved water–phytagel mixture under constant stirring. Prepare medium plates and store them at 4 °C until use (*see* **Note 4**).
10. Regeneration medium (RM) without selection, *see* Subheading 2.3, **item 7**.

3 Methods

3.1 Selection of the sgRNA Target Sequences

1. Select 20 nt target sequences with G as the start of transcription and with appropriate 4-bp overhangs that complement the sticky ends arising from BsmBI digestion of the vector (AGCT for the sense and CAAA for the antisense oligo). The 3′ end of the genomic sequence must contain a 5’-NGG-3′ PAM. Select

target sequences with high purine content in the seed (6-8 nucleotides adjacent to the PAM) region [13]. According to Jiang et al. [14] sgRNAs with more than 50% CG content are more efficient.

3.2 Cloning of the Target Sequences in the pENTRY Vector/ Fusion of the Target Sequence to the sgRNA Scaffold

1. Digest pENTRY vector with BsmBI according to the manufacturer's protocol. Purify the product in order to remove enzyme and undigested vector.
2. Phosphorylate and anneal target sense and antisense oligonucleotides. In a total volume of 10 μL the reaction contains: 6.0 μL water, 2.0–2.0 μL 10 μM oligos, 1 μL T4 ligase buffer and 1 μL PNK. The reaction is heated to 95 °C for 5 min, then ramped down to 25 °C at a rate of 5 °C/min.
3. Ligate the oligos into the predigested pENTRY vector. The reaction (10 μL total) is composed of 6.0 μL water, 1.0 μL T4 ligase buffer, 0.5 μL pENTRY (digested with BsmBI), 2.0 μL annealed sense and antisense oligos, and 0.5 μL T4 ligase. Incubate the reaction for 1–2 h at room temperature or overnight at 14 °C. Transform the products into *E. coli* and confirm the presence of the insert by test restriction digest using EcoRI/EcoRV and sequencing using a primer binding in the T-nos region (5′-TATGAGATGGGTTTTTATGAT-3′).

3.3 Barley Genetic Transformation and Tissue Culture

Excision of the embryos, their co-culture with *Agrobacterium tumefaciens* strain AGL1, microspore isolation and successive tissue culture steps must be carried out under sterile conditions in a laminar flow bench. It is recommended that the embryos are isolated under a stereo microscope using forceps and lancet.

1. Grow 10 mL overnight culture of strain AGL1 [15] containing the pcas9:sgRNA binary vector at 28 °C and shaking at 180 rpm in MG/L medium without antibiotics (*see* **Note 7**). Adjust optical density OD_{600} to 0.2.
2. Use immature embryos as explants for the genetic transformation. Harvest developing caryopses approximately 12 days after pollination. Sterilize the surface of the caryopses by stirring them for 3 min in 70% ethanol, followed by a washing step for 20 min in 3.7% NaOCl–Tween solution. Finally, rinse them in autoclaved distilled water 3–5 times. If necessary, the material can be stored overnight at 4 °C until use.
3. Excise barley embryos from the caryopses by using forceps and lancet needle under a stereo microscope (*see* **Note 8**) and remove the embryonic axis from the scutellum. Place 30 scutella in each well of a 6-well-plate filled with 2.5 mL co-culture medium (CCM). For the co-culture with agrobacteria, remove CCM and add 600 μL *Agrobacterium* suspension. Vacuum infiltrate the plate for 1 min at 500 mbar, cover and incubate

for 10 min. Remove the suspension and wash embryos with 2.5 mL CCM medium. Incubate for 15 min and carry out another washing step with 2.5 mL CCM. Incubate the plates at 21 °C in the dark for 2–3 days. After co-culture transfer the embryos to CIM medium supplemented with antibiotics for plant selection. Place ten embryos on each plate. Incubate at 24 °C in the dark for 2 weeks, then transfer the developing calli onto fresh CIM (+ selection) medium, and incubate for another 2 weeks. Transfer the well-developed calli to RM, supplemented with selective agent and incubate, in a light chamber (24 °C, 16/8 h light/dark photoperiod, 10,000 lux). Repeat this step three times in 2-week intervals. Transfer regenerating plantlets to sterile boxes containing RM (supplemented with selective agent). Transfer plants to soil when first roots appear, and move them to a growth chamber (18/16 °C day/night, 16-h photoperiod, min. 25,000 lux and 70% humidity).

3.4 Detection of Cas9-Induced Site-Specific Mutations

1. Isolate plant genomic DNA (gDNA) as described by Pallotta et al. [16]. Grind approximately 200 mg leaf material (snap-frozen in liquid nitrogen) with an autoclaved metal ball (2 mm diameter) in a 2 mL Eppendorf tube using a Retsch mill (*see* **Note 9**). Add 800 μL DNA extraction buffer and vortex thoroughly to obtain a homogeneous suspension. Add 800 μL phenol–chloroform–isoamyl alcohol and vortex for 30 s. Centrifuge (5000 rpm, 2.3 rcf) at room temperature for 3 min. Pipette 700 μL supernatant into a clean 1.5-mL Eppendorf tube (*see* **Note 10**). Add 70 μL 3 M Na-acetate (pH 5.2) and 700 μL 2-propanol. Mix until precipitates of genomic DNA become visible, then centrifuge (13,000 rpm, 15.7 rcf) at 4 °C for 20 min. Discard the supernatant, wash pellet with 700 μL 70% ethanol, and centrifuge at 4 °C for 5 min. Carefully remove all supernatant with a pipette without disturbing the pellet, and air-dry gDNA. Add 100 μL TE-buffer/RNAse, adjust DNA concentration to 1 μg/μL, and store DNA at 4 °C or at −20 °C for a longer time period.
2. Analyze the regenerated plants for the presence of the cas9 gene using Taq polymerase and primers CAS-F and CAS-R. Set up the PCR reaction according to the manufacturer's recommendation, add 0.5 μL of genomic DNA and carry out the reaction in a thermocycler using the following steps: initial denaturing step at 95 °C for 5 min followed by 35 cycles of 95 °C for 30 s, 60 °C for 30 s, and 72 °C for 1 min, and then a final extension step at 72 °C for 2 min.
3. Analyze the selected target region of the putative barley ENGase gene using Q5 HiFi high-fidelity DNA polymerase. The expected product size using primers ENG-F and ENG-R is 616 bp. Set up the PCR reaction according to the manufacturer's recommendation (*see* **Note 11**), add 0.5 μL genomic

DNA and carry out the reaction in a thermocycler using the following steps: initial denaturing step at 95 °C for 5 min followed by 35 cycles of 95 °C for 30 s, 53 °C for 30 s, and 72 °C for 1 min, and then a final extension step at 72 °C for 2 min.

4. Subject the obtained PCR fragments to direct sequencing or insert them into an intermediate vector containing standard primer binding sites, such as M13 and M13r, for sequencing. Compare the sequencing results to the wildtype gene sequence.

3.5 Embryogenic Pollen Culture

1. Harvest spikes of selected genome edited barley lines containing microspores at the late uninucleate stage. Spray them with 70% ethanol, remove awns and store in sterile petri dishes. Apply cold treatment for 2–3 weeks at 6 °C. Cut spikes into pieces of 1 cm length using a sterile scalpel, and place them in an autoclaved and precooled blender. Add 20 mL precooled 0.4 M D-mannitol using a pipette and homogenize for 2 × 10 s (level "low"). Filter the suspension through a 100 μm nylon mesh and collect the filtrate in a Falcon tube on ice. Wash tank with 5 mL 0.4 M D-mannitol. Collect spike residues and place them back in the blender. Add 10 mL 0.4 M D-mannitol and homogenize again. Pass the suspension again through the nylon mesh, and wash blender with 5 mL 0.4 M D-mannitol. Centrifuge for 10 min at 100 × *g* and 4 °C. Discard supernatant, resuspend the pellet in 5 mL ice cold 0.55 M maltose and transfer to a 12-mL screw-cap tube. Wash the falcon tube with 1.5 mL 0.4 M D-mannitol and carefully place it on top of the maltose/microspore suspension without mixing. Centrifuge at 100 × *g* for 10 min at 4 °C (*see* **Note 12**). Collect the microspores accumulated in a ring at the interface between maltose and D-mannitol (Fig. 1a), and transfer them to a clean Falcon tube. Fill up the tube with D-mannitol to 20 mL. Estimate the number of isolated microspores using a Burker-Türk haemocytometer. Centrifuge again at 100 × *g* for 10 min at 4 °C. Discard the supernatant, and dissolve the pellet in starvation medium (SM) adjusting microspore density to approximately 2–4 × 10^5 per mL. Incubate culture at 21 °C in a dark incubator. After 2 days replace starvation medium with pollen medium, and incubate again at 21 °C without light.
2. Sterilize the surface of harvested wheat spikes (cultivar "Bobwhite") with 70% ethanol. Dissect pistils from immature florets, and store in KBP medium at 21 °C until use.
3. After 1 week of microspore culture, add 1 mL pollen medium and five freshly or previously isolated (max. 3 days old) wheat pistils. Incubate on a rotary shaker at 24 °C. After three weeks calli derived from embryogenic pollen should be visible (Fig. 1b). Transfer these structures to solid pollen medium,

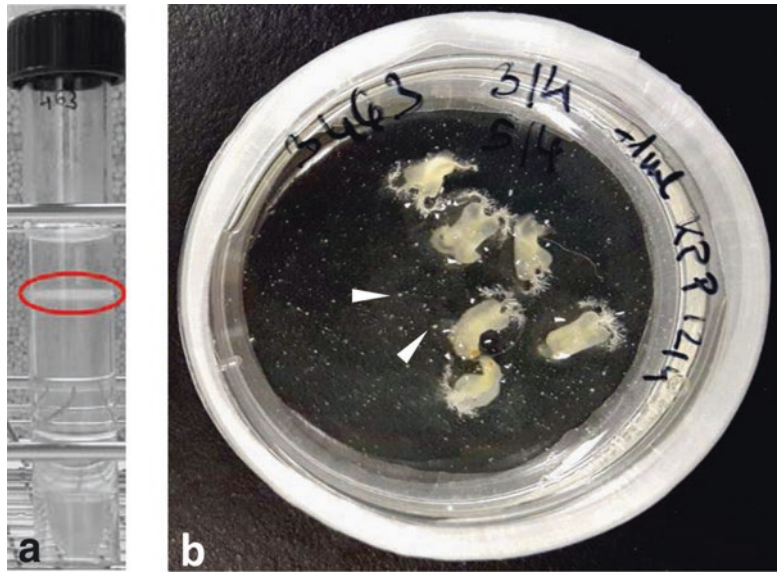

Fig. 1 (**a**) Isolated late uninucleate microspores after gradient centrifugation. (**b**) Calli derived from embryogenic pollen become visible approximately 1 month after microspore isolation

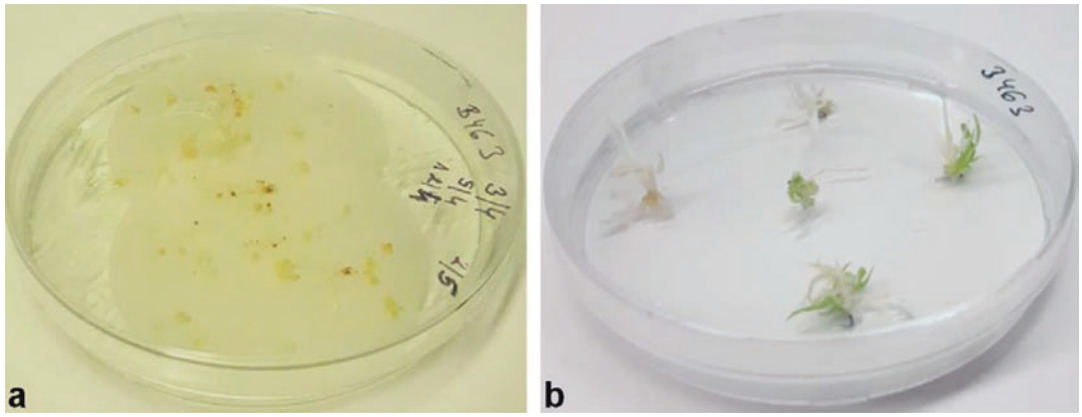

Fig. 2 Production of doubled haploid plants derived from immature pollen. (**a**) Callus induction ca. 1 month after microspore isolation. **(b**) Regenerating calli from embryogenic pollen culture

and incubate at 24 °C in dark for two weeks. Finally, transfer the well-developed calli onto fresh regeneration medium in 2-week intervals (Fig. 2). First regenerating plantlets appear after approximately 2 weeks. Analyze doubled haploid plants by PCR and Sanger sequencing to identify the edited allele (Fig. 3).

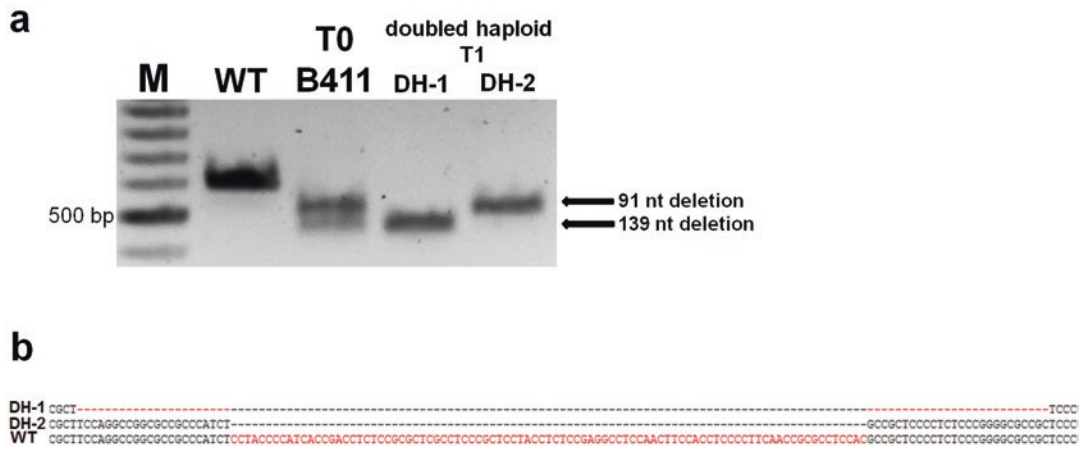

Fig. 3 Analysis of doubled haploid progeny (DH-1 and DH-2) by (**a**) PCR and (**b**) Sanger sequencing. *WT* wild-type. An edited line (B411, shown in lane 3) containing biallelic fragment deletions (one allele with a deletion of 91 nucleotides and a second allele with a deletion of 139 nucleotides) was selected for the generation of doubled haploids. Plants DH-1 and DH-2, shown in lanes 4 and 5, were derived from microspores of B411. DH-1 is homozygous for the 139 nt deletion, and DH-2 is homozygous for the 91 nt deletion

4 Notes

1. L-Cysteine is an antioxidant and prevents tissue culture from browning and oxidation processes.
2. Sterile filtration of medium (instead of sterilization by autoclaving) preserves vitamins and sensitive chemicals.
3. Prepare fresh or store max. Overnight.
4. Solid medium plates can be stored for approximately 1 month at 4 °C.
5. When preparing the K-macro solution measure and dissolve all components separately. Then mix them and add water to the required volume. Finally, sterilize solution by autoclaving.
6. Cefotaxime prevents microspore culture from infections. Its use is optional, but recommended.
7. *Agrobacterium tumefaciens* cultures should not be grown at temperatures exceeding 28 °C, because they might lose their plasmid.
8. Genetic transformation efficiency is strongly influenced by the developmental stage of the isolated barley embryos. The most suitable ones have a diameter of 1.5–2 mm and are transparent in the middle. The radicle and epicotyl axis must be removed using a sterile lancet or needle in order to prevent their germination and to promote callus growth.
9. To achieve optimal grinding of the snap-frozen leaf material precool the containers of the Retsch mill at −80 °C.

10. Pipette carefully in order to avoid the transfer of proteins and cell debris.
11. When amplifying a DNA sequence with high CG content, such as the putative barley ENGase target area, it is recommended to add Q5 High GC Enhancer (5×) to the PCR reaction.
12. When centrifuging microspores the acceleration and deceleration steps should progress slowly.

Acknowledgment

We thank Stanislav Melnik for sequence analysis and Maria Corcuera-Gómez for technical assistance. This work was supported by the Austrian Research Fund FWF (I1461-B16).

References

1. Buchholz F (2009) Engineering DNA processing enzymes for the postgenomic era. Curr Opin Biotechnol 20(4):383–389
2. Hilscher J, Burstmayr H, Stoger E (2017) Targeted modification of plant genomes for precision crop breeding. Biotechnol J 12(1). https://doi.org/10.1002/biot.201600173
3. Bortesi L, Zhu C, Zischewski J, Perez L, Bassié L, Nadi R, Forni G, Lade SB, Soto E, Jin X, Medina V, Villorbina G, Muñoz P, Farré G, Fischer R, Twyman RM, Capell T, Christou P, Schillberg S (2016) Patterns of CRISPR/Cas9 activity in plants, animals and microbes. Plant Biotechnol J 14:2203–2216. https://doi.org/10.1111/pbi.12634
4. Pacher M, Puchta H (2016) From classical mutagenesis to nuclease-based breeding–directing natural DNA repair for a natural end-product. Plant J. https://doi.org/10.1111/tpj.13469
5. Vuylsteker C, Cuvellier G, Berger S, Faugeron C, Karamanos Y (2000) Evidence of two enzymes performing the de-N-glycosylation of proteins in barley: expression during germination, localization within the grain and set-up during grain formation. J Exp Bot 51:839–845
6. Rademacher T, Sack M, Arcalis E, Stadlmann J, Balzer S, Altmann F, Kunert R, Fischer R, Stoger E (2008) Recombinant antibody 2G12 produced in maize endosperm efficiently neutralizes HIV-1 and contains predominantly single-GlcNAc N-glycans. Plant Biotechnol J 6:189–201. https://doi.org/10.1111/j.1467-7652.2007.00306.x
7. Hensel G, Floss DM, Arcalis E, Sack M, Melnik S, Altmann F, Rutten T, Kumlehn J, Stoger E, Conrad U (2015) Transgenic production of an anti HIV antibody in the barley endosperm. PLoS One 10:e0140476. https://doi.org/10.1371/journal.pone.0140476
8. Kapusi E, Corcuera-Gómez M, Melnik S, Stoger E (2017) Heritable genomic fragment deletions and small indels in the putative ENGase gene induced by CRISPR/Cas9 in barley. Front Plant Sci 8:540. https://doi.org/10.3389/fpls.2017.00540
9. Kapusi E, Hensel G, Coronado MJ, Broeders S, Marthe C, Otto I, Kumlehn J (2013) The elimination of a selectable marker gene in the doubled haploid progeny of co-transformed barley plants. Plant Mol Biol 81:149–160. https://doi.org/10.1007/s11103-012-9988-9
10. Tingay S, McElroy D, Kalla R, Feig S, Wang M, Thornton S, Brettell R (1997) *Agrobacterium tumefaciens*-mediatedbarley transformation. Plant J 11:1369–1376
11. Hensel G, Kumlehn J (2004) Genetic transformation of barley (Hordeum vulgare L.) by co-culture of immature embryos with Agrobacteria. In: Curtis IS (ed) Transgenic corps of the world – essential protocols. Kluwer, Dordrecht, pp 35–44
12. Garfinkel DJ, Nester EW (1980) *Agrobacterium tumefaciens* mutants affected in crown gall tumorigenesis and octopine catabolism. J Bacteriol 144:732–743
13. Wang T, Wei JJ, Sabatini DM, Lander ES (2014) Genetic screens in human cells using the CRISPR-Cas9 system. Science 343:80–84

14. Jiang W, Zhou H, Bi H, Fromm M, Yang B, Weeks DP (2013) Demonstration of CRISPR/Cas9/sgRNA-mediated targeted gene modification in Arabidopsis, tobacco, sorghum and rice. Nucleic Acids Res 41(20):e188. https://doi.org/10.1093/nar/gkt780
15. Lazo GR, Stein PA, Ludwig RA (1991) A DNA transformation-competent arabidopsis genomic library in agrobacterium. Biotechnology (N Y) 9(10):963–967
16. Pallotta MA, Graham RD, Langridge P, Sparrow DHB, Barker SJ (2000) RFLP mapping of manganese efficiency in barley. Theor Appl Genet 101:1100–1108

Chapter 3

Vacuolar Sorting Determinants: Isolation and Study

Bruno Peixoto, Susana Pereira, Cláudia Pereira, and José Pissarra

Abstract

As it serves an important function in the compartmentalization of a series of components, from secondary metabolites to proteins, the vacuole is a central organelle in plant cell biology and development. One of the most important mechanisms regulating not only vacuolar biogenesis but also its luminal content, is the vacuolar sorting of proteins. This sorting mechanism is based upon the recognition of specific signal sequences, vacuolar sorting determinants, by sorting receptors, which then act by redirecting vacuolar cargo away from the default secretory pathway, and into the vacuolar lumen. One of the most direct ways of understanding if a given peptide possesses vacuolar sorting determinant capability is to isolate it, fuse it with a marker and express it in a plant system such as *Nicotiana tabacum*, a pipeline which will be described in more detail in this chapter.

Key words *Nicotiana tabacum*, Vacuolar sorting determinants, Fluorescent markers, Trafficking, Vacuole, Endomembrane system, Transient expression

1 Introduction

Vacuoles are multipurpose, ubiquitous organelles present in several eukaryotic systems, including plants. In vegetative tissues they may occupy up to 90% of a cell's total volume, and will have important water and solute storage functions, as well as function as a hydrostatic skeleton for maintaining plant architecture. Vacuolar morphology is known to vary during the cell's life cycle and in response to the plant's environmental conditions and one of the mechanisms behind the modulation of both vacuolar morphology and chemical composition is vacuolar trafficking [1].

Vacuolar trafficking of proteins relies on the interaction between sorting receptor molecules and their target sequences, vacuolar sorting determinants (VSDs). VSDs are peptide sequences that by being capable of interacting with specific cargo receptors become both necessary and sufficient for directing its host protein toward the vacuole. These signal sequences can be classified into three different classes—N-terminal, C-terminal, and internal signals—depending on their localization within the protein [2].

Cláudia Pereira (ed.), *Plant Vacuolar Trafficking: Methods and Protocols*, Methods in Molecular Biology, vol. 1789,
https://doi.org/10.1007/978-1-4939-7856-4_3,

Membrane-bound receptors can recognize and bind to these sorting determinants, in order to redirect soluble proteins from the plasma membrane-directed bulk flow, toward the lumen of the plant vacuole [3].

Recognized signals are typically between 4 and 17 residues long, but some exceptions to this rule exist [2, 3]. Some of these determinants can be easily swapped between different proteins, making them of practical interest for the manipulation of recombinant proteins' subcellular localization. Sequence specific vacuolar sorting determinants (ssVSDs) such as barley's proaleurain NPIR sequence are not amenable to changes in their sequence composition, are generally N-terminally located and can be easily transferred to a novel protein sequence, since they can retain their VSD function even when localized in other regions of the original protein [2, 4]. C-terminal vacuolar sorting determinants (ctVSDs) are not known to have a conserved sequence, provided the constituting residues are hydrophobic in nature and are located at the carboxy-terminus of a peptide, they can maintain functionality. Traditionally, these ctVSDs will direct a given protein to the protein storage vacuole, but they have been known to also direct proteins to the lytic vacuole, when expressed in heterologous systems/tissues [2, 5]. Physical structure VSDs (psVSDs) are commonly found in storage proteins and the residues comprising these determinants are sometimes dependent upon correct three dimensional conformational folding of the protein for proper formation of the final motif, making these determinants particularly hard to predict or manipulate [4, 6, 7].

Currently, in order to characterize a protein's VSDs there are two different complementary approaches that may be employed. The first one is a loss-of-function approach, in which the putative VSD is removed from the original protein sequence through mutagenesis. If the new protein loses its ability to reach the vacuole in a plant system, then it is safe to say that the determinants responsible for its correct vacuolar sorting have been disrupted, either by having been removed, or due to misfolding of the protein.

Another, complimentary approach is the isolation of the putative VSD and its transfer to a fluorescent extracellular marker, such as secmCherry. If this transfer results in a gain-of-function phenotype, in which the marker becomes redirected toward the central vacuole when expressed in a plant system, then it is safe to say that a vacuolar sorting determinant has been identified. In this chapter, the reader will be introduced to this gain-of-function approach, from primer design and construct design, up to the final observation of the fluorescent marker in the confocal laser scanning microscope.

2 Materials

2.1 Integrating a ctVSD in the Reporter Through PCR-Based Approaches

1. *Pfu* DNA polymerase.
2. dNTPs.
3. mCherry-specific primers with ctVSD sequence incorporated in Rev. primer.
4. secmCherry cDNA template.
5. Thermocycler.
6. Restriction enzymes.
7. T4 DNA ligase.
8. Agarose (molecular biology grade).
9. Blunt cloning kit (*see* **Note 1**).
10. Luria Bertani Broth (LB),1% (w/v) tryptone, 0.5% (w/v) yeast extract, 1% (w/v) NaCl, pH 7.0 (autoclaved).
11. Appropriate antibiotics (filter sterilized) (usually stored as 1000x stock solutions).
12. Incubator with shaker and controlled temperature.
13. Agrobacterium-compatible binary expression vector (*see* **Note 2**).
14. *Escherichia coli* DH5α competent cells.

2.2 Transient Expression Assay

2.2.1 Agrobacterium Transformation

1. Temperature controlled shaker/incubator.
2. 250 mL glass flasks.
3. 50 mL conical tubes.
4. Swing-out rotor in conical tube-compatible centrifuge.
5. Spectrophotometer.
6. Ice cold 20 mM $CaCl_2$.
7. Liquid nitrogen.
8. Water bath.
9. Petri dishes.
10. Luria–Bertani broth (LB), 1% (w/v) tryptone, 0.5% (w/v) yeast extract, 1% (w/v) NaCl, pH 7.0 (autoclaved).
11. Appropriate antibiotics (filter sterilized) (usually stored as 1000× stock solutions).
12. 1 M $CaCl_2$ (filter sterilized) (stored at 4 °C).

2.2.2 Nicotiana tabacum Leaf Infiltration Assay

1. Tabletop centrifuge for 1.5 mL micro tubes.
2. Spectrophotometer and compatible plastic cuvettes.
3. Needleless, 1-mL syringes.
4. 10× Infiltration Buffer, 100 mM $MgCl_2$, 100 mM MES (pH 5.6). Filter-sterilize and store at −20 °C in 5 mL aliquots.

5. 1000× acetosyringone: 100 mM 4′-hydroxy-3′,5′-dimethoxyacetophenone in DMSO. Store at −20 °C in 50 μL aliquots. Each aliquot should be thawed only once and used immediately.

2.2.3 Confocal Microscope Analysis

1. Glass slides.
2. Scalpel blades.
3. dH_2O (or another compatible mounting medium).
4. Rectangular coverslips (22 × 50 mm or 22 × 60 mm).
5. (OPTIONAL) Immersion oil (depending on the microscope setup being used).
6. Access to a confocal laser scanning microscope (or fluorescence microscope with appropriate filters).

3 Methods

3.1 VSD Incorporation Through PCR-Based Approaches

1. Start by designing secmCherry-specific primers (Forward and Reverse), and incorporating the putative ctVSD in the reverse primer, just before the stop codon sequence; you may also add appropriate restriction enzyme adapter sequences, flanking the cDNA, to facilitate downstream manipulation of the insert (Fig. 1).
2. Prepare a standard PCR reaction with *Pfu*, or any other proof-reading DNA polymerase, according to the manufacturer's protocol (adjustments may be required, depending on the enzyme used, primers, or product size).
3. Run the totality of the PCR reaction in an agarose gel and cut the band corresponding to the amplicon of the expected molecular size, under UV light (*see* **Notes 3** and **4**).

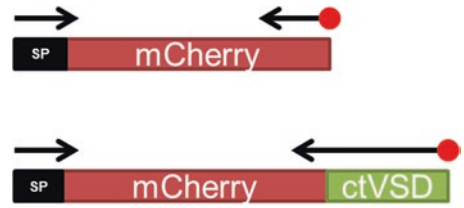

Fig. 1 Using secmCherry as a starting point (and as our negative control), the primers should be designed in a way that the original STOP codon from mCherry is removed, and the ctVSD is introduced in its stead, with a new STOP codon afterward.Control secmCherry should maintain its original signal peptide and STOP codons. The differently colored boxes represent the cDNA segments of the marker constructs, the black colored arrows represent the annealing location for the primers, and the red dot represents the location the STOP codon should be placed. *ctVSD* c-terminal vacuolar sorting determinant, *SP* signal peptide

4. Purify the DNA from the agarose and quantify the final concentration of your preparation.
5. Employ a blunt cloning kit, in order to clone the purified amplicon into a vector backbone (Invitrogen's pCR Blunt® can be used), following the manufacturer's protocol.
6. Transform DH5α competent cells with the resulting ligation, plate in selective LB media and grow overnight at 37 °C.
7. Select 3–5 clones and screen them through miniprep and restriction digest of the obtained DNA; sequence 1–2 positive clones to confirm no undesired mutations were incorporated during PCR or band excision.
8. Select one of the positive sequenced clones for subcloning the insert into the final, binary Agro vector (*see* **Notes 2** and **5**).

3.2 Competent Cell Preparation and Heat Shock Transformation of Agrobacterium

1. Grow Agrobacterium strain in 5 mL LB supplemented with all relevant antibiotics overnight at 28 °C.
2. Add 2 mL of the overnight culture to 50 mL LB in a 250 mL flask (*see* **Note 6**) and shake vigorously (250 rpm) at 28 °C until the culture reaches an OD_{600} of 0.5–1.0 (this will take several hours).
3. Add culture to a 50 mL conical tube, chill on ice for 10 min and centrifuge for 20 min at max speed in a 4 °C swing out rotor centrifuge.
4. Discard the supernatant and resuspend cells in 1 mL of ice cold 20 mM $CaCl_2$. Dispense into pre-chilled 1.5 mL micro tubes, in 50 μL aliquots and store at −80 °C.
5. For transformation, add 500 ng of DNA per 20 μL of competent cells to a 50 μL aliquot of competent Agrobacteria (*see* **Note 7**).
6. Let cells thaw on ice for 10–15 min.
7. Freeze tubes in liquid nitrogen (*see* **Note 8**).
8. Heat shock in a water bath at 37 °C for 5 min.
9. Add 200 μL of LB medium (no antibiotic) to the cells and incubate at 28 °C for 2–4 h, without shaking.
10. Centrifuge at 2500 × *g* for 3 min at room temperature.
11. Discard the supernatant and resuspend the pellet in 200 μL of LB medium (no antibiotics).
12. Spread the entire volume in LB plates supplemented with the appropriate antibiotics, and incubate the plates at 28 °C for 36–48 h.
13. Bacterial clones may be stored as glycerol stocks at −80 °C until required for plant transformation.

3.3 Transient Expression Assay

1. Use the previously stored Agrobacterium clone to initiate a small (5 mL) LB culture supplemented with the appropriate antibiotics. Grow overnight at 37 °C at 180–220 rpm.
2. Transfer 1 mL of the saturated Agrobacterium culture into a 1.5 mL micro tube (*see* **Note 9**).
3. Centrifuge at maximum speed for 1 min and discard the supernatant.
4. Resuspend the bacterial pellet in 1 mL of 1× Infiltration Buffer.
5. Centrifuge as above and discard the supernatant.
6. Supplement the remaining 1× Infiltration buffer with 100 μM acetosyringone and use 1 mL to resuspend the bacterial pellet (*see* **Notes 10–12**).
7. Centrifuge as above and discard the supernatant
8. Resuspend the bacterial pellet once more in 1× Infiltration buffer with 100 μM acetosyringone.
9. After careful homogenization of the bacterial suspension, prepare a 1:5 dilution (200 μL of cells + 800 μL of Infiltration buffer with acetosyringone) in a spectrophotometer cuvette. Measure the optical density of the dilution at 600 nm.
10. Prepare mixtures for infiltration with a final volume of 1 mL, by using the following formula (*see* **Notes 9**, and **13–15**):

$$\left[\left(\frac{\text{Desired OD}_{600\text{nm}}}{\text{Measured OD}_{600\text{nm}}}\right)\times 1000\right]\times\frac{1}{5} = x\mu L \text{ cells / mL infiltration mixture.}$$

11. After careful homogenization of the Agrobacteria infiltration mix, perform infiltration by using a 1 mL needleless syringe and pressing the open tip against the abaxial side of the leaf. You should be able to see the liquid spreading inside the leaf's tissue as you press the plunger (*see* **Notes 16** and **17**).
12. Incubate the plant in the original growth conditions for 2 days before imaging in the confocal laser scanning microscope (*see* **Notes 18** and **19**).

3.4 Laser Scanning Confocal Microscopy Analysis

1. Cut a small fragment of the infiltrated leaf (1 cm^2 is enough), being careful to avoid damaged sections of the leaf or thick veins (*see* **Note 20**).
2. Mount the leaf section on a glass slide, abaxial side facing upward (*see* **Note 21**).
3. Carefully place a drop of water (or mounting media) (*see* **Note 22**) on top of the leaf segment. Holding coverslip by its edges between thumb and forefinger place the bottom edge of the coverslip on the slide as the coverslip forms a 45°

angle with the slide. Slowly lower the coverslip into its position with the help of a dissecting needle (in the other hand) until it touches the mounting medium. Gently remove the dissecting needle, avoiding creating air bubbles in between the sample and the coverslip, as this could create optical artifacts due to refraction.

4. The confocal microscope settings should match your chosen fluorescent marker. Red mCherry emission can be detected between 595 and 647 nm using a 561 nm laser for excitation, but the overall setting may change. It is also important to take photographs of transmission light emission in Nomarski mode differential interference contrast (DIC) to have an idea as to how the tissue was affected by the expression of your sample. Under ideal conditions, the laser power, gain and pinhole settings should be as low as possible, but these settings can all be adjusted to your own particular samples. Figure 2 represents an expected, positive result, if the isolated fragment has VSD capacity.

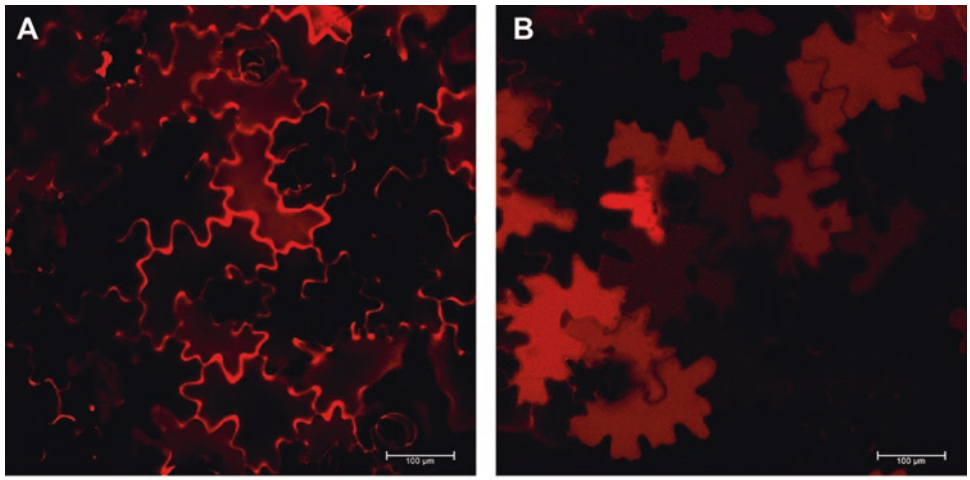

Fig. 2 Illustrative example of expected results of an infiltration of *N. tabacum* with a secmCherry marker (**a**) and secmCherry fused to cardosin A's ctVSD (**b**). It is easily observable that not all cells show the same level of expression, or are even transformed. In case of overexpression there may be leakage of the marker to unexpected "endpoint" subcellular compartments, such as the extracellular compartment or the vacuole. It is thus important to observe a high number of cells and eventually quantify the predominantly marked subcellular compartment, or to test different concentrations of *Agrobacterium* in the infiltration medium. In (**a**), the secmCherry marker clearly marks preferentially the periphery of the "zigzaw puzzle" shaped epidermal cells, whereas its accumulation is shifted toward the lumen of the central vacuole after cardosin A's ctVSD is attached to the marker (**b**)

4 Notes

1. Invitrogen's Zero Blunt® PCR cloning kit can be used, but any similar system should work.
2. The pVK binary vector [8] can be used with its 6×35S promoter system, but many other better annotated alternatives are currently available and may be employed. Depending on promoter strength, the expression protocol may have to be adjusted accordingly (*see* Subheading 3.3).
3. During band excision from the gel, it is important to expose the DNA to the UV illumination for the least amount of time possible, as there is danger of incorporating unwanted mutations in the amplicon during this step.
4. Be aware that some DNA-staining dyes, such as RedSafe, are suspected of interfering with the subsequent cloning protocols. Ethidium bromide is commonly used for these applications. GelRed works well too, but tends to alter band migration patterns.
5. The final expression vector does not need to have a 6x35S promoter driving expression, like the pVK vector does. In fact, too much expression of the fluorescent reporter may result in overloading of the cellular's trafficking system, resulting in mislocalization of the marker and making interpretation of the results nearly impossible. Expression strength may be indirectly controlled by diluting the Agrobacteria concentration in the final infiltration mix (*see* Subheading 3.3).
6. All and every step that requires preparation of competent cells may be upscaled as required but, as a rule of thumb, it is important to remember that the culture volume should not exceed 1/5 of the total vessel volume, to allow for better aeration of the culture.
7. It is usually sufficient to just add 5 μL of miniprep DNA to the frozen bacteria.
8. Alternatively, in case no liquid nitrogen is immediately available, you can also incubate the tubes in the −80 °C freezer for 5 min, followed by immediate immersion of the tubes in the 37 °C water bath.
9. The initial volume of Agrobacterium to be prepared can vary depending on how much plant material you need to infiltrate. For visualization of fluorescent markers the space between secondary veins (side veins) of the leaf will be enough. If protoplasts have to be isolated, or for time-course experiments, half a leaf or more may be required. As a rule of thumb, 1 mL of culture will be comfortable for infiltrating one of these spaces between vascular bundles. If more than 1 mL of Agrobacteria

needs to be prepared, it is better to process them in separate micro tubes, joining them together and homogenizing them only prior to measuring the OD_{600} of the suspension.

10. Acetosyringone aliquots are single-use only, do not freeze them after thawing. Thaw them on ice just before use and use it as freshly as possible. The infiltration buffer should be ice-cool before supplementation with acetosyringone and should always remain on ice from that step forward.
11. To prepare your stock solutions, always prepare a minimum of 50 mL of 1x Infiltration buffer (1 aliquot of 10× stock), which is used for the initial washes of the Agro pellets, and then use a full acetosyringone aliquot (50 μL of 1000× stock) in the remaining volume of 1× buffer. Usually it is not necessary to calculate the few milliliters of buffer that were previously used in the washes, to make sure that the final concentration of acetosyringone is exactly 100 μM, as long as the final volume does not deviate by a huge amount.
12. If for any reason a large amount of 1× Infiltration buffer is prepared unnecessarily, the diluted buffer may be stored again at −20 °C for the next infiltration protocol. Never freeze buffer that was already supplemented with acetosyringone.
13. The same way the initial volume of Agrobacterium can be adjusted, depending on the amount of tobacco leaf to be infiltrated, so should the final amount of infiltration mix be adjusted. As a rule of thumb, 1 mL of final infiltration mix should be enough for comfortably infiltrating the space between secondary veins.
14. The "Desired OD_{600}" value must be assessed experimentally in the first infiltration experiment. Expression of the fluorescent marker will vary a lot depending on the promoter sequences used in the expression vector, the Agrobacterium strain, leaf age and health, or marker size (in amino acids). For trafficking and sorting studies, one thing to avoid is overexpression, as it may result in overloading of the cell's sorting machinery and marker missorting, meaning that for this type of studies "less is more." Using the 6×35S promoter in pVK, GV3101 Agro strain and a small marker, such as a secmCherry with a ctVSD, a final OD_{600} of 0.01–0-05 is usually employed in the infiltration mixture. Larger fluorescent markers, such as an entire protein tagged with a mCherry marker may require this final OD value to go up to 0.3. Ideally, the very first infiltration experiment will be used to assess the ideal Agrobacterium density in the infiltration mix by testing them out experimentally—0.01, 0.05, 0.1, 0.3, and 1.0 may be used as reference values for that test.

15. Co-expression may be achieved by mixing up the different Agrobacteria bearing the different constructs in the final infiltration mix. By using this strategy 2 constructs can be successfully co-expressed simultaneously, but attempting 3 constructs or more is often ineffective. It is important to bear in mind that the transfection process is random, meaning that a pool of cells expressing construct #1, construct #2 and both constructs will occur. Transfection is also not 100% efficient, so some cells may not be expressing any construct whatsoever (This effect may be reduced by increasing the Agro density in the final infiltration mix, but will also result in increasing expression levels per cell, so the ideal density has to be optimized.).
16. During infiltration it is important to cause the least amount of mechanical damage to the leaf as possible. This means that if you can successfully infiltrate a large area of the leaf with only one application of the syringe, you should aim for that. During infiltration, it is easy to see the liquid spreading through the mesophyll, meaning you can have a very good idea if any section of the leaf was not completely infiltrated. Try to avoid these "dry spots," as they will have become invisible by the time of sample collection.
17. As the infiltration mix penetrates the leaf through the open stomata, certain physiological conditions may result in a more impermeable leaf. Tobacco plants should be well watered and young, as this results in easier to infiltrate leaves. If the leaf is still impermeable, one way to force the stomata to open is to leave the plant under intense light for 5–10 min. As a last resort, you may use either the syringe opening or some quartz sand to induce some mechanical damage to the leaf, allowing for easier infiltration.
18. Plants for infiltration experiments can be grown in either continuous light or 16:8 (L:D) photoperiod, 60% humidity and 21 °C, but these conditions may be adjusted to your own experimental requirements as needed.
19. Usually wait a minimum of 48 h prior to imaging, as this allows for infection, expression and sorting of the fluorescent marker all the way to the vacuolar lumen to occur, but the first signs of fluorescence can be visualized as early as 24 h after infiltration. Signal stability may vary according to the fluorescent marker used, but for mCherry it can be detected in the vacuolar lumen as late as 2 weeks after infiltration (although with much lower fluorescence intensity).
20. It is important to note that (a) regions that were not properly infiltrated, (b) regions that were mechanically damaged, and (c) the plant's vascular tissues will not be expressing the fluorescent protein, and may even present some autofluorescence.

A second reason to avoid cutting your sample too close to the leaf's veins is that they increase the sample's thickness, making its observation in the microscope more complicated.

21. There are several reasons why it is important to mount the leaf abaxial side-up, the most important of which is that the transformed tissues are the lower epidermis and the spongy parenchyma of the mesophyll. The absence of trichomes also facilitates imaging, by allowing the transformed cells to be localized more superficially.
22. One very interesting alternative to water as mounting medium is the use of the chemical perfluorodecalin, which was described by Littlejohn and Love [9] as a powerful alternative in the sense that it decreases refraction and increases the depth at which imaging can be performed. The paper cited in this chapter links to a filmed experimental protocol, which may be of use to the budding microscopist.

References

1. Zhang C, Hicks GR, Raikhel NV (2014) Plant vacuolar morphology and vacuolar trafficking. Front Plant Sci 5:476–485
2. Peixoto B, Pereira S, Pissarra J (2016) Plant vacuolar sorting: an overview. In: Cánovas FM, Lüttge U, Matyssek R (eds) Progress in botany, vol 78. Springer International Publishing, Cham, p 67
3. de Marcos LC, Denecke J (2016) Lysosomal and vacuolar sorting: not so different after all! Biochem Soc Trans 44:891–897
4. Neuhaus JM, Rogers JC (1998) Sorting of proteins to vacuoles in plant cells. Plant Mol Biol 38:127–144
5. Pereira C, Pereira S, Satiat-Jeunemaitre B, Pissarra J (2013) Cardosin A contains two vacuolar sorting signals using different vacuolar routes in tobacco epidermal cells. Plant J 76:87–100
6. Jolliffe NA, Craddock CP, Frigerio L (2005) Pathways for protein transport to seed storage vacuoles. Biochem Soc Trans 33:1016–1018
7. Zouhar J, Rojo E (2009) Plant vacuoles: where did they come from and where are they heading? Curr Opin Plant Biol 12:677–684
8. Batoko H, Zheng HQ, Hawes C, Moore I (2000) A rab1 GTPase is required for transport between the endoplasmic reticulum and golgi apparatus and for normal golgi movement in plants. Plant Cell 12(11):2201–2218
9. Littlejohn G, Love J (2012) A simple method for imaging *Arabidopsis* leaves using perfluorodecalin as an infiltrative imaging medium. J Vis Exp 59:e3394. https://doi.org/10.3791/3394

Chapter 4

Vacuole-Targeted Proteins: Ins and Outs of Subcellular Localization Studies

Inês Carqueijeiro, Liuda J. Sepúlveda, Angela Mosquera, Richard Payne, Cyrielle Corbin, Nicolas Papon, Thomas Dugé de Bernonville, Sébastien Besseau, Arnaud Lanoue, Gaëlle Glévarec, Marc Clastre, Benoit St-Pierre, Lucia Atehortùa, Nathalie Giglioli-Guivarc'h, Sarah E. O'Connor, Audrey Oudin, and Vincent Courdavault

Abstract

Accurate and efficient demonstrations of protein localizations to the vacuole or tonoplast remain strict prerequisites to decipher the role of vacuoles in the whole plant cell biology and notably in defence processes. In this chapter, we describe a reliable procedure of protein subcellular localization study through transient transformations of *Catharanthus roseus* or onion cells and expression of fusions with fluorescent proteins allowing minimizing artefacts of targeting.

Key words Vacuole, Tonoplast, *Catharanthus roseus*, *Allium cepa*, YFP, GFP, Protein localization, Vacuolar targeting, Transient transformation, Onion peel, Biolistic

1 Introduction

Studies of protein targeting to plant organelles are intimately influenced by the physiological functions ensured by each of the subcellular compartments, ranging from plastids, nucleus, endoplasmic reticulum, mitochondria, and peroxisomes to vacuoles for instance. For a long time, involvement of vacuoles in the whole cell biology has been hugely underestimated and restricted to sink roles as a direct consequence of their large size reaching up to 90% of the plant cell volume. Over the last 20 years, this erroneous and incomplete vision has evolved. It now appears that vacuoles fulfil a myriad of functions such as turgor pressure maintenance, storage and accumulation of inorganic ions, amino acids, proteins, sugars and secondary

Inês Carqueijeiro, Liuda J. Sepúlveda, and Angela Mosquera contributed equally to this work.

Cláudia Pereira (ed.), *Plant Vacuolar Trafficking: Methods and Protocols*, Methods in Molecular Biology, vol. 1789,
https://doi.org/10.1007/978-1-4939-7856-4_4,

compounds, sequestration and inactivation of toxic compounds, cell homeostasis, signal transduction and plant development, by using a plethora of imported soluble or tonoplast-localized proteins [1–3]. These functional roles are usually attributed in an organ- and/or tissue-dependant manner and can differ throughout development [4]. Furthermore, this vast set of functions can be achieved within the cells either by a single vacuole, by different vacuole types including the lytic vacuoles, the protein storage vacuoles, or even by their fusion in a single hybrid vacuole, adding a supplemental level of complexity to the study of protein vacuolar localization [3, 5–7]. The targeting of soluble proteins to vacuoles is a highly complex process relying on at least two distinct sorting routes that remain only partially characterized. The first one, associated to lytic vacuole sorting, is dependent on sequence-specific sorting determinants (ssVSDs) while the second one dedicated to vacuolar storage proteins involves C-terminal sorting determinants (ctVSDs) [3]. N-terminal determinants have also been reported in plants and usually include a NPIR motif or other NPIR-related sequences such as NXI and LRMP identified in sweet potato sporamin and castor bean 2S albumin or a vacuolar sorting-like sequence (SPIL-) in papain like cysteine proteases [8–11]. In addition, very little is known about the targeting mechanisms of tonoplast proteins except requirement of the (D/E)X_{3-5}L(L/I) motif for some transporters [12–16]. Such complex routes to vacuole and tonoplast constitute the main pitfall to the elucidation of protein subcellular localization studied by overexpression of fluorescent protein (FP) fusions and can lead to protein mistargeting caused by the masking of targeting sequences, due to FP addition at the N- or C-terminal of the investigated proteins. It thus hinders the characterization of the potential involvement of vacuoles in new physiological mechanisms such as plant defence whose vacuoles are recognized actors withal. Indeed, besides storing toxic specialized metabolites such as alkaloids using dedicated import systems, vacuoles may directly contribute to their production by hosting biosynthetic enzymes [17, 18]. Furthermore, vacuoles can be part of complex systems of spatial segregation between phytoanticipins and their activating enzymes such as in the well-known mustard oil bomb system relying on the vacuolar sequestration of myrosinases [19]. Interestingly, this type of organization has also been evolved for other plant specialized metabolites and notably monoterpene indole alkaloids (MIAs) that are synthetized in the Apocynaceae family whose *Catharanthus roseus* (Madagascar periwinkle) constitutes one of the prominent members [20, 21]. *C. roseus* synthesizes more than 130 distinct MIAs that are a part of the chemical arsenal deployed by this plant to face pathogens and pest attacks [22, 23]. Their high biological activities also confer to MIAs valuable pharmaceutical properties such as the antineoplastic vinblastine and vincristine, which were one of the first natural anticancer products to be clinically used, and are still among the most

potent agents used in chemotherapy [24, 25]. Such outstanding properties have stimulated the interest of the scientific community for MIA metabolism and have prompted the elucidation of the MIA biosynthetic pathway in *C. roseus* ultimately leading to the development of bioengineered approaches of MIA production [26–28]. The MIA biosynthetic pathway involves from 30 to 40 enzymes and is highly compartmentalized at the cellular level, by being distributed in at least four different leaf cell types, but also at the subcellular level with no less than seven distinct subcellular compartments hosting MIA biosynthetic enzymes [29]. Within this organization, the vacuole holds a central place by ensuring storage and accumulation of the final MIAs after synthesis in the cytosol and active internalization [30–33]. In addition, vacuoles play a main organizational role by hosting enzymes catalyzing cornerstone steps of MIA biosynthesis based on precursor condensations. This includes for instance peroxidase 1 (PRX1) that carries out the oxidative coupling of vindoline and catharanthine leading to vinblastine/vincristine [18, 34] and strictosidine synthase (STR) that performs the condensation of tryptamine and secologanin to from strictosidine the first and universal precursor of all MIAs [17, 35]. This vacuolar synthesis of strictosidine is highly inducible and can result in a substantial pool of vacuole-sequestered strictosidine. This gives birth to a type of defence process related to the myrosinase/glucosinolate system, the so-called nuclear time bomb mechanism that relies on the massive deglucosylation of strictosidine catalyzed by a nuclear glucosidase yielding to the production of a highly reactive aglycone upon aggressor attacks [17, 23]. As a corollary, the existence of this system also implies that *C. roseus* cells tightly regulate export of strictosidine to the cytosol to ensure the synthesis of downstream MIAs under physiological conditions and to avoid plant cell intoxication. Recent advances demonstrate that such a transport is achieved by tonoplast-localized nitrate/peptide family (NPF) transporter, CrNPF2.9 [36].

Overall the characterization of the central role of the vacuole in synthesis of important specialized metabolites such as MIA, and its role in plant defence, illustrates how important are the firm demonstrations of the vacuolar and/or tonoplastic localizations of proteins to decipher the molecular processes underlying these mechanisms. To this aim, as mentioned above, studying protein subcellular localizations by transiently expressing fusions with FP remains a convenient and efficient approach, albeit potentially suffering from technical issues needing to be alleviated. Here, we describe an optimized procedure of transient expression of FP fusions through a biolistic-mediated transformation of *C. roseus* and onion cells yielding reliable vacuole/tonoplast protein localizations. We notably recommend (1) carrying out experiments on two different cell types to generate complementary data that prove to be required for unequivocal localization and (2) to keep in mind that long time-course of expression as well as minimal amounts of

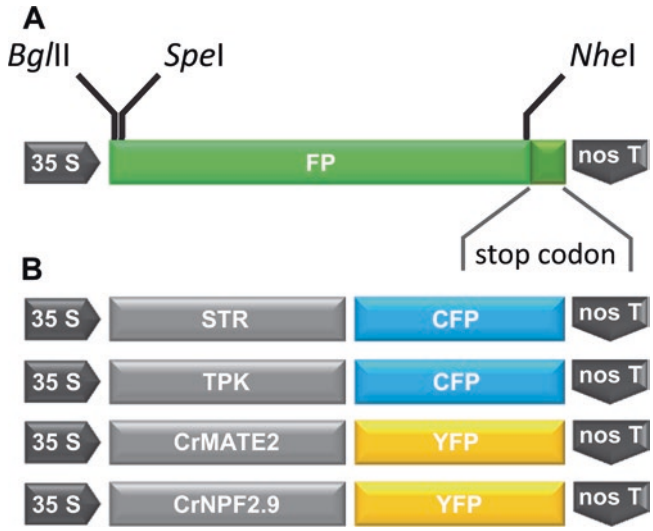

Fig. 1 Scaffold of the expression cassette of the pSCA-cassette series (**a**) allowing cloning of the coding sequence of the investigated protein at the 5′ or 3′ end of the FP coding sequence via the compatible *Spe*I and *Nhe*I restriction sites (**a**). Schematic representation of the cloning strategy used to express the different FP fusions. STR and TPK were fused at the N-terminal of CFP, while CrMATE2 and CrNPF2.9 were fused at the N-terminal of YFP (**b**)

transforming DNA usually provides the best results. We illustrated this procedure with the subcellular localization study of *C. roseus* proteins including STR, CrNPF2.9 and the multidrug and toxic compound extrusion (MATE) proteins CrMATE2 (Fig. 1; [17, 36]) but warrant that this system is versatile enough to study the targeting of proteins from many other plants.

2 Materials

2.1 Plant Material and Culture Medium

1. *C. roseus* suspension cultures (C20A and C20D dark-grown strains), propagated in Gamborg B5 medium (pH 5.5 adjusted with KOH; *see* **Note 1**) supplemented with 15 mM sucrose and 10 μM naphthalene acetic acid (NAA) at 24 °C under continuous shaking (100 rpm). Cells are subcultured every 7 days by adding 5 mL of full growth culture into 45 mL of fresh medium in 250 mL flasks [37, 38].
2. Onion bulbs (*Allium cepa* L.), obtained in a regular organic market and kept at 4 °C in the dark upon transformation (*see* **Note 2**).
3. Walk-in chamber at 25 °C in the dark.

2.2 Constructs

1. Vectors used to generate fusion protein (FP) derived from a pSCA-cassette plasmid (*see* **Note 3**; [39]) harbouring the desired FP (green FP (GFP), yellow FP (YFP), cyan (CFP))

(Fig. 1a). This vector series has been designated to allow the cloning of the coding sequence(s) of the investigated protein(s) at the 5′ or 3′ end of the FP coding sequence using the same PCR product via the compatible restriction sites *Spe*I and *Nhe*I located at each extremity. For cotransformation experiments, we recommend to use the marker set developed by [40].

2. Isolated supercoiled plasmids from *Escherichia coli* cultures (*see* **Note 4**).
3. Set of diverse material needed for the cDNA amplification and FP constructions, primers, thermal cycler, electrophoresis gel system, bench-top centrifuge, UV transilluminator.
4. Conventional material required for *E. coli* manipulation, chemically *E. coli* competent cells (according to [41]), and orbital shaker at 37 °C.

2.3 Cell Transformation by Particle Bombardment

2.3.1 Plating C. roseus Cells and Onion Peels

1. Gamborg B5 medium as described above (*see* Subheading 2.1) with 0.8% (w/v) plant agar and 0.2 mg/L cefotaxime. Pour in small petri dishes (50 × 15 mm) and keep at 4 °C (up to 4–6 months) until use (*see* **Note 5**).
2. Sterile porcelain Büchner funnel maximum content 25 mL, for 40 mm diameter filters.
3. Vacuum pump and Erlenmeyer vacuum flask.
4. Filter paper disc (49 mm) autoclaved.
5. For onion cells: sterile blades, a set of scalpels and forceps (dry heat sterilized).

2.3.2 Pretreatment and Coating of Particles

1. 2.5 M $CaCl_2$ stock solution, autoclaved.
2. 0.1 M spermidine (*see* **Note 6**): prepare a 1 M (w/v) stock solution in water and sterilize by passing through a 0.22-μm filter. Store the solution in small aliquots at −20 °C.
3. 1 μm gold particles.
4. Ethanol (100% and 70%).
5. 50% glycerol (w/v) prepared in sterile conditions.
6. Tabletop centrifuge (16,000 × *g*).
7. Constructs (*see* Subheading 2.2)
8. Water bath sonicator.

2.3.3 Particle Bombardment Procedure

1. Biolistic macrocarriers.
2. Biolistic stopping screens.
3. Biolistic rupture disks 1100 psi.
4. Bio-Rad PDS1000/He delivery system according to manufacturer's recommendations, helium cylinder.

Table 1

Filter set combinations used for fluorescent signal acquisition

Experiment	Fluorochromes emission filters	Filter set name (reference)	Excitation filter (nm)	Emission filter (nm)
YFP/CFP	YFP	JP2 (Chroma#31040)	500–520	540–580 band pass
YFP/CFP	CFP	Cyan GFP (Chroma#31044v2)	426–446	460–500 band pass
GFP/ mCherry	GFP	JP1(Chroma#31039)	460–480	500–520 band pass
GFP/ mCherry	mCherry	Texas Red (Olympus U-MWIY2)	545–580	610 long pass

5. Sterile forceps.
6. Freshly prepared ethanol (100% and 70%).
7. Water sonication bath (50 kH).
8. Parafilm strips.

2.4 Post-transformation Analysis and Image Capture

1. Walk-in chamber at 25 °C in the dark.
2. Epifluorescence microscope armed with a proper light source (mercury short arc HBO or LED) and the specific filter set described in Table 1. The microscope should be equipped with a digital camera (such as Olympus DP71) and a proper imaging software
3. Coverslips (22.32 mm), microscope slides (76 x 26 mm)
4. Sterile sawn-off 20–200 μL micropipette tips; sterile forceps.

3 Methods

3.1 Construct Design and Generation (See Notes 7 and 8)

1. Execute an extensive and careful in silico study of the full-length protein sequence(s) in order to identify potential subcellular sorting signals. Those can be routinely performed with several available bioinformatics tools such as PSORT, TargetP, PredPlant, NLS mapper [42–45]. Alternatively, target sequences may be subjected to Interproscan. Depending on the position of the subcellular sorting signals, design the right orientation for your fusion to avoid any potential masking of the targeting sequences: upstream or downstream of FPs, each configuration should be tested when predictions are not highly confident, or within the protein coding sequence when targeting sequences are located at both extremities (Fig. 1a). In this

example, analysis of the *C. roseus* STR sequence led to the identification of a putative vacuolar/secretory signal peptide at the N-terminal end (1-MANFSESKSMMAV-FFMFFLLLL SSSSSSSSSPIL-35). As a consequence, to maintain access to this sequence, STR was fused at the N-terminal end of FP to generate the STR-CFP fusion protein (Fig. 1b). For *C. roseus* NPF2.9 and MATE2, no highly reliable targeting sequences were retrieved from the prediction analysis except an acidic di-leucine motif involved in tonoplast targeting for NPF2.9 [36] and both types of fusions with YFP were thus designed (Fig. 1b). Nevertheless, specific targeting was only observed with both proteins fused at the N-terminal end of YFP (data not shown). As a tonoplast marker, we used the Arabidopsis two-pore K^+ channel, AtTPK1, fused to CFP (TPK–CFP), which is known to localize to this membrane [46].

2. Proceed with the amplification of the coding sequence of the studied protein(s) by using a high-fidelity DNA polymerase and adapted primers designed with adequate restrictions sites to allow cloning into a pSCA-cassette vector at the selected end of the FP coding sequence. In our particular case, STR primers (STR-for 5′-CTGAGA*ACTAGT*ATGGCAAAC TTTTCTGAATCTAAA-3′ and STR-rev 5′-CTGAG A*ACTAGT*ATGGGATCTAAAGATGATCAGTCC-3′) as well as CrNFP2.9 and CrMATE2 primers were designed with *Spe*I sites to clone each protein sequence upstream or downstream CFP (since *Spe*I is compatible with *Nhe*I—Fig. 1a) and express the STR-CFP and CFP-STR, MATE2-YFP and YFP-MATE2 or NFP2.9-YFP and YFP-NFP2.9 fusions.
3. After cloning into pSCA-cassette vector through classical restriction/ligation procedures, sequence recombinant plasmids to warrant the absence of point mutations. For plant cell transformation, fresh plasmid preparations at a final concentration of 1 μg/μL are recommended.

3.2 Biolistic-Mediated Transformation of C. roseus and Onion Cells

The choice for the most suitable approach to study protein subcellular localizations through FP imaging procedures depends on the need to generate stably or transiently transformed cells. While stable transformations allow long-term studies, this approach is time-consuming and requires up to 2–4 months to select homogenous transformed cell lines rendering stable transformations less compatible with the subcellular localizations of numerous proteins. By contrast, transient transformations enable the rapid generation (12–48 h) of thousands of individual transformants per single transformation experiment allowing rapid determination of protein subcellular localizations and high confidence in targeting determination by simultaneously studying hundreds of independent transformation events. We thus recommend to use this approach to conduct most of protein subcellular localization studies.

Several methods have been described to perform transient transformations including for instance protoplast transformation [47]. Albeit it constitutes a cheap and relatively efficient procedure, cell wall removal during protoplast preparation results in huge cell stresses that can give rise to artefactual localizations caused by the rerouting of the secretory pathway to re-form the cell wall. This context can thus affect final localization of vacuolar proteins and special care should be taken for interpretation of results. *Agrobacterium* infiltration of *Nicotiana benthamiana* leaves also constitutes a powerful method to study protein subcellular localizations at a low cost without lab-intensive manipulations [48, 49]. However, efficient observations of transformed cells require specific leaf mounting and/or equipment such as a confocal microscope and are more difficult to conduct. Finally, biolistic-mediated transient transformation of plant cells constitutes our preferential choice by combining several key advantages. Albeit this approach is by far being the most expensive, it allows efficient transformations of all plant cells with very low amounts of transforming DNA (around 100 ng per particle bombardment) thus avoiding any artefact caused by protein overexpression as described later. Furthermore, except cells located at the centre of the bombarding area, most of FP expressing cells integrates a single particle in the nucleus, which corresponds to a relatively nontraumatic event given the small size of the particle, thus reducing stress-induced mistargeting of proteins. Finally, using cell suspension also enables easier cell mounting and observation. The protocol described below is an adaptation of the procedures developed by [39, 50] and has been initially developed for transformation of *C. roseus* cells.

3.2.1 Preparation of C. roseus Cells for Particle Bombardment

While studying the subcellular localization of proteins in homologous plant cell systems definitely constitutes the ideal condition to avoid any problems of targeting sequence recognition, such a situation is not always technically possible due to unavailability of efficient protocols of transient transformation and/or easy-handling plant material. Our procedure of transformation relying on the bombardment of *C. roseus* suspension cells can therefore be used to study subcellular localizations of proteins from this plant but also provides excellent results for proteins from other plant species such as *Arabidopsis thaliana* [51], *Populus trichocarpa* [52], *Pastinaca sativa* [53], or *Malus domestica* [54].

1. Grow *C. roseus* cells as described in Subheading 2.1.
2. Prepare small petri dishes with 6 mL of Gamborg B5 medium as described in Subheading 2.3.1 (*see also* **Notes 1** and **5**).
3. Three days after subculture of *C. roseus* cells, pour 4 mL of cells onto a sterile filter paper (45 mm diameter) in a sterile filtration funnel (or Büchner funnel) and apply weak vacuum.

Be sure that cells form an uniform thin layer above the filter paper (*see* **Note 9**).

4. Carefully transfer the plated cells onto the petri dish containing solid Gamborg B5 medium. Cover and close the plate with sterile Parafilm strips. Cultivate the cells at 24 °C in dark for 48 h before bombardment.

3.2.2 Preparation of Onion Peels for Particle Bombardment

Confirmation of protein subcellular localization in a distinct plant system can be hugely useful to provide additional evidences of targeting to a dedicated subcellular compartment. Furthermore, it can also be used to demonstrate that localization or protein interactions are independent of the presence of other proteins from the parental plant species when transformation are performed in phylogenetically distant plants [17]. For such type of applications, we recommend to use onion peels since it constitutes an efficiently transformable system allowing easy cell treatment when required.

1. Prepare petri dishes as described in Subheading 2.3.1.
2. Peel the inner layers of onions with sterile razor blades and forceps in laminar flow hood (*see* **Note 2**). Cut peels in 2 × 1 cm parts and place 4–5 cut pieces per petri dish with the inner side facing up. Close plates with ethanol-sterilized Parafilm strips.
3. Transformation can be performed in the week of peel preparation or keep the plates at 4 °C upon transformation up to 2–3 days (*see* **Note 10**).

3.2.3 Pretreatment of Gold Particles

1. Weigh 30 mg of 1 μm gold particles in a glass tube, cover with an aluminium foil and dry heat autoclave for 8 h at 180 °C.
2. In the laminar flow hood, add 1 mL of ethanol 70%, vortex and sonicate for 5 min in a 50 kHz sonication bath (*see* **Note 11**).
3. Transfer the gold particles in 2 mL eppendorf tubes and centrifuge at 16,000 × *g* for 2 s.
4. In the flow hood, remove the supernatant. Wash the beads three times with 1 mL of sterile ultrapure (milliQ) water.
5. Centrifuge at 16,000 × *g* for 2 s and resuspend particles in 500 μL of sterile glycerol 50% (v/v). Keep at −20 °C upon use.

3.2.4 Coating of Transforming DNA onto Gold Particles

As illustrated in Fig. 2, transformation with the higher amount of plasmid expressing CrMATE2-YFP resulted in protein agglutination in endoplasmic reticulum corpuscles since the yield of fusion proteins probably exceeds the capacity of the cell machinery to correctly target the protein to the appropriated subcellular compartment. By contrast, with 150 and 300 ng of transforming plasmids, the CrMATE2-YFP fusion protein is targeted to the tonoplast of a small large vacuole or small multiple vacuoles. For each tested protein, a

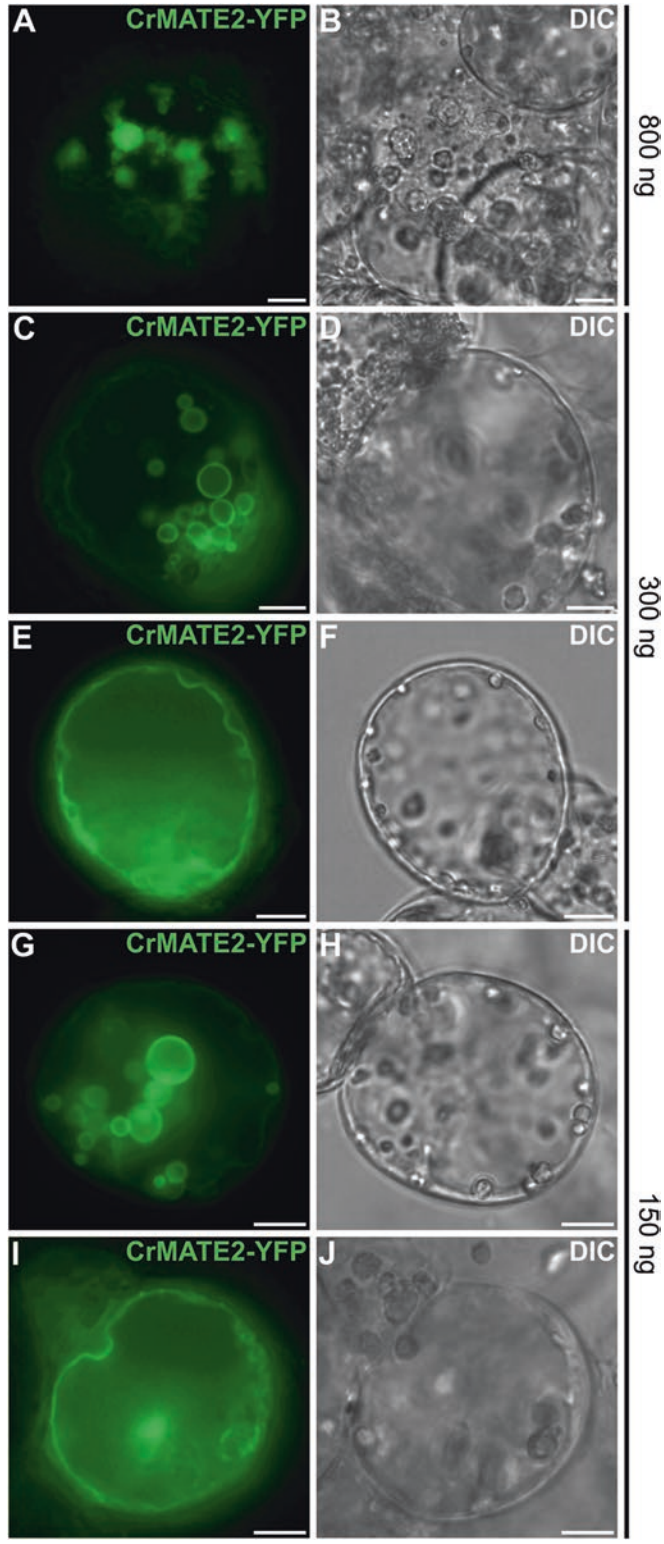

Fig. 2 Impact of the transforming DNA amount on the tonoplast localization of the CrMATE2 transporter fused to YFP (CrMATE2-YFP) in *C. roseus* cells. Cells were transiently transformed with different amounts of the

plasmid concentration range should be tested in order to determine the best experimental conditions. For instance, in the following sections, transformations have been performed with 150–300 ng of plasmids/500 μg of gold particles per transformation for CrMATE2 (Figs. 2 and 5) or with 600–800 ng for STR localization (Fig. 4) in *C. roseus* cells but also 150–300 ng for CrNPF2.9 in onion cells (Figs. 3 and 6).

1. For each petri dish bombardment, we recommend to coat 150–800 ng of the transforming plasmids onto 500 μg of gold particles (roughly 8 μL). A crucial determinant affecting protein targeting, notably for vacuole and tonoplast-targeted proteins, is the amount of transforming DNA used for transfection.
2. Sonicate the glycerol stock of gold particles for 15 min in 50 kHz sonication bath. Homogenize during sonication by vigorous vortexing every 3 min. While vortexing, collect 8 μL of the gold particle solution and transfer to a new 1.7 mL Eppendorf tube. Repeat as many times as planned transformations.
3. Under constant vortex, add 5 μL of 0.1 M spermidine to each 8 μL of gold beads. Vortex and sonicate during 30 s.
4. Under constant vortex, add the proper amount of plasmid(s), 150–800 ng of plasmid expressing the investigated protein and a similar amount of the plasmid expressing a subcellular marker. To maximize the efficiency of coating, let rest at room temperature for 3 min by vortexing each minute (*see* **Note 12**).
5. While vigorously vortexing, add 6 μL of 2.5 M $CaCl_2$, and vortex for additional 15 min at room temperature (*see* **Note 13**).
6. Centrifuge the tube at 16,000 × *g* for 2 s and discard the supernatant under flow hood.
7. Wash the beads with 500 μL of freshly prepared 70% ethanol without affecting integrity of the particle pellet. Discard the supernatant and repeat the washing step with 100% ethanol.
8. Remove supernatant and resuspend the pellet in 10 μL of 100% ethanol by vortexing.
9. Spread the DNA-coated gold particles onto each macrocarrier and allow to total solution drying. Proceed immediately to cell transformation.

Fig. 2 (continued) CrMATE2-YFP expressing construct (provided as supercoiled plasmid) ranging from 800 ng per 500 μg of gold particles (**a**) to 300 ng (**c**, **e**) and 150 ng (**g**, **i**). While a high amount of plasmid (800 ng) leads to mistargeting of the fusion protein appearing as aggregates in the cytosol (**a**), lower amounts (300 or 150 ng) result in a perfect tonoplast targeting in multiples small vacuoles (**c**, **g**) or unique large vacuole (**e**, **i**). Cell morphology (**b**, **d**, **f**, **h**, **j**) was observed with differential interference contrast (DIC). Bars 10 μm

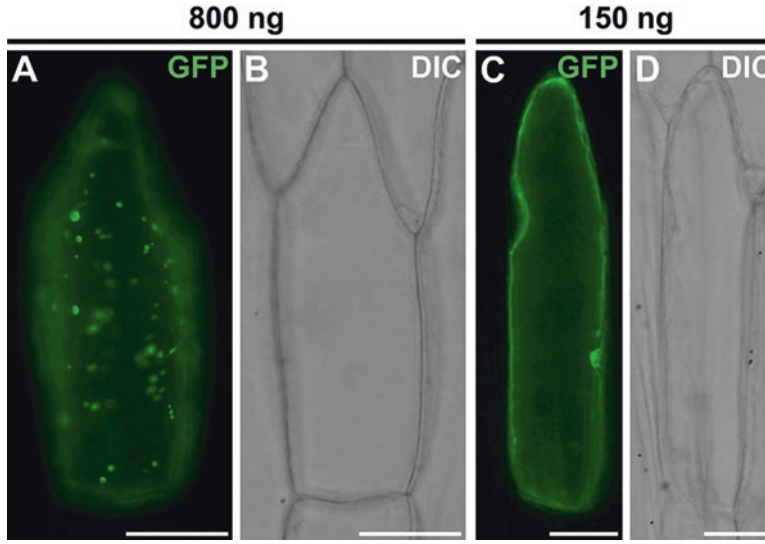

Fig. 3 Impact of the transforming DNA amount on the tonoplast localization of the CrNPF2.9 transporter fused to YFP (CrNPF2.9-YFP) in onion cells. Cells were transiently transformed with either 800 ng of the CrNPF2.9-YFP expressing construct (provided as supercoiled plasmid) per 500 μg of gold particles (**a**) or 150 ng (**c**). While a high amount of plasmid (800 ng) leads to mistargeting of the fusion protein appearing as aggregates in the cytosol (**a**), the lower amount (150 ng) results in a perfect tonoplast targeting. Cell morphology (**b**, **d**) was observed with differential interference contrast (DIC). Bars 50 μm

3.2.5 Particle Bombardment of Plant Cells with a Helium Powered Particle Gun

Transformation of plant cells by particle bombardment is performed with the PDS1000/He device (Bio-Rad), according to the manufacturer's recommendations. For *C. roseus* and onion cell transformations, particle bombardments are performed at a shooting distance of 9 cm with a 1 cm distance-of-flight of the macrocarriers, under pressure vacuum of 28 in. of Hg, using 1100 psi rupture discs.

1. Place the PDS100/He biolistic device in a laminar flow hood and clean all surfaces with 70% ethanol.
2. Sterilize all the biolistic consumables by dipping in 70% ethanol during 15 min: macrocarriers, ring loaders, stopping screens, rupture disks, forceps or tweezers needed to handle and Parafilm strips. Let air-dry until complete evaporation inside the flow hood.
3. After loading and drying of the DNA-coated particle mixture onto macrocarriers, assemble each part of the firing device according to manufacturer's indications: close the gas acceleration tube with a rupture disk, install the macrocarrier in a macrocarrier holder and load in microcarrier launch assembly with stopping screen. Place an open petri dish containing plated cells (*C. roseus* or onion) at 9 cm distance onto the target shelf in the bombardment chamber.

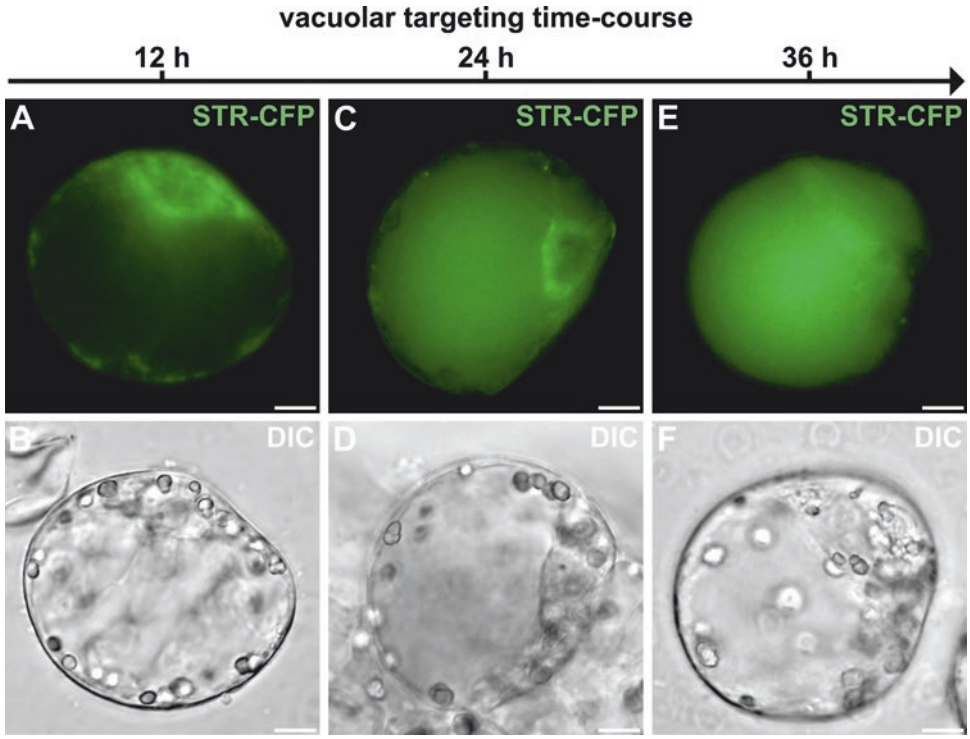

Fig. 4 Time course of the vacuolar targeting of STR-CFP in *C. roseus* cells. Cells were transiently transformed with the STR-CFP expressing construct and the subcellular localization was monitored over 36 h. At 12 h (**a**), the fusion FP was only detected in the endoplasmic reticulum while at 24 h (**c**), the fluorescent signal was observed in both the endoplasmic reticulum and the vacuole. The complete targeting to the vacuole was only achieved after 36 h (**e**). Cell morphology (**b**, **d**, **f**) was observed with differential interference contrast (DIC). Bars, 10 μm

4. Evacuate chamber and hold vacuum at 28 in. of mercury (*see* **Note 14**).
5. Bombard sample by continuously depressing the fire button until rupture disk bursts and helium pressure gauge drops to zero. Close the petri dish and seal with sterile Parafilm strips.
6. Incubate the cells for 1–2 days, in the dark at 25 °C (*see* Subheading 3.2.6; *see* **Note 15**)
7. After determining the amount of plasmid suitable to obtain the best targeting results, one plate for each construct should be enough for image acquisition.

3.2.6 Post-transformation, Observation and Image Acquisition

The right procedure to acquire the best images mainly depends on the FP selected to create fusion and on the microscope equipment, especially when coexpressing two proteins, such as the investigated protein and a subcellular compartment marker, fused with distinct FP. Care should be taken to specifically acquire the fluorescent signal of each FP without cross-fluorescence detection. For the illustrations presented in this work, images were captured with an

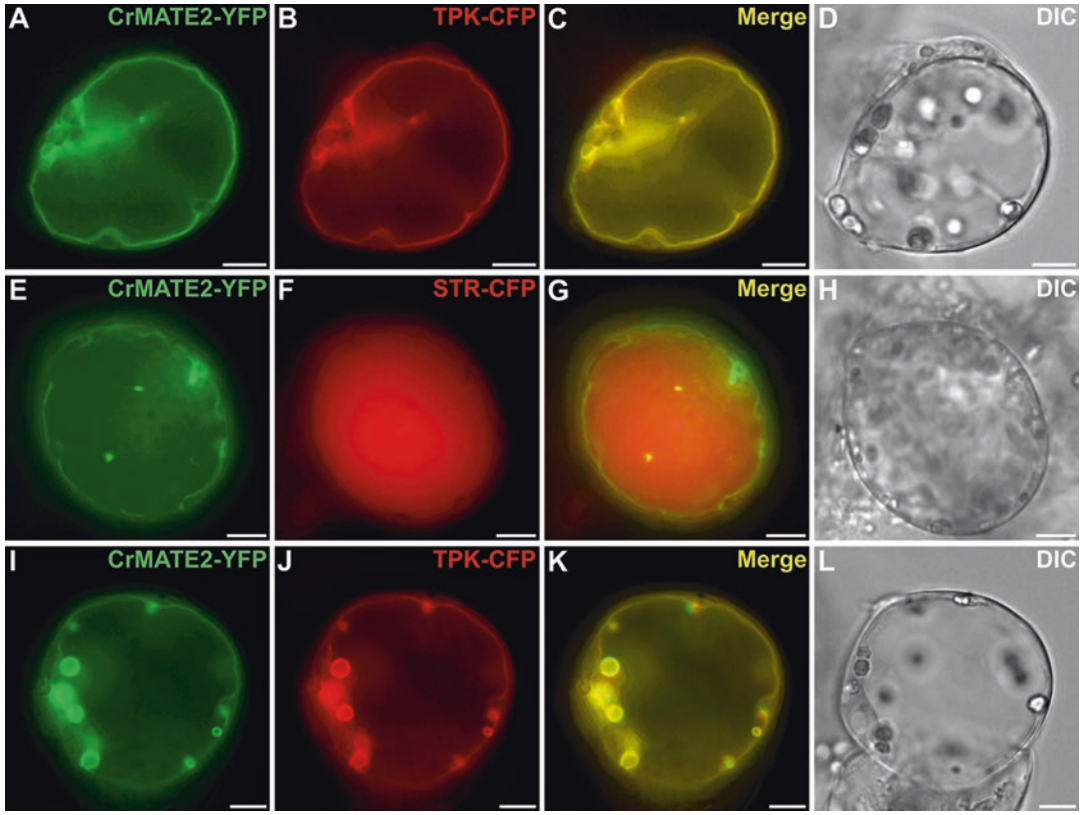

Fig. 5 Validation of the tonoplast localization of the CrMATE2-YFP fusion proteins in *C. roseus* cells. Cells were transiently cotransformed with the plasmid expressing CrMATE2-YFP and the plasmid encoding the tonoplastic AtTPK1 (TPK)–CFP marker (**a**–**b**; **i**–**l**) or the plasmid encoding the vacuolar localized strictosidine synthase (STR–CFP) marker (**e**–**h**). Colocalization of the fluorescence signals appears in yellow when merging the two individual (green/red) false color images (**c**, **g**, **k**). The tonoplast localization of CrMATE2-YFP was observed in either a large single vacuole (**a**) or in small multiple vacuoles (**i**). Cell morphology (**d**, **h**, **l**) is observed with differential interference contrast (DIC). Bars, 10 μm

Olympus BX51 epifluorescence microscope equipped with an Olympus DP71 digital camera and the CellD imaging software (Olympus). For double labelling experiment, we recommend to combine YFP- to CFP-fusions and GFP- to mCherry-fusions with the filter set described in Table 1.

1. Harvest transiently transformed cells from the petri dish with a sterile inoculation loop and resuspend in 500 μL liquid Gamborg B5 medium. Homogenize, deposit on a slide and shield with a coverslip. When cell aggregation occurs and renders image acquisition difficult, protoplasting of transformed cells may be envisaged. The protoplasting treatment (*see* **Note 16**) performed during a short period post-transformation are not likely to interfere with cell localization.

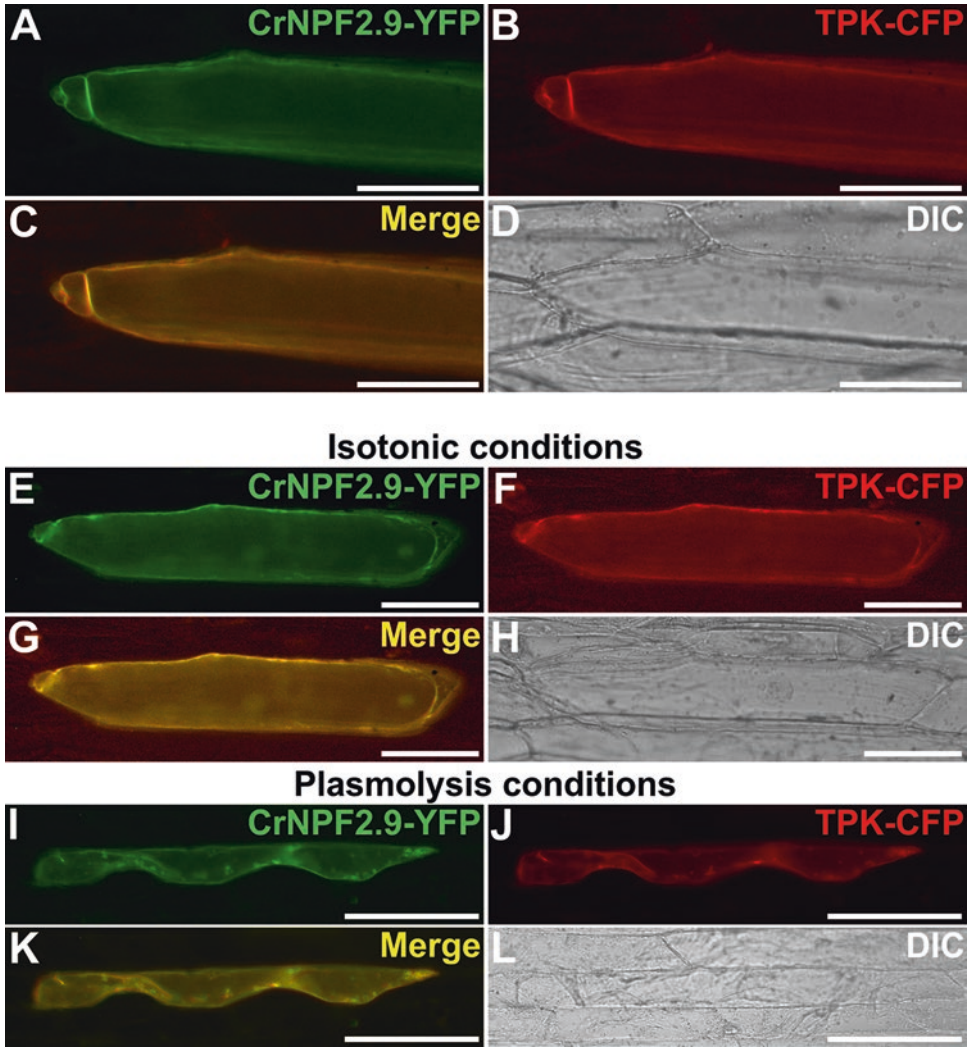

Fig. 6 Validation of the tonoplast localization of the CrNPF2.9-YFP fusion proteins in onion cells by cotransformation with marker and osmotic treatment. Cells were transiently cotransformed with the plasmid expressing CrNPF2.9-YFP and the plasmid encoding the tonoplastic AtTPK1 (TPK)–CFP marker (**a**–**d**; **e**–**h**; **i**–**l**). Colocalization of the fluorescence signals appears in yellow when merging the two individual (green/red) false color images (**c**, **g**, **k**). As compared to isotonic conditions (**a**–**d**; **e**–**h**), plasmolysis (**i**–**l**) induces a similar shift of localization of CrNPF2.9-YFP and TPK-CFP due to tonoplast retraction. Cell morphology (**d**, **h**, **l**) is observed with differential interference contrast (DIC). Bars, 50 μm

2. Harvesting and observation of transiently transformed cells can be performed from 12 up to 72 h post-transformation depending on the subcellular localization of the investigated protein(s). Targeting of vacuolar proteins is usually achieved after 24–48 h as illustrated for STR (Fig. 4). A time-course analysis of the subcellular localization of each new protein is thus recommended.

3. Before beginning image capture, ensure that localization is representative of circa 50–100 observed cells to avoid misinterpretation.
4. For each transformed cell, successively acquire the fluorescent signal of each fusion protein according to the filter set configuration described in Table 1, and illustrate cell morphology with differential interference contrast (DIC) or bright field (Fig. 5). We recommend to acquire fluorescence signals in monochrome and to numerically attribute false colors according to the green/red or green/magenta conventions. Figure 5a–c illustrates the overlay of the fluorescent signal of CrMATE2-YFP (a, i), with that of the tonoplast TPK-CFP marker (b, j) on the merge image (c, k) while CrMATE2-YFP (e) signal remains distinct from the STR-CFP fluorescent located in the vacuole (f) after superimposition (g).

3.2.7 Hypertonic and Hypotonic Conditions (Onion Cells)

Confirmation of the tonoplast localization of a transporter can be obtained by performing osmotic treatments of transiently transformed cells in order to induce membrane contraction (plasmolysis conditions) or relaxation (isotonic or turgescent condition). Such type of treatments usually gives better results by using transformed onion cells (Fig. 6).

1. To induce plasmolysis, prepare a saturated sucrose solution (sucrose 30%) in ultrapure (milliQ) water.
2. Collect transformed onion peels with a forceps and transfer on a slide. Cover with a drop of saturated sucrose solution to induce a plasmolysis, Gamborg B5 medium for isotonic condition or milliQ water for turgidity. Wait for 30 min at room temperature and cover with a glass slip.
3. Acquire images as described in Subheading 3.3.6.

4 Notes

1. As Gamborg B5 is a rich medium that tends to easily get contaminated, it should be autoclaved immediately after preparation, according to classical autoclaving conditions. Auxin, provided as Naphthalene acetic acid (NAA) is prepared as a 100 mg/L (w/v) water stock solution, sterilized by filtration (0.22 μm Pore Size), and kept at 4 °C.
2. Better ratios of transformation efficiency are obtained with organic onions that have not been subjected to pesticides during production or any conservation treatments, and preferentially from the year of production. Better visualization results are also obtained by using white onions versus purple onions since those latter present a higher vacuolar content of anthocyanin that may interfere with observations.

3. A countless number of vectors are now available for expressing fusion proteins with multiple FP variants, under the control of constitutive or inducible promoters. In this report, we mentioned a homemade developed plasmid based on a pSCA scaffold and bearing an expression cassette with the different FP colors, allowing the overexpression of the investigated protein under a constitutive expression CaMV 35S promoter [39]. Depending on the nature of the studied protein and the specificities of the fluorescence microscopy, a proper FP variant and/or proper combination with marker(s) have to be selected. Additional particular care has also to be taken due to the acidic nature of the vacuole, which can reach pH values ranging from 3 to 6, and this, combined with light exposure of GFP expressing cells can rapidly led to GFP degradation [55, 56]. Fluorescent signals of high quality were obtained for mGFP5, YFP, CFP, and mCherry by using our procedure of localization for vacuolar and tonoplastic proteins [17, 50] as exemplified for CFP (Fig. 2). The use of enhanced GFP (eGFP), red FP (RFP) has also been reported for soluble vacuole proteins [57, 58]. Validation of protein localization usually requires a cotransformation of both localization construct and subcellular compartment marker (Figs. 5 and 6). In this case, the choice of suitable and compatible FPs for localization constructs and markers becomes even more crucial, especially when using an epifluorescence microscope, for which an overlap of the excitation spectrum of one FP with the emission spectrum of the second one can alter capture of individual fluorescent signal. Combining yellow FP (YFP) with cyan FP (CFP) or green FP with red FP (RFP) or mCherry circumvents this problem.
4. Checking the integrity of the plasmids used for transformation by analytical electrophoresis gel is mandatory for the success of the procedure. Presence of salts in the plasmid solutions also impairs the efficiency of the transformation. Additional ethanol precipitation can be performed to avoid this trouble.
5. The antibiotic cefotaxime is prepared as a stock solution of 200 mg/mL (w/v) in water, sterilized by filtration (0.22 μm pore size), aliquoted and kept at −20 °C upon use. Cefotaxime is added to the medium after autoclaving and progressive temperature cooldown (around 65 °C) to avoid heat mediated degradation.
6. Spermidine degradation is one of the issues that might decrease cell transformation efficiency. The aliquots should be kept at −20 °C for a short period (few months) and only suffer one cycle of freeze/thaw.
7. The pSCA-cassette plasmid series allows creating protein fusion at both extremities of the FP. Internal fusions can also be created as described in [51].

8. Correct targeting of fusion proteins notably relies on the orientation of the fusion that has to be designed to avoid masking the targeting sequence and the resulting altered localization. Therefore, when the targeting sequence is located at N-terminal end of the protein, fusion should be performed at N-terminal of FP, while in contrast opposite fusion has to be done when targeting sequence is at the C-terminal end [17, 46] You might also consider adding six neutral amino acids (such as arginine) between the sorting signal and the FP to prevent the sandwiched effect and maintain a full accessibility of the sorting signal [46, 56]. For tonoplast localized proteins, less is known about the sequence of sorting signals. In such a case, we advise to test both type of fusions as reported for the *C roseus* transporters described in this work.
9. Use weak vacuum for plating cells to avoid damages or excessive stress. However, ensure to remove all liquid culture medium and that cells cover the entire filter paper surface before transferring in petri dishes.
10. Onion peels can be stored at 4 °C for several days by keeping environment wet enough.
11. Sonicate the beads for 5 min and interrupt with shot vortex-homogenization steps.
12. Higher transformation efficiencies are usually obtained with freshly prepared plasmids. Before proceeding to DNA coating, plasmid integrity should be checked by agarose gel electrophoresis. For cotransformations, the final amount of plasmids should be adjusted. From our experience, we advise to use 200–300 ng of plasmid per transformation (150 ng of each plasmid). The volume of plasmid (both for single or cotransformation) should not exceed the 7 μL per coating mixture.
13. In perfect conditions, you should observe the precipitation of the gold particles after adding the $CaCl_2$ solution.
14. Typically one bombardment per plate is sufficient to generate several thousands of transformants; nonetheless, two bombardments of the same cell plate can be performed for low-expression constructs.
15. Better results are obtained when cells are submitted to dark treatment (16 h to 48 h) prior observations, particularly for soluble proteins localized in the vacuole.
16. The protoplasting method mentioned herein has been described previously [50] and adapted from [59].

Acknowledgments

We gratefully acknowledge support from the University François-Rabelais of Tours and from the "Région Centre-Val de Loire" (France): ABISAL grant, CatharSIS program and BioPROPHARM Project – ARD2020 Biomédicaments). IC was financed by a postdoctoral fellowship from Région Centre Val de Loire. We thank Marie-Antoinette Marquet, Evelyne Danos, and Cédric Labarre (EA2106 BBV) for help in maintaining cell cultures and plants; Emeline Marais and Céline Mélin (BBV) for valuable technical assistance.

References

1. Endler A, Meyer S, Schelbert S et al (2006) Identification of a vacuolar sucrose transporter in barley and arabidopsis mesophyll cells by a tonoplast proteomic approach. Plant Physiol 141:196–207. https://doi.org/10.1104/pp.106.079533
2. Jaquinod M, Villiers F, Kieffer-Jaquinod S et al (2007) A proteomics dissection of *Arabidopsis thaliana* vacuoles isolated from cell culture. Mol Cell Proteomics 6:394–412. https://doi.org/10.1074/mcp.M600250-MCP200
3. Zouhar J, Rojo E (2009) Plant vacuoles: where did they come from and where are they heading? Curr Opin Plant Biol 12:677–684. https://doi.org/10.1016/j.pbi.2009.08.004
4. Martinoia E, Meyer S, De Angeli A et al (2012) Vacuolar transporters in their physiological context. Annu Rev Plant Biol 63:183–213. https://doi.org/10.1146/annurev-arplant-042811-105608
5. Hunter PR, Craddock CP, Di Benedetto S et al (2007) Fluorescent reporter proteins for the tonoplast and the vacuolar lumen identify a single vacuolar compartment in Arabidopsis cells. Plant Physiol 145(4):1371–1382. https://doi.org/10.1104/pp.107.103945
6. Olbrich A, Hillmer S, Hinz G et al (2007) Newly formed vacuoles in root meristems of barley and pea seedlings have characteristics of both protein storage and lytic vacuoles. Plant Physiol 145(4):1383–1394. https://doi.org/10.1104/pp.107.108985
7. Frigerio L, Hinz G, Robinson DG (2008) Multiple vacuoles in plant cells: rule or exception? Traffic 9:1564–1570. https://doi.org/10.1111/j.1600-0854.2008.00776.x
8. Masclaux FG, Galaud JP, Pont-Lezica R (2005) The riddle of the plant vacuolar sorting receptors. Protoplasma 226(3–4):103–108. https://doi.org/10.1007/s00709-005-0117-3
9. Brown JC, Jolliffe NA, Frigerio L et al (2003) Sequence-specific, Golgi-dependent targeting of the castor bean 2S albumin to the vacuole in tobacco protoplasts. Plant J 36:711–719. https://doi.org/10.1046/j.1365-313X.2003.01913.x
10. Nakamura K, Matsuoka K, Mukumoto F et al (1993) Processing and transport to the vacuole of a precursor to sweet potato sporamin in transformed tobacco cell line BY-2. J Exp Bot 44:331–338
11. Paris N, Neuhaus J-M (2002) BP-80 as a vacuolar sorting receptor. Plant Mol Biol 50(6):903–914. https://doi.org/10.1023/A:1021205715324
12. Gattolin S, Sorieul M, Frigerio L (2011) Mapping of tonoplast intrinsic proteins in maturing and germinating arabidopsis seeds reveals dual localization of embryonic TIPs to the tonoplast and plasma membrane. Mol Plant 4:180–189. https://doi.org/10.1093/mp/ssq051
13. Yamada K, Osakabe Y, Mizoi J et al (2010) Functional analysis of an *Arabidopsis thaliana* abiotic stress-inducible facilitated diffusion transporter for monosaccharides. J Biol Chem 285:1138–1146. https://doi.org/10.1074/jbc.M109.054288
14. Larisch N, Schulze C, Galione A et al (2012) A N-terminal dileucine motif directs two-pore channels to the tonoplast of plant cells. Traffic 13:012–1022. https://doi.org/10.1111/j.1600-0854.2012.01366.x
15. Komarova NY, Meier S, Meier A et al (2012) Determinants for Arabidopsis peptide transporter targeting to the tonoplast or plasma membrane. Traffic 13:1090–1105. https://doi.org/10.1111/j.1600-0854.2012.01370.x
16. Wolfenstetter S, Wirsching P, Dotzauer D et al (2012) Routes to the tonoplast: the sorting of tonoplast transporters in Arabidopsis mesophyll protoplasts. Plant Cell 24:215–232. https://doi.org/10.1105/tpc.111.090415

17. Guirimand G, Courdavault V, Lanoue A et al (2010) Strictosidine activation in Apocynaceae: towards a "nuclear time bomb"? BMC Plant Biol 10:182. https://doi.org/10.1186/1471-2229-10-182
18. Costa MMR, Hilliou F, Duarte P et al (2008) Molecular cloning and characterization of a vacuolar class III peroxidase involved in the metabolism of anticancer alkaloids in *Catharanthus roseus*. Plant Physiol 146:403–417. https://doi.org/10.1104/pp.107.107060
19. Kissen R, Rossiter JT, Bones AM (2009) The 'mustard oil bomb': not so easy to assemble?! Localization, expression and distribution of the components of the myrosinase enzyme system. Phytochem Rev 8(1):69–86. https://doi.org/10.1007/s11101-008-9109-1
20. Guirimand G, Courdavault V, St-Pierre B et al (2010) Biosynthesis and regulation of alkaloids. In: Pua E, Davey M (eds) Plant developmental biology – biotechnological perspectives, vol 2. Springer, Heidelberg, pp 139–160. https://doi.org/10.1007/978-3-642-04670-4_8
21. St-Pierre B, Besseau S, Clastre M et al (2013) Deciphering the evolution, cell biology and regulation of monoterpene indole alkaloids. Adv Bot Res 68:73–109. https://doi.org/10.1016/B978-0-12-408061-4.00003-1
22. Parage C, Foureau E, Kellner F et al (2016) Class II cytochrome P450 reductase governs the biosynthesis of alkaloids. Plant Physiol 172:1563–1577. https://doi.org/10.1104/pp.16.00801
23. Dugé de Bernonville T, Carqueijeiro I, Lanoue A et al (2017) Folivory elicits a strong defense reaction in *Catharanthus roseus*: metabolomic and transcriptomic analyses reveal distinct local and systemic responses. Sci Rep 7:40453. https://doi.org/10.1038/srep40453
24. Stanton RA, Gernert KM, Nettles JH et al (2011) Drugs that target dynamic microtubules: a new molecular perspective. Med Res Rev 31:443–481. https://doi.org/10.1002/med.20242
25. Muto A, Atsukol Nakagawa MD et al (2005) Antineoplastic agents for pediatric anaplastic large cell lymphoma: vinblastine is the most effective *in vitro*. Leuk Lymphoma 46(10):1489–1496. https://doi.org/10.1080/10428190500126547
26. Dugé de Bernonville T, Clastre M, Besseau S et al (2015) Phytochemical genomics of the Madagascar periwinkle: unravelling the last twists of the alkaloid engine. Phytochemistry 113:9–23. https://doi.org/10.1016/j.phytochem.2014.07.023
27. Brown S, Clastre M, Courdavault V et al (2015) De novo production of the plant-derived alkaloid strictosidine in yeast. PNAS 112(11):3205–3210. https://doi.org/10.1073/pnas.1423555112
28. Qu Y, Easson MLAE, Froese J et al (2015) Completion of the seven-step pathway from tabersonine to the anticancer drug precursor vindoline and its assembly in yeast. Proc Natl Acad Sci U S A 112(19):6224–6229. https://doi.org/10.1073/pnas.1501821112
29. Courdavault V, Papon N, Clastre M et al (2014) A look inside an alkaloid multisite plant: the Catharanthus logistics. Curr Opin Plant Biol 19:43–50. https://doi.org/10.1016/j.pbi.2014.03.010react-text:72
30. Deus-Neumann B, Zenk MH (1984) A highly selective alkaloid uptake system in vacuoles of higher plants. Planta 162:250–260. https://doi.org/10.1007/BF00397447
31. Blom TJM, Sierra M, Van Vliet TB et al (1991) Uptake and accumulation of ajmalicine into isolated vacuoles of cultured cells of *Catharanthus roseus* (L.) G. Don and its conversion into serpentine. Planta 183(2):170–177. https://doi.org/10.1007/BF00197785
32. Wink M (1993) The plant vacuole: a multifunctional compartment. J Exp Bot 44:231–246
33. Carqueijeiro I, Noronha H, Duarte P et al (2013) Vacuolar transport of the medicinal alkaloids from *Catharanthus roseus* is mediated by a proton-driven antiport. Plant Physiol 162:1486–1496. https://doi.org/10.1104/pp.113.220558
34. Sottomayor M, Lopez-Serrano M, DiCosmo F et al (1998) Purification and characterization of alpha-3′,4′-anhydrovinblastine synthase (peroxidase-like) from *Catharanthus roseus* (L) G. Don. FEBS Lett 428:299–303. https://doi.org/10.1016/S0014-5793(98)00551-1
35. Stevens LH, Blom TJM, Verpoorte R (1993) Subcellular localization of tryptophan decarboxylase, strictosidine synthase and strictosidine glucosidase in suspensioncultured cells of *Catharanthus roseus* and Tabernaemontana divaricata. Plant Cell Rep 12:573–576. https://doi.org/10.1007/BF00233063
36. Payne RME, Xu D, Foureau E et al (2017) An NPF transporter exports a central monoterpene indole alkaloid intermediate from the vacuole. Nat Plants 3:16208. https://doi.org/10.1038/nplants.2016.208
37. Mérillon JM, Doireau P, Guillot A et al (1986) Indole alkaloid accumulation and tryptophan decarboxylase activity in *Catharanthus roseus* cells cultured in three different media. Plant Cell Rep 5(1):23–26. https://doi.org/10.1007/BF00269710

38. Kodja H, Liu D, Mérillon JM et al (1989) Stimulation of indole alkaloid accumulation in suspension cell cultures of *Catharanthus roseus* (G. Don) by cytokinins. C R Acad Sci Life Sci 309:453–458
39. Guirimand G, Burlat V, Oudin A et al (2009) Optimization of the transient transformation of *Catharanthus roseus* cells by particle bombardment and its application to the subcellular localization of hydroxymethylbutenyl 4-diphosphate synthase and geraniol 10-hydroxylase. Plant Cell Rep 28(8):1215–1234. https://doi.org/10.1007/s00299-009-0722-2
40. Nelson BK, Cai X, Nebenführ A (2007) A multicolored set of in vivo organelle markers for co-localization studies in Arabidopsis and other plants. Plant J 51(6):1126–1136. https://doi.org/10.1111/j.1365-313X.2007.03212.x
41. Hanahan D (1983) Studies on transformation of with plasmids. J Mol Biol 166(4):557–580. https://doi.org/10.1016/S0022-2836(83)80284-8
42. Yu NY, Wagner JR, Laird MR et al (2010) PSORTb 3.0: Improved protein subcellular localization prediction with refined localization subcategories and predictive capabilities for all prokaryotes. Bioinformatics 26(13):1608–1615. https://doi.org/10.1093/bioinformatics/btq249
43. Emanuelsson O, Nielsen H, Brunak S, von Heijne G (2000) Predicting subcellular localization of proteins based on their N-terminal amino acid sequence. J Mol Biol 300:1005–1016. https://doi.org/10.1006/jmbi.2000.3903
44. Reumann S, Buchwald D, Lingner T (2012) PredPlantPTS1: a Web server for the prediction of plant peroxisomal proteins. Front Plant Sci 3:194. https://doi.org/10.3389/fpls.2012.00194
45. Kosugi S, Hasebe M, Tomita M, Yanagawa H (2009) Systematic identification of yeast cell cycle-dependent nucleocytoplasmic shuttling proteins by prediction of composite motifs. PNAS 106(25):10171–10176. https://doi.org/10.1073/pnas.0900604106
46. Latz A, Becker D, Hekman M et al (2007) TPK1, a Ca2+-regulated Arabidopsis vacuole two-pore K^+ channel is activated by 14-3-3 proteins. Plant J 52:449–459. https://doi.org/10.1111/j.1365-313X.2007.03255.x
47. Duarte P, Memelink J, Sottomayor M et al (2010) Fusion with fluorescent proteins for subcellular localization of enzymes involved in plant alkaloid biosynthesis. In: Fett-Netto A (ed) Plant secondary metabolism engineering: methods and applications. Methods in molecular biology, vol 643. Springer protocols. Humana, New York, pp 275–290. https://doi.org/10.1007/978-1-60761-723-5_19
48. Ueki S, Magori S, Lacroix B et al (2013) Transient gene expression in epidermal cells of plant leaves by biolistic DNA delivery. Methods Mol Biol 940:17–26. https://doi.org/10.1007/978-1-62703-110-3_2
49. Xu K, Huang X, Wu M et al (2014) A rapid, highly efficient and economical method of Agrobacterium-mediated in planta transient transformation in living onion epidermis. PLoS One 9(1):e83556. https://doi.org/10.1371/journal.pone.0083556
50. Foureau E, Carqueijeiro I, Dugé de Bernonville T et al (2016) Prequels to synthetic biology: from candidate gene identification and validation to enzyme subcellular localization in plant and yeast cells. In: O'Connor S (ed) Synthetic biology and metabolic engineering in plants and microbes part B: metabolism in plants, methods in enzymology, vol 576. Elsevier, Amsterdam, pp 167–206. https://doi.org/10.1016/bs.mie.2016.02.013
51. Guirimand G, Guihur A, Phillips MA et al (2012) A single gene encodes isopentenyl diphosphate isomerase isoforms targeted to plastids, mitochondria and peroxisomes in *Catharanthus roseus*. Plant Mol Biol 79(4):443–459. https://doi.org/10.1007/s11103-012-9923-0
52. Bertheau L, Chefdor F, Guirimand G et al (2012) Identification of five B-type response regulators 1 as members of a multistep phosphorelay system interacting with Histidine-containing Phosphotransfer partners of Populus osmosensor. BMC Plant Biol 12:241–254. https://doi.org/10.1186/1471-2229-12-241
53. Munakata R, Olry A, Karamat F et al (2016) Molecular evolution of parsnip (*Pastinaca sativa*) membrane-bound prenyltransferases for linear and/or angular furanocoumarin biosynthesis. New Phytol 211:332–344. https://doi.org/10.1111/nph.13899
54. Navarro Gallon SM, Elejalde-Palmett C, Daudu D et al (2017) Virus-induced gene silencing of the two squalene synthase isoforms of apple tree (Malus x domestica L.) negatively impacts phytosterol biosynthesis, plastid pigmentation and leaf growth. Planta 246:45. https://doi.org/10.1007/s00425-017-2681-0
55. Tamura K, Shimada T, Ono E et al (2003) Why green fluorescent fusion proteins have not been observed in the vacuoles of higher plants. Plant J 35:545–555. https://doi.org/10.1046/j.1365-313X.2003.01822.x

56. Epimashko S, Meckel T, Fischer-Schliebs E et al (2004) Two functionally different vacuoles for static and dynamic purposes in one plant mesophyll leaf cell. Plant J 37:294–300. https://doi.org/10.1046/j.1365-313X.2003.01958.x
57. Duarte P, Ribeiro D, Henriques G et al (2011) Cloning and characterization of a candidate gene from the medicinal plant *Catharanthus roseus* through transient expression in mesophyll protoplasts. In: Brown G (ed) Molecular cloning-selected applications in medicine and biology. Intech, New York, pp 291–308. https://doi.org/10.5772/23323
58. Pereira C, Pereira S, Pissarra J (2014) Delivering of proteins to the plant vacuole-an update. Int J Mol Sci 15(5):7611–7623. https://doi.org/10.3390/ijms15057611
59. Duarte P, Ribeiro D, Carqueijeiro I et al (2016) Protoplast transformation as a plant-transferable transient expression system. In: Fett-Netto A (ed) Biotechnology of plant secondary metabolism. Methods for field and laboratory, methods in molecular biology, vol 14. Springer protocols. Humana, New York, pp 137–148. https://doi.org/10.1007/978-1-4939-3393-8_13

Chapter 5

Plant Cell Vacuoles: Staining and Fluorescent Probes

Giovanni Stefano, Luciana Renna, and Federica Brandizzi

Abstract

In plant cells, vacuoles are extremely important for growth and development, and influence important cellular functions as photosynthesis, respiration, and transpiration. Plant cells contain lytic and storage vacuoles, whose size can be different depending on cell type and tissue developmental stage. One of the main roles of vacuoles is to regulate the cell turgor in response to different stimuli. Thus, studying the morphology, dynamics, and physiology of vacuole is fundamentally important to advance knowledge in plant cell biology at large. The availability of fluorescent probes allows marking vacuoles in multiple ways. These may be fast, when using commercially available chemical dyes, or relatively slow, in the case of specific genetically encoded markers based on proteins directed either to the membrane of the vacuole (tonoplast) or to the vacuole lumen. Any of these approaches provides useful information about the morphology and physiology of the vacuole.

Key words Vacuole, Vacuole lumen, Tonoplast, Chemical dyes, Fluorescent-tagged vacuolar proteins

1 Introduction

The plant vacuole is one of the largest subcellular compartments, mainly enriched in water, that in some conditions can occupy up to 90% of the total cell volume [1, 2]. The plant vacuoles exist as storage and lytic compartments [3, 4]. Beside a role as water storage compartment, which is a critical element in cell turgor and cell growth processes, the vacuole is also extremely important to accumulate metabolites [1]. The vacuole is also important for seemingly unrelated processes, including photosynthesis. For example, changes in vacuole morphology and size control the aperture or closure of the stomata by guard cells. This in turn modulates CO_2 intake and O_2 extrusion [5, 6], a process that is critical for photosynthesis. Additionally, in CAM-based photosynthesis, vacuoles store CO_2 that is taken up at night and used during the day for photosynthesis. Thus studying how and when the morphology of the vacuole is regulated can provide important clues to understand mechanisms that directly or indirectly drive important processes

Cláudia Pereira (ed.), *Plant Vacuolar Trafficking: Methods and Protocols*, Methods in Molecular Biology, vol. 1789,
https://doi.org/10.1007/978-1-4939-7856-4_5,

including cell expansion, cell growth and photosynthesis [1]. Intriguingly, key mechanisms governing vacuole morphology are yet to be discovered and their identification may be facilitated by the use of fluorescent probes which mark this subcellular compartment in several ways. The probes provide a good degree of flexibility to investigators to study the physiology and morphology of the vacuole as well as cargo traffic to the tonoplast or the vacuole lumen.

As follows, we will describe different vacuolar labeling methods, which can be used for different purposes.

1.1 Chemical Dyes

1.1.1 Neutral Red

Neutral red (NR) (3-amino-7-dimethylamino-2-methylphenazine) is a lipophilic phenazine dye and is considered a nontoxic compound, at least for plant systems [7]. Root growth and cytoskeleton structures (actin and microtubules) are not affected after short NR staining treatment. It is also a relatively inexpensive chemical. The compound penetrates easily through biological membranes and has been used as a vital stain to label vacuoles in plant cells, but also in other organisms like fungi and the lysosomes of animal cells [7] using light microscopy [8]. In its unprotonated form, NR penetrates the plasma membrane and tonoplast. Once inside the vacuole, the fluorescent dye is protonated and trapped (Fig. 1). Although the dye can be used to stain the vacuole, it has also been described to visualize plant structures (such as protoxylem, metaxylem elements, and Casparian bands) [7]. In confocal microscopy analyses, NR can be excited using a 488, 514, or 543 nm laser line; the maximum fluorescence emission is in the range between 550 and 650 nm.

1.1.2 FM4-64

Another dye that can be used to label the vacuole is the lipophilic styryldye,N-(3-triethylammoniumpropyl)-4-(p-diethylaminophenylhexatrienyl) pyridinium dibromide (FM4-64). This dye binds the lipids of the outer leaflet of the plasma membrane, which consists predominantly of phosphatidylcholine, sphingomyelin, and glycolipids. From the plasma membrane, FM4-64 reaches endosomal compartments and ultimately the vacuole [9] (Fig. 1). Because a delay of the dye in reaching the vacuole indicates plasma membrane to vacuole trafficking defects, FM4-64 has been used in mutagenesis screens based on time-course internalization of the dye to identify trafficking elements in yeast [10]. In confocal microscopy, FM4-64 can be excited using 488, 514, 543, and 561 nm laser lines; the maximum fluorescence emission is in the range between 600 and 650.

1.2 Fluorescent-Tagged Vacuolar Proteins

1.2.1 AFVY-RFP

A useful fluorescent marker for the central vacuole is AFVY-RFP, a soluble marker based on the fusion of a monomeric red fluorescent protein (RFP) to the tetrapeptide AFVY, a C-terminal sorting signal of soluble proteins to the vacuole [11] (Fig. 2) (*see* **Note 1**). The fluorescence can be detected using a 560 nm laser line (excitation); the emitted signal can be detected between 560 and 650 nm.

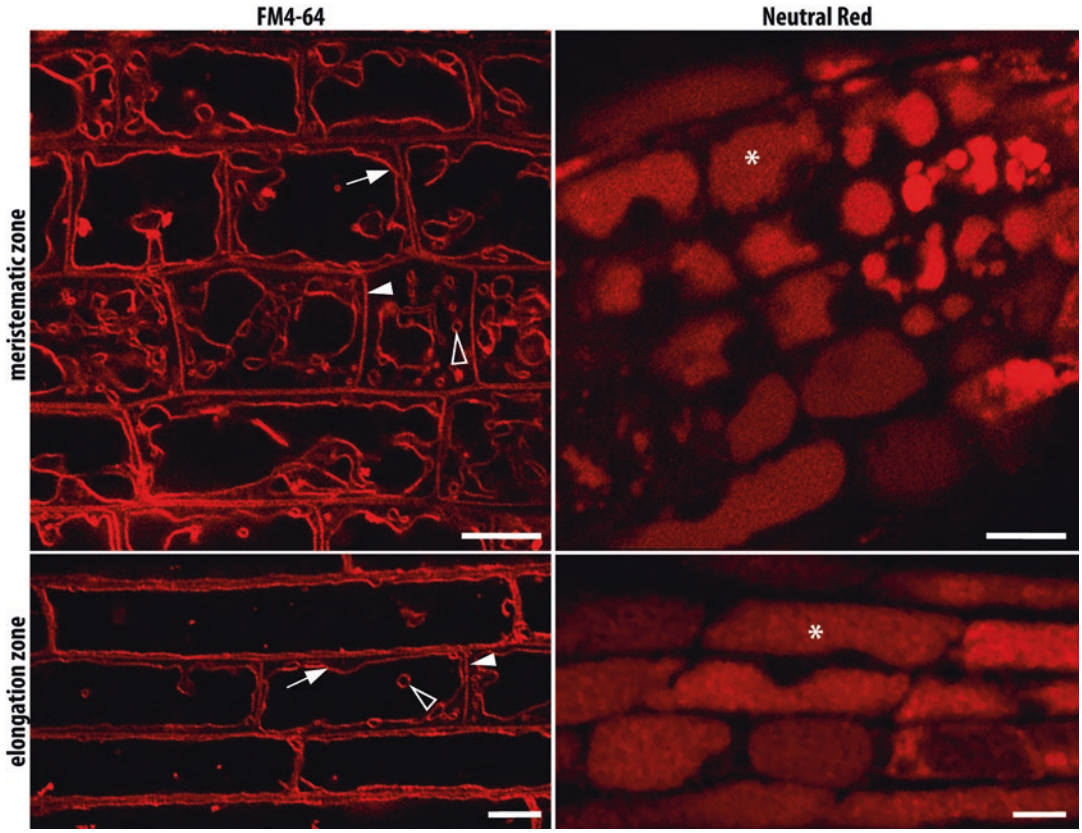

Fig. 1 Staining of vacuoles with fluorescent dyes. (*Left panels*) *A. thaliana* (6 DAG) root seedlings were incubated with FM4-64 (30 min), and observed after 2 h of incubation in ½ LS medium. Arrows indicate tonoplast, empty arrows points to bulbs, and arrowheads point to plasma membrane. Images were acquired with Nikon A1Rsi, using a 514 nm laser as excitation, and fluorescence signal was acquired with filter cube 595/50. (*Right panels*) Confocal images of roots of *A. thaliana* 6 DAG (days after germination) seedlings that were incubated with Neutral Red (15 min) to stain the vacuolar lumen. Asterisk indicates the vacuolar lumen. Imaging was performed with Zeiss LSM510 confocal microscope, using a 543 nm laser as excitation, and fluorescence signal was acquired with filter cube LP560. Bar = 10 μm

1.2.2 VAC-YFP

To mark the tonoplast, various fluorescent-tagged proteins have been used. Here we describe VAC-YFP, a tonoplast marker based on the fusion of the C-terminus of a γ-TIP protein [12] to the yellow fluorescent protein (YFP) (Fig. 2). The fluorescence can be detected using a 488 or 514 nm laser line (excitation) and the emitted signal can be detected between 560 and 600 nm, as previously described [12].

1.3 Additional Fluorescent Vacuolar Markers Available

Among the numerous fluorescent markers used to label the vacuole, two have been used to label either the lytic vacuole (LV), which can be marked by Aleu-GFP [4], or the protein storage vacuole (PSV), which can be labeled using GFP-Chi [13, 14]. Another important marker to mention is δTIP-GFP (tonoplast intrinsic pro-

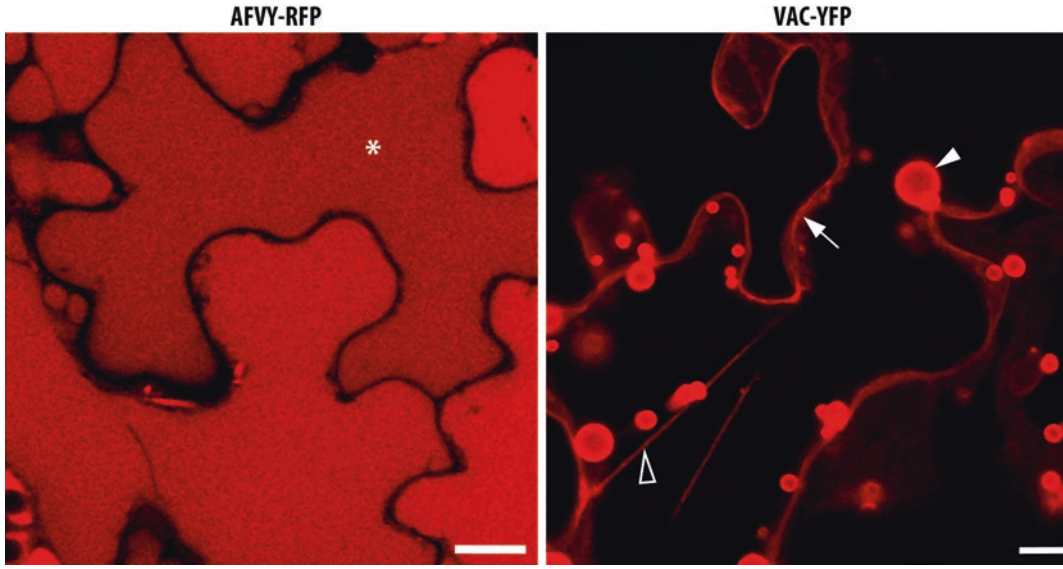

Fig. 2 Staining of vacuoles with fluorescent proteins. (*Left panel*) Confocal images of Arabidopsis abaxial epidermal cells (9 DAG) stably expressing AFVY-RFP, which marks the vacuolar lumen indicated by an asterisk. Imaging was performed with Zeiss LSM510 confocal microscope, using a 543 nm laser as excitation, and fluorescence signal was acquired with LP560 filter. (*Right panel*) VAC-YFP (12 DAG) in abaxial epidermal cells. Arrow points to tonoplast, arrowhead indicates bulbs, and empty arrowhead indicates transvacuolar-strand. A Zeiss LSM510 confocal microscope, with a 514 nm laser as excitation was used, and fluorescence signal was detected with filter cube BP580/40. Bar = 10 μm

tein), a tonoplast fluorescent marker. This marker in the past has been used as tool to screen for vacuolar mutants after ethyl methanesulfonate (EMS) treatment, a chemical inducing nucleotides changes throughout the genome [15]. VAMP711-YFP can also be used to the list of useful markers for tonoplast labelling [16].

2 Materials

2.1 Plant Growth

1. Linsmaier and Skoog medium (LS) plates, with the pH buffered to 5.7 ± 0.2 containing macronutrients, micronutrients, and vitamins. For 1 L of medium (here named 1/2 LS) use 2.35 g of LS, 1% (w/v) sucrose, and 0.8% (w/v) agar, and then autoclave the media for 25 min.

2.2 Preparation of Dye Solution

1. Neutral Red: stock solution of 1 mM in ethanol, keep at −20 °C. Aliquot the stock solution to avoid cycle of thawing and freezing. Protect the dye from light exposure.
2. FM4-64: stock solution of 500 μM in DMSO. Aliquot the stock solution in eppendorf tube an amount equal to 2 μL, then store at −20 °C. Protect the dye from light exposure. Add

500 μL of ½ LS medium to each eppendorf tube containing 2 μL of stock solution to prepare the working solution.

2.3 Stable or Transient Expression of Vacuolar Reporters in Arabidopsis Lines

1. Seeds stratification: LS medium plates. For 1 L of medium (here named 0.25× LS) use 1.18 g of LS, 1% (w/v) sucrose, and 0.8% (w/v) agar, and then autoclave the media 25 min.
2. Cocultivation medium: LS Medium 0.25×, 100 μM acetosyringone, 0.005% Silvet L-77 [17].
3. Wash solution: 10 mM $MgCl_2$ (*see* **Note 2**), 100 μM acetosyringone [17].

2.4 Microscope

Confocal imaging can be performed with a variety of confocal microscopes, including, Zeiss LSM510 META and a Nikon A1Rsi, using a 40×, 60×, or 63× oil objective. Set for each fluorescent probe, the excitation and emission wavelengths as follow:

- For Neutral Red: 543 nm (excitation) and 560–650 nm (emission).
- For FM4-64: 514 nm (excitation) and 600–750 nm (emission).
- For YFP: 514 nm (excitation) and 530–600 nm (emission).
- For RFP: 560 nm (excitation) and 560–650 nm (emission).

3 Methods

3.1 Arabidopsis Root Staining with Neutral Red

1. Stratify *A. thaliana* seeds on ½ LS plate, seal the plate with micropore tape 3M and incubate in a growth chambers from Percival Scientific under standard *A. thaliana* growth conditions (22 °C of temperature, 55% of humidity) in 16 h of light and 8 h of dark cycle.
2. Dispose the plates vertically to image root seedlings or position horizontally to take picture of the abaxial pavemental cells in cotyledon or leaf cells.
3. Use 3–12 DAG Arabidopsis seedlings.
4. Incubate seedlings (a number max of 3 for tube or well) or young leaf (25 mm^2) with 1 μM working solution for 5–15 min (*see* **Note 3**). The seedlings can be incubated directly in an eppendorf tube; if the number of samples to analyze is elevated then a multiwell plate (24 wells) can be used. Add 1 mL of liquid medium for each well used.
5. Add the fluorescent probes to the medium to a final concentration of 1 μm and mix up and down with the pipette.

6. Transfer the seedlings into the eppendorf or multiwell plate containing the medium with the fluorescent probe and incubate for 15–30 min in the dark (*see* **Note 4**).
7. Wash the seedlings by transferring them into a new well supplemented with fresh medium without the probe. Wash the sample at least three times.
8. Place the seedlings on a glass slide and image with a confocal microscope. If you want to image only the root, keep the cotyledons out of the coverslip. In this way you may be able to flatten the sample easily. Vice versa if you want to capture images of cotyledons it possible to cut one cotyledon off the seedling and observe it. Another option is to germinate the seeds directly on plate containing Neutral Red.

3.2 Arabidopsis Root Staining with FM4-64

1. Use 3–9 DAG Arabidopsis seedlings.
2. Incubate the roots (a number max of 3 for tube or well) with 1 μm working solution for 30–45 min (*see* **Note 5**).
3. The seedlings can be incubated directly in an eppendorf tube or a multiwell plate (24 wells) as in Subheading 3.1, **step 2**.
4. Add the fluorescent probes to the medium to a final concentration of 1 μm and mix up and down with the pipette.
5. Transfer the seedlings into the eppendorf tube or well containing the medium with the fluorescent probe and incubate for 30–45 min in the dark (*see* **Note 6**).
6. Wash the seedlings by transferring them into a new well supplemented with fresh medium without the probe. Let the incubation proceed for 1.5–2 h to get a noticeable signal at the tonoplast membrane. Wash the sample at least three times.
7. Place the seedlings on a glass slide and image to a confocal microscope. For sample handling procedures *see* Subheading 3.1, **step 6**.

3.3 AVFY-RFP and VAC-YFP Samples for Confocal Microscopy Analyses

3.3.1 Stable Expression of Genetically Encoded Vacuolar Markers in A. thaliana

1. Sterilize *A. thaliana* seeds expressing the transgene (AFVY-RFP or VAC-YFP), as follow: Pour around 40 seeds in an eppendorf tube, then add 1 mL of ethanol 70%, invert the tube, centrifuge to low speed and discard the solution. Add 1 mL of 20% bleach solution invert the tube few times, centrifuge and discard the liquid by pipette. Wash three times with water then stratify the seeds on plate (LS 0.25× medium) and vernalize at 4 °C for 48 h.
2. Transfer the plates in the growth chamber in a 16 h light and 8 h dark cycle, at 22 °C.
3. Perform confocal microscopy analyses on seedlings starting a 3 days after germination until desired to follow the vacuole marker. Usually, we observe seedlings up to 12 DAG.

3.3.2 Transient Expression of Genetically Encoded Vacuolar Markers in A. thaliana

1. Wild-type *A. thaliana* seeds were sterilized as follow: Pour around 200 seeds in an eppendorf tube, then add 1 mL of ethanol 70%, invert the tube, centrifuge to low speed and discard the solution. Add 1 mL of 20% bleach solution invert the tube few times, centrifuge and discard the liquid by pipette. Wash three times with water then stratify the seeds on plate (LS 0.25× medium) and vernalize at 4 °C for 48 h.
2. Transfer the plates in the growth chamber with 16 h light and 8 h dark, at 22 °C.
3. Two days after germination prepare the cocultivation media. In this way we make sure to use young seedlings with an age of 4–5 days after germination.
4. Three days after germination inoculate the agrobacterium (GV3101) carrying the binary vector with the vacuolar marker of interest, into LB with appropriate antibiotics, shake at 200 rpm, 28 °C until the optical density (OD) read at 600 nm reach a value which is greater than 1.5.
5. Centrifuge the agrobacteria culture at low speed 5000 rpm (2655 × *g*) for 3 min then discard the supernatant.
6. Resuspend the agrobacteria in 10 mL of wash solution by vortex. Repeat the last two steps one more time.
7. Resuspend the agrobacteria pellet in 1 mL of wash solution.
8. Add Agrobacteria to 10 mL of cocultivation media to reach a final optical density of 0.5, then pour the media in the plate.
9. Incubate the plates in the dark for about 24 h.
10. Open the plates remove the media, and wash at least twice with 10 mL of cocultivation media.
11. Seal the plate with micropore 3M and incubate in standard growth conditions.
12. Perform confocal microscopy on cotyledons or root tissue 48–96 h after transformation (*see* **Note 7**).

4 Notes

1. To tag proteins into the vacuole lumen it is suggested to use monomeric RFP because is less sensitive to acidic pH.
2. It is suggested not to autoclave $MgCl_2$, but only sterilize by 0.22 μm filter.
3. The experimental conditions described in this protocol are for young cotyledons (3–12 DAG) and or a young true leaf. It suggested increasing the amount of dye used or the incubation time for older tissues.

4. The incubation time depends on the age of the seedlings: 15 min for 3 DAG root while 30 min for 12 DAG roots.
5. The experimental conditions described in this protocol are for young root seedlings (3–9 DAG). Increasing the amount of dye used or the incubation time will increase the possibility to stain also older tissue.
6. The incubation time depends on the age of the seedlings, 30 min for 3 DAG root while 45 min for 12 DAG seedlings.
7. For transient expression to image a good fluorescent signal into the vacuole or tonoplast it is necessary to observe the sample after 48 h because the signal could be higher in the endoplasmic reticulum before this time.

Acknowledgment

We acknowledge the support by the Chemical Sciences, Geosciences and Biosciences Division, Office of Basic Energy Sciences, Office of Science, US Department of Energy (award number DE-FG02-91ER20021), and the National Science Foundation (MCB1243792).

References

1. Zhang C, Hicks GR, Raikhel NV (2014) Plant vacuole morphology and vacuolar trafficking. Front Plant Sci 5:476
2. Marty F (1999) Plant vacuoles. Plant Cell 11:587–600
3. Paris N, Stanley CM, Jones RL, Rogers JC (1996) Plant cells contain two functionally distinct vacuolar compartments. Cell 85:563–572
4. Di Sansebastiano GP, Paris N, Marc-Martin S, Neuhaus JM (2001) Regeneration of a lytic central vacuole and of neutral peripheral vacuoles can be visualized by green fluorescent proteins targeted to either type of vacuoles. Plant Physiol 126:78–86
5. Gao XQ, Li CG, Wei PC, Zhang XY, Chen J, Wang XC (2005) The dynamic changes of tonoplasts in guard cells are important for stomatal movement in *Vicia faba*. Plant Physiol 139:1207–1216
6. Gao XQ, Wang XL, Ren F, Chen J, Wang XC (2009) Dynamics of vacuoles and actin filaments in guard cells and their roles in stomatal movement. Plant Cell Environ 32:1108–1116
7. Dubrovsky JG, Guttenberger M, Saralegui A, Napsucialy-Mendivil S, Voigt B, Baluska F, Menzel D (2006) Neutral red as a probe for confocal laser scanning microscopy studies of plant roots. Ann Bot 97:1127–1138
8. Schwab B, Hulskamp M (2010) Neutral red staining for plant vacuoles. Cold Spring Harb Protoc 2010(6):pdb.prot4953
9. Bolte S, Talbot C, Boutte Y, Catrice O, Read ND, Satiat-Jeunemaitre B (2004) FM-dyes as experimental probes for dissecting vesicle trafficking in living plant cells. J Microsc 214:159–173
10. Vida TA, Emr SD (1995) A new vital stain for visualizing vacuolar membrane dynamics and endocytosis in yeast. J Cell Biol 128:779–792
11. Hunter PR, Craddock CP, Di Benedetto S, Roberts LM, Frigerio L (2007) Fluorescent reporter proteins for the tonoplast and the vacuolar lumen identify a single vacuolar compartment in Arabidopsis cells. Plant Physiol 145:1371–1382
12. Nelson BK, Cai X, Nebenfuhr A (2007) A multicolored set of in vivo organelle markers for co-localization studies in Arabidopsis and other plants. Plant J 51:1126–1136
13. Fluckiger R, De Caroli M, Piro G, Dalessandro G, Neuhaus JM, Di

Sansebastiano GP (2003) Vacuolar system distribution in Arabidopsis tissues, visualized using GFP fusion proteins. J Exp Bot 54:1577–1584

14. Di Sansebastiano GP, Paris N, Marc-Martin S, Neuhaus JM (1998) Specific accumulation of GFP in a non-acidic vacuolar compartment via a C-terminal propeptide-mediated sorting pathway. Plant J 15:449–457
15. Avila EL, Zouhar J, Agee AE, Carter DG, Chary SN, Raikhel NV (2003) Tools to study plant organelle biogenesis. Point mutation lines with disrupted vacuoles and high-speed confocal screening of green fluorescent protein-tagged organelles. Plant Physiol 133:1673–1676
16. Geldner N, Denervaud-Tendon V, Hyman DL, Mayer U, Stierhof YD, Chory J (2009) Rapid, combinatorial analysis of membrane compartments in intact plants with a multicolor marker set. Plant J 59:169–178
17. Li JF, Park E, von Arnim AG, Nebenfuhr A (2009) The FAST technique: a simplified Agrobacterium-based transformation method for transient gene expression analysis in seedlings of Arabidopsis and other plant species. Plant Methods 5:6

Chapter 6

Vacuolar Targeting and Characterization of Recombinant Antibodies

Carolina Gabriela Ocampo and Silvana Petruccelli

Abstract

Plant-based platforms are extensively use for the expression of recombinant proteins, including monoclonal antibodies (mAbs). Generally, immunoglobulins (Igs) are sorted to the apoplast, which is often afflicted with intense proteolysis. Here, we describe methods to transiently express mAbs sorted to central vacuole in *Nicotiana benthamiana* leaves and to characterize the obtained IgG. Central vacuole is an appropriate compartment for the efficient production of Abs, consequently vacuolar sorting should be considered as an alternative strategy to obtain high protein yields.

Key words Immunoglobulin, N-glycosylation, Vacuolar sorting signals, Secretory pathway, Vacuolar transport, Molecular farming

1 Introduction

The plant vacuole is a multifunctional and dynamic organelle essential for the regulation and maintenance of plant cell growth and development, which share some of their properties with the lysosomes in animal cells [1]. Vacuoles can be divided into two main groups in terms of its functions: protein storage vacuoles (PSV) and lytic vacuoles (LV) [2]. Protein storage vacuoles (PSV) are special compartments found in seeds and specialized tissues, in which large amounts of foreign proteins can be accumulated for long periods in stable form [3]. In contrast, lytic vacuoles (LVs) are specialized in breaking down cellular material destined for degradation [2]. In vegetative tissues, deposition of recombinant proteins in central vacuoles has not been considered adequate for the hydrolytic characteristic expected for this compartment [4]. Nevertheless, several proteins such as avidin, cellulolytic enzymes, endolysin, human transglutaminase, human collagen, glucocerebrosidase, α1-proteinase inhibitor, complement-5a, interleukin-6, and immunoglobulins stably accumulated at high yields in vacuoles of leaves and/or suspension culture cells [5].

Cláudia Pereira (ed.), *Plant Vacuolar Trafficking: Methods and Protocols*, Methods in Molecular Biology, vol. 1789,
https://doi.org/10.1007/978-1-4939-7856-4_6,

Proteins destined to vacuoles are introduced into the plant secretory pathway by mean of a signal peptide and then they can follow different trafficking routes. The conventional transport pathway involves endoplasmic reticulum (ER) export via coat protein complex II (COPII) vesicles followed by Golgi and post-Golgi transport [6]. In addition, a direct transport from the ER to the vacuole, independent of COPII vesicles has also been described [7]. These different trafficking routes will have an impact in foreign protein N-glycosylation pattern [8].

Vacuolar transport requires of positive targeting information since the default pathway is the secretion [9]. Different vacuolar sorting signals (VSSs) have been described: sequence specific (ss) signals consist in the NPIXL or NPIR motif and work independent of its position in the protein sequence. On the other hand, hydrophobic C-terminal signals (Ct) do not have e consensus motif but are always located in the carboxyl-terminus of the protein [2, 10]. Stable accumulation of foreign proteins sorted to vacuole has been obtained by means of both types of VSSs [5]. For example, when the heavy chain of mAb14D9 was fused to the Ct VSS (KISIA) and the ssVSS (NIFRGF) accumulations levels of vacuolar antibodies was 10–15-fold higher than secretory's mAb version [8].

Immunoglobulins (Igs) are usually sorted to the apoplast, in which intense proteolysis often occurs [11–13]. Thus, protein accumulation in other cellular organelles, such as vacuoles, is an alternative strategy used to optimize protein yields, though glycosylation pattern will be dependent of the vacuolar trafficking route [8]. Protein N-glycosylation starts in the ER with the transfer of the oligosaccharide precursor Glc3Man9GlcNAc2 to specific asparagine residues of the nascent polypeptide, this process is follow by a limited glycan trimming in both the ER and Golgi. A subsequent addition of monosaccharides occurs as the protein travel through the Golgi apparatus, to form complex N-glycans, usually GlcNAc2 Man3XylFucGlcNAc2 (GnGnXF) structures [14]. Further modifications include the addition of galactose β-1,3 and fucose α-1,4 linked to the terminal GlcNAc forming the called Lewis A (Le^a) epitope for apoplast proteins [15, 16]. In vacuoles, removal of terminal GlcNAc residues from complex N-glycans results in the formation of paucimannosidic Man3XylFucGlcNAc2 (MMXF) structures [17, 18], however, we have shown that vacuolar sorted immunoglobulin carried mainly oligomannosidic (Man 7-9) followed by GnGnXF forms [8]. In contrast, Ig fused to the ssVSS (NPIRL) of sporamin at N terminus synthesized in transgenic tobacco BY2 cells, showed mainly paucimannosidic MMXF as main N-glycan structure [19]. Therefore N-glycosylation of vacuolar antibodies should be study to be sure that is adequate for the intended application.

This chapter describes optimized protocols for transient expression and purification of vacuolar targeting mAbs in *Nicotiana*

benthamiana leaves. IgG localization, quantification and antigen binding determination, integrity and glycan profile analysis methods are described as well.

2 Materials

2.1 Biological Material

1. *Agrobacterium tumefaciens* GV3101 possess integrated to its chromosome a Rifampicin resistance gen and also harbors a deleted version of pTiC58 called pMP90, from which the entire T-DNA region has been deleted and replaced with a gene conferring resistance to Gentamicin (*see* **Note 1**).
2. *Nicotiana benthamiana*: plants grown for 6–8 weeks in a growth chamber at 22 °C in a 16-h-light/8-h-dark cycle.

2.2 Buffers, Solutions and Reagents

All solutions are prepared using *Milli-Q ultrapure water* and analytical grade reagents. Unless indicated otherwise, all reagents are at RT.

1. *Bacteria medium*: Yeast Extract–Beef extract, YEB (1 L): 5 g of beef extract, 1 g of yeast extract, 5 g of tryptone, 5 g sucrose, 2 mL $MgSO_4$ 1 M. Sterilize by autoclave.
2. Kanamycin sulfate: Dissolve 50 mg in 1 mL of sterile H_2O to obtain a 1000× stock solution. Store at −20 °C.
3. Gentamicin: Dissolve 50 mg in 1 mL of sterile H_2O to obtain a 1000× stock solution. Store at −20 °C.
4. Infiltration buffer: 10 mM $MgCl_2$, 10 mM 2-(N-morpholino) ethanesulfonic acid (MES), 200 μM acetosyringone. Adjust to pH 5.6 with NaOH 1 N.
5. Extraction buffer: 1.5 M NaCl, 1 mM EDTA, 45 mM Tris, 40 mM ascorbic acid, pH 7.4. Prepare a fivefold extraction buffer without ascorbic acid and store at 4 °C. Dilute to 1× and add ascorbic acid prior to use, adjust to pH 7.4 with NaOH (*see* **Note 2**).

2.3 SDS-PAGE

1. Sodium dodecyl sulfate (SDS) solution: SDS prepared a 10% (w/v) stock solution. Stored at room temperature (RT).
2. 4× Stacking Gel Buffer: 0.5 M Tris–HCl (pH 6.8), 0.4% SDS. Store at 4 °C.
3. 4× Separating Gel Buffer: 1.496 M Tris–HCl (pH 8.9), 0.4% SDS. Store at 4 °C.
4. 4× SDS-PAGE Sample Buffer: 1 M Tris–HCl (pH 8), 2% SDS, 50% (v/v) glycerol, 0.15% (w/v) bromophenol blue, 5% β-mercaptoethanol. Prepare the buffer without β-mercaptoethanol and store at 4 °C. Add β-mercaptoethanol prior to use.

5. 5× SDS-PAGE Running Buffer: 125 mM Tris–HCl, 0.95 M Glycine, 1% SDS. Adjust to pH 8.3. Store at 4 °C.
6. Ammonium persulfate: Prepare a 10% (w/v) stock solution. Fractionate 500 μL aliquots and store at −20 °C.
7. Polyacrylamide solution: Prepare a 30% (w/v) acrylamide, 0.2% (w/v) bis-acrylamide solution. Filtrated through 0.45 μm filter. Handle with care, since both components are neurotoxins. Store at 4 °C in a bottle wrapped with aluminum foil (*see* **Note 3**).
8. *N*,*N*,*N*,*N*′-tetramethyl-ethylenediamine (TEMED): Store at 4 °C.
9. Gel Staining Solution: 0.1% (w/v) Coomassie Brilliant Blue R250, 50% (v/v) Methanol and 16% (v/v) glacial acetic acid in H_2O. Filtrate. Store at RT.
10. Destain Solution: 25% (v/v) Ethanol (*see* **Note 4**) and 10% (v/v) glacial acetic acid in H_2O. Store at RT.

2.4 In-Gel Digestion

1. Gel destaining: Prepare a 50% (v/v) Acetonitrile solution.
2. Neat acetonitrile.
3. 50 mM ammonium bicarbonate buffer.
4. 100 mM ammonium bicarbonate buffer.
5. 10 mM dithiothreitol (DTT) solution: Dissolve DTT in 100 mM ammonium bicarbonate buffer.
6. 55 mM iodoacetamide solution: Dissolve iodoacetamide in 100 mM ammonium bicarbonate buffer.
7. Trypsin solution: 1:6 dilution of 100 ng/μL trypsin in 25 mM NH_4HCO_3 solution.
8. 5% (v/v) Formic acid.

2.5 LC-ESI-MS Measurement

1. Solvent A: 65 mM ammonium formate buffer. Adjust to pH 3.0 with 25% NH_4 solution. Degas either by vacuum or by treatment in an ultrasonic bath (at least 10 min).
2. Solvent B: HPLC-grade acetonitrile. Degas in an ultrasonic bath (at least 10 min).

2.6 Western Blot

1. 5× FastBlot Buffer: 125 mM Tris–HCl (pH 8.3), 0.75 M glycine, 20% (v/v) methanol. Prepare the solution without methanol. Store at 4 °C. Dilute to 1× and add the methanol prior to use.
2. 10× Phospate Buffered Saline (PBS): 1.37 M NaCl, 27 mM KCl, 100 mM Na_2HPO_4, 10 mM KH_2PO_4. Adjust to pH 7.4 with HCl. Store at 4 °C.

Table 1
Antibodies and dilutions used in our laboratory

Assay	Primary antibody	Secondary antibody
RFP fusion	Rabbit anti-RFP antibody (1/1000)	Biotinylated goat anti-rabbit antibody (1/20,000)
Antibody chains integrity	Biotinylated goat anti-mouse antibody (1/3000)	–

3. Ponceau S Red: 0.2% (w/v) Ponceau S Red, 5% (v/v) acetic acid (*see* **Note 5**) in H_2O.
4. Blocking Buffer: PBS supplemented with 5% (w/v) nonfat dry milk.
5. Antibody Dilution Buffer: PBS supplemented with 1% (w/v) nonfat dry milk.
6. Antibodies: Dilutions used for each assay are given in Table 1.
7. Luminol: 0.2 mg Luminol/5 µL DMSO. Prepare the solution in the moment. Store at −20 °C (*see* **Note 6**).
8. p-Coumaric acid: 0.15 mg p-coumaric acid/10 µL DMSO. Prepare the solution in the moment. Store at −20 °C (*see* **Note 7**).
9. Chemiluminescent solution A: 5 µL Luminol, 2.2 µL p-coumaric acid, 33 µL 5× separation gel buffer, and 470 µL H_2O. Prepare prior to use.
10. Chemiluminescent solution B: 3.3 µL H_2O_2, 33 µL 5× separation gel buffer, and 470 µL H_2O. Prepare prior to use.
11. Antibodies dilutions commonly used are described in Table 1.

2.7 Enzyme-Linked Immunosorbent Assay (ELISA)

1. Blocking Buffer: PBS supplemented with 3% (w/v) nonfat dry milk.
2. Antibody Dilution Buffer: PBS supplemented with 1% (w/v) nonfat dry milk.
3. Antibodies: goat anti-mouse antibody specific to LC and to HC.
4. Tetramethylbenzidine (TMB) peroxidase substrate.

2.8 Microsome Insolation

1. 1.5× High Density Extraction Buffer: 150 mM Tris–HCl, 37.5% (w/w) sucrose, 5.7% (v/v) glycerol, 15 mM EDTA, 15 mM EGTA, 5.7 mM KCl, and 1.5 mM DTT. Adjust to pH 7.5. Store at −20 °C.
2. Wash Buffer: 20 mM Tris–HCl (pH 7.5), 5 mM EDTA, and 5 mM EGTA.

2.9 Special Equipment

1. Greenhouse or plant growth chamber with controlled temperature, photoperiod, and humidity.
2. Incubator (28 or 37 °C) with horizontal shaker.
3. Spectrometer and plate lector.
4. Vacuum concentrator.
5. Reversed-phase LC column: BioBasic C18, 5 μm particle size, 0.32 × 150 mm (ThermoScientific).
6. LC-ESI-MS system: Q-TOF Ultima Global mass spectrometer (Waters Corporation, MA, USA).
7. Centrifuge: Refrigerate Hermle z326k centrifuge with 1.5-mL tube and 15- or 50-mL Falcon tube rotor.

3 Methods

3.1 Agroinfiltration

1. Inoculate YEB medium (*see* **Notes 8** and **9**) with the agrobacterium carrying LC, HC; LC-FP and HC-FP constructs (Fig. 1), ER-GFP and silencer suppressor P19. Add the corresponding antibiotics to the liquid medium. Incubate overnight at 28 °C and 200 rpm.
2. Harvest bacterial cells by centrifugation at 5000 × *g* for 5 min at RT.
3. Carefully discard supernatant and resuspend the pellet in 1–3 mL of infiltration buffer by carefully pipetting up and down.
4. Measure the optical density at 600 nm (OD_{600}).

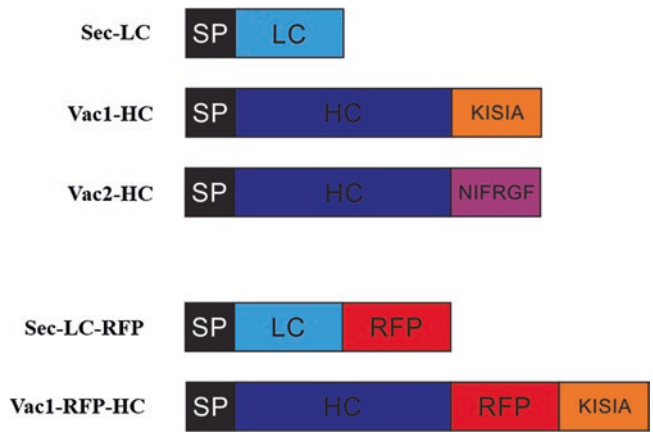

Fig. 1 Schematic representation of the 14D9 antibody constructions used for *Agrobacterium tumefaciens*-mediated transient expression in *Nicotiana benthamiana* leaves. *SP* murine signal peptide, *LC* light chain, *HC* high chain, *RFP* red fluorescent protein, *KISIA* Ct-VSS, *NIFRGF* ss-VSS

Table 2
Amount of agrobacteria used in leaf infiltration

Assay	Construct	OD_{600}
Antibody purification Microsome isolation	Sec-LC	0.6
	Vac1-HC	0.6
	Vac2-HC	0.6
Subcellular localization	Sec-LC-RFP	0.1
	Sec-LC	0.1
	Vac1-HC	0.3
	Vac2-HC	0.3
	Vac1-HC-RFP	0.3

5. Mix the necessary volumes of resuspended agrobacteria to obtain the desired OD_{600} for each construction and fill up with infiltration buffer to the final volume needed. The values used in our laboratory for each assay are given in Table 2.
6. Infiltrate onto the lower epidermal surface of leaves using a 1 mL needleless plastic syringe applying gentle pressure (*see* **Note 10**).
7. Grown plants for 5 days before harvest (*see* **Note 11**).
8. Proceed to section 3.2 for immunoglobulin purification for glycan analysis, to section 3.5 for antibody quantification and hapten recognition assays, and to section 3.4 for confocal microscopy analysis.

3.2 Immunoglobulin Purification

All the steps were performed at 4 °C unless indicated otherwise.

1. If needed, weight the leaf material and frozen at −80 °C or proceed immediately.
2. Ground 10 g of agroinfiltrated leaves until a fine powder with mortar and pestle in liquid N_2.
3. Extract the soluble proteins with extraction buffer for 15 min at 4 °C with agitation in a 1 mL of buffer per 1 g of fresh leaf.
4. Centrifuge the extracts three times at 10,000 × *g* for 10 min at 4 °C (*see* **Note 12**).
5. Incubate the supernatant with 2 μL of Protein G Sepharose with gentle agitation for 1 h 30 min at 4 °C.
6. Pass the extract through a Micro Bio-Spin column (*see* **Note 13**).
7. Wash the column three times with 800 μL of extraction buffer without ascorbic acid or PBS.

8. Elute adding 50 μL of SDS-PAGE sample buffer and heating at 95 °C 5 min (*see* **Note 14**). Centrifuge at 500 × *g* 1 min.
9. Store at −20 °C or use immediately. Proceed to Subheading 3.6.

3.3 Microsome Isolation

All steps were performed at 4 °C unless indicated otherwise.

1. Ground 200 mg (~20 leaves discs) with ice-cold 200 μL of 1.5× high-density extraction buffer (*see* **Note 15**) and a tip of spatula of polyvinylpolypyrrolidone (PVPP).
2. Centrifuge at 600 × *g* for 5 min. Collect the supernatant in a new tube.
3. Reextract the pellet with 100 μL of ice-cold 1.1× high-density extraction buffer.
4. Repeat **step 2**.
5. Reextract the pellet with 67 μL of ice-cold 1× high-density extraction buffer.
6. Repeat **step 2**.
7. Put all the supernatant together and centrifuge at 600 × *g*.
8. Calculate the final sucrose concentration in the homogenate and dilute to a 12% (w/v) sucrose concentration.
9. Fractionate the sample in 200 μL aliquots (*see* **Note 16**) and centrifuge at 21,000 × *g* for 2 h.
10. Keep the supernatant as the soluble fraction.
11. Wash the pellet with 150 μL of wash buffer and centrifuge at 21,000 × *g* for 45 min.
12. Resuspend the pellet in 100 μL of SDS-PAGE sample buffer.
13. Store at −20 °C or use immediately. Proceed to Subheading 3.6.

3.4 Confocal Microscopy

1. Cut out a small square (0.5 × 0.5 cm) from the agroinfiltrated region of the leaf.
2. Place the square in a microscope slip with the lower epidermis facing upward.
3. Mount the leaf square with water or perfluorodecalin (*see* **Note 17**). Put a cover slip on top of the leaf.
4. Follow standard confocal microscopy procedure. The parameters used for our laboratory are described in Table 3.
5. Agroinfiltrated leaves could be store at −80 °C or used immediately. Proceed to Subheading 3.5 for fusion integrity analysis.

3.5 Total Protein Extraction

All steps were performed at 4 °C unless indicate otherwise.

1. Ground leaves in extraction buffer. Extract for 15 min.
2. Centrifuge at 10,000 × *g* for 20 min.

Table 3
Confocal microscopy parameters

Fluorophore	Laser	Laser Intensity	Excitation (nm)	Detection (nm)
RFP	HeNe 1.5 mW	54%	543	570–630
GFP	Argon 100 mW	24%	480	496–532

3. Measure soluble protein concentration in the supernatant using Bradford assay (*see* **Note 18**).
4. Store at −20 °C or use immediately. Proceed to Subheading 3.6 to fusion integrity analysis or to Subheading 3.12 to immunoglobulin quantification and Subheading 3.13 to hapten recognition assay.

3.6 SDS-PAGE

1. Clean the glasses.
2. Assemble the mini-gel system according to your model. Make sure it stands on a flat surface.
3. Prepare the monomer solution for a 12.5% gel by combining the following volumes in a 15 mL Falcon tube: 2.5 mL 5× separating gel buffer; 4.1 mL polyacrylamide solution; 50 µL persulfate solution; 10 µL TEMED; and 3.4 mL H_2O. Mix well.
4. Immediately pour the monomer solution between the glasses (*see* **Note 19**).
5. Prevent exposure to oxygen by adding 70% (v/v) ethanol on top of the monomer mix.
6. Allow gel to polymerization for about 30 min (*see* **Note 20**).
7. Remove ethanol.
8. Prepare the stacking gel solution in a 15 mL Falcon tube: 650 µL 4× stacking buffer; 0.4 mL polyacrylamide solution; 20 µL persulfate solution; 5 µL TEMED; and 1.5 mL H_2O. Mix well.
9. Immediately pour the stacking solution on top of the polymerized running gel.
10. Allow polymerization for about 30 min.
11. After removing the gel sandwich from the casting stand, install the gel according to the instructions, specific to your model. Remove the comb carefully.
12. Fill the lower and upper buffer chambers with 1× running buffer.
13. Load molecular weight markers and your samples into the lanes (*see* **Note 21**).

14. Run the gels using 15 mA constant current per gel in the stacking zone and 25 mA in the running zone. The run is complete when the blue dye front reaches the bottom of the gel.
15. Disassemble the gel sandwich and remove the stacking gel. Remove the top right corner of the running gel for orientation purposes.
16. Proceed to the Subheadings 3.7 or 3.10 to western blot analysis.

3.7 Gel Staining

1. Put the running gel in staining buffer for 1 h (*see* **Note 22**).
2. Detain using detaining buffer for 1 h.
3. Conserve the gel or proceed to the Subheading 3.8.

3.8 In-Gel Digestion

All procedures are carried out at RT unless otherwise specified.

1. Excise band of interest from the gel and cut into small pieces (*see* **Note 23**).
2. Transfer the gel pieces to a tube with H_2O (the pieces of gel in water can be stored at 4 °C for at least 1 week).
3. Throw away the water and add 50 μL of 50% acetonitrile, incubate for 5 min at RT (*see* **Note 24**), and discard liquid.
4. Repeat **step 3** once.
5. Add 50 μL of 100% acetonitrile, shake for a few seconds, gel pieces should get white, and discard liquid.
6. Add 30 μL of 100 mM ammonium bicarbonate buffer and incubate for 5 min.
7. Add 30 μL of 100% acetonitrile and incubate for 15 min.
8. Discard liquid and dry gel pieces in a vacuum concentrator for 15 min.
9. Add 50 μL of 10 mM DTT and incubate at 56 °C for 45 min. Submerge sample complete in buffer.
10. Cool down to RT and discard liquid.
11. Add 50 μL of 55 mM iodoacetamide solution and incubate in dark for 30 min at RT.
12. Discard liquid and dry gel pieces in a vacuum concentrator for 15 min.
13. Repeat **steps 3–8** once.
14. Add 20 μL of Trypsin solution. Incubate overnight at 37 °C. Submerge sample complete in buffer.
15. Add 50 μL of 50 mM ammonium bicarbonate buffer and shake for min on a vertical shaker.
16. Add 50 μL of 100% acetonitrile and shake for another 15 min.
17. Transfer the supernatant (contains the peptides) to a fresh vial.

18. Add 50 μL of 5% formic acid in H2O, shake for 15 min, and transfer the supernatant to this fresh vial.
19. Repeat **step 18** once.
20. Dry the peptides in a vacuum concentrator.
21. Peptides are now ready for analysis or can be stored at −20 °C.
22. Before analysis, redissolve peptides in a volume of H_2O appropriate for at least two injections.

3.9 LC-ESI-MS Measurement

1. Redissolve peptides in 10–40 μL of H_2O.
2. Inject a tryptic digest of bovine serum albumin to verify proper performance of the analytic system.
3. Prior to every queue, calibrate the instrument to ensure best mass accuracy possible.
4. Use 1% solvent B to equilibrate chromatographic system.
5. Inject sample to LC-ESI-MS system.
6. Elute glycopeptide (*see* **Note 25**) using a flow rate of 6 μL/min. After a 5 min hold time, develop a gradient from 1% B to 35% B in 45 min, followed by a 15-min ramp to 80% B.
7. Turn the instrument for the mass region of 800–1600 amu while measuring from 500–900 amu.
8. Perform the analysis with data-dependent acquisition (DDA).
9. Prepare a spreadsheet listing likely glycoforms with different charge states.
10. Identify eluting glycopeptide. In these conditions the sample generates one glycopeptide EEQFNSTFR [M+H]1+: 1157.52 Da.
11. In a not too narrow zone around the glycopeptide signal, sum up the spectra.
12. Deconvolute the obtained spectra to simplify the glycopeptide profile.
13. Assign glycan compositions to the multiple peaks in the deconvoluted profile (*see* **Note 26**).
14. Perform relative quantization by listing heights of the peaks of different glycoforms.

3.10 Gel Transference

1. Run the samples in a SDS-PAGE.
2. Place the running gel in ice-cold 1× FastBlot buffer with methanol. Do not left the gel in buffer more than 5 min.
3. Measure the dimensions of the running gel obtained. Cut four pieces of blotting paper and one piece of nitrocellulose membrane of the same dimensions. Remove the top right corner of the membrane for orientation purposes.

4. Put the nitrocellulose membrane and the blotting papers in ice-cold 1× FastBlot buffer with methanol.
5. Transfer two pieces of blotting paper to the bottom of the plate of the semidry transfer system. With a Pasteur's pipette smooth out any bubbles.
6. Put the nitrocellulose membrane in top of the blotting paper stack.
7. Take out the gel from the FastBlot buffer and lay it on top of the stack. Roll a Pasteur's pipette to smooth out any bubbles as before.
8. Repeat **step 5** placing the blotting papers in top of the gel.
9. Place the lid on the transfer system.
10. Apply a 5 mA/cm^2 for about 1 h (*see* **Note 27**).
11. Remove the lid and gently disassemble the transfer stack.
12. Stain the membrane with Ponceau S for about 1 min. Remove the dye and wash the membrane with water until the protein bands are visible. Gently mark the marker band and the position of the lanes with a pencil (*see* **Note 28**).
13. Proceed to the Subheading 3.11.

3.11 Immunolabeling

1. Place the membrane in blocking buffer for 1 h at 37 °C or overnight at 4 °C (*see* **Note 28**) to block nonspecific binding sites.
2. Discard the blocking buffer and wash the membrane three times with 1× PBS for 10 min.
3. Incubate the membrane with the primary antibody 1 h at 37 °C on a rocking platform or overnight at 4 °C (*see* **Note 29**).
4. Wash the membrane three times with 1× PBS for 10 min.
5. If appropriate, incubate the membrane with the secondary antibody for 1 h at 37 °C on a rocking platform.
6. Repeat **step 4**.
7. Incubate the membrane with streptavidin fused to horseradish peroxidase (HRP) for 45 min at 37 °C on a rocking platform.
8. Repeat **step 4**.
9. In a dark room, place the membrane between two acetate films.
10. Mix 500 μL of solution A and B and wet the membrane with it. Dry the excess of solution.
11. Put an X-ray film on top of the acetate and place the stack between two magnetic sheets. Fold the bottom right of the plate to orientation purpose.

12. After 10–20 min (*see* **Note 30**), transfer the film to developer solution. When the protein bands become visible, wash the film with water.
13. Transfer the film to fixer solution. Wash with water.

3.12 Sandwich ELISA

1. Coat wells with 1 μg/mL of goat anti-mouse antibody specific to LC overnight at 4 °C.
2. Block nonspecific binding sites with blocking buffer for 1 h at 37 °C.
3. Wash three times with 1× PBS 10 min at RT.
4. Incubate the plates with 100 μg of soluble protein leaf extract at 4 °C overnight.
5. Repeat **step 3**.
6. Incubate plates with 1 μg/mL biotinylated goat anti-mouse antibody specific to HC overnight at 4 °C.
7. Repeat **step 3**.
8. Incubate plates with high sensitive HRP conjugated streptavidin for 30 min at 37 °C.
9. Repeat **step 3**.
10. Incubate the plates with TMB peroxidase substrate for 20 min at 37 °C in dark. Measure OD at 650 nm (*see* **Note 31**).

3.13 Indirect ELISA

1. Coat the wells by passive absorption with 1 μg/mL of BSA couple 14D9 enol ether hapten and incubate overnight at 4 °C.
2. Follow **steps 2–10** from Subheading 3.12.

4 Notes

1. This strain develops spontaneous tetracycline resistance and should be used with care. Fast growing colonies after transformation are false. True transformants appear 1–2 days after fast growing colonies.
2. Ascorbic acid is not stable in solution. Do not store 1× extraction buffer.
3. For a 100 mL solution, weight 30 g of acrylamide and 0.2 g of bis-acrylamide, transfer to a 100 mL graduated tube with 40 mL of H_2O and make up to 100 mL.
4. The destain solution could also be prepared with methanol in the same proportion.
5. Do not freeze. Alternative recipe for stain solution 0.2% (w/v) Ponceau in 3% (v/v) acetic acid.

6. This solution should not be stored for more than 2 weeks.
7. This solution should not be stored for more than a month.
8. The volume of the liquid culture depends on the OD and final infiltration volumes needed.
9. Different agrobacterium could grow at different rates. We recommend to plate the bacteria from the cryo-stock onto a plate with the correspondent antibiotics 2 or 3 days before agroinfiltration and use these plates to inoculate the liquid cultures. The plates can be stored at 4 °C for 3, 4 weeks.
10. For microsome isolation, ELISA and subcellular localization experiment we used at least five plants per construct and three biological replicates. Starting with the youngest mature leaf, leaves were numbered from the top-down (Fig. 1) and each construct was infiltrated in leaves located at different positions (leaf 3–5, or counting from the top).
11. Maximal expression levels were obtained between day 5 and 8 post-infiltration. The leaves can be harvested between these days.
12. The extract can be filtrated with a Miracloth filter prior centrifugation.
13. The column can be centrifuged at low revolutions for less than 30 s.
14. If antibody functionality is needed, this elution method should be avoided. Elution can be performed using an elution with a pH 2.4 buffer.
15. A concentrated high-density extraction buffer is used to take into consideration tissue water content.
16. Whole supernatant can be centrifuged, but a minimum amount of extract is used to expose the whole sample to the maximum RFC possible.
17. Perfluorodecalin enhance in vivo microscopy resolution of mesophyll and significantly improves the optical qualities of the leaf compared with water. In addition, mounting the specimen in perfluorodecalin has minimal physiological impact when compared to water.
18. Do not use Bicichoninic Acid protein assay (BCA), since ascorbic acid interfere with the redox reaction of this assay.
19. Nonpolymerized polyacrylamide is a neurotoxin, handle with care.
20. Polymerization time is temperature dependent.
21. When working with total soluble protein extracts, we load the same amount of protein in each lane, normally, 20 μg.
22. Do not leave the gel staining for more than an hour. This is really important for glycan analysis, since particular care needs

to be taken in order to avoid unintended modifications of the analyte.

23. Higher extraction yields are reached if the gel pieces are small, however, too small pieces could cause problems during extraction.
24. The volume used depends on the size of the bands since all pieces need to be covered with liquid. Normally, 50 μL are sufficient.
25. The N-glycan composition of a protein can be analyzed by LC-ESI-MS after glycans release with PNGase A treatment. However, site-specific analysis of glycosylation is performed by mass spectrometric analysis of the generated glycopeptides. This approach has several advantages over analysis of release glycans: (a) It is sure that the detected glycoforms are linked to the protein of interest and do not belong to a highly glycosylated impurity. (b) It can be assumed that the different glycoforms of a peptide have similar detection sensitivity, since ionization efficiency is dominated by the peptide. (c) It can be used to analyze several glycosylation sites in a protein, which is of particular interest in the case of antibodies, since glycosylation of the Fc region has relevant functional implications.
26. The different variants of the glycopeptide elute essentially at the same time.
27. The transfer time depends on the sample.
28. It is no needed to completely destain the membrane; the blocking solution will take a pinkish color, which does not affect the outcome of the experiment.
29. In our experience, better sensibility and less background noise is obtained when incubate overnight at 4 °C, but the other option can also be used.
30. Exposition time depends on protein level obtained.
31. OD can also be measured at 450 nm after stopping the reaction with 200 μL of 0.16 M sulfuric acid.

Acknowledgment

This work was supported by the Agencia Nacional de Promoción Científica y Tecnológica (ANPCyT) through the grants PICT Start Up 2015-0010 and PICT 2016-1722 and by Universidad Nacional de La Plata (grant 11X/754) to S.P. S.P. is a researcher from CONICET and Full Professor of the Facultad de Ciencias Exactas-UNLP; CGO is a fellow at CONICET.

References

1. Marty F (1999) Plant vacuoles. Plant Cell 11:587–599
2. Vitale A, Raikhel NV (1999) What do proteins need to reach different vacuoles? Trends Plant Sci 4:149–155
3. Herman EM, Larkins BA (1999) Protein storage bodies and vacuoles. Plant Cell 11:601–613
4. Tamura K, Shimada T, Ono E, Tanaka Y, Nagatani A, Higashi S-i, Watanabe M, Nishimura M, Hara-Nishimura I (2003) Why green fluorescent fusion proteins have not been observed in the vacuoles of higher plants. Plant J 35:545–555
5. Marin Viegas VS, Ocampo CG, Petruccelli S (2017) Vacuolar deposition of recombinant proteins in plant vegetative organs as a strategy to increase yields. Bioengineered 8:203–211
6. Xiang L, Etxeberria E, Van Den Ende W (2013) Vacuolar protein sorting mechanisms in plants. FEBS J 280:979–993
7. De Marchis F, Bellucci M, Pompa A (2013) Traffic of human alpha-mannosidase in plant cells suggests the presence of a new endoplasmic reticulum-to-vacuole pathway without involving the Golgi complex. Plant Physiol 161:1769–1782
8. Ocampo CG, Lareu F, Marin Viegas VS, Mangano S, Loos A, Steinkellner H, Petruccelli S (2016) Vacuolar targeting of recombinant antibodies in Nicotiana benthamiana. Plant Biotechnol J 14:2265–2275. https://doi.org/10.1111/pbi.12580
9. Denecke J, Botterman J, Deblaere R (1990) Protein secretion in plant cells can occur via a default pathway. Plant Cell 2:51–59
10. Matsuoka K, Neuhaus JM (1999) Cis-elements of protein transport to the plant vacuoles. J Exp Bot 50:165–174
11. Goulet C, Khalf M, Sainsbury F, D'Aoust MA, Michaud D (2012) A protease activity-depleted environment for heterologous proteins migrating towards the leaf cell apoplast. Plant Biotechnol J 10:83–94
12. Benchabane M, Goulet C, Rivard D, Faye L, Gomord V, Michaud D (2008) Preventing unintended proteolysis in plant protein biofactories. Plant Biotechnol J 6:633–648
13. Niemer M, Mehofer U, Torres Acosta JA, Verdianz M, Henkel T, Loos A, Strasser R, Maresch D, Rademacher T, Steinkellner H et al (2014) The human anti-HIV antibodies 2F5, 2G12, and PG9 differ in their susceptibility to proteolytic degradation: down-regulation of endogenous serine and cysteine proteinase activities could improve antibody production in plant-based expression platforms. Biotechnol J 9:493–500
14. Castilho A, Steinkellner H (2012) Glyco-engineering in plants to produce human-like N-glycan structures. Biotechnol J 7:1088–1098
15. Fitchette AC, Cabanes-Macheteau M, Marvin L, Martin B, Satiat-Jeunemaitre B, Gomord V, Crooks K, Lerouge P, Faye L, Hawes C (1999) Biosynthesis and immunolocalization of Lewis a-containing N-glycans in the plant cell. Plant Physiol 121:333–344
16. Strasser R (2016) Plant protein glycosylation. Glycobiology 26:926–939
17. Gomord V, Fitchette A, Menu-Bouaouiche L, Saint-Jore-Dupas C, Plasson C, Michaud D, Faye L (2010) Plant-specific glycosylation patterns in the context of therapeutic protein production. Plant Biotechnol J 8:564–587
18. Lerouge P, Cabanes-Macheteau M, Rayon C, Fischette-Lainé AC, Gomord V, Faye L (1998) N-glycoprotein biosynthesis in plants: recent developments and future trends. Plant Mol Biol 38:31–48
19. Misaki R, Sakai Y, Omasa T, Fujiyama K, Seki T (2011) N-terminal vacuolar sorting signal at the mouse antibody alters the N-linked glycosylation pattern in suspension-cultured tobacco BY2 cells. J Biosci Bioeng 112(5):476–484

Chapter 7

Isolation of Vacuoles from the Leaves of the Medicinal Plant *Catharanthus roseus*

Inês Carqueijeiro, Henrique Noronha, Sara Bettencourt, Joana G. Guedes, Patrícia Duarte, Hernâni Gerós, and Mariana Sottomayor

Abstract

The isolation of vacuoles is an essential step to unravel the important and complex functions of this organelle in plant physiology. Here, we describe a method for the isolation of vacuoles from *Catharanthus roseus* leaves involving a simple procedure for the isolation of protoplasts, and the application of a controlled osmotic/thermal shock to the naked cells, leading to the release of intact vacuoles, which are subsequently purified by density gradient centrifugation. The purity of the isolated intact vacuoles is assayed by microscopy, western blotting, and measurement of vacuolar (V)-H^+-ATPase hydrolytic activity. Finally, membrane functionality and integrity is evaluated by measuring the generation of a transtonoplast pH gradient by the V-H^+-ATPase and the V-H^+-pyrophosphatase, also producing further information on vacuole purity.

Key words Plant vacuoles, Vacuole isolation, Protoplasts, *Catharanthus roseus*, ATPase hydrolytic activity, Vacuolar (V)-H^+-ATPase, Vacuolar (V)-H^+-pyrophosphatase, Proton pumping activity

1 Introduction

Vacuoles occupy most of the volume of plant cells and play an array of key roles for plant physiology which are still under debate. Vacuoles maintain the turgor pressure needed for cell growth and support of the plant body, perform the lytic functions of animal cell lysosomes, and accumulate protons, inorganic ions, amino acids, proteins, sugars, specialized metabolites, etc. [1]. As such, it is thought that vacuoles have a central role in plant cell homeostasis, signal transduction and plant development that is still poorly acknowledged. Vacuoles are also very important for all sorts of plant environmental interactions, namely due to their role in the metabolism and accumulation of a massive array of specialized metabolites with defense, protection, and communication properties [2].

Cláudia Pereira (ed.), *Plant Vacuolar Trafficking: Methods and Protocols*, Methods in Molecular Biology, vol. 1789,
https://doi.org/10.1007/978-1-4939-7856-4_7,

In order to tackle the complexity of vacuole functions, it will be essential do determine the qualitative and quantitative profiles of proteins and metabolites of isolated vacuoles, for different organs, developmental stages, and stress conditions. These approaches will allow to address plenty of specific functional biology questions as well as to apply systems biology tools to reach more integrative levels of understanding of vacuole function.

Isolation of vacuoles is usually achieved by the application of a gentle osmotic or osmotic/thermal shock to protoplasts, leading to the rupture of plasma membrane with release of intact vacuoles, which are subsequently purified by density gradient centrifugation. This procedure was first reported by Cocking in 1960 [3], for root tips of tomato seedlings, and variants of the method have since been applied to different plant species and tissues (*see* references in [4]). In 1976, Leigh and Branton described an alternative method for the large-scale isolation of vacuoles from root storage tissue of red beet, involving slicing of the tissue in an apparatus specifically designed to avoid high shear forces [5]. Nevertheless, the method of election remains the isolation of vacuoles from disturbed protoplasts. A simple method for the large-scale isolation of vacuoles from Arabidopsis leaves using osmotic/thermal shock of protoplasts has been described by Robert et al. [4] and extended to the isolation of tonoplast by Zouhar [6]. In spite of the improvements, the big size and instability of vacuoles still make of their isolation a challenging procedure, which is seldom applied. Moreover, given the current view that not all the above mentioned functions are accumulated by a single multifunctional vacuole, but are rather performed in a complementary way by two or more different types of vacuoles [7], it is urgent to further refine experimental procedures to achieve isolation of vacuole subpopulations.

Here, we describe the optimization of two methods for the isolation of intact vacuoles from the leaves of *Catharanthus roseus*, a medicinal plant known by the production and accumulation of anticancer alkaloids in the vacuoles of its leaf cells [8]. The two methodologies include: (1) isolation of protoplasts using a simple and effective protocol that is easily adaptable to different plant species and tissues [9], (2) release of vacuoles by osmotic/thermal shock of protoplasts followed by density gradient purification of vacuoles, (3) characterization of vacuole purity by microscopy, western blotting and assay of vacuolar (V)-H^+-ATPase hydrolytic activity, and (4) evaluation of membrane functionality and integrity by demonstrating the generation of a transtonoplast pH gradient by an active V-H^+-ATPase and/or an active V-H^+-pyrophosphatase (PPase). We also include a description of staining with calcofluor-white (CFW) to test for the presence of cell wall during protoplast isolation, and a description of staining with fluorescein diacetate (FDA) to evaluate protoplast viability.

The isolation of intact vacuoles with high purity is dependent on several factors including: (1) the delicate equilibrium of the osmotic/

thermal shock leading to an efficient protoplast lysis without compromising vacuole integrity; (2) the cleaning capacity of the Ficoll interphase to trap chloroplasts, which are also released upon protoplast disruption and are one of the major sources of contamination of intact vacuoles and (3) the capacity of the vacuole suspension buffer to keep the homeostasis and integrity of the vacuoles. Here, we describe two protocols proficient in the isolation of vacuoles from *C. roseus* leaves, whose improvement resulted from different needs. Method 1 was tailored for studies where a high yield is important, even if with a lower purity, and where the integrity of the vacuolar membrane has to be maintained. In this method, the presence of bovine serum albumin (BSA) and protease inhibitors in the vacuole buffer impairs the use of the vacuoles in proteomics, but the high yield and stability makes them suitable for functional studies. Method 2 was tailored to achieve a very high purity in the absence of any added proteins. This comes with the cost of a lower yield and more unstable vacuoles, but the purity of the obtained organelles makes them particularly suitable for omic studies.

2 Materials

2.1 Plant Materials

Plants of *C. roseus* (L.) G. Don cv. Little Bright Eye were grown at 25 °C, under a 16 h photoperiod, using light with a maximum intensity of 70 μmol/m^2/s. Young, healthy plants should be used for protoplast and vacuole isolation (*see* **Note 1**).

2.2 Isolation of Protoplasts

All buffers and solutions should be made fresh.

1. MM buffer (*see* **Notes 2** and **3**): 0.4 M mannitol in 20 mM MES, pH 5.7–5.8 adjusted with 1 M KOH. Autoclave at 120 °C for 20 min and keep at 4 °C until use.
2. Digestion medium (*see* **Note 4**): 2% (w/v) cellulase Onozuka R-10, 0.3% (w/v) macerozyme R-10 and 0.1% (v/v) pectinase dissolved in MM buffer. Stir very gently at least for 30 min, in the dark, at room temperature. Prepare immediately prior to tissue harvest.
3. Excicator; vacuum pump; orbital shaker; haemocytometer; 20–200 μL micropipette; bright-field optical microscope.
4. Sterile surgical blades; 50–200 μm nylon mesh; disposable plastic Pasteur pipettes; plastic Petri dishes; sterile sawn-off 20–200 μL micropipette tips; 15 mL plastic centrifuge tubes without any inside edges or bulges.

2.3 Staining of Protoplasts with Calcofluor-White (CFW) and Fluorescein Diacetate (FDA)

1. CFW (*see* **Note 5**): prepare 1% (w/v) in water.
2. FDA (*see* **Note 6**): prepare 10 μg/μL in acetone.
3. 20–200 μL Micropipette; fluorescence or confocal microscope equipped with (1) excitation wavelengths of 387 ± 11 nm and emission wavelengths of 457 ± 22 nm (for CFW staining visual-

ization), (2) excitation wavelengths of 494 ± 20 nm and emission wavelengths of 530 ± 20 nm (for FDA staining visualization).

4. Sterile sawn-off 20–200 μL micropipette tips; slides; coverslips.

2.4 Isolation of Vacuoles

2.4.1 Isolation of Vacuoles—Method 1 (See Note 7)

1. Lysis buffer: 150 μg/mL BSA, 2 mM dithiothreitol (DTT), 0.2 M mannitol, 10% (w/v) Ficoll 400 P, 15 mM EDTA, and 10 mM MOPS pH 8, adjusted with 1 M KOH. The buffer without BSA and DTT may be kept frozen. Upon use, DTT is added from a 1 M stock solution and BSA powder is dissolved directly in the buffer.
2. Vacuole buffer: 2 mM DTT, 0.5 M mannitol, 0.67 mM protease inhibitor cocktail, 10 mM MOPS pH 7.5 adjusted with 1 M KOH. The buffer without DTT and protease inhibitor may be kept frozen. Upon use, DTT is added from a 1 M stock solution, and 10 μL of 1 M protease inhibitor cocktail is added per 15 mL of vacuole buffer.
3. Ficoll buffer: mix lysis buffer, already supplemented with DTT and BSA, with vacuole buffer, already supplemented with protease inhibitor and DTT, in order to achieve a final concentration of 3% (w/v) Ficoll (e.g., to prepare 15 mL, mix 4.5 mL of lysis buffer with 10.5 mL of vacuole suspension buffer).
4. Water bath; 20–200 μL, 1 mL, and 5 mL micropipettes; refrigerated orbital centrifuge; haemocytometer; bright-field optical microscope.
5. Disposable plastic Pasteur pipettes; sterile sawn-off 20–200 μL and 1 mL micropipette tips; 5 mL micropipette tips; 15 mL plastic centrifuge tubes; 1.7 mL eppendorff tubes; disposable 15 mL serological pipettes; liquid nitrogen.

2.4.2 Isolation of Vacuoles—Method 2 (See Note 8)

1. Lysis buffer: 0.2 M mannitol, 10% (w/v) Ficoll 400 P, 10 mM EDTA (from a 0.5 M stock solution with pH 8), and 5 mM sodium phosphate (from a 0.2 M stock solution with pH 8.0).
2. Vacuole buffer: 0.45 M mannitol, 2 mM EDTA and 5 mM sodium phosphate pH 7.5. Upon use add 2 mM DTT from a 1 M stock solution.
3. Ficoll buffer: mix lysis and vacuole buffers in a proportion of 4.5 to 3 in order to achieve a final concentration of 4% Ficoll.
4. Water bath; 20–200 μL, 1 mL and 5 mL micropipettes; refrigerated orbital centrifuge; utltracentrifuge; haemocytometer; bright-field optical microscope.
5. Disposable plastic Pasteur pipettes; sterile sawn-off 20–200 μL and 1 mL micropipette tips; 5 mL micropipette tips; 15 mL plastic centrifuge tubes; 1.7 mL eppendorff tubes; disposable 15 mL serological pipettes; liquid nitrogen.

2.5 Yield and Purity of Vacuole Fraction—Microscopy

1. 1 mg/mL Neutral red (*see* **Note 9**). The neutral red solution is stable for several months at 4 °C.
2. 10 mM FM1-43 (fluorescence membrane marker) (*see* **Note 10**).
3. 20–200 µL Micropipette; bright-field optical microscope; fluorescence or confocal microscope equipped with (1) an excitation wavelength of 488 nm and an emission wavelength window from 500 to 650 nm (for FM1-43 staining visualization), (2) excitation wavelengths of 490/20 nm and emission wavelengths of 705/72 nm (for chlorophyll visualization).
4. Sterile sawn-off 20–200 µL micropipette tips; slides; coverslips.

2.6 Purity of Vacuole Fraction—Western Blotting

1. Protein solution: 1 mM NaCl, 1 mM $CaCl_2$, 1 mM $MgCl_2$, and 1 mM $MnCl_2 \cdot 4H_2O$.
2. Reagents for protein quantification with Bradford method [10]: Bio-RAD Protein Assay Dye Reagent Concentrates (#5000006). Reagents for sodium dodecyl sulfate polyacrylamide gel electrophoresis (SDS-PAGE): (1) loading buffer 4× — 40% (v/v) glycerol, 250 mM Tris–HCl pH 6.8, 8% (w/v) SDS, 0.0004% (w/v) bromophenol, 5% (v/v) beta-mercaptoethanol; (2) running buffer — 190 mM glycine, 25 mM Tris, 0.1% SDS. 10% polyacrylamide gels.
3. Western blot reagents as described in [11, 12]: (1) transfer buffer — 20% (v/v) methanol, 190 mM glycine, 25 mM Tris, 0.003% (w/v) SDS; (2) Tris-buffered saline (TBS) buffer — 50 mM Tris pH 7.6, 200 mM NaCl. Addition of 0.1% SDS to the transfer buffer might be needed when membrane proteins are the target of research. Nitrocellulose membranes.
4. Membrane blocking solution: Tris-buffered saline (TBS) containing 0.15% (v/v) Tween-20, 5% (w/v) skimmed milk powder, 1% (w/v) BSA and 0.1% (v/v) goat serum.
5. Primary antibodies: ER marker — rabbit antiserum raised against calreticulin (a gift from J. Denecke, University of Leeds), at a 1:10,000 dilution, or rabbit antiserum raised against STM1 at a 1:1000 dilution; chloroplast marker — rabbit antiserum raised against the chloroplast inner envelope TIC 40 protein, at a 1:2500 dilution; tonoplast markers — rabbit antisera raised against a V-H^+-ATPase and against a V-H^+-PPase [13] (may be requested to Prof. M. Maeshima—maeshima@agr.nagoya-u.ac.jp), both at a 1:2000 dilution.
6. Secondary antibody: peroxidase conjugated goat anti-rabbit at 1:7500 dilution.
7. Chemiluminescent substrate ECL™.
8. Micropipettes; X-ray film; developing cassette; gel documentation system.

2.7 Purity of Vacuole Fraction—V-H^+-ATPase Hydrolytic Activity

1. General stock solutions: 200 mM adenosine 5′-triphosphate dipotassium salt (ATP) in 200 mM Bis-Tris Propane buffer (stored at −20 °C, in 100 μL aliquots); 10 mM NaH_2PO_4 in 0.02% Triton X-100.
2. Reaction solution: 3 mM ATP, 0.02% Triton X-100, 50 mM KCl, 1 mM sodium molybdate, and 6 mM MgSO4 in 30 mM Tris-MES, pH 8. Always prepare fresh, add ATP and Triton only immediately before reaction.
3. Stock solutions of inhibitors: 50 mM sodium azide (mitochondria F-H^+-ATPase inhibitor); 50 mM sodium orthovanadate (plasma membrane P-H^+-ATPase inhibitor).
4. Stop solution: 10% TCA and 4% perchloric acid.
5. Ames solution [14]: 1 volume of 10% ascorbic acid plus 6 volumes of a solution containing 4.2 g ammonium molybdate and 28.6 mL of H_2SO_4 in 1 L of H_2O.
6. Calibration solutions: 0.2, 0.4, 0.6, 0.8 and 1 mM NaH_2PO_4 prepared with the 10 mM stock solution described in 1.
7. Incubator with agitation; table top centrifuge (2400 × *g*); spectrophotometer (O.D. 820 nm).
8. Glass tubes washed with phosphate free solutions (MiliQ water and ethanol 100%).

2.8 Tonoplast Integrity and Functionality—Activity of Proton Pumps

1. General stock solutions: 200 mM ATP as above; 20 mM potassium pyrophosphate (PPi) (store at −20 °C); 2 mM ACMA prepared in 100% ethanol (stable for several months when protected from light and kept at −20 °C); 500 mM $MgCl_2{\cdot}6H_2O$ (filter sterilize and store at room temperature).
2. Reaction buffer: 30 mM KCl, 50 mM NaCl, 20 mM Hepes, pH 7.2, supplemented with 0.1% (w/v) BSA. Filter sterilize and store at 4 °C.
3. Stock solutions of inhibitors and uncoupling agents: 150 mM NH_4Cl; 5 M KNO_3; 50 mM sodium azide (mitochondria F-H^+-ATPase inhibitor); 10 mM concanamycin A (V-H^+-ATPase inhibitor); 50 mM sodium orthovanadate (plasma membrane P-H^+-ATPase inhibitor).
4. Spectrofluorometer with excitation and emission wavelengths set at 415 and 485 nm respectively; 2 mL UV spectrofluorometer cuvette; small magnetic stirrer.

3 Methods

3.1 Isolation of Protoplasts

1. Choose a healthy plant with 3–8 months (*see* **Note 1**). To guarantee perfect physiological conditions, water well the plants on the day before. Select 8–10 healthy fully developed leaves (approximately 2 g) and cut the leaves in ~1 mm strips

with a chirurgic blade, excluding the central vein. Soak the blade with the medium several times as you cut and change the blade every 3–4 leaves.

2. Immediately transfer the leaf strips, abaxial face down, to a Petri dish with 10 mL of digestion medium. Start with three plates.
3. Put the open Petri dishes inside the dessicator and apply a −50 to −100 mBar vacuum for 15 min to infiltrate the medium into the leaf strips. Apply gentle disruptions of the vacuum every 30 s.
4. Incubate the leaf strips in the digestion medium for 3 h at 25 °C, in the dark (*see* **Note 11**).
5. After this incubation, place the Petri dishes on an orbital shaker, at ~60 rpm, for 25 min, in the dark, at room temperature (RT), to help release the protoplasts.
6. Further release the protoplasts from leaf strips with the help of a sawn-off plastic Pasteur pipette, by gently pressing the leaf strips against the side wall of the Petri dish and slowly flushing the medium over them.
7. Use a new sawn-off plastic Pasteur pipette to carefully transfer the protoplasts into a funnel of nylon mesh to filter the protoplasts into a new Petri dish. Maintain the mesh in contact with the dish to guarantee a continuous flow of solution and avoid dripping. Wash the leaf strips with 2 mL of MM buffer to recover the maximum number of protoplasts and press gently the strips in the end.
8. Gently transfer the protoplasts to six 15 mL plastic tubes (two per Petri dish), using sawn-off plastic Pasteur pipettes, always avoiding dripping. Wash the Petri dish with 2 mL of MM buffer. Do not fill the tubes with more than 5–6 mL.
9. Centrifuge the protoplast suspension at 65 × *g*, with Acc/Dcc 1, for 5 min, at RT, to pellet the protoplasts. Remove the supernatant with a pipette and discard it.
10. Wash the protoplasts of each tube three times with 5 mL of MM buffer. Pipette 1 mL of MM buffer using a swan-off tip, allowing the medium to gently drain against the wall of the tube and resuspend the protoplasts by tapping gently the tube with your fingertips. Add the remaining washing volume with the same precautions, invert gently the tube to homogenize the suspension, and centrifuge as in **step 9**. At this point you may inspect the yield and purity of the protoplast suspension under the bright-field optical microscope (Fig. 1a).
11. Resuspend the last pellets in a minimum volume of MM buffer and pool together the protoplast suspensions.
12. Determine the protoplast concentration using a haemocytometer under the optical microscope (you may leave the protoplast suspension at RT). To pipette the protoplast suspension

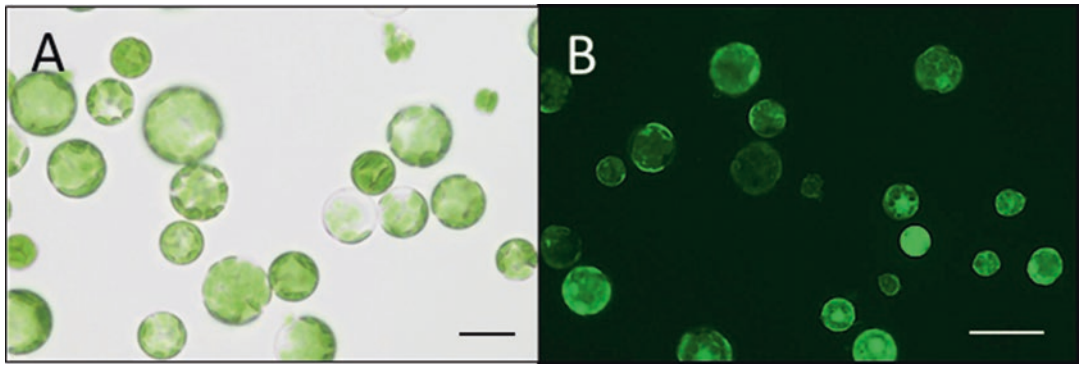

Fig. 1 *Catharanthus roseus* protoplasts. (**a**) Bright field image of protoplasts. (**b**) Fluorescence image of protoplasts labeled with fluorescein diacetate (FDA). Bars = 20 μm (**a**), 50 μm (**b**)

use a 20–200 μL micropipette with a sawn-off tip with no irregularities. Dilute an aliquot of the suspension if needed.

13. After this time, protoplasts settle at the bottom of the tube by gravity. Discard the supernatant and resuspend the protoplasts in the volume of MMg buffer needed to obtain a final concentration of 10^6–10^7 protoplasts in a maximum volume of 5 mL.

3.2 Characterization of Cell Wall Digestion and Protoplast Viability

The generation of cell wall free protoplast cells can be followed using CFW staining (*see* **Note 5**), at any point of the digestion incubation. This procedure is useful when you are optimizing a digestion protocol.

3.2.1 Characterization of Cell Wall Digestion—Staining with Calcofluor-White (CFW)

1. Stir gently the Petri dish where digestion is taking place for around 20 s. Pipette ~100 μL of digestion medium / protoplast suspension, using a 20–200 μL micropipette with a sawn-off tip with no irregularities, onto a slide, and add 2 μL of 1% CFW gently into the centre of the suspension on the slide. Lay a coverslip very slowly to avoid disruption of protoplasts.
2. Incubate for 10 min, at RT, in the dark, and observe under a fluorescence microscope using a filter with excitation wavelengths of 387 ± 11 nm and emission wavelengths of 457 ± 22 nm. The presence of blue fluorescence around the cells indicates there is still cell wall present (cellulose).

3.2.2 Characterization of Protoplast Viability—Staining with Fluorescein Diacetate

The viability of the final isolated protoplasts can be measured using FDA (Fig. 1b) (*see* **Note 6**).

1. Add 5 μL of 10 μg/μL FDA to ~5×10^5 protoplasts (100 μL of cells using a 20–200 μL micropipette with a sawn-off tip with no irregularities, diluted with 400 μL of MM) in an Epperdorf tube.
2. Incubate for 10 min in the dark and pipette ~100 μL onto a slide, using a 20–200 μL micropipette with a sawn-off tip with

no irregularities. Lay a coverslip very slowly to avoid disruption of protoplasts.

3. Observe under a fluorescence microscope using a filter with excitation wavelengths of 494 ± 20 nm and emission wavelengths of 530 ± 20 nm. Viable protoplasts will display green fluorescence as can be seen in Fig. 1b.

3.3 Isolation of Vacuoles

3.3.1 Isolation of Vacuoles—Method 1 (See Note 7)

This method is based on the method described by [15] for *Vitis vinifera* suspension cells, with some modifications. This method enables a high yield of stable vacuoles, but a lower purity than method 2.

1. Start with 10^6–10^7 protoplasts in a maximum volume of 5 mL.
2. Centrifuge the protoplast suspension at 65 × *g*, with Acc/Deacc 1, for 5 min, at RT, to pellet the protoplasts. Discard the supernatant using a 1 mL micropipette with a sawn-off tip with no irregularities, and chill the protoplasts on ice for at least 30 min and no more than 45 min.
3. Add 2 mL of lysis buffer prewarmed at 42 °C to the chilled pelleted protoplasts, and resuspend the cells by pipetting up and down with a 5 mL micropipette or with a disposable 15 mL serological pipette (5–8 times) (*see* **Note 12**). Add 5 mL more of lysis buffer and invert the tube gently to guarantee full homogeneization. Make sure protoplasts are well resuspended.
4. Allow lysis to occur for 10 min at 42 °C in a water bath (*see* **Note 13**). At 5 min invert the tubes gently to assure protoplasts do not sediment.
5. Remove the tubes from the water bath and carefully overlay 3.5 mL of 3% Ficoll buffer at RT, using a 1 mL micropipette with a sawn-off tip with no irregularities. Finally, carefully overlay 1 mL of vacuole buffer at RT. The three phases must be distinguishable. Be aware to choose a sawn-off tip (around 5–10 mm cut) with a fine regular edge.
6. Centrifuge at 1000 × *g*, for 15 min, at 20 °C, in a swing-out rotor, selecting Acc/Dcc 2 (*see* **Note 14**).
7. Carefully collect the upper phase containing the vacuoles using a 1 mL micropipette with a sawn-off tip with no irregularities. In the vacuole buffer, vacuoles do not tend to precipitate. Ordinarily, this method yields ~2 × 10^6 vacuoles in a total of 2–3 mL.
8. Use the vacuoles immediately to evaluate purity by microscopy/staining, to perform functional assays (such as in Subheading 3.5 below) or aliquot as needed, freeze with liquid nitrogen and store at −80 °C for later characterization.

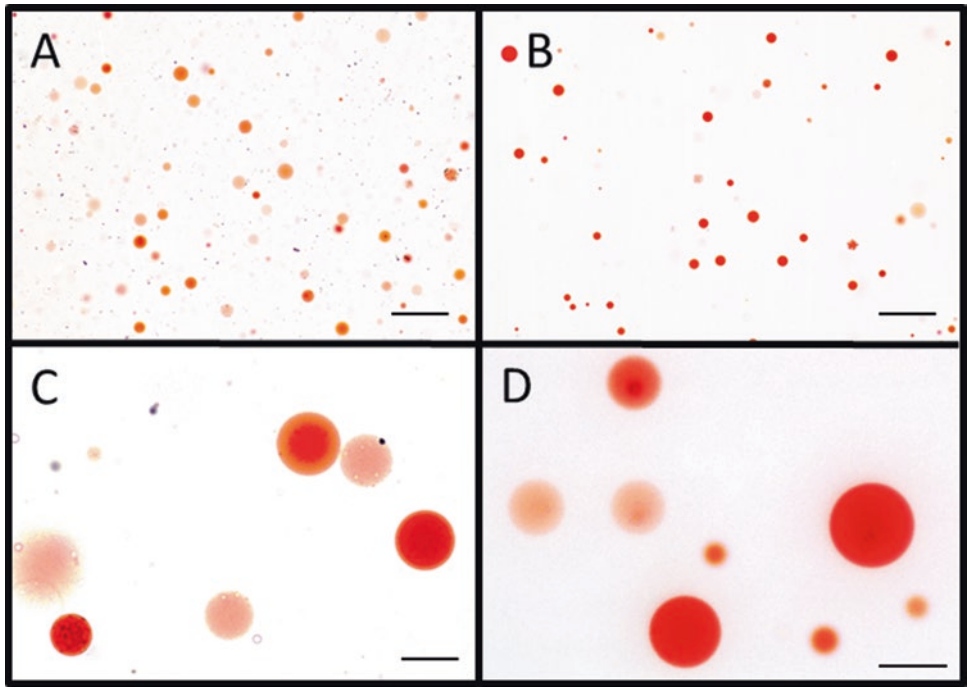

Fig. 2 Bright field images of *Catharanthus roseus* intact vacuoles stained with neutral red. Intact vacuoles isolated with method 1 (**a**, **c**) and method 2 (**b**, **d**). Bars = 20 μm (**a**, **b**), 100 μm (**c**, **d**)

3.3.2 Isolation of Vacuoles—Method 2 (See Note 8)

This method is based on the method described in [4] for Arabidopsis leaves, with some modifications. This method enables to achieve a very high purity in the absence of any added proteins, but has a lower yield than method 1 and vacuoles are more unstable (Fig. 2).

1. Start with a minimum of 10^7 protoplasts per mL in a total of 1–3 mL and pellet through centrifugation.
2. Centrifuge the protoplast suspension at 65 × *g*, with Acc/Dcc 1, for 5 min, at RT, to pellet the protoplasts. Discard the supernatant using a 1 mL micropipette with a sawn-off tip with no irregularities, and chill the protoplasts on ice for at least 30 min and no more than 45 min.
3. Add 4 mL of lysis buffer prewarmed at 37 °C to the chilled pelleted protoplasts and resuspend the cells by pipetting up and down with a disposable 15 mL serological pipette (5–8 times) (*see* **Note 12**). Add 8 mL more of lysis buffer and invert the tube gently to guarantee full homogeneization. Make sure protoplasts are well resuspended.
4. Allow lysis to occur for 4 min at RT. At 2 min invert the tubes gently to assure protoplasts do not sediment.
5. Transfer each 6 mL of lysed protoplasts per ultracentrifuge tube (two tubes) using a 5 mL micropipette. Overlay 3.6 mL of 4% Ficoll buffer at 25 °C, using a 1 mL micropipette with a sawn-off tip with no irregularities. Finally, carefully overlay

1 mL of ice-chilled vacuole buffer. Be aware to choose a sawn-off tip (around 5–10 mm cut) with a fine regular edge.

6. Centrifuge at 71,000 × *g*, for 30 min, at 10 °C, in a swing-out rotor, selecting Acc/Dcc 8 (*see* **Note 15**).
7. Vacuoles will rise and resolve in the interface between the 4% Ficoll buffer and the vacuole buffer, and will be identifiable by the presence of a yellowish color. Carefully collect the vacuoles at the interface using a 1 mL micropipette with a sawn-off tip with no irregularities. Ordinarily, this method yields ~7–10 × 10^5 vacuoles in 1 mL.
8. Use the vacuoles immediately to evaluate purity by microscopy/staining, to perform functional assays (such as in Subheading 3.5 below), and/or aliquot as needed, freeze with liquid nitrogen and store at −80 °C for later characterization.

3.4 Characterization of Vacuole Yield, Integrity and Purity, by Microscopy, by Staining with Neutral Red and by Staining with FM1-43

1. Mount the vacuole suspension in a microscope slide. Pipette ~100 μL of vacuole suspension using a 20–200 μL micropipette with a sawn-off tip with no irregularities onto a slide, and lay a coverslip very slowly on the suspension, to avoid disruption of vacuoles.

3.4.1 Characterization of Vacuole Purity by Microscopy

2. Observe under the bright-field optical microscope, using a magnification of 400× and closing the diaphragm to increase contrast. You should be able to visualise the vacuoles and contaminants such as protoplasts, chloroplasts, xylem cell walls, and aggregates. For a better visualization of vacuoles use neutral red staining (Subheading 3.4.2 below) or FM1-43 staining (Subheading 3.4.3 below), which enables the visualization of vacuole substructures and specific types of contaminants.
3. To evaluate rigorously the contamination with chloroplasts, which are also released upon protoplast disruption and are one of the major sources of contamination of intact vacuoles, observe the vacuole preparation under a fluorescence or confocal microscope equipped with excitation wavelengths of 490/20 nm and emission wavelengths of 705/72 nm. Chloroplasts are easily detectable with a high sensitivity as red fluorescing particles. When using method 1 for isolation of vacuoles, we can detect the presence of some chloroplasts in our vacuole suspensions, while method 2 yields vacuole suspensions virtually devoid of chloroplasts.

3.4.2 Characterization of Vacuole Yield and Integrity Using Neutral Red

1. Stain vacuoles with neutral red (*see* **Note 9**). Pipette ~100 μL of vacuole suspension onto a slide, using a 20–200 μL micropipette with a sawn-off tip with no irregularities, then add slowly 10 μL of 1 mg/mL neutral red to the centre of the suspension on the slide. Lay a coverslip very slowly to avoid disruption of vacuoles.
2. Incubate for 5 min, at RT, in the dark.

3. Observe under the bright-field optical microscope. Acidic vacuoles will accumulate the cationic red form of neutral red and will become rose to deep red, depending on their pH (Fig. 2). Staining by neutral red shows that vacuoles have a pH different from the medium, and have therefore retained tonoplast integrity.
4. Use a haemocytometer to count the neutral red stained vacuoles, and calculate the yield and the percentage of contaminants such as protoplasts, chloroplasts and undetermined structures/debris. Pipette the suspension to the haemocytometer according to the respective instructions, using a 20–200 µL micropipette with a sawn-off tip with no irregularities. Add 5 µL of 1 mg/mL neutral red to the side of the coverslip very slowly, allowing the dye to penetrate. Perform counting after 3–5 min.

3.4.3 Characterization of Vacuole Purity Using FM1-43

1. Stain vacuoles with FM1-43 (*see* **Note 10**). Pipette ~100 µL of vacuole suspension onto a slide, using a 20–200 µL micropipette with a sawn-off tip with no irregularities, and add 2 µL of 10 µM FM1-43 to the centre of the suspension on the slide. Lay a coverslip very slowly to avoid disruption of vacuoles.
2. Incubate for 30 min at RT in the dark.
3. Observe under a fluorescence or confocal microscope using excitation wavelength of 488 nm and an emission wavelength window from 500 to 650 nm. FM1-43 will stain membranes, enabling a clear visualization of vacuoles as well as of membrane structured contaminants. This procedure also enables the visualization of membrane compartments inside the vacuoles, which were described for instance in [16], and should enable to distinguish between vacuoles and vacuoplasts—cells that have released most organelles upon disruption of plasma membrane, suffering subsequent sealing of plasma membrane to become cells with a vacuole, some cytosol and the plasma membrane.

3.5 Characterization of Tonoplast Integrity and Properties by Assaying the Activity of Proton Pumps

The generation of a transtonoplast pH gradient by the V-H^+-ATPase and/or the V-H^+- PPase is tested using the fluorescent probe ACMA according to [17], with minor modifications (*see* **Notes 16** and **17**).

1. Set the spectrofluorometer to 25 °C, use excitation and emission wavelengths of 415 and 485 nm respectively (*see* **Note 18**).
2. Add 1 mL of reaction buffer, 10 µL of 500 mM $MgCl_2$ and ~10^4 intact vacuoles in no more than 100 µL into a 2 mL UV spectrofluorometer cuvette with a small magnetic stirrer.
3. Set the spectrofluorometer to medium stirring and allow to equilibrate for 1 min.
4. Add 1 µL of 2 mM ACMA and monitor fluorescence stabilization—it should take 2–4 min.

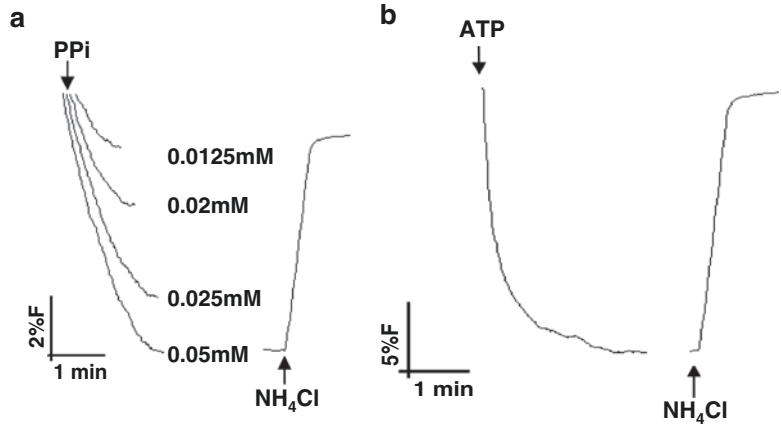

Fig. 3 Pumping activity of V-H$^+$-PPase and V-H$^+$-ATPase in intact vacuoles from *C. roseus* leaves isolated with method 1, measured by the fluorescence quenching of the pH-sensitive probe ACMA. (**a**) H$^+$ pumping activity upon addition of PPi (substrate of the V-H$^+$-Ppase). (**b**) H$^+$ pumping activity upon addition of ATP (substrate of the V-H$^+$-ATPase)

5. Start the reaction by adding ATP to a final concentration of 0.05–1.5 mM ATP, or PPi to a final concentration of 0.0125–0.1 mM, in order to activate proton pumping by the V-H$^+$-ATPase or the V-H$^+$-PPase respectively, and register fluorescence with a 1 s resolution (*see* **Note 19**). If these pumps are active and the membranes are intact, a transmembrane pH gradient is generated resulting in fluorescence quenching of ACMA (Fig. 3).
6. Add 10 μL of 150 mM NH_4Cl. This weak base will dissipate any transmembrane pH gradient and induce a strong recovery of the ACMA fluorescence, if the previous quenching was indeed due to a transmembrane pH gradient.
7. If desired, the initial rates of fluorescence quenching for different concentration of ATP or PPi may be used to estimate the kinetic parameters of the proton pumps [8]. The rates are expressed as Δ fluorescence in % min^{-1} μg^{-1} protein.
8. In order to confirm if (or which part of) the transmembrane pH gradient, observed when ATP is added, results from V-H$^+$-ATPase proton pump activity, and not from other ATPase proton pumps present in contaminant compartments, the following inhibitors may be used, added after ACMA, and 3–4 min before the addition of ATP: 100 μM vanadate—inhibits the plasma membrane P-H$^+$-ATPase and should not inhibit quenching if vacuoles are pure; 100 μM KNO_3 and 0.1 μM concanamycin—inhibit the V-H$^+$-ATPase and should inhibit completely the ATP induced quenching if vacuoles are pure.

3.6 Characterization of Vacuole Purity by Western Blotting

1. Lyophilize the vacuole samples. Reconstitute in 1 mM NaCl, 1 mM $CaCl_2$, 1 mM $MgCl_2$, and 1 mM $MnCl_2.4H_2O$, dialyze against the same solution (*see* **Note 20**) and determine protein concentration using the Bradford method [10]. Store at −20 °C until use.
2. Resolve the proteins in a 10% acrylamide gel as described in [11]. For immunodetection of soluble proteins, boil samples for 2 min prior to gel loading. For immunodetection of membrane proteins, heat samples at 70 °C for 10 min prior to gel loading, and load immediately onto the gel. Load 10 μg of protein for calreticulin and TIC 40 immunodetection, and 1 mg of protein for V-H^+-ATPase and V-H^+-PPase immunodetection.
3. Transfer the proteins to a nitrocellulose membrane for 1 h and 30 min, at 100 V, according to the method described in [12]. For the immunodetection of membrane proteins, add 0.1% of SDS to the transfer buffer.
4. Probe the membranes against the different primary antibodies in the appropriate dilutions (*see* Subheading 2.6 above). Determine the optical density of the western blot bands and plot the results (Fig. 4a).

3.7 Characterization of Vacuole Purity by Measurement of V-H^+-ATPase Hydrolytic Activity (See Note 21)

The rate of ATP hydrolysis is determined by measuring the release of inorganic phosphate by the hydrolytic domain of the ATPase pumps, according to [18], with some modifications.

1. Thaw a vacuole aliquot and determine protein concentration using the Bradford method[10].
2. Mix a maximum volume of 15 μL of vacuole sample, corresponding to 15 μg of protein, with 300 μL of reaction solution, and incubate for 30 min at 37 °C with slow agitation. Perform a similar reaction in the presence of 0.5 mM azide + 0.1 mM vanadate. In parallel, perform reactions using 0.2, 0.4, 0.6, 0.8, 1, and 1.2 mM NaH_2PO_4 in 0.1% Triton X100 as standards, to build the calibration curve.
3. Stop the reaction by adding 500 μL of cold stop solution, keep samples on ice for 2 min, vortex and centrifuge at 2400 × *g* for 3 min.
4. Collect 500 μL of supernatant, mix with 1.3 mL of Ames solution and incubate for 15 min at room temperature in the dark.
5. Read absorbance at 820 nm using a blank control performed without protein.
6. Build a calibration curve in nmol PO_4^{3-} min^{-1} and express the estimated ATPase hydrolytic activity in nmol PO_4^{3-} min^{-1} mg^{-1} protein.

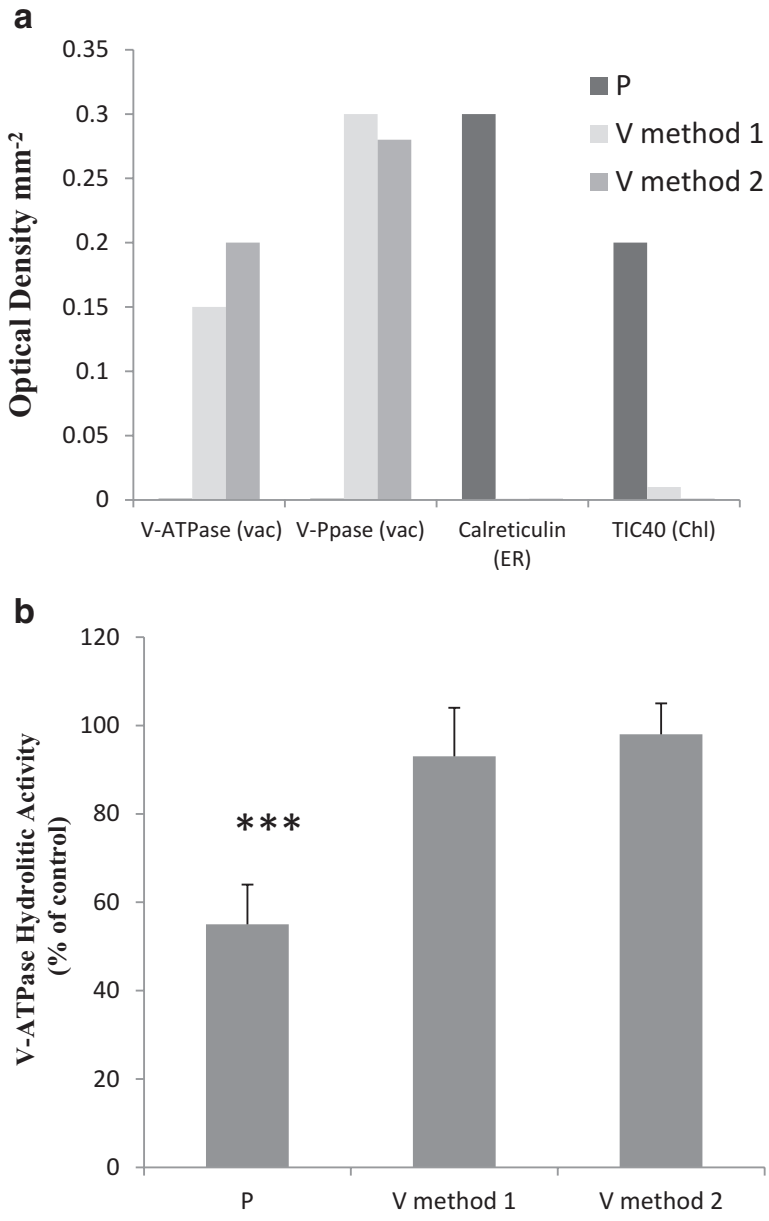

Fig. 4 Characterization of the purity of *C. roseus* vacuoles isolated using method 1 and 2, through western blot and ATPase hydrolytic activity. (**a**) Western blot quantitative analysis of protein extracts from protoplasts (P) and vacuoles (V), isolated with method 1 and method 2, using specific antibodies raised against the chloroplast inner envelope protein TIC40, the vacuole specific V-H^+-PPase and V-H^+-ATPase (subunit epsilon), and the ER resident protein calreticulin. (**b**) V-H^+-ATPase hydrolytic activity of protein extracts from protoplasts (P) and vacuoles (V), isolated with method 1 and method 2. For each fraction, ATP hydrolytic activity was measured in the presence of 0.5 mM azide (mitochondrial ATPase inhibitor) and 100 μM vanadate (plasma membrane ATPase inhibitor) and expressed as the percentage of the total ATP hydrolytic activity in the absence of inhibitor, revealing the residual % of activity corresponding to the V-H^+-ATPase present in each fraction. Statistical significance was evaluated using Student's *t* test for pairwise comparison ($^{***}P < 0.01$). Data significantly different from control are indicated. Error bars indicate SD from three biological replicates with two biochemical replicates each

7. Express the V-H^+-ATPase activity as the percentage of ATP hydrolytic activity detected in the presence of inhibitors compared with the activity observed in their absence (Fig. 4b).

4 Notes

1. There was a seasonal effect in the protoplast and vacuole yield, as well as in membrane integrity and H^+ pumping activity of intact vacuoles. Although plants were growing in a growth chamber, under constant conditions, maximum yield and activity were typically obtained in March–June and September–October.
2. The MM buffer tends to easily contaminate, autoclave immediately after preparation, and respect the autoclaving conditions. You may consider also to sterilize using Millipore Steritop-GV SCGVT05RE Polystyrene Bottle Top Vacuum Filter Unit, 0.22 μm Pore Size, 45 mm Thread. It is mandatory to use KOH to adjust the pH, since NaOH promotes protoplast instability.
3. The osmotic pressure stabilizing agents and the presence of protecting agents such as BSA, $CaCl_2$, and KCl in the digestion buffer are considered important factors in protoplast isolation. In our hands, Mes and mannitol alone were sufficient to uphold membrane integrity with several plant materials [9].
4. The key step in protoplast isolation is the enzyme mixture used for cell wall digestion. Several other mixtures have been described, with the combinatorial use of cellulase Onozuka RS with pectolyase Y23 being the most widely used. These enzymes indeed work quite well with *C. roseus* mesophyll cells (data not shown) but they are very expensive, and good results were also obtained here using a balanced mixture of the cheaper cellulase Onozuka R10, macerozyme R10 and pectinase. However, the use of highly active enzymes allows the use of lower concentrations, what may be important for sensitive cells susceptible to enzyme toxicity. Optimal enzyme concentrations may change considerably depending on the species, the nature of the tissue, the period of incubation and the vacuum infiltration conditions, with cellulase typically ranging from 0.5% to 3%, and macerozyme and pectinase from 0.1% to 0.4%, although they can be raised at least up to 1.5% for recalcitrant tissues. Storage of digestion medium in aliquots at −20 °C is often described, but is diminishes severely the activity of the enzymes.
5. CFW is a special fluorescent stain that binds to cellulose and is used for the staining of cell walls of algae and higher plants.
6. The intact plasma membrane is permeable to FDA, which is accumulated inside the cells, due to conversion into a mem-

brane impermeable green fluorescent dye (fluorescein) by cytoplasmic esterases. Thus, accumulation of fluorescein in the cytoplasm is a measure of two independent processes, membrane integrity and the presence of active esterases, and represents a highly reliable indication of cell viability [15].

7. Method 1 is tailored for studies where a high yield is important, even if with a lower purity, and where the integrity of the vacuolar membrane is crucial. The presence of BSA and protease inhibitors in the vacuole suspension buffer impairs the use of these vacuoles in proteomics, but the high yield and stability makes them suitable for functional studies.
8. Method 2 was tailored to achieve a very high purity in the absence of any added proteins. This comes with the cost of a lower yield and more unstable vacuoles, but the high purity of the obtained vacuoles makes them particularly suitable for omic studies.
9. Neutral red is a weak cationic azine vital dye that presents red color at acid pH, changing to yellow at 6.8–8 range. It accumulates in acidic compartments, where it is trapped as a cation with red color.
10. FM1-43 is a membrane marker previously used to observe vacuole membranes and membranous contaminants namely in Arabidopis and *Vitis vinifera* suspension cells [15].
11. It is important to improve conditions to obtain the shortest possible digestion incubation period, in order to avoid physiological changes and enzyme toxicity, which can render protoplasts too sensitive to subsequent manipulations. Many protoplast isolation protocols do this incubation under weak orbital shaking, but with our protocol that is not necessary or advisable, possibly because we use a low osmotic concentration.
12. The pipetting should be performed fast; gentleness at this point is not essential since we want to disrupt the cells.
13. Lysis must be performed in a water bath and not in a dry chamber.
14. The centrifuge model influences the efficiency of vacuole isolation (purity and yield). In our case Eppendorf 5810 R or Sigma 2-16K centrifuges enabled the best results, likely due to the gentleness of the deacceleration, since any abrupt movement may disrupt the interfaces and allow contamination with undisrupted protoplasts, otherwise retained by the 3% Ficoll buffer.
15. Once again the centrifuge model influences the success of the procedure. Our choice lies in Beckman Coulter Ultracentrifuge or Sorvall Utracentrifuge (ThermoFisher).
16. The generation of a transmembrane pH gradient will simultaneously demonstrate that membrane proteins are active and

that the membrane is impermeable to protons, conserving its main in vivo properties.

17. Fluorescent amines such as ACMA are permeable through membranes in their neutral form and accumulate inside acidic compartments due to protonation. This equilibrium redistribution upon the generation of a transmembrane pH gradient (acidic inside) is associated with a quenching of their fluorescence. According to [19] this is a consequence of the fact that the only fluorescent form of ACMA is the one present in the aqueous external compartment.
18. We obtained optimal sensitivity and stability for this assay with a LS-5B fluorescence spectrophotometer (PERKIN ELMER, USA).
19. The addition of ATP produces a direct and immediate quenching of ACMA fluorescence independent of any transport, which should be unvalued. The quenching resulting from proton pumping appears later with a slower slope. The part of the quenching corresponding to proton pumping by the V-H^+-ATPase is confirmed by the dissipation of the transmembrane pH gradient by addition of NH_4Cl (Fig. 3). This artifact due to the addition of ATP does not happen upon addition of PPi, and is excluded from final figures.
20. Dialysis is important to remove the mannitol, which can interfere with immunodetection.
21. It is postulated that the remnant ATP hydrolytic activity observed upon simultaneous inhibition with the plasma membrane H^+-ATPase (P-H^+-ATPase) inhibitor vanadate and the mitochondria H^+-ATPase (F-H^+-ATPase) inhibitor azide represents the V-H^+-ATPase hydrolytic activity (in the presence of Triton X100 ABC transporters lose their ATPase activity and do not interfere in this measurement). Therefore, if a ~100% activity is observed in the presence of the two inhibitors, this indicates the absence of contamination with plasma membrane and with mitochondrial membranes, confirming a high purity of the vacuole suspension.

Acknowledgments

This work was supported by (1) Fundo Europeu de Desenvolvimento Regional funds through the Operational Competitiveness Programme COMPETE and by National Funds through Fundação para a Ciência e a Tecnologia (FCT) under the projects FCOMP-01-0124-FEDER-037277 (PEst-C/SAU/LA0002/2013) and FCOMP-01-0124-FEDER-019664 (PTDC/BIA-BCM/119718/2010); (2) the FCT scholarships cosupported by FCT and POPH-QREN (European

Social Fund), SFRH/BD/41907/2007 (I.C.) and SFRH/BD/74257/2010 (H.N.); (3) a Scientific Mecenate Grant from Grupo Jerónimo Martins.

References

1. Neuhaus JM, Martinoia E (2011) Plant vacuoles. In: eLs. John Wiley & Sons, Ltd: Chichester. https://doi.org/10.1002/9780470015902.a0001675.pub2
2. Hartmann T (2007) From waste products to ecochemicals: fifty years research of plant secondary metabolism. Phytochemistry 68:2831–2846. https://doi.org/10.1016/j.phytochem.2007.09.017
3. Cocking EC (1960) A method for the isolation of plant protoplasts and vacuoles. Nature 187:962–963. https://doi.org/10.1038/187962a0
4. Robert S, Zouhar J, Carter C, Raikhel N (2007) Isolation of intact vacuoles from Arabidopsis rosette leaf-derived protoplasts. Nat Protoc 2:259–262. https://doi.org/10.1038/nprot.2007.26
5. Leigh RA, Branton D (1976) Isolation of vacuoles from root storage tissue of *Beta vulgaris* L. Plant Physiol 58:656–662. https://doi.org/10.1104/pp.58.5.656
6. Zouhar J (2017) Isolation of vacuoles and the tonoplast. In: Taylor NL, Millar AH (eds) Isolation of plant organelles and structures. Methods and protocols, methods in molecular biology, vol 1511. Springer Science + Business Media, New York, pp 113–118. https://doi.org/10.1007/978-1-4939-6533-5_9
7. Zouhar J, Rojo E (2009) Plant vacuoles: where did they come from and where are they heading? Curr Opin Plant Biol 12:677–684. https://doi.org/10.1016/j.pbi.2009.08.004
8. Carqueijeiro I, Noronha H, Duarte P et al (2013) Vacuolar transport of the medicinal alkaloids from *Catharanthus roseus* is mediated by a proton-driven antiport. Plant Physiol 162:1486–1496. https://doi.org/10.1104/pp.113.220558
9. Duarte P, Ribeiro D, Carqueijeiro, Bettencourt S, Sottomayor M (2016) Protoplast transformation as a plant-transferable transient expression system. In: Fett-Netto A (ed) Biotechnology of plant secondary metabolism. Methods for field and laboratory, methods in molecular biology, vol 14. Springer protocols. Humana Press, Totowa, NJ, pp 137–148. https://doi.org/10.1007/978-1-4939-3393-8_13
10. Bradford MM (1976) A rapid and sensitive method for the quantitation of microgram quantities of protein utilizing the principle of protein-dye binding. Anal Biochem 72:248–254. https://doi.org/10.1016/0003-2697(76)90527-3
11. Laemmli UK (1970) Cleavage of structural proteins during the assembly of the head of bacteriophage T4. Nature 227:680–685. https://doi.org/10.1038/227680a0
12. Burnette WN (1981) "Western blotting": electrophoretic transfer of proteins from sodium dodecyl sulfate–polyacrylamide gels to unmodified nitrocellulose and radiographic detection with antibody and radioiodinated protein A. Anal Biochem 112:195–203. https://doi.org/10.1016/0003-2697(81)90281-5
13. Maeshima M, Yoshida S (1989) Purification and properties of vacuolar membrane proton-translocating inorganic pyrophosphatase from mung bean. J Biol Chem 264:20068–20073
14. Ames BN (1966) Assay of inorganic phosphate, total phosphate and phosphatases. Methods Enzymol 8:115–118. https://doi.org/10.1016/0076-6879(66)08014-5
15. Fontes N, Silva R, Vignault C et al (2010) Purification and functional characterization of protoplasts and intact vacuoles from grape cells. BMC Res Notes 3:19. https://doi.org/10.1186/1756-0500-3-19
16. Bottanelli F, Gershlick DC, Denecke J (2012) Evidence for sequential action of Rab5 and Rab7 GTPases in prevacuolar organelle partitioning. Traffic 13:338–354. https://doi.org/10.1111/j.1600-0854.2011.01303.x
17. Façanha AR, de Meis L (1998) Reversibility of H^+-ATPase and H^+-pyrophosphatase in tonoplast vesicles from maize coleoptiles and seeds. Plant Physiol 116:1487–1495. https://doi.org/10.1104/pp.116.4.1487
18. Vera-Estrella R, Barkla BJ, Higgins VJ et al (1994) Plant defense response to fungal pathogens: activation of host-plasma membrane H^+-ATPase by elicitor-induced enzyme dephosphorylation. Plant Physiol 104:209–215. https://doi.org/10.1104/pp.104.1.209
19. Casadio R (1991) Measurements of transmembrane pH differences of low extents in bacterial chromatophores. A study with the fluorescent probe 9-amino, 6-chloro, 2-methoxyacridine. Eur Biophys J 19:189–201. doi.org/10.1007/BF00196345

Chapter 8

Flow Cytometry and Fluorescence Microscopy as Tools for Structural and Functional Analysis of Vacuoles Isolated from Yeast and Plant Cells

Jorge M. P. Rodrigues, Cátia S. Pereira, Natacha Fontes, Hernâni Gerós, and Manuela Côrte-Real

Abstract

A series of optimized protocols to isolate vacuoles from both yeast and plant cells, and to characterize the purified organelles at a functional and structural level, are described. For this purpose, we took advantage of the combined use of cell fractionation techniques with different fluorescence-based approaches namely flow cytometry, fluorescence microscopy and spectrofluorimetry. These protocols altogether constitute valuable tools for the study of vacuole structure and function, as well as for the high-throughput screening of drug libraries to identify new molecules that target the vacuole.

Key words Isolated vacuoles, Flow cytometry, Fluorescence microscopy, Yeast, Plant cell

1 Introduction

Vacuoles were traditionally viewed as simply the terminal compartments of the biosynthetic and endocytic pathways, playing a role in protein degradation, ion and metabolite storage, as well as in cell detoxification. However, nowadays it is known that these organelles are highly sensitive and responsive to different cellular challenges being strongly regulated and playing important functions in ion homeostasis, response to nutrient deprivation, osmotic and ionic stress, autophagy, and even in cell death. In plants, they are also responsible for the maintenance of turgor pressure ([1–7]).

As storage compartments, vacules generally accumulate amino acids, nucleic acids, ions, heavy metals, proteins, carbohydrates, secondary metabolites, and signaling molecules [8, 9]. Vacuoles

Jorge Rodrigues and Cátia Pereira contributed equally to this work.

Cláudia Pereira (ed.), *Plant Vacuolar Trafficking: Methods and Protocols*, Methods in Molecular Biology, vol. 1789, https://doi.org/10.1007/978-1-4939-7856-4_8,

can also accumulate more specialized molecules such as hydrolytic proteins [10], nucleases [11] and defense proteins [12]. In plant cells, vacuoles are involved in the protection against oxidative stress, participating in the regulation of the reactive oxygen species content [13]. Plants also use vacuoles and vacuolar proteases in regulated cell death (RCD) processes either in a destructive or nondestructive way. The destructive way, in contrast to the nondestructive way, is triggered by vacuolar membrane collapse. Also in yeast, vacuole and its proteases are involved different cell death scenarios (reviewed by [14]).

Almost all vacuolar functions depend either on the acidic pH of the lumen or on the pH gradient across the membrane. The vacuolar acidification in both yeast and plants is maintained through the action of the proton pump V-H^+-ATPase, which is located at the vacuolar membrane and couples the energy of ATP hydrolysis to actively transport protons to the vacuolar lumen ([1, 15, 16]). In plants, the proton pump V-H^+-PPase cooperates with the V-H^+-ATPase in the acidification of the vacuole but relies on inorganic pyrophosphate (PPi) as the energy source, instead of ATP. V-H^+-PPase is able to generate a pH gradient 1.4-fold higher than V-H^+-ATPase, depending on the plant species [17].

Some of the vacuolar functions and of their molecular components are difficult to study in a cellular context, and therefore the use of cell-free systems is an important approach to gain further insight into the different molecular mechanisms required for vacuolar function. In this regard, the biochemical characterization of V-H^+-ATPase using isolated vacuoles is a very good example of such an in vitro approach. Isolated vacuoles have been also a valuable tool to further understand vacuolar morphology and function, as well as to analyze the membrane and luminal proteome ([1, 18–20]). For example, isolated vacuoles were used to identify novel tonoplast transporters [21] and to obtain new insights on yeast protein trafficking to the vacuole [22].

Here, we describe a series of optimized protocols to isolate vacuoles from both yeast and plant cells and to characterize the purified organelles at a functional and structural level. For this purpose, we took advantage of the combined use of cell fractionation techniques with different fluorescence-based approaches namely flow cytometry, fluorescence microscopy and spectrofluorimetry. Flow cytometry provides the possibility of performing a cell/organelle-based quantitative analysis of thousands of cells/vacuoles in few minutes, and offers considerable advantages over classical biochemistry analysis, namely the assessment of the homogeneity/heterogeneity of the sample, and a much more robust statistical analysis [1]. Fluorescence microscopy, although less quantitative, allows visualizing the intracellular fluorescence compartmentation and to control specific/unspecific fluorescence, and hence validates the flow cytometric determinations. A set of different flow cytometry and fluorescence microscopy protocols to

stain isolated intact vacuoles are described. In addition, protocols to evaluate the activity of V-H^+-ATPase and V-H^+-PPase by spectrofluorimetry are provided. Some protocols were optimized from reports available in the literature when we studied vacuole structure and function using isolated vacuoles and vacuole membrane vesicles from yeast and plant cells [1, 17, 23–27]. The images presented throughout this chapter are adapted from Rodrigues and coworkers [1] and Fontes and coworkers [17]. Altogether, these protocols constitute valuable tools for the study of vacuole structure and function, as well as for the high-throughput screening of drug libraries to identify new molecules that target the vacuole.

2 Materials

The buffers and solutions are prepared with deionized water. The probes are dissolved in ultrapure water, ethanol, or DMSO according to manufacture instructions. All the buffers, solutions, and probes are prepared at room temperature. The buffers are stored at 4 °C, the majority of solutions are stored also at 4 °C, some can be stored at room temperature, and the probes are stored at −20 °C. Buffers and solutions should be stored no longer than 1 week, to avoid contaminations. The residues must be treated according to the appropriate regulation.

2.1 Vacuole Isolation from Yeast Cells

1. YEPD medium (1% yeast extract, 1% peptone, and 2% glucose).
2. Orbital shaker.
3. Spectrophotometer.
4. Digestion Buffer: 1.35 M sorbitol, 10 mM citric acid, 30 mM Na_2HPO_4, 1 mM EGTA, pH 7.5.
5. Zymolyase (Seikagaku, Japan).
6. Potter-Elvehjem.
7. 12% Ficoll (w/v).
8. 8% Ficoll (w/v).
9. Beckman Optima XL-90 ultracentrifuge with swing-out rotor.

2.2 Vacuoles Isolation from Plant Cells

1. Grape cell suspensions (CSB, *Cabernet Sauvignon Berry*).
2. 250-mL flasks.
3. Rotatory shaker.
4. Mineral medium supplemented with 2% (w/v) sucrose.
5. Incubation Buffer: Gamborg B5 Medium supplemented with 0.4 M sucrose.
6. Enzymatic cocktail: 0.007% (w/v) cellulose Y-C and 0.0007% (w/v) pectolyase Y-23, prepared in the Incubation Buffer before each experiment.

7. W5 Medium: 0.05 M glucose, 154 mM NaCl, 125 mM $CaCl_2$, and 5 mM KCl, pH 5.8.
8. MM Medium: 0.4 M mannitol, 15 mM $MgCl_2$, 5 mM MES, pH 5.8.
9. Lysis Buffer: 0.2 M mannitol, 0.5% BSA, 10% Ficoll 400, 20 mM EDTA, 10 mM HEPES, 2 mM DTT, pH 8.0. DTT is added before each experiment.
10. Vacuole Buffer: 0.5 M mannitol, 10 mM MOPS, pH 7.5, protease inhibitor cocktail (Complete, Roche Applied Science, Germany).

2.3 Flow Cytometry

1. Staining Buffer: 100 mM KCl, 1 mM MOPS adjusted to pH 7.2 with Tris.
2. Stocks of Acridine Orange, MDY-64, FM1-43, Lysosensor Green, $Dibac_4(3)$, and Fluo4-AM (Invitrogen, USA) in appropriate concentrations.
3. Flow cytometer tubes.
4. Flow cytometer equipped with a laser with a beam emitting at 488 nm.

2.4 Light and Fluorescence Microscopy

1. Staining Buffer: 100 mM KCl, 1 mM MOPS adjusted to pH 7.2 with Tris.
2. Stocks of MDY-64, FM1-43, and Neutral Red in appropriate concentrations.
3. Fluorescence and light microscope.

2.5 Analysis of the Functionality of the Isolated Vacuoles

1. ATPase Buffer: 100 mM KCl, 1 mM MOPS adjusted to pH 7.2 with Tris. Before each experiment complete with 2 μM ACMA and 1 mM $MgCl_2$.
2. PPase Buffer: 100 mM KCl, 10 mM MOPS adjusted to pH 7.2 with Tris. Before each experiment complete with 2 μM ACMA, 2 mM $MgCl_2$, and 0.1% BSA (w/v).
3. 200 mM ATP.
4. 200 mM PPi.
5. Quartz cuvette.
6. Spectrofluorimeter equipped with a UV light.

3 Methods

3.1 Culture Conditions

1. For vacuole isolation from yeast cells, grow 600 mL of W303-1A cells in YEPD medium in a 3 L sterile Erlenmeyer until OD_{640nm} 0.7–1.0 in a 30 °C orbital shaker at 200 rpm.
2. For vacuole isolation from plant cells, cultivate the grape cell suspensions (CSB, *Cabernet Sauvignon Berry*) for 1 week in

250-mL flasks on a rotatory shaker at 100 rpm in the dark, at 25 °C on mineral medium supplemented with 2% (w/v) sucrose. Cells are subcultured weekly by transferring 10-mL aliquots into 70 mL of fresh medium.

3.2 Vacuoles Isolation from Yeast

1. Collect the cells to 250 mL flasks, centrifuge at 4050 × *g* for 2 min and wash twice with 50 mL ice-cold distilled water.
2. Resuspend the pellet with 15 mL Digestion Buffer containing 30 mM DTT. Incubate the cells in an orbital shaker at 200 rpm for 15 min at 30 °C. Centrifuge the cells for 2 min at 2740 × *g* and discard the supernatant.
3. Add 15 mL of Digestion Buffer containing 2 mg/mL zymolyase. Incubate the cells under gentle shaking for up to 1 h at 32 °C and check regularly for the cell wall digestion (*see* **Note 1**).
4. Collect spheroplasts by centrifugation at 2740 × *g* for 5 min and wash once with Digestion Buffer without zymolyase.
5. Add 10 mL of 12% Ficoll (w/v) to the pellet, resuspend and transfer the suspension to a Potter-Elvejhem homogeneizer (*see* **Note 2**).
6. Homogenize the suspension of spheroplasts with the "loose" piston with gentle strokes, and check regularly for vacuole release (*see* **Note 3**).
7. Centrifuge at 2740 × *g* for 3 min, collect the supernatant containing the vacuoles and store on ice (*see* **Note 4**).
8. Prepare a Ficoll gradient transferring the supernatant containing 12% Ficoll to an ultracentrifuge tube and add carefully 12 mL of 8% (w/v) Ficoll on the top (*see* **Note 5**).
9. Centrifuge in a swing-out bucket rotor at 80,000 × *g* for 30 min at 4 °C (*see* **Note 6**).
10. Collect the white membranous fraction floating on the top of the tube containing the vacuoles (*see* **Note 7**).
11. Vacuoles can then be freshly used or frozen in aliquots in liquid nitrogen and stored at −80 °C. Vacuoles remain active up to several weeks (*see* **Note 8**).

3.3 Vacuoles Isolation from Plant Cells

1. Perform the protoplasting by enzymatic digestion of the cell walls (450 × 10^6 CSB cells) in Incubation buffer supplemented with the Enzymatic cocktail at pH 5.8 in a final volume of 50 mL.
2. Perform the cell's digestion overnight under gentle shaking at 50 rpm and 22 °C and collect the resulting protoplasts to 50 mL Corex tubes.
3. Prepare a discontinuous gradient to purify protoplasts by overlaying 1 volume of the W5 Medium, pH 5.8, on the protoplast suspension and centrifuge at 150 × *g* for 8 min.

4. Resuspend the floating protoplasts recovered from the interface of the gradient in 3 volumes of W5 Medium and sediment at 150 × *g* for 8 min.
5. Wash the pellet in MM Medium at 150 × *g* for 5 min, resuspend in the same medium and store at 4 °C.
6. Count the protoplasts in a Malassez chamber under the light microscope (*see* **Note 9**).
7. Perform protoplast lysis by diluting the protoplast suspension with 2.5 volumes of prewarmed (37–45 °C) Lysis buffer.
8. For the isolation of intact vacuoles, prepare a Ficoll gradient in a 25 mL Corex with 7:3:1 volumes of the following layers: a bottom layer containing lysed protoplasts in 10% (w/v) Ficoll, one intermediate layer of 3.0% (w/v) Ficoll and a top layer of Vacuole Buffer (*see* **Note 10**).
9. Collect the vacuoles from the Vacuole buffer layer after the one-step Ficoll gradient centrifugation at 1000 × *g* for 15 min and estimate vacuole number on a Malassez chamber under the light microscope (*see* **Notes 7** and **11**).

3.4 Characterization of Isolated Yeast and Plant Vacuoles by Flow Cytometry

For all the staining protocols add 20 μg protein of isolated vacuoles to flow cytometer tubes containing 1 mL of staining buffer. For each experimental condition prepare a nonstained sample to measure autofluorescence. Flow cytometry analysis of isolated vacuoles should be performed in a flow cytometer equipped with an argon-ion laser with a beam emitting at 488 nm. Green fluorescence and red fluorescence should be collected through a 525 nm band-pass filter and a 620 nm band-pass filter, respectively (*see* **Note 12**).

3.4.1 Correct Gating of Vacuoles Population

1. The acquisition protocol should include a biparametric histogram to measure forward scatter (FS) and side scatter (SS) in a logarithmic scale.
2. Define the gate on the vacuoles to proceed with the analysis (Fig. 1). In this figure, a mixed sample containing intact yeast cells, vacuoles, and vacuolar vesicles was analyzed.
3. Add monoparametric histograms for green and red fluorescence, and apply the vacuoles gate to these histograms.
4. Acquire the data corresponding to the autofluorescence of the vacuolar samples and define the gate for "positive staining."
5. Acquire the labeled samples.

3.4.2 Structural Staining of Isolated Yeast Vacuoles with MDY-64 and FM1-43

1. Stain the vacuole membrane with MDY-64 (10 μM, final concentration) or FM1-43 (5 μM, final concentration) under incubation in the dark for 10 min at room temperature (*see* **Note 13**).
2. Acquire data on the flow cytometer using the settings for green fluorescence (Fig. 2).

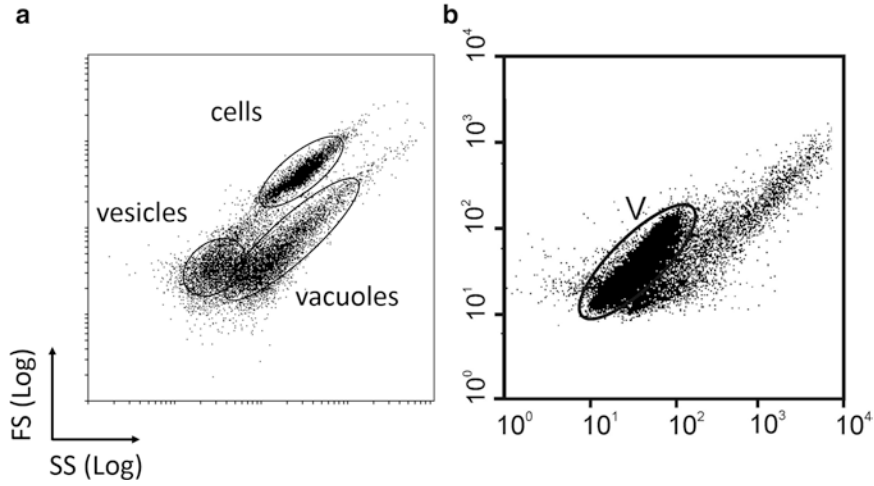

Fig. 1 Flow cytometry analysis of yeast and plant vacuoles. (**a**) Histogram with distinguishable populations of cells, vacuoles, and vesicles obtained with a mixed sample of intact cells, intact vacuoles, and vacuolar membrane vesicles isolated from yeast. (**b**) Correct gating of vacuoles isolated from plant cells in an SS FS histogram. Adapted from [1, 17] (original publishers: Microbiology Society and BioMed Central, respectively)

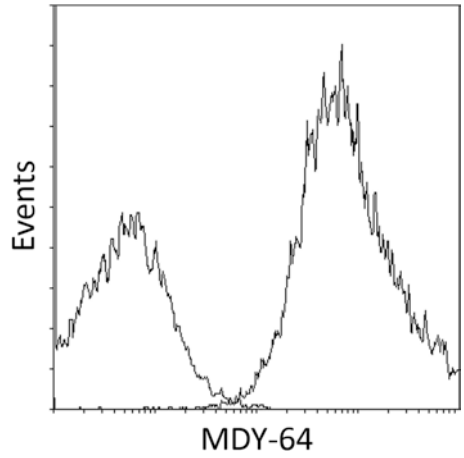

Fig. 2 Overlay of histograms of a yeast vacuole-gated population showing the autofluorescence of isolated yeast vacuoles (left histogram) and fluorescence of vacuoles stained with MDY-64 (right histogram). The fluorescence was acquired with the green channel of the flow cytometer. Adapted from [1] (original publisher: Microbiology Society)

3.4.3 Functional Staining of Isolated Yeast Vacuoles with Acridine Orange, Lysosensor Green and Dibac$_4$(3)

1. Stain the vacuoles with the pH-sensitive probes Acridine Orange (AO, 30 μM final concentration) or LysoSensor Green (5 μM, final concentration) under incubation in the dark for 10 min at room temperature. Stain the vacuoles with the membrane potential-sensitive probe DiBAC$_4$(3) (13 μM, final concentration) and incubate for 5 min in the dark at room temperature (*see* **Note 14**).

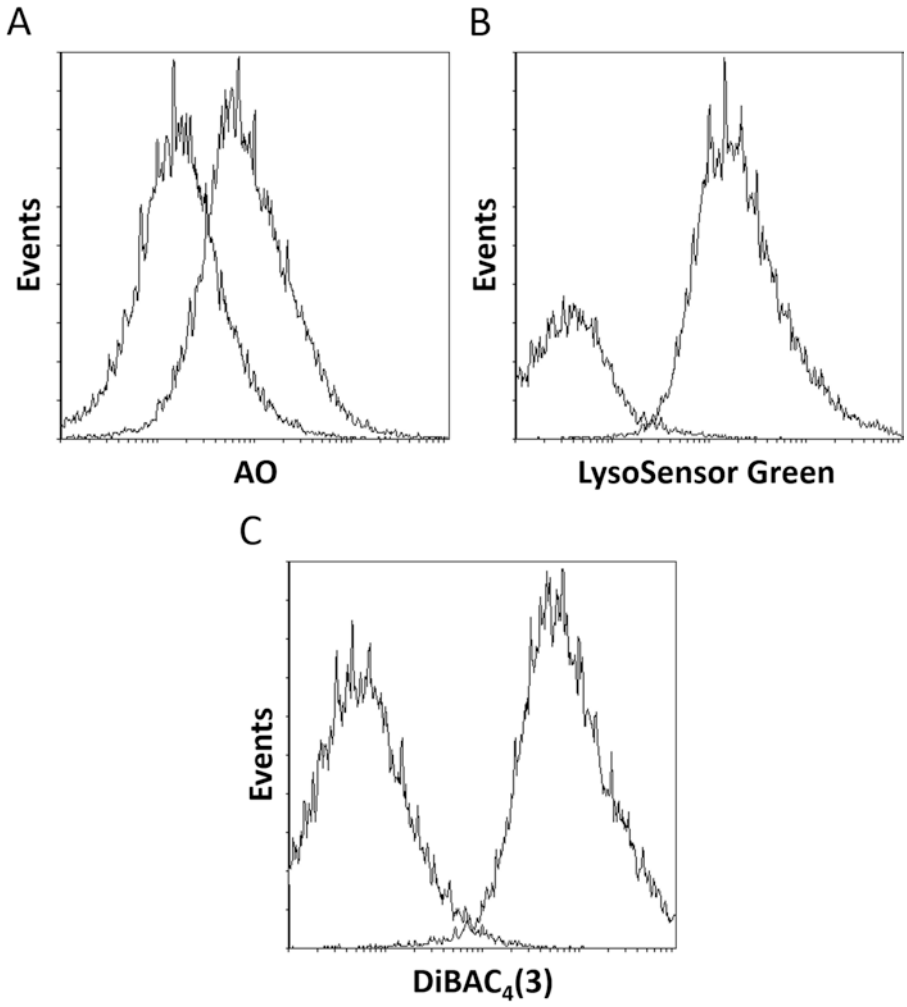

Fig. 3 Overlay of histograms of a yeast vacuole-gated population stained with functional dyes. (**a**) Staining with Acridine Orange, (**b**) LysoSensor Green and (**c**) DiBAC4(3). Autofluorescence of vacuoles (histograms on the left) and fluorescence from stained samples (histograms on the right). Adapted from [1] (original publisher: Microbiology Society)

2. Acquire data on the flow cytometer using the settings for green (LysoSensor Green and $DiBAC_4(3)$) and red (AO) fluorescence (Fig. 3).

3.4.4 Assessment of Calcium Accumulation in Yeast and Plant Vacuoles by Fluo-4 AM Staining

1. Stain the vacuoles with Fluo-4 AM (5 μM, final concentration) and incubate for 1 h in the dark at room temperature (*see* **Note 15**).
2. Acquire data on the flow cytometer using the settings for green fluorescence (Fig. 4).

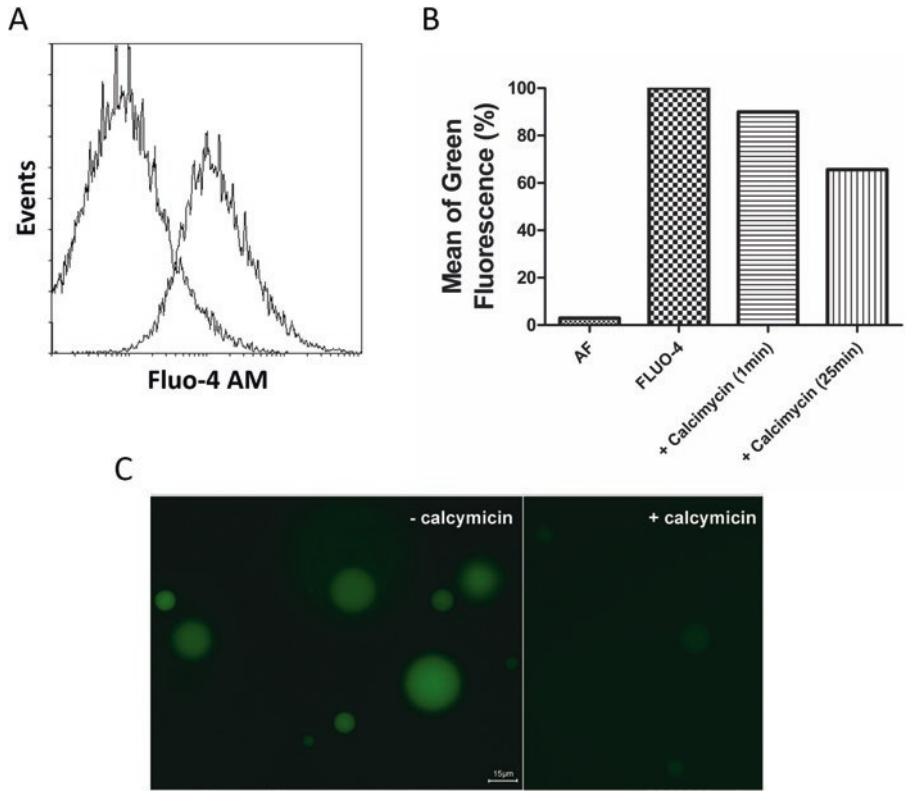

Fig. 4 Characterization of vacuoles isolated from yeast and plant cells with Fluo-4 AM. (**a**) Overlay of histograms showing on the left the autofluorescence of the yeast vacuoles and on the right the fluorescence of the vacuoles stained with Fluo-4AM. (**b**) Mean green fluorescence intensity measured by flow cytometry of yeast vacuole population nonstained (AF) and stained with Fluo-4AM, in the absence or presence of 300 μM calcimycin. (**c**) Intact plant vacuoles labeled with Fluo-4AM in the absence and the presence of 300 μM calcimycin, observed under the fluorescence microscope. Adapted from [1] (**a**, **b**) and [17] (**c**) (original publishers: Microbiology Society and BioMed Central, respectively)

3.5 Characterization of Isolated Vacuoles from Yeast and Plant Cells by Fluorescence Microscopy

For all staining protocols add 100 μg protein of isolated vacuoles to eppendorfs containing 0.05 mL staining buffer.

3.5.1 MDY-64 or FM1-43 Staining

1. Stain the vacuoles with MDY-64 (10 μM, final concentration) or FM1-43 (5 μM, final concentration) and incubate in the dark for 10 min at room temperature (*see* **Note 16**).
2. Acquire the images under a fluorescence microscope with the settings for green fluorescence (Fig. 5).

3.5.2 Neutral Red Staining

1. Stain the vacuoles with Neutral Red (Sigma) (4 μM, final concentration), a lipophilic phenazine dye that accumulates in intact and acidic vacuoles (*see* **Note 17**).
2. Acquire the images under a bright field microscope (Fig. 6).

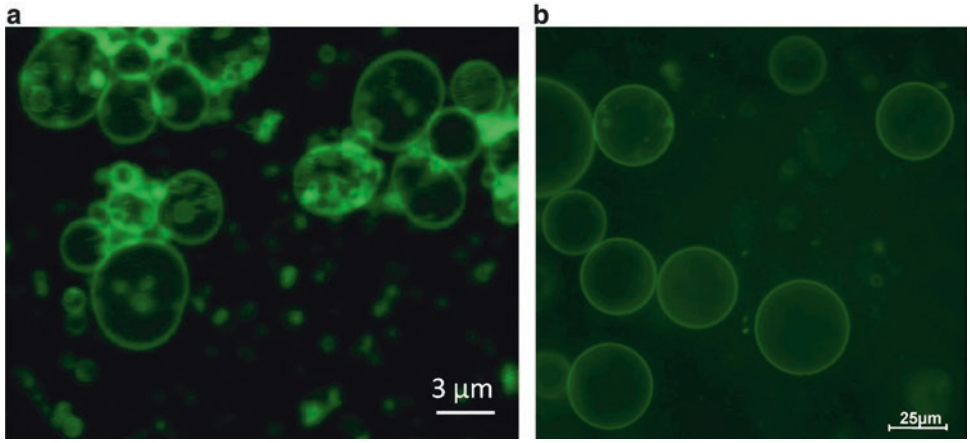

Fig. 5 Microscopy analysis of vacuoles (**a**) isolated from yeast stained with MDY-64 and (**b**) from plant cells stained with FM1-43. Adapted from [1, 17] (original publishers: Microbiology Society and BioMed Central, respectively)

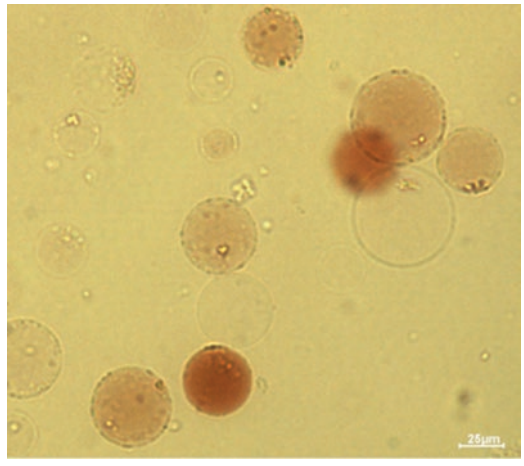

Fig. 6 Vacuoles isolated from plant cells stained with Neutral Red. Adapted from [17] (original publisher: BioMed Central)

3.6 Study of the Activity of Proton Pumps in Isolated Yeast and Plant Vacuoles

3.6.1 Proton Pumping Activity of V-H^+-ATPase in Yeast Isolated Vacuoles

V-H^+-ATPase can be evaluated in vacuoles isolated from yeast and plant cells. V-H^+-PPase activity is only measurable in plant cell vacuoles.

1. In a quartz cuvette add 2 mL ATPase buffer, 2 µM of the pH-sensitive fluorescent probe ACMA, and 20 µg protein of isolated yeast vacuoles.
2. Set the excitation and emission wavelengths to 415 and 485 nm, respectively.
3. When a baseline is reached, start the reaction by adding 0.2–1 mM ATP and record the rate of initial fluorescence quenching (*see* **Note 18**).

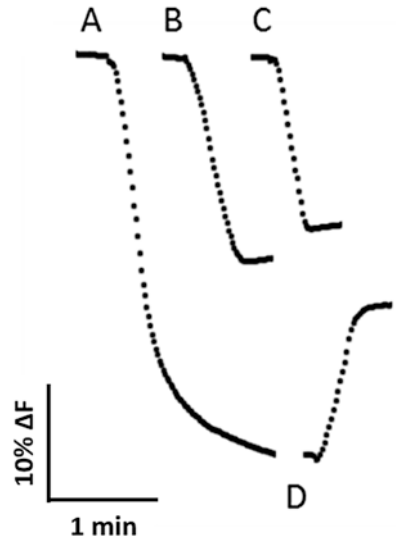

Fig. 7 V-H$^+$-ATPase activity in intact vacuoles purified from yeast. (**a**) Typical fluorescence signal of the initial velocity of proton pumping by V-H$^+$-ATPase in a vacuolar suspension after adding 1 mM ATP, (**b**) nonspecific effect on the fluorescence intensity after the addition of ATP in the absence of vacuoles, (**c**) inhibition of proton pumping activity by concanamycin A added before ATP addition, and (**d**) dissipation of the proton gradient by addition of 1 mM $CaCl_2$ at the steady-state. Adapted from [1] (original publisher: Microbiology Society)

4. At the steady-state, add 1 mM $CaCl_2$ or 50 nM concanamycin A (Fig. 7) (*see* **Notes 19** and **20**).
5. Estimate the initial rates of proton uptake (or proton dissipation) as $\Delta\%F$ min^{-1} (mg protein)$^{-1}$ and estimate the kinetic parameters, K_m and V_{max}, from Michaelis–Menten kinetics.

3.6.2 Proton Pumping Activity of V-H$^+$-PPase in Isolated Plant Vacuoles

1. In a quartz cuvette add 2 mL PPase buffer, 2 μM ACMA, and 1×10^4–1×10^5 of isolated plant vacuoles and set the excitation and emission wavelengths to 415 and 485 nm, as reported above.
2. When a baseline is reached, start the reaction by adding 1–150 μM PPi and record the rate of initial fluorescence quenching.
3. Add 150 mM NH_4Cl or 25 μM CCCP at the steady state (*see* **Note 21**).
4. Estimate the initial rates of proton uptake (or proton dissipation) as $\Delta\%F$ min^{-1} (mg protein)$^{-1}$ and estimate the kinetic parameters, K_m and V_{max}, from Michaelis–Menten kinetics.
5. To measure V-H$^+$-ATPase activity in plant vacuoles add ATP-Mg instead of PPi (Fig. 8).

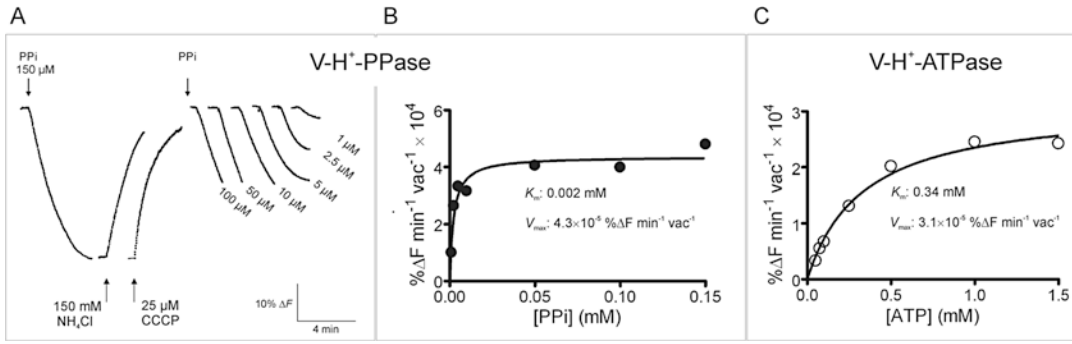

Fig. 8 Proton pumping activity in vacuoles purified from plant cells. (**a**) Initial velocities of proton pumping by V-H$^+$-PPase after addition of 1–150 μM PPi and dissipation of the gradient by addition of 150 mM NH_4Cl and 25 μM CCCP. (**b**) Michaelis–Menten plot of the initial velocities presented in (**a**). (**c**) Michaelis–Menten plot of the initial velocities of proton pumping by V-H$^+$-ATPase for 0.05–1.5 mM ATP. Reproduced from [17] (original publisher: BioMed Central)

4 Notes

1. The birrefringency of the cell walls observed under the phase contrast microscope decreases during the digestion and spheroplasts acquire rounded shapes. As they become osmotically fragile, spheroplasts will suffer lysis observable under the bright field microscope in the presence of 0.1% SDS.
2. Ficoll is a hydrophilic polysaccharide which dissolves readily in aqueous solutions. Solutions below 20% (w/v) have a density of 1.07 g/cm^3 and are considered osmotically inert.
3. Cell membrane disruption should be monitored under a bright field microscope every ten strokes so as not to compromise vacuolar integrity with longer homogeneization times.
4. To increase vacuole yield, the pellet can be resuspended with 10 mL of 12% Ficoll and the homogenization step be repeated.
5. Special care must be taken when preparing the gradient. The tube may be placed at a 45° position and the 8% Ficoll solution added very slowly so as not to disturb the gradient.
6. Maximum acceleration may be applied, but maximum deceleration will damage the gradient, so set this value between maximum deceleration and no brake (in the Beckman Optima XL 90 ultracentrifuge you can set deceleration to 6).
7. Protein concentration of the vacuole and protoplast suspensions can be determined by the Lowry method [28].
8. A further step of purification can be performed using the silicone oil technique [29]. Briefly, mix 20 μg vacuoles with buffer containing 40% (v/v) Percoll, 0.45 M sorbitol and 30 mM HEPES, pH 7.4. On the top of the mixture add Wackman

silicone oil AR-200, and then 0.4 M mannitol and 0.01 M HEPES pH 7.4. Centrifuge at 14,000 × *g* for 1 min and recover the purified vacuoles in the mannitol fraction (*see* Ref. 1).

9. A protoplast yield of 13% can be obtained as a result of a 12 h digestion protocol. Shorter digestion periods should result in lower protoplast yield.
10. The 3% Ficoll solution is prepared by diluting the lysis buffer with the vacuole buffer.
11. In a typical fractionation procedure, an average amount of 4.0×10^6 vacuoles is obtained, corresponding to about 12% of the total number of protoplasts (purified by a 12-h digestion protocol) subjected to lysis.
12. For each experiment, analyze up to 20,000 events at a low flow rate. Data may be analyzed in a proper software such as Flowing Software or FlowJo.
13. To ascertain if the obtained vacuolar fraction is contaminated with mitochondria stain the vacuoles in the same conditions with the mitochondrial marker NAO (5 μM, final concentration) [30–32].
14. Membrane potential dissipation can be monitored by the addition of 5 mM NH_4Cl to vacuoles pre-stained with $DiBAC_4(3)$.
15. Dissipation of the calcium accumulated in the vacuole can be monitored by the addition of 300 μM of the calcium ionophore calcimycin.
16. FM1-43 is a lipophilic die that shines when inserted in the hydrophobic core of the biological membrane. MDY-64 specifically binds to the yeast vacuole membrane according to the manufacturer.
17. Make a stock solution of 500 mM Neutral Red in mannitol, pH 7.5 prior to use.
18. The nonspecific effect on the fluorescence intensity after the addition of ATP in the absence of vacuoles (observed in Fig. 7) can be avoided by the addition of 2 mM $MgCl_2$ instead of ATP (This should be previously dissolved in the reaction mixture).
19. When the isolated fraction is enriched in pure and active vacuoles, $CaCl_2$ dissipates the gradient formed by ATP hydrolysis through CAX (H^+/cation exchanger) transporters of the vacuole membrane. Concanamycin A is a specific inhibitor of V-H^+-ATPase.
20. At this stage, 100 μM sodium azide (NaN_3) or 100 μM orthovanadate (Na_3VO_4), specific inhibitors of the mitochondrial F-ATPase and the plasma membrane P-ATPase, respectively, may be used to check for the purity of the vacuole fraction.
21. To dissipate the pH gradient which induces a recovery of the ACMA fluorescence.

References

1. Rodrigues J, Silva RD, Noronha H et al (2013) Flow cytometry as a novel tool for structural and functional characterization of isolated yeast vacuoles. Microbiology 159:848–856
2. Guicciardi ME, Leist M, Gores GJ (2004) Lysosomes in cell death. Oncogene 23:2881–2890
3. Klionsky DJ, Herman PK, Emr SD (1990) The fungal vacuole: composition, function, and biogenesis. Microbiol Rev 54:266–292
4. Li SC, Kane PM (2009) The yeast lysosome-like vacuole: endpoint, function, and biogenesis. Microbial Rev 54:266–292
5. Pereira C, Chaves S, Alves S et al (2010) Mitochondrial degradation in acetic acid-induced yeast apoptosis: the role of Pep4 and the ADP/ATP carrier. Mol Microbiol 76:1398–1410
6. Schauer A, Knauer H, Ruckenstuhl C et al (2009) Vacuolar functions determine the mode of cell death. Biochim Biophys Acta 1793:540–545
7. Andreev IM (2012) Role of the vacuole in the redox homeostasis of plant cells. Russ J Plant Physiol 59(5):611–617. Original Russian Text, IM Andreev, 2012, published in Fiziologiya Rastenii, 2012, 59(5): 660–667
8. Zhang C, Hicks GR, Raikhel NV (2015) Molecular composition of plant vacuoles: important but less understood regulations and roles of tonoplast lipids. Plants 4:320–333
9. Yang S-Y, Huang T-K, Kuo H-F et al (2016) Role of vacuoles in phosphorous storage and remobilization. J Exp Bot. https://doi.org/10.1093/jxb/erw481
10. Hirawa N, Kondo M, Nishimura M et al (1997) An aspartic proteinase is involved in the maturation of storage proteins in concert with the vacuolar processing enzyme. Eur J Biochem 246:133–141
11. Obara K, Kuriyama H, Fukuda H (2001) Direct evidence of active and rapid nuclear degradation triggered by vacuole rupture during programmed cell death in zinnia. Plant Physiol 125:615–626
12. Ueda H, Nishiyama C, Shimada T et al (2006) AtVAM3 is required for normal specification of idioblasts, myrosin cells. Plant Cell Physiol 47:164–175
13. Martinoia E, Maeshima M, Neuhaus HE (2007) Vacuolar transporters and their essential role in plant metabolism. J Exp Bot 58:83–102
14. Hara-Nishimura I, Hatsugai N (2011) The role of vacuole in plant cell death. Cell Death Differ 18:1298–1304
15. Graham LA, Flannery AR, Stevens TH (2003) Structure and assembly of the yeast V-ATPase. J Bioenerg Biomembr 35:301–312
16. Kane PM (2006) The where, when, and how of organelle acidification by the yeast vacuolar H^+-ATPase. Microbiol Mol Biol Rev 70:177–191
17. Fontes N, Silva R, Vignault C et al (2010) Purification and functional characterization of protoplasts and intact vacuoles from grape cells. BMC Res Notes 3:19
18. Michaillat L, Baars TL, Mayer A (2012) Cell-free reconstitution of vacuole membrane fragmentation reveals regulation of vacuole size and number by TORC1. Mol Biol Cell 23:881–895
19. Sarry JE, Chen S, Collum RP et al (2007) Analysis of the vacuolar luminal proteome of *Saccharomyces cerevisiae*. FEBS J 274:4287–4305
20. Wiederhold E, Gandhi T, Permentier HP et al (2009) The yeast vacuolar membrane proteome. Mol Cell Proteomics 8:380–392
21. Schmidt UG, Endler A, Schelbert S et al (2007) Novel tonoplast transporters identified using a proteomic approach with vacuoles isolated from cauliflower buds. Plant Physiol 145(1):216–229. Epub 2007 July 27
22. Decker BL, Wickner WT (2006) Enolase activates homotypic vacuole fusion and protein transport to the vacuole in yeast. J Biol Chem 281:14523–14528
23. Carqueijeiro I, Noronha H, Duarte P et al (2013) Vacuolar transport of the medicinal alkaloids from *Catharanthus roseus* is mediated by a proton-driven antiport. Plant Physiol 162(3):1486–1496
24. Martins V, Hanana M, Blumwald E et al (2012) Copper transport and compartmentation in grape cells. Plant Cell Physiol 53(11):1866–1880
25. Sousa MJ, Azevedo F, Pedras A et al (2011) Vacuole-mitochondrial cross-talk during apoptosis in yeast: a model for understanding lysosome-mitochondria-mediated apoptosis in mammals. Biochem Soc Trans 39(5):1533–1537
26. Silva P, Façanha AR, Tavares RM et al (2010) Role of tonoplast proton pumps and Na+/H+ antiport system in salt tolerance of populus eufrática oliv. J Plant Growth Regul 29(1):23–34
27. Queirós F, Fontes N, Silva P et al (2009) Activity of tonoplast protón pumps and Na+/H+ exchange in potato cell cultures is modulated by salt. J Exp Bot 60(4):1363–1374

28. Lowry OH, Rosebrough NJ, Farr AL et al (1951) Protein measurement with the Folin phenol reagent. J Biol Chem 193:265–275
29. Tohge T, Ramos MS, Nunes-Nesi A et al (2011) Toward the storage metabolome: profiling the barley vacuole. Plant Physiol 157:1469–1482
30. Maftah A, Petit JM, Ratinaud MH et al (1989) 10-N nonyl-acridine Orange: a fluorescente probe which stains mitochondria independently of their energetic state. Biochem Biophys Res Commun 164:185–190
31. Petit JM, Maftah A, Ratinaud MH et al (1992) 10N-nonyl acridine orange interacts with cardiolipin and allows the quantification of this phospholipid in isolated mitochondria. Eur J Biochem 209:267–273
32. Septinus M, Seiffert W, Zimmermann HW (1983) Hydrophobic acridine dyes for fluorescence staining of mitochondria in living cell. 1. Thermodynamic and spectroscopic properties of 10-n-alkylacridine orange chlorides. Histochemistry 79:443–456

Chapter 9

Live Cell Imaging and Confocal Microscopy

Luciana Renna, Giovanni Stefano, and Federica Brandizzi

Abstract

The availability of more specific dyes for a subset of endomembrane compartments, combined with the development of genetically encoded probes and advanced microscopy technologies, makes live cell imaging an approach that goes beyond the microscopically observation of cell structure. Here we describe the latest improved techniques to investigate protein–protein interaction, protein topology, and protein dynamics.

Furthermore, we depict new technical approaches to identify mutants for chloroplast morphology and distribution through the tracking of chlorophyll fluorescence, as well as mutants for chloroplast movement.

Key words Plant cell, FRAP, iFRAP, BIFC, Protein interaction, Protein topology, Chloroplast movement, Photosynthesis, VAEM

1 Introduction

Cell biology has made huge progresses with the advent of confocal microscopy applied with genetically encoded fluorophores. The combination of these tools allows for in vivo studies at cellular level and in entire organisms. Also, the broad variety of the molecular dyes now available has made a strong impact. For example, dyes such as FM4-64 and DiOC6 have been used in several studies for membrane staining in live cells; nonetheless, the incorporation of these lipophilic dyes in prolonged time stains most the endomembranes making it very difficult to perform single organelles analyses. Advances in this field led to the development of new chemical dyes that allow the identification of new cellular structures. Furthermore, with the advent of genetically encoded fluorescent probes, studies at specific organelle level have become possible.

The use of molecular markers that target specific endomembrane compartment combined with the confocal microscopy allows for studying not only mechanisms for organelle targeting but also the identification of specific machinery components, protein–protein

Cláudia Pereira (ed.), *Plant Vacuolar Trafficking: Methods and Protocols*, Methods in Molecular Biology, vol. 1789,
https://doi.org/10.1007/978-1-4939-7856-4_9,

interactions, as well as the study of protein topology and protein intraorganelle and interorganelle dynamics. Confocal microscopy methodologies that enable this kind of analyses include fluorescence recovery after photobleaching (FRAP) (with all its variants like iFRAP and two-color FRAP) and bimolecular fluorescence complementation (BiFC).

Specific protein targeting to organelles in vivo is fundamental to investigate organelle function and biogenesis but also organelle interactions with other cellular compartments and components, underling that analyses in vivo using specific probes may be highly relevant to the understanding of the physiology of a specific cell type or entire organism.

Among all the cell types that best allow for high-resolution imaging of the secretory pathway are the leaf epidermal cells. This specific cell type has indeed the advantage not only to be large but also to have a large central vacuole that makes the cytoplasm confined to a cortical thin layer, which makes endomembrane imaging easier. Moreover in photosynthetic organisms, through the imaging of epidermal and mesophyll cells live cell confocal microscopy allows investigating chloroplasts morphology, biogenesis, and conduct chloroplast photo-relocation experiments by simply using the autofluorescence of chlorophyll without the need of introducing foreign fluorescence markers into the organism. Thanks to this kind of analysis, it is possible to have information also on the photosynthetic performance of plants. The newest methodologies that can be applied through live cell confocal allow also the study of important components of plant structures, an example is the total internal reflection fluorescence (TIRF) variant, also named variable epifluorescence microscope (VAEM). This technique can be applied to image cellulose microfibrils to study their orientation through the vital molecular dye Direct 23.

1.1 FRAP, iFRAP, and Two-Color FRAP

In order do study protein dynamics in vivo, it is possible to use techniques like FRAP (fluorescence recovery after photobleaching) and iFRAP (inverse FRAP). Photobleaching analysis allows monitoring the dynamics of proteins with a highly refined precision and in the range of subseconds. This method provides information such as protein retention at membrane level, interaction with other proteins and prediction of trafficking mechanisms. FRAP and iFRAP techniques can be performed to measure protein diffusion and the ratio of protein exchange between compartments. FRAP is performed by irreversibly photobleaching a fluorochrome in a specific area of the cell called region of interest (ROI) using high intensity illumination of a laser line that excites the fluorochrome; in contrast, for iFRAP a whole cell area or organelle is photobleached, except a selected small area of interest. By disrupting a fluorochrome integrity, the protocol enables monitoring only the pool of fluorochrome that has not been bleached. Only the

nonbleached fluorochromes, such as those of fluorescent proteins, can diffuse into the bleached area (FRAP) or outside (iFRAP) with a recovery rate that is specific for each protein fusion. From this kind of experiments, one obtains information about kinetic plots of the fluorescence changes in the ROI [1–4]. It is therefore possible to calculate protein mobile fraction and immobile fraction. The mobile fraction represents the fraction of fluorescent probes that can exchange between the bleached region of interest and nonbleached area, while the immobile fraction is the fraction that cannot exchange between these two regions. The evaluation of mobile fraction values can be important to understand protein–protein interactions or protein–membrane domain association.

FRAP can also reveal the existence of intercompartmental communication and rates of movement of molecules within or between compartments. This kind of information generally is useful to capture a broad picture of the functional organization of the cell. For example, in plant cells FRAP is useful to examine protein exchange between compartments that could be functionally or physically connected. Indeed, using a fluorescent protein targeted to the stroma of plastid this approach has been used to test whether chloroplasts could exchange protein molecules through stromules, which are narrow chloroplast–chloroplast connecting structures [5].

Another useful variant of FRAP is the two-color FRAP. Two-color FRAP is used to investigate mutual mobility of two proteins which belongs or form a complex. The principle of technique is similar to the single channel FRAP; the only difference is that we can use two proteins, fused to different fluorophore (which possesses different spectral properties to avoid signal overlapping). Simultaneous FRAP of both fluorophores can be performed using two channels with specific excitation and emission wavelength ranges. This allows for measuring the protein turnover of the two molecules at the same time.

1.2 Use of Chlorophyll Autofluorescence to Identify Possible Photosynthetic Mutant and Chloroplast Fractal Analysis

The use of confocal microscopy is convenient for studying photosynthetic organelles like chloroplast in plants or algae. By taking advantage of chlorophyll autofluorescence, it is possible to visualize these organelles without tagging them with foreign fluorophores. With this approach, it is possible to identify chloroplast mutants with defects in the morphology or distribution of these photosynthetic organelles [6]. Furthermore, the availability of fast scan Z-drive available in the newest microscope systems now gives the possibility to acquire Z-stacks in a very short time without, thus limiting the potential artifacts owing to movement of chloroplasts during the image acquisition. The images acquired and reconstructed in the Z-direction provide abundant information, including number and size of each chloroplast, shape, and spatial arrangement. The latter can be analyzed in detail using fractal

analysis from which we can obtain fractal dimensions (D) and lacunarity parameter (Λ) for each acquired image. The obtained values of D allow establishing the geometric complexity of the distribution of chloroplasts for comparison across different experimental conditions or mutants. Instead, the heterogeneity (e.g., the gaps) in the distribution of chloroplasts is defined by Λ (Fig. 1).

Another useful analysis is the photo relocation of chloroplasts, which can be performed to calculate the velocities of this organelle in different conditions or mutants. Chlorophylls can be excited with laser line of 514 nm and light emitted can be detected at 650–700 nm.

1.3 Bimolecular Fluorescence Complementation (BIFC)

BIFC is a useful technique to study protein topology, protein–protein interaction or to screen a prey genomic library tagged with half moiety fluorescent protein for possible interactors against bait fused with the other half fluorescent protein [7]. Unfortunately, if not properly executed, this technique can provide false positive results, so specific precautions and improvements have been developed in the recent years.

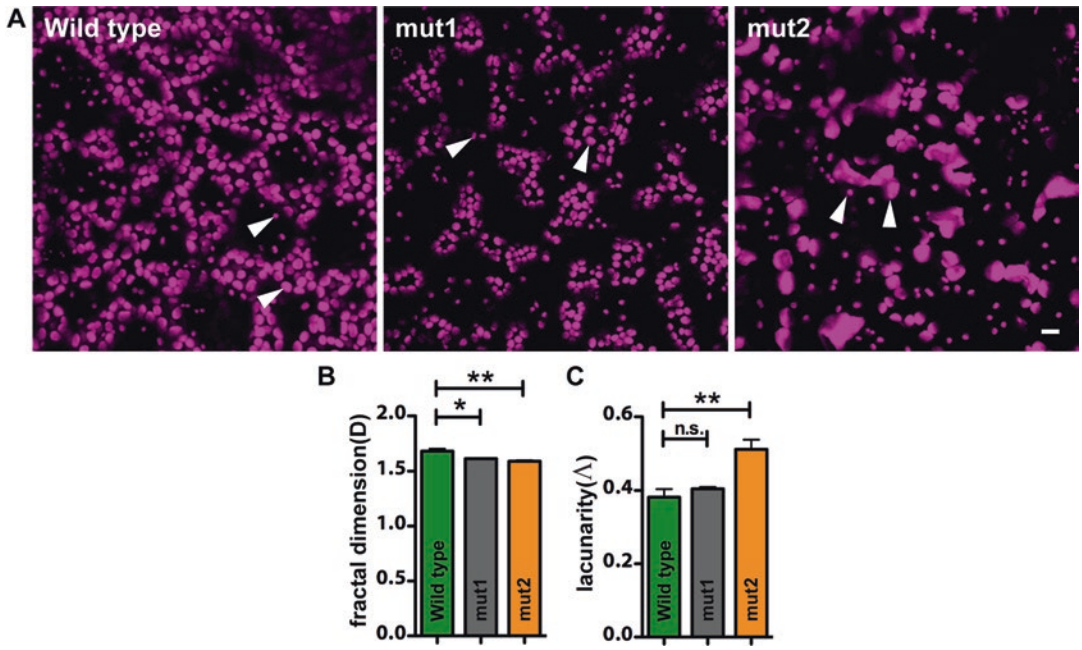

Fig. 1 (**a**) Confocal images of the chloroplasts from wild type, mut1 (mutant 1), and mut2 (mutant 2) plant leaves. Arrowheads indicate chloroplasts. Each image in panel A is the result of a Z-stack obtained from 25 confocal planes acquired starting from the abaxial surface of the leaf. Scale bar = 10 μm. (**b**) Fractal dimensions (D) of the wild type and mutant plants calculated from 10 images to compare the chloroplast distribution and geometry. (**c**) Lacunarity parameters (∧) calculated from 10 images. Error bars indicate SEM. **0.001 > P < 0.01; *0.01 > P < 0.05; n.s., not significant

1.3.1 BiFC for Topology

The classical BIFC experiments have been performed by splitting the YFP in a first half containing amino acids 1–154 (N terminal YFP) and the second half containing amino acids 155–239 (C terminal YFP). These two halves are generally fused to the proteins for which an interaction is to be tested. In this classical setup the nonspecific reconstitution of the entire YFP protein is recurrent. However, such feature has proven advantageous to establish protein topology. Specifically, this method can be used to study protein orientation with respect to a membrane in most organelle with the premises that a reference protein for each side of the compartment under investigation is available. Once a reference protein with an established subcellular is selected (preferable a soluble protein) then it should be fused to either the N or C terminal half of YFP while the complementary half should be fused to the protein to be investigated. It is worth to mention that for this approach YFP is commonly used; however, any fluorescent variant can be used [8]. Detection of a fluorescence signal will inform us if the two proteins are facing the same compartment with respect to a membrane or to the organelle investigated, and as a result it is possible to determine the protein orientation (Fig. 2) (*see* **Note 1**).

1.3.2 BIFC for Protein Interaction

As stated before the commonly used BiFC approaches are generally prone to false results, showing fluorescent protein reconstitution even when the two proteins are not true interactors [9–11]. A more reliable system has been optimized to test and quantify the level of interaction at the same time. This is the ratiometric BIFC (rBIFC) approach [12] that consists of a single binary vector that has multiple expression cassettes. The system named "2 in 1" has the half N-terminal YFP (1–155) in one cassette and the other C-terminal YFP (156–239) in another cassette. This system possesses also a soluble monomeric red fluorescent protein (mRFP) that allows the ratiomentric analysis because it works as internal control of expression. This system can be used in different organism (*see* **Note 2**).

Recently, after different attempts of splitting the fluorescent proteins in different positions or introducing point mutations to eliminate nonspecific self-assembling of the complementary halves, a novel modified approach has been proposed, which, as stated by the authors, should have "zero background" BIFC [13]. In this new system a binary vector is composed of two expression cassettes driven by the same promoter and contains an additional fluorescent marker (mTurquoise2) to discriminate between transformed and non transformed cells (internal control of successful transformation). In one cassette, the vector contains the half N-terminal YFP (1–210) and in the other cassette the C-terminal YFP (211–239). This split position reduces the nonspecific signal frequently obtained with the approaches described above to a zero background signal [13].

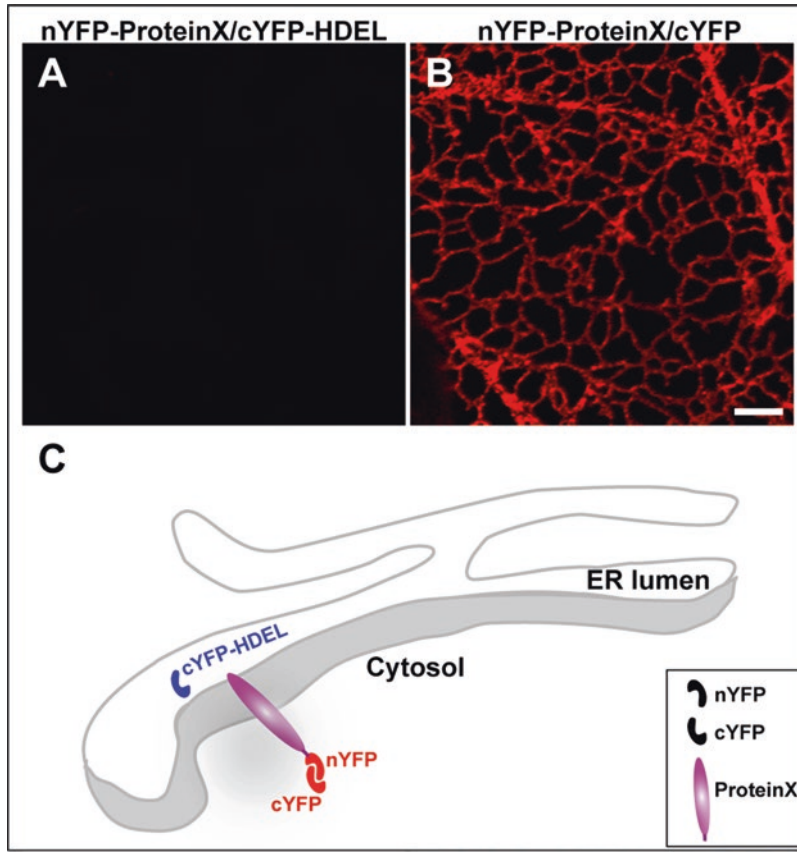

Fig. 2 Example of BIFC to investigate membrane protein topology. To map the N-terminal region of a ProteinX fused with half YFP, coespression analysis is performed in presence of the other half YFP expressed in the cytosol or ER lumen. (**a**) Confocal image of *N. tabacum* epidermal cells expressing ProteinX fused with half YFP and half YFP fused to an ER luminal protein. (**b**) Confocal image of *N. tabacum* epidermal cells expressing ProteinX fused with half YFP and half YFP fused to a cytosolic protein. Fluorescence detection in this case indicates that the protein face the cytosol with its N-terminal region. (**c**) Cartoon depicting the approach used to map the N-terminal of an ER ProteinX

1.4 Variable-Angle Epifluorescence Microscopy (VAEM)

VAEM technique derives from total internal reflection fluorescence microscopy (TIRFM). TIRFM is a useful technique to observe fluorescent probes on the plasma membrane edge of animal cells. In plant cells, the thick cell walls surrounding the plasma membrane form a barrier, limiting the use of the TIRF. However, VAEM represents a useful variant which allows for imaging plasma membrane molecules and study their behavior [14]. Here we describe how to use VAEM technique to investigate the behavior and orientation of cellulose microfibrills in *A. thaliana* seedlings stained using a well-characterized fluorescent probes known as Pontamine Fast Scarlet 4B or Direct RED 23 (Fig. 3) [15].

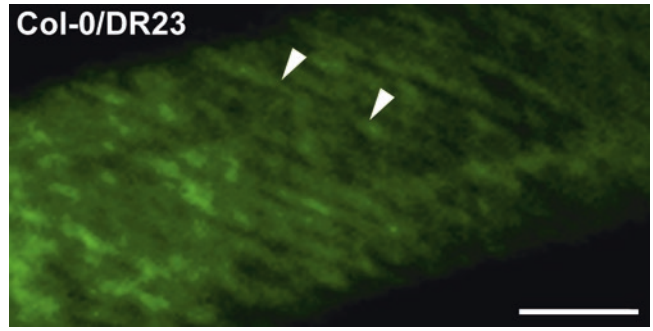

Fig. 3 Direct RED 23 (DR23) fluorescence acquisition by VAEM of *A. thaliana* hypocotyl epidermal cells. Arrowheads indicate cellulose microfibril. Scale bar = 5 μm

2 Material

2.1 FRAP

1. Plant plasmids: The gene of interest can be fused to any fluorescent protein variant in two ways: (1) Subcloning the gene in plant binary vectors already containing the XFP. (2) Fusing the CDNA of the gene of interest with the XFP by overlapping PCR [4, 16] and then cloning the obtained product in a binary vector without the XFP sequence.
2. Agrobacterium and Media:
   (a) Strain of agrobacterium: GV3101::mp90 containing the binary vector created as described above.
   (b) Antibiotics to select agrobacteria and plasmid: for GV3101::mp90 selection Gentamycin 25 μg/mL and rifampicin 50 μg/mL, plasmid selection varies depending on the specific resistance of the plasmid utilized, for the binary vector pVKH18En6 the antibiotic added to the media for selection in addition to gentamicin and rifampicin, will be kanamycin 100 μg/mL.
   (c) LB media for bacteria growth: tryptone (10 g/L), yeast extract (5 g/L), sodium chloride (10 g/L) pH 7.0.
   (d) Infiltration Buffer: 0.5% D-glucose, 50 mM MES, 2 mM Na_3PO_4* 12 H_2O, 0.2 mM acetosyringone.
3. Three-four weeks old *Nicotiana tabacum*, grown in growth chambers at 23 °C for 18 h light and 18 °C for 6 h dark.
4. Stable lines of *Arabidopsis thaliana* obtained accordingly to the protocol of Clough and Bent [17] and expressing the gene of interest can be used at different growth stages.
5. 25 mM latrunculin B solution.
6. Confocal microscope equipped with 10×, 40× and 60× objectives.

2.2 Chlorophyll Autofluorescence Imaging and Chloroplast Fractal Analysis

1. *Arabidopsis thaliana* EMS mutagenized or tDNA insertion lines grown in chambers with controlled temperature conditions 20 °C and 125 μmol m^{-2} s^{-1} white light with a photoperiod of 16 h of light followed by 8 h of dark.
2. Growth substrate:
   (a) Substrate for stratification: 0.1% Phytoblend.
   (b) Soil: sterilized mixture of Bacto High Porosity Professional Planting Mix, vermiculite and perlite with ratio 1:1:1
   (c) Sterile substrate for in vitro growth: Linsmaier and Skoog (LS) medium containing 0.5% Phytoblend, 2% sucrose.
3. Sterilization solutions:
   (a) 70% ethanol containing 0.5% Triton X-100.
   (b) 95% ethanol.
   (c) Sterilized filter paper.
4. Confocal microscope equipped with 10× and 40× objectives.

2.3 BIFC

1. Plant plasmids—the gene of interest can be fused to the half N or C terminal portion of YFP in two ways: (1) Subcloning the gene in plant binary vectors already containing the N terminal or C terminal half portion of YFP. (2) Fusing the CDNA of the gene of interest with the half YFP by overlapping PCR [4, 16] and then cloning the obtained product in a binary vector without the YFP sequence.
2. Agrobacterium and Media:
   (a) Strain of agrobacterium: GV3101::mp90 containing the binary vector created as described above.
   (b) Antibiotics to select agrobacteria and plasmid.
   (c) LB media for bacteria growth: Tryptone (10 g/L), yeast extract (5 g/L), sodium chloride (10 g/L) pH 7.0.
   (d) Infiltration Buffer: 0.5% D-glucose, 50 mM MES, 2 mM Na_3PO_4*$12H_2O$, 0.2 mM acetosyringone.
3. Plants: 3–4 weeks old Nicotiana tabacum, grown in growth chambers at 23 °C for 18 h light and 18 °C for 6 h dark.
4. Confocal microscope equipped with 10×, 40× and 60× objectives.

2.4 Variable-Angle Epifluorescence Microscopy (VAEM)

1. 0.01% (w/v) Direct RED 23 in liquid 0.5× LS or MS medium.
2. LS or MS medium.
3. Confocal laser scanning microscopy (CLSM) with VAEM mode (100× objective)

3 Methods

3.1 FRAP

FRAP and iFRAP techniques can be applied to endomembrane compartments or structures that are non-cytoskeleton driven or endomembranes/organelles that are guided by actin or microtubules. In this case the use of depolymerizing agents prior to imaging is generally necessary to reduce organelle movement significantly. For example, latrunculin B (actin depolymerizing agent) is generally used to stop Golgi movement [18, 19] and microtubule depolymerizing agents (oryzalin, nocodazole) can be used for organelles whose motility is driven by this cytoskeletal component.

FRAP analysis with the newest confocal systems has been very easy to perform thanks to the user-friendly software preinstalled in most of the systems available on the market. Here we describe a FRAP setup for Golgi bodies in a stable transgenic line of *A. thaliana* expressing a Golgi-specific fluorescent marker.

1. Use a cotyledon of young seedlings (i.e., 9 days after germination (DAG) (*see* **Note 3**).
2. Start the experiment by treating the sample to be investigated with an actin-depolymerizing agent in order to stop the movement of the Golgi stacks. To do so, submerge the tissue into 25 mM latrunculin B solution for at least 30 min (*see* **Note 4**).
3. Mount the tissue on the slide with the same solution using coverslips with the same thickness for all the experiments (*see* **Note 5**).
4. Open the microscope software and set up excitation and emission wavelengths for the fluorochrome of choice. Keep in mind that they should provide maximum signal yield with minimal laser intensity power and avoid pixel imaging oversaturation or undersaturation.
5. Acquire one image and select the following areas:
   (a) Draw a control region of interest (background ROI), where the fluorescent signal is visible. This ROI will allow checking for nonspecific bleaching during the process and will define the levels of fluorescence that should be reached upon the bleaching.
   (b) Select the number of preferred bleached regions (typically we use 2–3 ROIs), away from the background ROI. These regions should all be of similar area.
   (c) During FRAP analysis the background fluorescence curve will be analyzed against the bleached curve to eventually correct for any nonspecific bleaching.
6. Set up the confocal microscope software to acquire 10 frames before the bleaching period (prebleach time), and then acquires

images until the recovery of the fluorescence reaches a plateau in the bleached area (The acquisition time for postbleach depends on the protein investigated.).

7. Acquire at least 20 scans containing ROI background and bleached ROIs. Perform all the experiments using the same confocal settings, which include laser intensity, pinhole, objective, and zoom [20].

3.2 Chlorophyll Autofluorescence Imaging and Chloroplast Fractal Analysis

1. Use a rosette leaf from an Arabidopsis plant grown for 3 weeks under standard condition (22 °C temperature, 50% humidity with 16 h light and 8 h dark cycle).
2. Place the leaf sample (around 25 mm^2) (*see* **Note 6**) on a glass slide and place the abaxial or adaxial side facing the objective.
3. Make sure to use the fast scan Z-drive in order to minimize the imaging time and avoid long exposure of the sample to the laser.
4. Use a 20× or 40× objective. Here we used a 40×/1.30 objective mounted on an inverted confocal laser-scanning microscope.
5. Excite chlorophylls using at 514 nm using argon laser and collect the fluorescence between 650 and 700 nm [21, 22].
6. To compare the different samples, acquire the images using the same fixed laser intensity, pinhole, gain, and zoom.
7. Acquire for each Z stack between 25 and 50 sections of 1 μm (make sure to collect the same amount of section between samples) from the abaxial or adaxial surface scanning up to the region of the spongy mesophyll cells.
8. Collect at least ten scans for each sample or mutant to be analyzed.
9. Using the software provided with the confocal or ImageJ plugin extrapolate the maximum intensity projections from each Z-stack acquired.
10. Calculate the fluorescence values for each image using the software provided with the microscope and plot the values.
11. Calculate fractal dimensions and lacunarity parameters using the same maximum intensity projections by fraclac, an ImageJ plugin [23].

3.2.1 Photorelocation of Chloroplasts

1. Use a rosette leaf from an Arabidopsis plant grown for 3 weeks under 35 μmol m-2 s-1 white light (22 °C temperature, 50% humidity with 16 h light and 8 h dark cycle).
2. Place the leaf sample (around 25 mm^2) (*see* **Note 6**) on a glass slide and place the adaxial side facing the objective.
3. Use a 20× or 40× objective.

4. Set the confocal software to perform chloroplast irradiation (bleaching set-up on the software) by repeatedly laser pulse the region of interest for 2–3 s with a 488 nm laser at 2–5% of maximum power throughout the photorelocation experiment.
5. Acquire images of chlorophyll fluorescence between irradiations of the region of interest, using a 633 nm laser and collect fluorescence from 650 to 700 nm [21, 22].
6. The movement of the chloroplasts located in the cortical region of the spongy mesophyll was acquired.
7. Calculate chloroplast velocities using the Multi Kymograph plugin from ImageJ.
8. Analyze at least 25 and 40 kymographs, from ten independent cells to obtain a good statistics.

3.3 BIFC

3.3.1 Binary Vector

Use any of the binary vectors described above that is helpful for your experiment based on the requirements of the background levels. Here we used and describe the methodology for pVKH18En6 with the N- or C-terminal half of YFP fused to a protein of interest, but the same approach can be used for other vectors. The YFP in this vector is split at amino acid 155. The half YFP portion can be fused at the N- or C-terminus of our protein of interest; this choice depends on the properties of the protein investigated in order to preserve its functionality without affecting distribution and function.

3.3.2 Tobacco Infiltration

BIFC experiments lead generally to a stable protein–protein interaction. Therefore, transient expression should be preferred to stable transformation where reconstitution of the YFP bearing two irreversibly interacting proteins may cause developmental problems. Here we describe a BiFC protocol for transient transformation in tobacco leaf epidermal cells:

1. Prepare the infiltration buffer using 50 mg of D-glucose, 1 mL from a stock solution of 500 mM MES, 1 mL from a stock solution of 20 mM Na_3PO_4 $12H_2O$ (*see* **Note 7**), and 10 μL from a stock 200 mM of acetosyringone.
2. Perform Agrobacterium infiltration in tobacco leaf epidermis using 1 mL syringe containing the resuspended agrobacteria solution that will be pushed through the abaxial side of the leaf, balancing the pressure with your finger on the adaxial corresponding region.
3. Use the lowest bacterial optical density (OD) at 600 nm to limit protein overproduction, which can lead to false positives. To avoid nonspecific results, successful experiments have been performed using an OD with range between 0.0025 and 0.005 [11].
4. Observe the samples transformed, 48–72 h after bacterial infiltration.

3.3.3 Microscope Observations

1. Place the sample (around 25 mm^2 of leaf section) on a glass slide with the abaxial side towards the coverslip and scan with a confocal microscope.
2. Use a low magnification objective, for example, a 10×.
3. Check first the negative control for nonspecific results; this sample should not be fluorescent. On the contrary if it is fluorescent do not proceed to the next step, but repeat the whole experiment reducing the OD of bacteria.
4. Observe the sample containing the protein of interest to test occurrence of an interaction.
5. If an interaction takes place, acquire images with a 40× or 60× objective to obtain more information about the localization of the interactors.

3.4 Variable-Angle Epifluorescence Microscopy (VAEM)

1. Use young seedlings (3–12 DAG).
2. Incubate a seedling with 0.01% (w/v) Direct RED 23 in liquid 0.5× LS or MS medium for 30–45 min (*see* **Note 8**). The seedlings can be incubated in a 1 mL eppendorf tube.
3. Wash the seedling by transferring them into a new tube supplemented with fresh medium without the probe. Wash the sample at least three times.
4. Place the seedling on a glass slide and observe the sample with confocal laser scanning microscopy (CLSM) to confirm that the fluorescent probes stained your tissue.
5. Switch from CLSM to VAEM mode and set-up the system to image the sample of interest. Below the procedure for Nikon A1RSi TIRF system equipped with ANDOR camera (iXon Ultra):
   (a) Turn on all the components of the microscope.
   (b) Install the TIRF stage.
   (c) Select the 100× (NA 1.49) TIRF objective.
   (d) Open the NIS Elements software using ANDOR.
   (e) Open the following windows available through the software: TiPad, DU-897 settings, TIRF/SR-active, LUT.
6. Place the sample mounted on glass slide on the stage and cover with the TIRF stage coverplate.
7. Focus on the sample.
8. Perform a coarse alignment of TIRF as follow:
   (a) Select from top toolbar the TIRF_UP optical alignment configuration specific for the laser being used.
   (b) Turn the laser ON using the icon AOTF located in the TIRF/SR-active window.

(c) Center the laser using the knob on TIRF arm (*see* **Note 9**).

(d) With the apposite slider in unlock position focus the laser beam until the beam is as tight as possible.

(e) Turn the laser OFF using the same icon as in **step b**.

9. Perform a fine alignment of the TIRF angle as follow:

(a) Select the TIRF_ optical configuration specific for the laser being used.

(b) Using the DU-897 settings window select NO Binning, 1 frame exposure time, EM Gain 17 MHz at 16 bit, EM gain ~300.

(c) Turn the laser ON using the same icon as in **step 8b**.

(d) Select PLAY to turn the camera ON to acquire images. (*see* **Note 10**)

10. Use TiPad window to tune the TIRF angle in live mode. (*see* **Note11**)

11. Record movies for further analysis.

4 Notes

1. In the specific case of the localization of the protein in compartment that might affect fluorescent protein stability compartment the YFP can be replaced with more resistant for of fluorescent proteins like RFP, or mCherry.
2. The 2in1 system can be used in different cell or expression systems cloning using the enzymes SpeI and PsiI [12].
3. Different age seedling can be used, as well as leaf form mature plants.
4. Incubation with Latrunculin B should be performed for a time no longer than 90 min in order to reduce excessive cellular stress that may confound the results.
5. Coverslip thickness influences the results of the experiment.
6. On a glass slide and place the adaxial side facing the objective.
7. MES and Na3PO4 12H2O Stock should be sterilized by filtration and stored at 4 °C. Acetosyringone stock solution is prepared in DMSO and aliquoted in an Eppendorf tube and stored at −20 °C until use.
8. Incubation time with the fluorescent probe depends on the age of the seedlings.
9. Wear laser safety goggles.

10. If you do not see image, increase the laser power until fluorescence is detected.
11. Keep in mind that a value of TIRF equal to 4000 is close to the critical angle.

References

1. Renna L, Stefano G, Majeran W, Micalella C, Meinnel T, Giglione C, Brandizzi F (2013) Plant Cell 25:1756–1773
2. Stefano G, Renna L, Rossi M, Azzarello E, Pollastri S, Brandizzi F, Baluska F, Mancuso S (2010) Plant J 64:790–799
3. Takagi J, Renna L, Takahashi H, Koumoto Y, Tamura K, Stefano G, Fukao Y, Kondo M, Nishimura M, Shimada T, Brandizzi F, Hara-Nishimura I (2013) Plant Cell 25:4658–4675
4. Higuchi R, Krummel B, Saiki RK (1988) Nucleic Acids Res 16:7351–7367
5. Kohler R, Hanson M, Wildman S (1997) Trends Cell Biol 7:392–392
6. Larkin RM, Stefano G, Ruckle ME, Stavoe AK, Sinkler CA, Brandizzi F, Malmstrom CM, Osteryoung KW (2016) Proc Natl Acad Sci U S A 113:E1116–E1125
7. Berendzen KW, Bohmer M, Wallmeroth N, Peter S, Vesic M, Zhou Y, Tiesler FK, Schleifenbaum F, Harter K (2012) Plant Methods 8:25
8. Miller KE, Kim Y, Huh WK, Park HO (2015) J Mol Biol 427:2039–2055
9. Lalonde S, Ehrhardt DW, Loque D, Chen J, Rhee SY, Frommer WB (2008) Plant J 53:610–635
10. Kodama Y, Hu CD (2012) BioTechniques 53:285–298
11. Stefano G, Renna L, Brandizzi F (2015) Methods Mol Biol 1242:173–182
12. Grefen C, Blatt MR (2012) BioTechniques 53:311–314
13. Gookin TE, Assmann SM (2014) Plant J 80:553–567
14. Wan Y, Ash WM 3rd, Fan L, Hao H, Kim MK, Lin J (2011) Plant Methods 7:27
15. Anderson CT, Carroll A, Akhmetova L, Somerville C (2010) Plant Physiol 152:787–796
16. Ho SN, Hunt HD, Horton RM, Pullen JK, Pease LR (1989) Gene 77:51–59
17. Clough SJ, Bent AF (1998) Plant J 16:735–743
18. Brandizzi F, Snapp EL, Roberts AG, Lippincott-Schwartz J, Hawes C (2002) Plant Cell 14:1293–1309
19. Stefano G, Renna L, Brandizzi F (2014) J Cell Sci 127:947–953
20. Stefano G, Osterrieder A, Hawes C, Brandizzi F (2013) Methods Cell Biol 118:69–83
21. Serodio J, Ezequiel J, Frommlet J, Laviale M, Lavaud J (2013) Plant Physiol 163:1089–1102
22. Muller SM, Galliardt H, Schneider J, Barisas BG, Seidel T (2013) Front Plant Sci 4:413
23. Karperien A., http://rsb.info.nih.gov/ij/plugins/fraclac/FLHelp/Introduction.htm., (1999-2013)

Chapter 10

Imaging Vacuolar Anthocyanins with Fluorescence Lifetime Microscopy (FLIM)

Alexandra Chanoca, Brian Burkel, Erich Grotewold, Kevin W. Eliceiri, and Marisa S. Otegui

Abstract

Anthocyanins are intrinsically fluorescent pigments that accumulate in plant vacuoles. We have developed a platform to analyze the fluorescence decay of anthocyanins by fluorescence lifetime imaging microscopy (FLIM), under in vitro and in vivo conditions. Fluorescence lifetime of a fluorophore can be influenced by temperature, pH, oxygen concentration, and other environmental conditions. Within plant cells, the anthocyanin fluorescence lifetime correlates with distinct subcellular compartments. Vacuolar anthocyanins exhibit shorter fluorescence lifetime than the cytoplasmic pool. Consistent with these observations, lower pH of anthocyanins solutions correlated with shorter fluorescence lifetimes. We discuss here the use of FLIM as a tool for analyzing the subcellular distribution of anthocyanins and estimating variation in vacuolar pH in intact cells.

Key words Fluorescence lifetime microscopy (FLIM), Anthocyanins, *Arabidopsis thaliana*, Plant vacuole, pH

1 Introduction

Vacuoles are prominent organelles in plant cells that occupy up to 90% of the cellular volume. They play diverse functions such as turgor pressure maintenance, degradation and recycling of cellular components, sequestration of xenobiotics, storage of proteins, specialized metabolites, ions, sugars, hormones, and other signaling molecules [1]. Through the activity of vacuolar H^+-translocating ATPases (V-ATPAse) and pyrophosphatases (V-PPAse) localized to the vacuolar membrane or tonoplast, the lumen of vacuoles is acidic (pH ~4.9–6.0) [2–6]. The proton electrochemical gradient established between the cytoplasm and vacuolar lumen is used by other vacuolar transporters at the tonoplast, such as Na^+/H^+ antiporters, to pump ions into vacuoles. The acidic pH also favors the activity of a diverse set of vacuolar hydrolytic enzymes.

Cláudia Pereira (ed.), *Plant Vacuolar Trafficking: Methods and Protocols*, Methods in Molecular Biology, vol. 1789,
https://doi.org/10.1007/978-1-4939-7856-4_10,

Vacuoles in both vegetative and reproductive tissues also store water-soluble pigments, such as anthocyanins. Anthocyanins are avonoids that consist of an anthocyanidin backbone (e.g., cyanidin, pelargonidin, delphinidin) with different modi cations (glycosylation, methylation, coumarylation). Anthocyanins show pink-to-blue colors depending on pH and modi cations of the anthocyanidin backbone. Their synthesis occurs in the cytoplasm but their nal accumulation site is the vacuolar lumen [7, 8]. Because of the lower pH, anthocyanins are stable and pigmented inside vacuoles but not in the cytoplasm. However, anthocyanins show intrinsic uorescence regardless of their subcellular localization [9–11], providing opportunities for their subcellular imaging and detection.

Vacuolar pH can be measured in intact vacuoles by different techniques, such as ^{31}P-nuclear magnetic resonance (NMR) [2, 12], pH sensitive dyes [3, 4, 6], and genetically encoded probes [5, 13]. Each approach offers advantages and disadvantages. NMR is noninvasive and does not require exogenous probes but it is time consuming and expensive. Dyes offer a relatively simple and economic option but their penetration into plant tissues can be limited and often requires disruption of tissues and removal of cells walls. A pH-sensitive, genetically encoded probe targeted to the vacuolar lumen can be powerful but requires plant transformation.

We have developed a platform to measure fluorescence lifetime of vacuolar anthocyanins using fluorescence lifetime imaging microscopy (FLIM) [14] to analyze the microenvironment in which these pigments are, including vacuolar pH [9, 15]. Fluorescence lifetime refers to the time (usually in the order of picoseconds to nanoseconds) an electron stays in the excited state before decaying to the ground state by emitting a photon [16]. Fluorescence lifetime of a fluorophore can be influenced by temperature, pH, oxygen concentration, and other environmental conditions [14, 17, 18]. Our approach combines detection of anthocyanin fluorescence and variations in their fluorescence lifetime to analyze their subcellular localization and variations in vacuolar pH without the need of genetically encoded sensors or dyes.

2 Materials

2.1 PlantMaterial

1. Sterile hood.
2. 10% (v/v) bleach.
3. 70% (v/v) ethanol.
4. Sterile water.

5. Sterile glass Pasteur pipettes or sterile 1 mL pipette tips.
6. *Arabidopsis thaliana* wild type (WT), *tt4* (SALK_020583), *and 35S:γTIP:CFP* (CS16256) [19] seeds available from the Arabidopsis Biological Resource Center (ABRC, Columbus, OH), and *vha-a2vha-a3* mutant seeds available from researchers [3].
7. Half strength Murashige and Skoog plant growth medium supplemented with 5% (w/v) sucrose.
8. 100 mM naringenin (Sigma-Aldrich) in ethanol (Stock solution).
9. #1.5 cover glass (0.16–0.19 mm thickness, Ted Pella, Inc.).
10. 2.8 mm CoverWell™ Imaging Chambers.
11. 35 mm diameter petri dishes.

2.2 Anthocyanin Extraction

1. Extraction buffer: 50% (v/v) methanol, 3% (v/v) formic acid.
2. 0.05% (w/v) MES adjusted to pH to 4.5, 5.5, and 6.5 with KOH.
3. 1.5 mL microcentrifuge tubes polypropylene pellet pestle (e.g., blue pellet pestles from Kimble Chase).
4. Freeze dryer/lyophilizer.
5. 0.2 m lter.
6. Rotary shaker.
7. Centrifuge.
8. Spectrophotometer.

2.3 FLIM of Anthocyanins

1. Custom-built Multiphoton laser scanning system with WiscScan 7.2.2 acquisition software (http://loci.wisc.edu/software/wiscscan), a Mai Tai DeepSee Ti:Sapphire solid state laser (Spectra Physics) producing 100 fs pulses at a repetition rate of 80Mhz, and a Hamamatsu GaAsP PMT (Gallium arsenide phosphide photomultiplier tube; H7422P-40) (*see* **Note1**).
2. Emission lters: 602–662 nm band-pass (ET632/60 m Chroma Technology Corp), 415–485 nm band pass (Semrock FF01–450/70), and 445/20 nm band pass (Semrock FF01–445/20–25).
3. Urea crystals, used as an instrument response function standard.

2.4 ImageAnalysis Software

1. Becker-Hickl (BH) SPCImage software (http://www.becker-hickl.com/software.htm).
2. FIJI [20].

3 Methods

3.1 Induction of Anthocyanin Synthesis in Arabidopsis Seedlings

Arabidopsis seedlings grown under light in ½ strength Murashige & Skoog plant growth medium supplemented with 5% (w/v) sucrose (modi ed anthocyanin inductive conditions or mAIC) synthesize anthocyanins in cotyledons and hypocotyls (Fig. 1a). The *35S::γTIP-CFP* line expresses a tonoplast protein (TIP) fused to Cyan Fluorescent Protein (CFP), offering the possibility to visualize the position of the tonoplast in anthocyanin-accumulating cells. The *tt4* mutant lacks the chalcone synthase required for anthocyanin biosynthesis [21] (Fig. 1b), and it is used here as a negative control for anthocyanin uorescence. It is possible to induce the synthesis of anthocyanins in *tt4* by adding to the growth medium naringenin (50–100 M), an intermediate in the anthocyanin pathway and the product of the chalcone synthase encoded by TT4 (Fig. 2).

1. Place *Arabidopsis* seeds in a plastic tube and add 10% (v/v) bleach for 5 min, mixing occasionally.
2. Remove bleach using sterile glass Pasteur pipette or sterile 1 mL pipette tips (open the pipette tip box inside the hood) and rinse three times with sterile water.
3. Add 70% (v/v) ethanol, mix, and discard after 5 min.
4. In a sterile hood, rinse three times with sterile water and place seeds on petri plates containing half strength Murashige and Skoog plant growth medium supplemented with 5% (w/v) sucrose.
5. Stratify seeds at 4 °C for 2 days.
6. Place petri dishes with seeds at 25 °C under continuous cool-white light at approximately 100 mol m^{-2} s^{-1} on a rotary shaker at 100 rpm. Under these conditions (mAIC), WT, *35S::γTIP-CFP,* and *vha-a2vha-a3* seedlings will actively synthesize anthocyanins and turn purple (Fig. 1a).
7. To induce the synthesis of anthocyanins in *tt4* mutant seedlings grown under mAIC, add to 2.5-day-old seedlings naringenin to a nal concentration of 100 M from a 100 mM stock in ethanol.

3.2 FLIM of Anthocyanins

As an example, we describe the procedure to image *35S::γTIP-CFP* and anthocyanin uorescence in the same cells (*see* **Note 2**). Pavement cells of cotyledons preferentially at the lower epidermis are ideal for imaging.

1. Place seedlings between #1.5 coverslips.
2. Image the lower epidermis of cotyledons (*see* **Note 3**) in a custom-built multiphoton optical system controlled by the WiscScan 7.2.2 acquisition software with an 80 Mhz Mai Tai

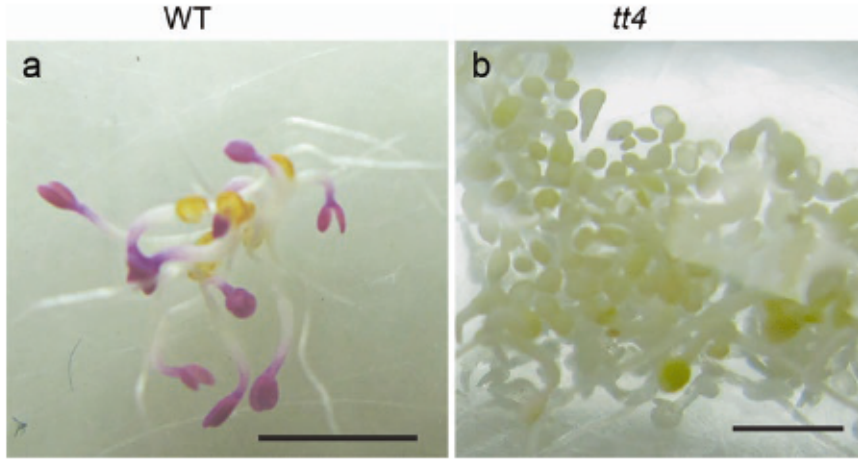

Fig. 1 5-day-old *Arabidopsis* seedlings grown in mAIC. Scale: 5 mm

DeepSee Ti:Sapphire solid laser yielding a 10 ns photon collection window.

3. To acquire the instrument response function used during image analysis, collect the second harmonic signal from urea crystals at 890 nm using a 445/20 nm filter and a 40× objective. Image the surface of one of the facets of the crystal.
4. To acquire fluorescence lifetime of anthocyanins, excite at 890 nm and collect emission using a 602–662 nm band-pass filter and time-correlated single-photon counting (TCSPC) electronics (Becker & Hickl GmbH; SPC-830). Each image is 256 × 256 with 256 time bins for each pixel. FLIM acquisition times typically range from 180 s to 240 s until approximately 1000 photons/pixel are collected. The power at the specimen should be adjusted to approximately 10–15 mW until the mean photon rate collected by the FLIM detector is at least 10^5 but not more than 10^6 to avoid fluorescence pileup. Save data as a ".sdt" file.
5. To detect *γTIP-CFP* at the tonoplast, excite CFP at 780 nm and collect emission with a 415–485 nm band pass filter (Fig. 2e).
6. The *tt4* seedlings grown in mAIC and without naringenin should be used as negative control to estimate the overall background fluorescence not related to anthocyanins.

3.3 Anthocyanin Extraction

1. Collect 7-day-old Ler-0 seedlings grown under mAIC, freeze them in liquid nitrogen, and grind them inside a plastic tube with a mini-pestle (*see* **Note 4**).
2. Freeze-dry seedlings and measure dry weight.
3. Add 1 µL of extraction solution per every 50 µg of dried weight plant material.

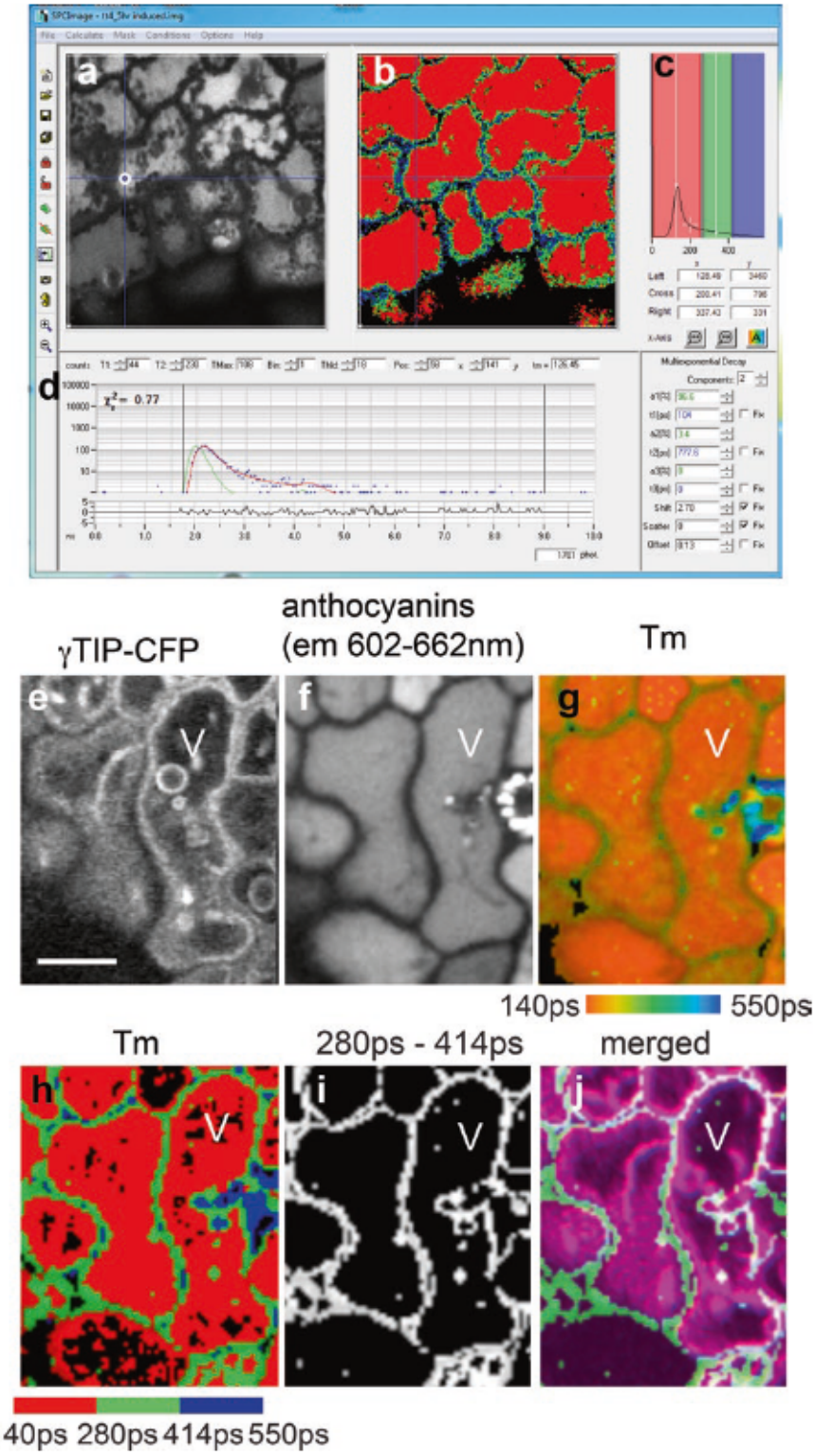

Fig. 2 FLIM analysis of anthocyanins by using the BH SPCImage software. Steady-state fluorescence intensity (**a**) and pseudo-colored according to three fluorescent lifetime (τ_m) range classes: 140–280 ps, 280–440 ps,

4. Incubate plant material in extraction solution at room temperature, overnight, on a rotary shaker.
5. Centrifuge at 13,500 × *g* for 2 min at room temperature.
6. Collect supernatant and pass it through a 0.2 m lter.
7. Collect ltrated anthocyanin extract.
8. Freeze-dry extracts and resuspend anthocyanins in distilled water to a nal concentration of 0.2 mg dry weight plant material/ L.
9. Optional: measure absorbance at 520 nm and 637 nm in a spectrophotometer and estimate anthocyanin content using Abs_{530}/g F.W. = [Abs_{530} (0.25 × Abs_{657})] × M-1, where A530 and A657 is the absorption at the indicated wavelengths and M is the weight of the plant material used for extraction in grams. This calculation does not provide absolute content but a corrected absorption value that is linearly correlated with anthocyanins content [22–24].
10. For adjusting to different pH, take 5 L of anthocyanin extract and add to 15 L of MES buffer equilibrated with KOH to pH 4.5, 5.5, and 6.5.

3.4 FLIM of Anthocyanin Extracts

1. Using a cork borer, puncture 5 mm holes on each corner of the 2.8 mm silicone imaging chamber before attaching the chamber to a 36 × 60 mm cover glass.
2. Place 5–10 L anthocyanin extracts in each hole for imaging and proceed as in Subheading 3.3 (**steps4** and **5**).

3.5 ImageAnalysis

The same general steps can be followed for images of cotyledon pavement cells and anthocyanin extracts.

1. Importing the "sdt" data le for the instrument response function (IRF) into the BH SPCImage software (*see* **Note 5**). Select the options and decay model that will be used for all

Fig.2 (continued) and 440–550 ps (**b**) in pavement cells of Arabidopsis cotyledons. (**c**) Histogram of the uorescence lifetime of the pixels from the FLIM image. (**d**) Fluorescence decay curve of anthocyanins from pixel indicated in (**a**) with a white circle. Photon decay values (blue points) are tted to a uorescence decay curve (red line) using double exponential function. The green lines represent the response function. The weighted least squares value or reduced Chi-square (X^2_r) is an indicator of the tting signi cance. (**e**) TIP-CFP detection in cotyledon pavement cells. (**f**) Steady-state uorescence of anthocyanins. (**g**) Pseudo-colored image of $_m$ values after analysis in the BH SPCImage software. (**h**) Pseudo-colored image according to three $_m$ range classes (140–280 ps, 280–440 ps, and 440–550 ps). (**i**) Pixels with $_m$ values within the 280–440 ps class. (**j**) Merged image of (**j**) in green and (**a**) in magenta. Colocalization is shown in white. The position of the tonoplast labeled with TIP-CFP coincides with pixels with intermediate anthocyanin lifetime values (280–440 ps, green) indicating that the pixels with shorter lifetime values (140–280 ps, red) correspond to the vacuolar lumen. V, vacuole. Scale bars: 10 m

subsequent image analysis. For anthocyanins, a double-exponential decay model seems most appropriate (*see* **Note5**). Set the bin to 10 and adjust to the trace of the urea crystal to include the initial rise and any instrumental features (afterpulsing, re ections, etc.) present in the data. Store this trace as the default IRF for subsequent deconvolutions.

2. Once the IRF has been inputted and stored, import the sdt le for the anthocyanins. Load stored IRF, set the bin to 1, and adjust trace window to include the full decay. Retaining information in the decay tails is important for getting good ts. Then select tting model by clicking into "Options, and then "Models."
3. Set the threshold so that pixels outside of the cell or region of interest are not modeled.
4. Calculate the lifetime decay curve of each pixel by a double-exponential curve (Fig. 2) by clicking into "Calculate" and then "Decay Matrix." Save the analyzed data as an ".img" le.
5. Once decay matrix has been generated, move the cursor over the uorescence intensity image to obtain the uorescence lifetime data for a given pixel. The software calculates the weighted mean of the uorescence lifetime ($_m$) for each pixel using $\tau_m = \sum_{i=1}^{N} a_i \tau_i \Big/ \sum_{i=1}^{N} a_i$ (*see* **Note6**). The SPCImage software creates a pseudocolor-image corresponding to the uorescence lifetime values.
6. The software will also provide parameters for the two components of this double-exponential curve, $_1$ and $_2$ (short and long lifetime components, respectively), and their relative fractional contributions, $_1(\%)$ and $_2(\%)$, where $_1(\%) + _2(\%) = 100\%$ (Fig. 2).
7. The anthocyanins in the vacuolar lumen exhibit shorter $_m$ values (Fig. 2g, h). To analyze the lifetime parameters of subcellular areas such as the vacuolar lumen, ROIs can be de ned in SPCImage and the measurement of each parameter can be done by selecting different parameters under Options/color/Coding of.
8. There are two modes of data display, continuous and discrete. This can be changed under Color/Mode. For the colocalization of anthocyanin $_m$ and the tonoplast, a discrete image of anthocyanin $_m$ was exported from SPCImage as a TIFF le.
9. Use Fiji [20] for colocalization analysis of anthocyanins and TIP-CFP in cotyledon pavement cells. Separate discrete anthocyanin uorescence lifetime images in channels and use individual channels for pixel intensity correlation over space analysis with the tonoplast CFP image using Coloc2 plugin (Fig. 2 i, j).

3.6 Estimation of Vacuolar pH Based on Anthocyanin Fluorescence Lifetime

The analysis of fluorescence lifetime of extracted anthocyanins solutions adjusted to different pH indicate that T_m values become shorter at acidic conditions (*see* Subheading 3.3. and [15]). Therefore, fluorescence lifetime analysis of vacuolar anthocyanins can be used to estimate differences in vacuolar pH. As an example, the *vha-a2 vha-a3* mutant that lacks VHA-a2 and VHA-a3 V-ATPase activity and shows higher vacuolar pH (6.4) than wild type plants (5.9) [3] can be used to detect changes in vacuolar pH based on FLIM of vacuolar anthocyanins (Fig. 3).

1. Collect time-resolved fluorescence emission of anthocyanins in WT and *vha-a2 vha-a3* as explained in Subheading 3.3 (**steps 4** and **5**).
2. Calculate the weighted mean of the fluorescence lifetime (T_m) for each pixel as explained in Subheading 3.5.
3. Select ROI corresponding to the vacuolar region to determine T_m of vacuolar anthocyanins in WT and *vha-a2 vha-a3* samples (**steps 1–5**).
4. Copy the values from each ROI from SPCImage into Excel.
5. Perform statistical analysis (e.g., t-test) to determine whether differences in T_m values are statistically significant.

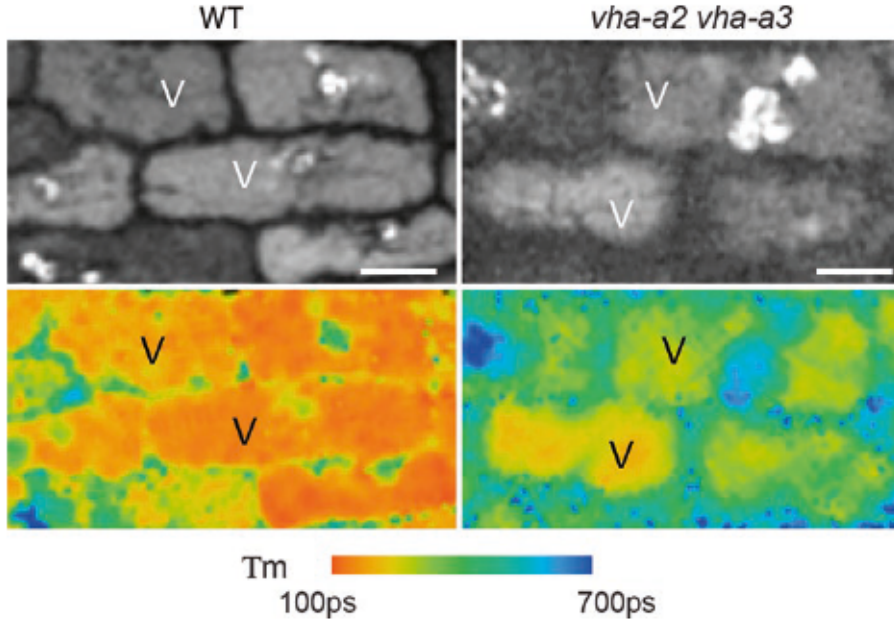

Fig. 3 FLIM analysis in WT and *vha-a2 vha-a3* cotyledon pavement cells showing the effect of different vacuolar pH on the fluorescence lifetime of anthocyanins. (**a**) and (**c**) Steady-steady fluorescence and (**b**) and (**d**) pseudocolor maps according to anthocyanin fluorescence τ_m values of wild type (WT) and *vha-a2 vha-a3* cotyledon pavement cells (100 ps to 700 ps). V, vacuole. Scale bars: 10 μm

4 Notes

1. Recently, commercial systems providing spectrally resolved FLIM have become available from Leica (http://www.leica-microsystems.com/products/confocal-microscopes/confocal-methods/sp- im/) and other vendors (www.becker-hickl.com).
2. Detailed analysis of properties of anthocyanin uorescence can be found in [10].
3. Pavement cells are ideal for imaging vacuolar anthocyanins.
4. Frozen seedlings can be stored at 80 °C until lyophilization.
5. The SPCImage handbook with more detail on how to analyze FLIM data can be found at http://www.becker-hickl.de/pdf/SPC-handbook-6ed-12-web.pdf.
6. The Chi-square (X^2_r) is an indicator of the tting signi cance. The closer X^2_r is to 1, the better the t.

Acknowledgments

This work was supported by NSF grant MCB-1048847 to EG and MSO.

References

1. Marty F (1999) Plant vacuoles. Plant Cell 11:587–599
2. Roberts JKM, Ray PM, Wade-Jardetzky N, Jardetzky O (1980) Estimation of cytoplasmic and vacuolar pH in higher plant cells by 31P NMR. Nature 283:870–872
3. Krebs M, Beyhl D, Gorlich E, Al-Rasheid KAS, Marten I, Stierhof YD, Hedrich R, Schumacher K (2010) *Arabidopsis* V-ATPase activity at the tonoplast is required for ef cient nutrient storage but not for sodium accumulation. Proc Natl Acad Sci U S A 107:3251–3256
4. Otegui MS, Herder R, Schulze J, Jung R, Staehelin LA (2006) The proteolytic processing of seed storage proteins in *Arabidopsis* embryo cells starts in the multivesicular bodies. Plant Cell 18:2567–2581
5. Martiniere A, Bassil E, Jublanc E, Alcon C, Reguera M, Sentenac H, Blumwald E, Paris N (2013) In vivo intracellular pH measurements in tobacco and *Arabidopsis* reveal an unexpected pH gradient in the endomembrane system. Plant Cell 25:4028–4043
6. Tang R-J, Liu H, Yang Y, Yang L, Gao X-S, Garcia VJ, Luan S, Zhang H-X (2012) Tonoplast calcium sensors CBL2 and CBL3 control plant growth and ion homeostasis through regulating V-ATPase activity in *Arabidopsis*. Cell Res 22:1650–1665
7. Harborne JB, Williams CA (2000) Advances in avonoid research since 1992. Phytochemistry 55:481–504
8. Grotewold E (2006) The genetics and biochemistry of oral pigments. Annu Rev Plant Biol 57:761–780
9. Chanoca A, Kovinich N, Burkel B, Stecha S, Bohorquez-Restrepo A, Ueda T, Eliceiri KW, Grotewold E, Otegui MS (2015) Anthocyanin vacuolar inclusions form by a microautophagy mechanism. Plant Cell 27:2545–2559
10. Poustka F, Irani NG, Feller A, Lu Y, Pourcel L, Frame K, Grotewold E (2007) A traf cking pathway for anthocyanins overlaps with the endoplasmic reticulum-to-vacuole protein-sorting route in *Arabidopsis* and contributes to the formation of vacuolar inclusions. Plant Physiol 145
11. Pourcel L, Irani NG, Lu Y, Riedl K, Schwartz S, Grotewold E (2010) The formation of anthocyanic vacuolar inclusions in *Arabidopsis*

thaliana and implications for the sequestration of anthocyanin pigments. Mol Plant 3:78–90

12. Faraco M, Spelt C, Bliek M, Verweij W, Hoshino A, Espen L, Prinsi B, Jaarsma R, Tarhan E, de Boer AH, Di Sansebastiano GP, Koes R, Quattrocchio FM (2014) Hyperacidi cation of vacuoles by the combined action of two different P-ATPases in the tonoplast determines ower color. Cell Rep 6:32–43
13. Reguera M, Bassil E, Tajima H, Wimmer M, Chanoca A, Otegui MS, Paris N, Blumwald E (2015) pH regulation by NHX-type antiporters is required for receptor-mediated protein traf cking to the vacuole in Arabidopsis. Plant Cell 27:1200–1217
14. Chang CW, Sud D, Mycek MA (2007) Fluorescence lifetime imaging microscopy. Methods Cell Biol 81:495–524
15. Chanoca A, Burkel B, Kovinich N, Grotewold E, Eliceiri KW, Otegui MS (2016) Using uorescence lifetime microscopy to study the subcellular localization of anthocyanins. Plant J 88:895–903
16. So PTC, Dong CY (2001) Fluorescence spectrophotometry. In eLSJohn Wiley & Sons Ltd, Chichester
17. Lakowicz JR (2006) Principles of uorescence spectroscopy. Springer
18. Lakowicz JR, Szmacinski H, Nowaczyk K, Johnson ML (1992) Fluorescence lifetime imaging of free and protein-bound NADH. Proc Natl Acad Sci U S A 89:1271–1275
19. Nelson BK, Cai X, Nebenfuhr A (2007) A multicolored set of *in vivo* organelle markers for co-localization studies in *Arabidopsis* and other plants. Plant J 51:1126–1136
20. Schindelin J, Arganda-Carreras I, Frise E, Kaynig V, Longair M, Pietzsch T, Preibisch S, Rueden C, Saalfeld S, Schmid B, Tinevez JY, White DJ, Hartenstein V, Eliceiri K, Tomancak P, Cardona A (2012) Fiji: an open-source platform for biological-image analysis. Nat Methods 9:676–682
21. Saslowsky DE, Dana CD, Winkel-Shirley B (2000) An allelic series for the chalcone synthase locus in *Arabidopsis*. Gene 255:127–138
22. Lange H, Shropshire W, Mohr H (1971) An analysis of phytochrome-mediated anthocyanin synthesis. Plant Physiol 47:649–655
23. Mancinelli AL, Yang C-PH, Lindquist P, Anderson OR, Rabino I (1975) Photocontrol of anthocyanin synthesis: III. The action of streptomycin on the synthesis of chlorophyll and anthocyanin. Plant Physiol 55:251–257
24. Lindoo SJ, Caldwell MM (1978) Ultraviolet-B radiation-induced inhibition of leaf expansion and promotion of anthocyanin production: lack of involvement of the low irradiance Phytochrome system. Plant Physiol 61:278–282

Chapter 11

The Use of Drugs in the Study of Vacuole Morphology and Trafficking to the Vacuole in *Arabidopsis thaliana*

Ricardo Tejos, Claudio Osorio-Navarro, and Lorena Norambuena

Abstract

Chemical compounds are useful to perturb biological functions in the same way as classical genetic approaches take advantage of mutations at the DNA level to perturb gene function. The use of bioactive chemicals currently called chemical genetic is especially valuable for cell biology. Chemical genetic approaches allow perturbations of cellular processes post-germination in a given time window controlling the severity of the effect by modifying or modulating the dose and/or the period of the treatment. Additionally, compounds can be applied directly to different mutants and translational fluorescent reporters/marker lines, expanding the repertoire of experimental setups addressing cell biology research. In this chapter, we describe standard protocols to visualize vacuole morphology and trafficking to the vacuole and the use of bioactive compounds as a proxy to study these biological processes.

Key words Vacuole, Tonoplast, Membrane trafficking, Protein trafficking, Endocytosis, Inhibitors

1 Introduction

Being the vacuole an essential organelle for plant cells implies the intrinsic difficulty of studying the vacuolar trafficking and morphology. Different types of vacuoles having specialized functions evidence a selective composition of membrane components and vacuole-resident proteins [1]. Thus, an accurate protein and membrane delivery process is essential for vacuole function. Vacuolar proteins are synthesized at the endoplasmic reticulum and delivered afterward to the vacuole following diverse trafficking pathways [2, 3]. Furthermore, the endocytic pathway delivers proteins and membrane to the vacuole where they are finally degraded as part of signaling pathways regulating physiological processes. Although classical genetics, i.e., the use of mutants, has contributed to understand the biogenesis and trafficking to the vacuole, in some cases, gene redundancy and/or lethality caused by gene loss-of-function knockouts made the unraveling of such cellular processes a difficult task. The use of

Cláudia Pereira (ed.), *Plant Vacuolar Trafficking: Methods and Protocols*, Methods in Molecular Biology, vol. 1789,
https://doi.org/10.1007/978-1-4939-7856-4_11,

bioactive chemicals able to distinguish among different trafficking pathways and vacuole morphology proved to be useful to circumvent mutant lethality and gene redundancy. One of the first fundamental chemicals to evidence the existence of two different vacuolar protein trafficking was wortmannin back in the 1990s [4]. Nowadays, a set of drugs altering vacuole morphology and vacuolar trafficking has been gathered by means of several chemical genetics strategies [5]. These bioactive compounds display dose-dependent and in many cases reversible effects, building a chemical toolbox of vacuole drugs to dissect diverse protein trafficking pathways and vacuole biogenesis and morphology. Depending on the aim of the research, the effect of these drugs could be combined with genetic mutants and fluorescent-tagged reporter proteins. In this chapter, we describe detailed protocols for testing both protein/membrane trafficking to the vacuole as well as vacuole morphology in response to a particular compound of interest. More importantly we compile the available bioactive drugs that affect vacuoles in *Arabidopsis thaliana*.

2 Materials

2.1 Plant Material

We routinely use *Arabidopsis thaliana* Col-0 as it is the ecotype most commonly used for the generation of mutant collections and marker lines as indicated. Nonetheless, any *Arabidopsis* ecotype can be used.

2.2 Reagents—Chemicals and Media

1. Dimethyl sulfoxide.
2. N-(3-Triethylammoniumpropyl)-4-(6-(4-(Diethylamino) Phenyl) Hexatrienyl) Pyridinium Dibromide (FM4-64).
3. Commercial house bleach (5-10% sodium hypochlorite).
4. 37% HCl.
5. Arabidopsis culture media: 0.5× MS basal salt mix, MES buffer 500 mg L^{-1}, sucrose 10 g L^{-1} (*see* **Note 1**), pH 5,7. When needed, 8 g L^{-1} plant tissue culture agar can be added prior autoclave.
6. Chemicals included in Table 1.

2.3 Equipment

1. Laminar flow bench.
2. Timer.
3. Confocal microscope.
4. 12-well plates.

Table 1

List of chemicals commonly used in *Arabidopsis* to interfere with vacuole morphology and trafficking to the vacuole

Compound	Concentration (μM)	Pathway affected	Cellular phenotypes	Ref.
Wortmanin	15–33	Inhibits phosphatidylinositol kinases, PI3K and PI4K, in vitro.	Inhibits differentially the trafficking to the vacuole of soluble proteins. Inhibits endocytosis and targeting to the vacuole. Also, induces the formation of PM cargoes in intracellular agglomerations.	[4, 6, 7]
Sortin 1	57	Unknown	Alters vacuolar cargoes trafficking to the vacuole and changes vacuole morphology	[8, 9]
Sortin 2	54	Unknown	Alters vacuolar cargoes trafficking to the vacuole and changes vacuole morphology	[8, 10]
Tyrphostin A23	5–50	Uncouples mitochondrial electrochemical gradient	Inhibits plasma membrane protein cargoes endocytosis. Alters vacuole morphology	Osorio and Norambuena, unpublished results and Fig. 3 [11, 12]
Brefeldin A	25–50	Binds and interfere ARF-GEF function	Inhibits exocytosis and trafficking to the vacuole in a concentration-dependent manner	[6]
Endosidin 2	40	Binds Exo70	Enhances protein targeting to the vacuole	[13]
Gravacin	1–5	Binds PGP19	Induces tonoplast intrinsic protein accumulation at ER-like structures	[14]
C834	55	Unknown	Disturbs the trafficking of GFP-TIP2;1 and TIP3;1-YFP to the tonoplast by inducing their accumulation at the endoplasmic reticulum; enhance plasma membrane cargoes trafficking to the vacuole in darkness	[15]

(continued)

Table 1
(continued)

Compound	Concentration (μM)	Pathway affected	Cellular phenotypes	Ref.
C410	62.34	Unknown	Inhibits the trafficking of GFP-TIP2;1, TIP3;1-YFP, and TIP1;1-YFP to the tonoplast	[15]
C755	88	Unknown	Disturbs the trafficking of GFP-TIP2;1, TIP3;1-YFP, and TIP1;1-YFP to the tonoplast, inducing their accumulation at cytoplasmic structures and at the endoplasmic reticulum	[15]
C103	79.14	Unknown	Disturbs the trafficking of TIP2;1-YFP, TIP3;1-YFP, and TIP1;1-YFP to the tonoplast	[15]
C578	80	Unknown	Disturbs TIP2;1-YFP trafficking to the tonoplast, inducing its agglomeration at the endoplasmic reticulum	[15]

5. Soft tweezers.
6. Micropipettes and sterile disposable tips.
7. Microscopy slides.
8. Coverslips.

3 Methods

3.1 Plant Culture Media and Growth Conditions

3.1.1 Surface Sterilized Arabidopsis Seeds Using the Chlorine Gas Method

1. Place seeds in a 2 mL polypropylene tube inside a hermetic desiccator were the reaction of 100 mL of commercial house bleach (5–10% sodium hypochlorite) and 2 mL 37% HCl is taking place (*see* **Note 2**).
2. Ventilate seeds inside the flow bench for 1 h prior sowing in solid *Arabidopsis* culture media.
3. Plate the seeds on the Arabidopsis culture plates and incubate them at 4 °C in darkness for at least 24 h. Place plates in vertical position inside a controlled growth chamber at 22 °C, with a 16:8 light-dark illumination regime for 4–7 days.

3.2 Evaluation of Endocytic Trafficking to the Vacuole and Vacuole Morphology

3.2.1 Use FM4-64 as a Tracer for Endocytic Trafficking to the Vacuole

The amphiphilic styryl dye FM4-64 is an important staining tool to track endocytic trafficking and to visualize the dynamic and structure of plant vacuoles (Fig. 1). As such, FM4-64 is the most versatile staining method to test for the effect of compounds on vacuole morphology and trafficking toward the vacuole. Indeed, FM4-64 staining allows for the immediate visualization of the tonoplast in different mutant backgrounds or in the presence of small compounds perturbing cellular functions. The following method can be used in wild type or mutant seedlings, and in fluorescent reporter lines.

A confocal microscope equipped with standard lasers and filter sets usually provide the appropriate settings to observe FM4-64. FM4-64 has maximum Em/Ex ~ 558/734 nm when dissolved in methanol. However, the emission peak varies considerably when inserted in the cell membrane and depends on the cell type or organism assayed. Nonetheless, the 488 nm or 514 nm Argon laser lines render clear and strong dye fluorescence in the red emission range (above 580 nm). Though we recommend using the 514 nm laser line as in this condition the plastid autofluorescence in *Arabidopsis*

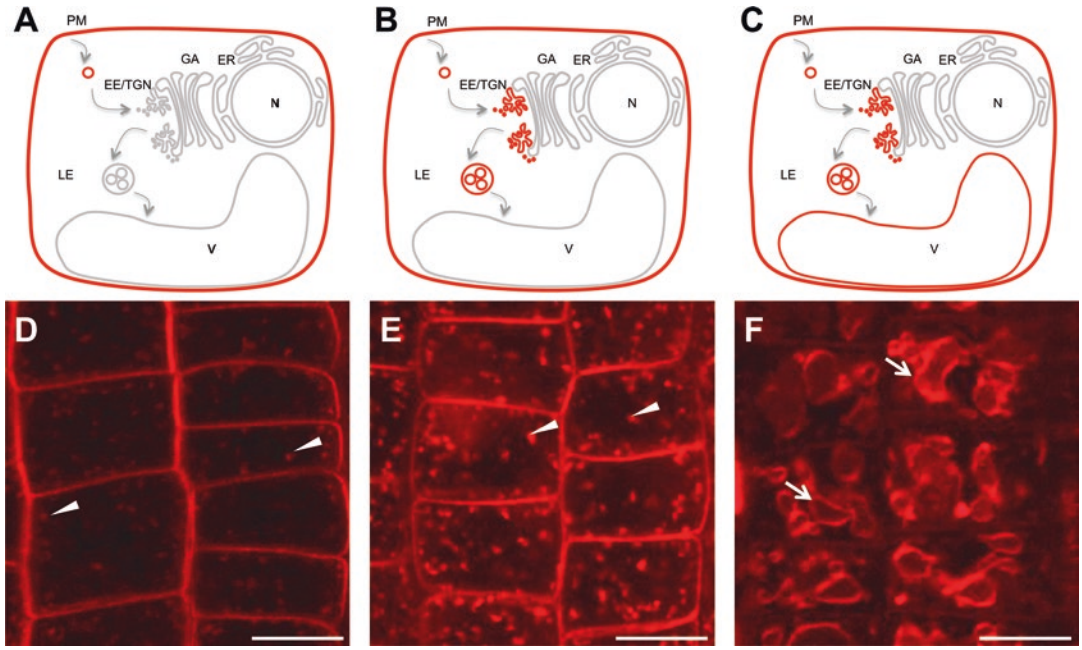

Fig. 1 FM dye-trafficking in Arabidopsis root cell: from plasma membrane to the tonoplast. The FM dye FM4-64 binds to the plasma membrane. The stained plasma membrane is internalized sequentially through the endocytic compartments. FM4-64-labeled plasma membrane vesicles (**a**, **d**) reach the early endosomes or trans-Golgi network (EE/TGN) and subsequently the late endosomes (LE) in about 30–60 min (**b**, **e**) depending in the experimental conditions. Finally, the dye reaches the tonoplast (**c**, **f**) in about 60–90 min. **d**, **e** and **f** show FM internalization in epidermal cells of Arabidopsis roots. Arrowheads and arrows show endosome population and vacuoles, repectively. Scale bars = 10 μm

root tips is avoided. The 543 laser also works well for FM4-64 fluorescence. In any case laser settings must be the same throughout the experiment. Alternatively, FM4-64 assay can be performed in the background of GFP- or YFP-tagged protein reporter lines.

1. Prepare a 4 mM FM4-64 stock solution by dissolving lyophilized dye in distillated water (*see* **Note 3**). This stock solution is light sensitive and should be stored in opaque microcentrifuge tubes or in inside a light-protected recipient.
2. Prepare a 12-well plate containing 1 mL liquid media per well. Add to each well 1 μL of FM4-64 stock solution. Mix well by pipetting to allow a homogeneous dispersion of the dye.
3. Place 4–7 day-post germination seedlings to each well using soft tweezers. Be sure to have all root tips completely submerged in the liquid media.
4. Incubate at 4 °C in darkness for 5 min (*see* **Note 4**) either by covering the plate with aluminum foil or placing the whole plate inside a light-protected container.
5. Wash the FM4-64 out by transferring the seedlings to a fresh and cold (4 °C) liquid media-containing well without dye using soft tweezers. Repeat once. Alternatively, the liquid media could be removed and replaced with fresh liquid media by pipetting.
6. Maintain the seedlings in the darkness. The endocytosis rate at 4 °C will be very low. In order to begin with normal endocytosis rate, seedling should be transferred to normal growth temperature that is 22 °C for Arabidopsis. This is time zero of endocytosis kinetics. The endocytic kinetics will be evaluated by confocal microscopy imaging (*see* Subheading 3.2.2).

3.2.2 Time-Dependent FM4-64 Endocytic Trafficking to the Vacuole

The following steps should be executed at constant temperature. Usually in the confocal room the temperature is kept at 22 °C being convenient for working with Arabidopsis.

1. Carefully place seedlings on a drop (10–20 μL) of Arabidopsis liquid media on top of a microscopy slide. Arrange seedling roots in a parallel fashion to facilitate finding root tips.
2. Place a coverslip gently over the roots leaving the hypocotyl and cotyledons out (*see* **Note 5**)
3. Search root tips and take a single image of the epidermal cell layer adjacent to the coverslip using 40× or 60× objective. Alternatively, a series of images can be obtained in the z-plane starting from the cell surface until the middle of the cell (i.e., from the focal plane where the FM4-64 stained compartments start to appear toward the area where the cell nucleus starts to appear) to build a 3D reconstruction.

4. Image the seedling in 30 min intervals after time zero. Intermediate points may be included to build the kinetics of endocytic trafficking to the vacuole with greater detail. We recommend starting by taking the first image at time 30 min and continuing at 60, 90, and 120 min (Fig. 1).
5. There is a natural variability among plants. Therefore, we recommend evaluating the kinetics of epidermal cells FM4-64 uptake from at least 15 seedlings. In each seedling image ten cells per root. Perform three replicates of the whole experiment.
6. Tonoplast labeling should be visible after 60 min in wild type Arabidopsis Col-0. Nonetheless, labeling depends on several experimental conditions. Therefore, the minimum time for observing FM4-64-labeled tonoplast has to be determined experimentally for the conditions in each lab.
7. Estimate the number of cells showing tonoplast FM4-64 labeling at each time point. Plot the frequency of cells with labeled tonoplast vs. the time of FM4-64 staining.

3.2.3 Evaluation of Vacuole Morphology

There are several strategies to evaluate vacuole morphology including staining the vacuole with fluorescent dyes (e.g., Lysotracker dyes, BCECF-AM)[16] or the use of fluorescent protein-tagged tonoplast resident proteins. For instance, the TONOPLAST INTRINSIC PROTEINs (TIPs) are all localized at the tonoplast. Arabidopsis expressing fluorescent-tagged TIP proteins are available allowing the direct observation of the vacuole morphology in different cell types including those in root epidermis, hypocotyl and cotyledons (Fig. 2a, b). In spite of that, the FM4-64 staining allows direct observation of vacuole structure and most of cell types in Arabidopsis (Fig. 2a, c). The convenience of FM4-64 of being applied to wild type or mutant plants and in combination with fluorescent reporter lines could be exploited as much as possible.

1. Follow **steps 1–5** in Subheading 3.2.2 and choose a time point where the tonoplast is visible among all assayed conditions for the experimental set up.
2. Evaluate the morphology of the vacuole in the cell type or tissue of interest. Different structures could be found in different tissues (Fig. 2). Therefore, the selection of the area to be examined depends on the physiological and cellular phenotypes to be addressed. Maintain this imaging condition, i.e., the zone where the vacuoles are being observed, among all conditions assayed in order to compare the effect of a particular drug treatment. For instance, the root epidermal cells from the root apical meristem until the root differentiation zone show a developmentally regulated vacuole morphology which is evident from the cells in the root apical meristem where vacuoles appear to be smaller and the vacuole lumens less abundant

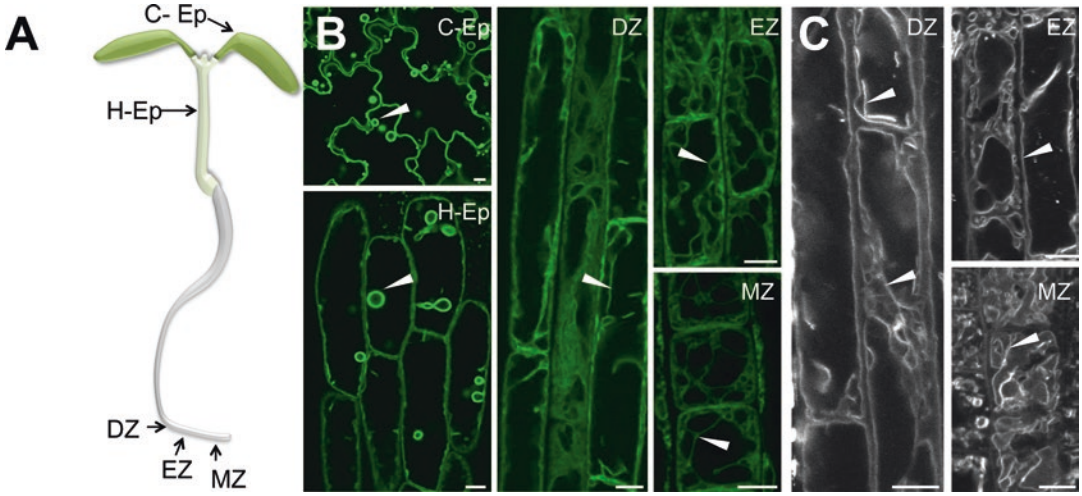

Fig. 2 Live imaging of vacuolar morphology in Arabidopsis. Tonoplast morphology and dynamics can be analyzed through fluorescent reporter proteins or fluorescent dyes. Arabidopsis seedling diagram highlight different tissues where the vacuole exhibits the morphology shown in **b** and **c** (**a**). C-EP and H-EP indicates epidermal cells in cotyledon and hypocotyl, respectively. In addition, DZ, EZ, and MZ indicate differentiation, elongation, and meristem zones in root epidermis, respectively. Vacuolar morphology in seedlings expressing the tonoplast reporter GFP-δTIP (**b**) and by FM4-64 labeling (**c**) is shown. The arrowheads indicate vacuole internal structures surrounded by tonoplast membranes. Scale bars = 10 μm

than the ones observed in the elongation and differentiation zones of the roots (Fig. 2).

3. There are several ways to compare the morphology of the vacuole among different conditions. One of the simplest is to count the number of vacuolar lumens observed per cell (*see* **Note 6**). Alternatively, quantifying the surface of those lumens, namely the area surrounded by the tonoplast membrane is possible. Then the relationship of the total area vs. the total cell area could be an index which can simplify the comparison among different conditions and in such way, facilitates finding perturbations or the effect of a particular drug.

3.3 Assaying the Effect of Small Bioactive Compounds on FM4-64 Endocytic Trafficking and Vacuolar Morphology

Several bioactive chemicals have been shown to perturb the trafficking to the vacuole and vacuole morphology (Table 1) [5]. The basic protocol presented here can be used in combination with any chemical compound for testing its effect on plant cells [17]. Additionally, Table 1 shows the recommended concentration range of the described chemicals to render clear effects and Fig. 3 show examples of the effect of some compounds. However, we recommend to experimentally obtaining the compounds minimum concentration or the concentration range and the preincubation time where the compound of interest (COI) has a clear effect. Usually a physiological or developmental phenotype is the quickest procedure to obtain such parameters for the compound. Similarly, it would be handy to

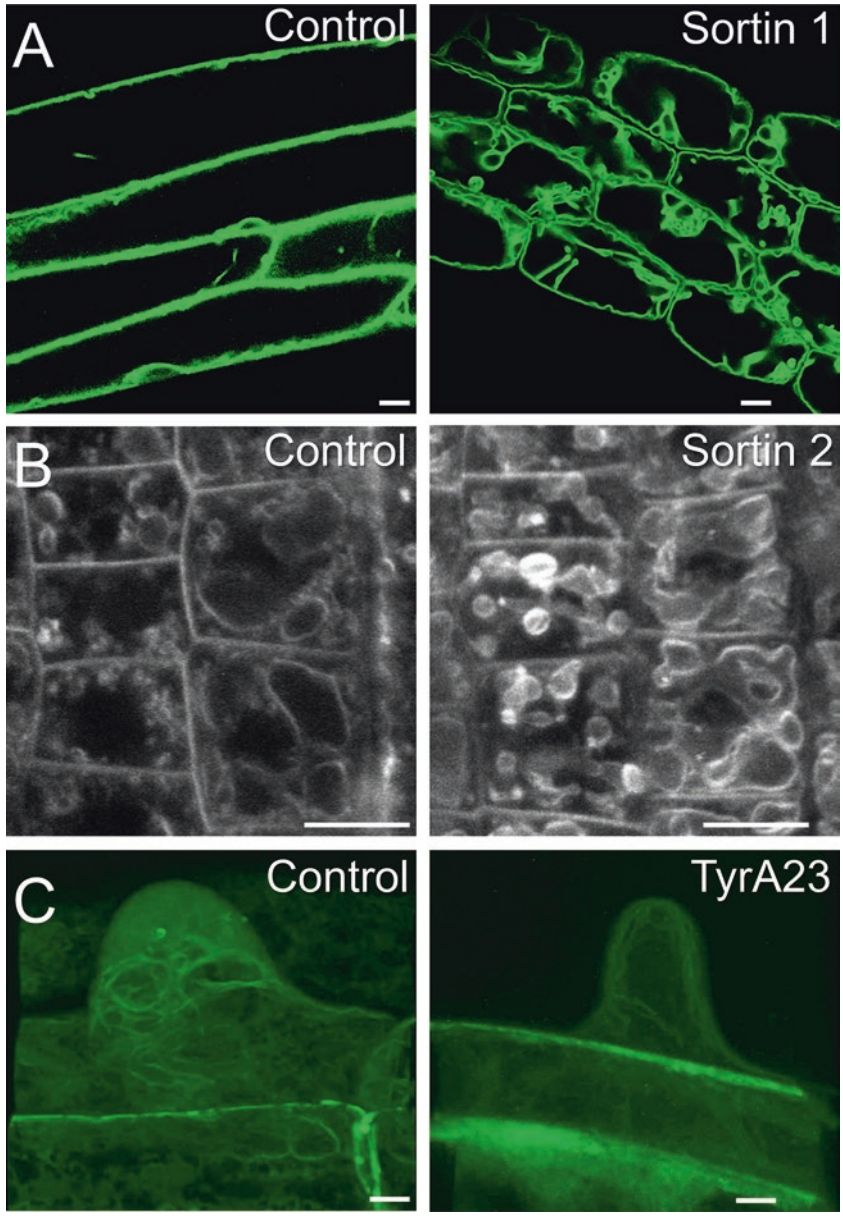

Fig. 3 Chemical modulation of vesicular trafficking impacts vacuolar morphology. Vacuolar trafficking through secretory or endocytic pathways can be perturbed by bioactive chemicals. In several cases, this alteration impacts the vacuolar morphology in different cells types. Vacuolar phenotype triggered by Sortin1 in hypocotyl epidermal cells (**a**), Sortin2 in root epidermal cells (**b**) and Tyrphostin A23 (TyrA23) in root hair of Arabidopsis (**c**) are shown as examples. Particularly, Sortin1 and Sortin2 increase the complex structures of tonoplast-like bulbs or membrane sheets. In contrast, TyrA23 reduces tonoplast complexity in the root hair. Vacuole morphology is visualized in GFP-δTIP Arabidopsis transgenic line in **a** and **c** or using FM4-64 in **b**. Scale bars = 10 μm

obtain and use an inactive structural homolog of the bioactive COI, i.e., a compound not exerting the same effect, to be used as a negative control. For most of the cases the chemicals described in chemical genetics approaches have several inactive analogs.

The following protocol uses *Arabidopsis thaliana* as a model for assaying the effect of COIs on vacuoles in root epidermal cells. However, it could be extrapolated to any cell type as long as the trafficking or the vacuole structure could be observed.

1. Seven-day-old Arabidopsis seedlings grew in normal condition are transferred to a MS solid media containing the bioactive chemical at the effective concentration (Table 1).
2. Always consider a mock control where the bioactive compound solvent (commonly DMSO) is at equal concentration as it will be in the experimental condition (*see* **Note 7**). We recommend preparing 1000× stocks of the bioactive compound to include a single mock control in the experimental set up.
3. Prepare a 12-well plate containing liquid media and the COI in the concentration ranges to be assayed.
4. Gently transfer seedlings to a well containing the chemical treatment.
5. Short preincubation periods, namely from 0 to 120 min, are usually enough to observe changes in the root epidermal cells although some COI need longer preincubation periods (*see* **Note 7**). This pretreatment time has to be obtained experimentally.
6. After the preincubation period on the bioactive chemical to be assayed proceed with FM4-64 staining as indicated in Subheading 3.2 maintaining the presence of COI.

4 Notes

1. The carbon source for early seedling growth comes from the storage sources in the embryonic leaves and from the culture media. A direct physiological assay that may indicate defects at the storage vacuole usually comes from comparing seedling growth in media with and without sucrose. Therefore, sucrose may be omitted from the recipe depending on the assay to be performed.
2. Extreme care should be taken when performing the chlorine gas method for seeds sterilization as such reaction produces toxic gases. Work inside a fume hood, wearing protective gloves and coat.
3. Repeated freeze and taw cycles of the FM4-64 solution should be avoided. We recommend preparing single use 5 μL aliquots and store them at −20 °C protected from light. Additionally,

FM4-64 staining solutions should be used only once for each staining to avoid unwanted reduction of the initial cells staining.

4. Several protocols for FM4-64 staining include an initial incubation in liquid media maintained in ice water (4 °C). Although we believe this may be a good approximation to obtain early FM4-64 uptake time points (e.g., 2–10 min), conclusions should be drawn with caution as the cold stress does affect the endocytosis rate. This effect most likely is not immediately reversed and could cause undesired effects on the intracellular trafficking pathways.
5. Alternatively, FM-4-64 uptake may be evaluated in hypocotyl epidermis or in other root tip cells. FM4-64 has good penetration in the root apical meristem, and labeling of tonoplast can be achieved in all cell types. Nonetheless, visualization of FM4-64 stained vesicles at early time points is not possible due to the difficult task of image the surface of those cells.
6. It has been shown that *Arabidopsis* root cells have a single, complex tubular vacuole, therefore the vacuolar lumen observed in confocal microscopy images correspond to a single compartment.
7. If the purpose is to test several concentrations of the same compound, we recommend preparing 1000× concentrated stocks to obtain the final dilution including a single mock control.

Acknowledgments

This work was supported by grants numbers 1170950 to LN and 1171442 to RT from the Fondo Nacional de Investigación Científica y Tecnológica (Fondecyt).

References

1. Frigerio L, Hinz G, Robinson DG (2008) Multiple vacuoles in plant cells: rule or exception? Traffic 9:1564–1570. https://doi.org/10.1111/j.1600-0854.2008.00776.x
2. Pedrazzini E, Komarova NY, Rentsch D, Vitale A (2013) Traffic routes and signals for the Tonoplast. Traffic 14:622–628. https://doi.org/10.1111/tra.12051
3. Xiang L, Etxeberria E, Van Den Ende W (2013) Vacuolar protein sorting mechanisms in plants. FEBS J 280:979–993. https://doi.org/10.1111/febs.12092
4. Matsuoka K, Bassham DC, Raikhel NV, Nakamura K (1995) Different sensitivity to wortmannin of two vacuolar sorting signals indicates the presence of distinct sorting machineries in tobacco cells. J Cell Biol 130:1307–1318. https://doi.org/10.1083/jcb.130.6.1307
5. Norambuena L, Tejos R (2017) Chemical genetic dissection of membrane trafficking. Annu Rev Plant Biol 68:197–224
6. Kleine-Vehn J, Leitner J, Zwiewka M et al (2008) Differential degradation of PIN2 auxin efflux carrier by retromer-dependent vacuolar targeting. Proc Natl Acad Sci U S A 105:17812–17817. https://doi.org/10.1073/pnas.0808073105

7. Alvarez AA, Han SW, Toyota M et al (2016) Wortmannin-induced vacuole fusion enhances amyloplast dynamics in Arabidopsis *zigzag1* hypocotyls. J Exp Bot 67:6459–6472. https://doi.org/10.1093/jxb/erw418
8. Zouhar J, Hicks GR, Raikhel NV (2004) Sorting inhibitors (Sortins): chemical compounds to study vacuolar sorting in Arabidopsis. Proc Natl Acad Sci U S A 101:9497–9501. https://doi.org/10.1073/pnas.0402121101
9. Rosado A, Hicks GR, Norambuena L et al (2011) Sortin1-hypersensitive mutants link vacuolar-trafficking defects and flavonoid metabolism in Arabidopsis vegetative tissues. Chem Biol 18:187–197. https://doi.org/10.1016/j.chembiol.2010.11.015
10. Pérez-Henríquez P, Raikhel NV, Norambuena L (2012) Endocytic trafficking towards the vacuole plays a key role in the auxin receptor SCFTIR-independent mechanism of lateral root formation in A. thaliana. Mol Plant 5:1195–1209. https://doi.org/10.1093/mp/sss066
11. Dejonghe W, Kuenen S, Mylle E et al (2016) Mitochondrial uncouplers inhibit clathrin-mediated endocytosis largely through cytoplasmic acidification. Nat Commun 7:11710. https://doi.org/10.1038/ncomms11710
12. Ortiz-Zapater E, Soriano-Ortega E, Marcote MJ et al (2006) Trafficking of the human transferrin receptor in plant cells: effects of tyrphostin A23 and brefeldin a. Plant J 48:757–770. https://doi.org/10.1111/j.1365-313X.2006.02909.x
13. Zhang C, Brown MQ, van de Ven W et al (2015) Endosidin2 targets conserved exocyst complex subunit EXO70 to inhibit exocytosis. Proc Natl Acad Sci U S A:E41–E50. https://doi.org/10.1073/pnas.1521248112
14. Rojas-Pierce M, Titapiwatanakun B, Sohn EJ et al (2007) Arabidopsis P-Glycoprotein19 participates in the inhibition of Gravitropism by Gravacin. Chem Biol 14:1366–1376. https://doi.org/10.1016/j.chembiol.2007.10.014
15. Rivera-Serrano EE, Rodriguez-Welsh MF, Hicks GR, Rojas-Pierce M (2012) A small molecule inhibitor partitions two distinct pathways for trafficking of Tonoplast intrinsic proteins in Arabidopsis. PLoS One 7:1–11. https://doi.org/10.1371/journal.pone.0044735
16. Scheuring D, Schöller M, Kleine-Vehn J, Löfke C (2015) Vacuolar staining methods in plant cells. Methods Mol Biol 1242:83–92. https://doi.org/10.1007/978-1-4939-1902-4_8
17. Rodriguez-Furlán C, Hicks GR, Norambuena L (2014) Chemical genomics: characterizing target pathways for bioactive compounds using the endomembrane trafficking network. Methods Mol Biol 1174:317–328. https://doi.org/10.1007/978-1-4939-0944-5_22

Chapter 12

Use of Brefeldin A and Wortmannin to Dissect Post-Golgi Organelles Related to Vacuolar Transport in *Arabidopsis thaliana*

Junpei Takagi and Tomohiro Uemura

Abstract

Eukaryotic cells comprise various organelles surrounded by the membrane. Each organelle is characterized by unique proteins and lipids and has its own specific functions. Single membrane-bounded organelles, including the Golgi apparatus, endosomes, and vacuoles are connected by membrane trafficking. Identifying the organelle localization of a protein of interest is essential for determining the proteins physiological functions. Here, we describe methods for determining protein subcellular localization using the inhibitors brefeldin A and wortmannin in *Arabidopsis thaliana*.

Key words Brefeldin A (BFA), Wortmannin, Vacuole, Endosome, *Trans*-Golgi network, Golgi stacks, Membrane trafficking, *Arabidopsis thaliana*

1 Introduction

Within plant cells, various single membrane-bounded organelles are connected via a membrane trafficking system that mediates the exchange of lipids and proteins (Table 1). Each organelle possesses a unique composition of proteins and lipids and plays unique roles in the cell; therefore, determining the organelle-specific localization of a protein of interest can provide new insights into its function. The endoplasmic reticulum (ER) is a network of tubules and cisternae that participates in protein and lipid synthesis [1]. Proteins from the ER are delivered to the Golgi apparatus, which comprises several stacks of cisternae and functions in protein modification. On the *trans* side of the Golgi apparatus there is a tubular-vesicular compartment called the *trans*-Golgi network (TGN), in which cargo proteins are selectively sorted to their final destination, such as a plasma membrane (PM) or vacuole [2]. In plant cells, the TGN functions as an early endosome (EE) [3], which does not occur in animal and yeast cells. Between the TGN and vacuole is an

Cláudia Pereira (ed.), *Plant Vacuolar Trafficking: Methods and Protocols*, Methods in Molecular Biology, vol. 1789,
https://doi.org/10.1007/978-1-4939-7856-4_12,

Table 1
List of organelle marker lines

Organelle	Marker name	Reference
ER	GFP-HDEL	[39]
	mCherry-HDEL	[39]
	EYFP-NIP1;1	[13]
	mCherry-NIP1;1	[13]
Golgi	ST-GFP	[40]
	ST-mRFP	[36]
	GFP-SYP32	[35]
	EYFP-SYP32	[13]
	mCherry-SYP32	[13]
	EYFP-MEMB12	[13]
	mCherry-MEMB12	[13]
TGN	GFP-SYP43	[36]
	mRFP-SYP43	[36]
	GFP-SYP61	[37]
	mRFP-SYP61	[37]
	VHAa1-GFP	[3]
	VHAa1-mRFP	[41]
	COV1-GFP	[42]
	COV1-mRFP	[42]
	ECHIDNA-EYFP	[43]
Endosome	ARA6-GFP	[44]
	ARA6-mRFP	[44]
	GFP-ARA7	[44]
	mRFP-ARA7	[44]
	SNX1-GFP	[45]
	SNX1-mRFP	[45]
	GFP-VAMP727	[38]
	tagRFP-VAMP727	[38]

(continued)

Table 1
(continued)

Organelle	Marker name	Reference
Vacuole	GFP-VAM3/SYP22	[38]
	mRFP-VAM3/SYP22	[46]
	γTIP-GFP	[39]
	γTIP-mCherry	[39]
	VHAa3-GFP	[3]
	VHAa3-mRFP	[47]
PM	GFP-LTI6b	[48]
	PIP2A-GFP	[39]
	PIP2A-mCherry	[39]
	GFP-SYP121	[46]
	GFP-SYP122	[46]
	GFP-SYP132	[46]
	GFP-KNOLLE/SYP111	[49]

intermediate prevacuolar compartment (PVC), in which vacuolar cargo receptors are recycled back. The PVC is also known as the multivesicular body (MVB) or late endosome (LE), and is involved in PM protein recycling and degradation [4]. Vacuoles are the largest organelles, occupying over 90% of the cell volume, and they function in protein storage and degradation. The PM separates the inside and the outside of the cell, and is therefore important in responses to the extracellular environment.

Membrane traffic is mediated by transport vesicles, the formation of which is initiated by ADP ribosylation factor (ARF) GTPases. ARF GTPase activity is regulated by guanine nucleotide exchange factors (ARF-GEFs) [5]. The *Arabidopsis* genome encodes eight ARF-GEFs that are grouped into two classes: GBF and BIG [6]. Six of these ARF-GEFs, including GNOM, can be inhibited by the fungal metabolite brefeldin A (BFA). In contrast, the other two ARF-GEFs—GNOM-LIKE 1 (GNL1) and BIG3—are BFA-resistant due to a difference in a specific residue within the catalytic SEC7 domain [5]. BFA can also influence organelle morphology, but the effects vary among species and tissues [7, 8]. BFA treatment of tobacco leads to the redistribution of some Golgi-localized proteins into the ER [9], as well as the formation of TGN/endosomes aggregates termed BFA compartments [10, 11]. On the other hand, BFA treatment of *Arabidopsis* root cells leads to the forma-

tion of BFA compartments comprising Golgi, TGN, and endosome aggregates [3, 12], but without resorption of Golgi stacks into the ER [13] (Fig. 1), possibly because BFA-resistant GNL1 is localized and functions at Golgi stacks [8, 14].

Phosphoinositides (PIs), a group of membrane lipids derived from phosphatidylinositol (PtdIns), are another key regulator of membrane trafficking. Specific lipid kinases can phosphorylate the hydroxyl groups at positions 3, 4, and 5 of the inositol head group of PtdIns, generating PtdIns monophosphates, bisphosphates, and one triphosphate [15]. Of the seven known PI species, only five have been detected in plants: PtdIns3P, PtdIns4P, PtdIns5P, PtdIns(3,5)P2, and PtdIns(4,5)P2 [16]. PI distribution varies among organelles [17], and each PI plays key roles in various steps of membrane trafficking [18]. For example, in *Arabidopsis*, PtdIns(4,5)P2 is enriched in the plasma membrane and participates in regulating exocytosis and clathrin-mediated-endocytosis [19–21]. PtdIns4P is distributed in the Golgi stacks, TGN, and PM, and reportedly mediates polarized exocytosis during tip growth [22, 23]. PtdIns3P is localized in late endosomes and vacuoles, and is required for vacuolar trafficking [24, 25]. Biosynthesis of these PIs can be inhibited by chemical compounds that specifically disturb phosphatidylinositol kinase (PIK) activity. LY294002 inhibits PtdIns3-kinase (PI3K), which generates PtdIns3P [26–29], and phenylarsine oxide (PAO) inhibits PtdIns4-kinase (PI4K), which generates PtdIns4P [29, 30]. Wortmannin (Wm) is the most broadly used inhibitor of PI3K and PI4K. Wm inhibits PI3K but not PI4K at a low concentration (<1 μM), and inhibits both PI3K and PI4K at a higher concentration [31, 32]. As each organelle has its own unique PIs distribution, they each show different responses to inhibitory compounds [29]. In *Arabidopsis*, Wm treatment induces endosome enlargement, but does not clearly change the phenotype of the Golgi stacks, TGN, or vacuoles (Fig. 2) [33].

Fluorescent proteins, such as GFP and RFP, are powerful tools for determining subcellular localizations of unknown proteins since they make it easy to visualize protein locations within living cells. However, it is difficult to distinguish the Golgi apparatus, TGN, and endosomes because they appear as punctate structures when labeled with fluorescent proteins and viewed under a confocal microscope. We can instead infer a protein's subcellular localization by observing the responses to BFA and Wm, since the Golgi stacks are insensitive to both BFA and Wm, the TGN is sensitive to BFA but insensitive to Wm, and endosomes are sensitive to both. However, it is better to determine localization by performing colocalization analysis using organelle markers (Table 1) because one cannot exclude the possibility that the drug induces protein mislocalization, as has been reported with GNOM [34]. Here, we describe and demonstrate subcellular localization

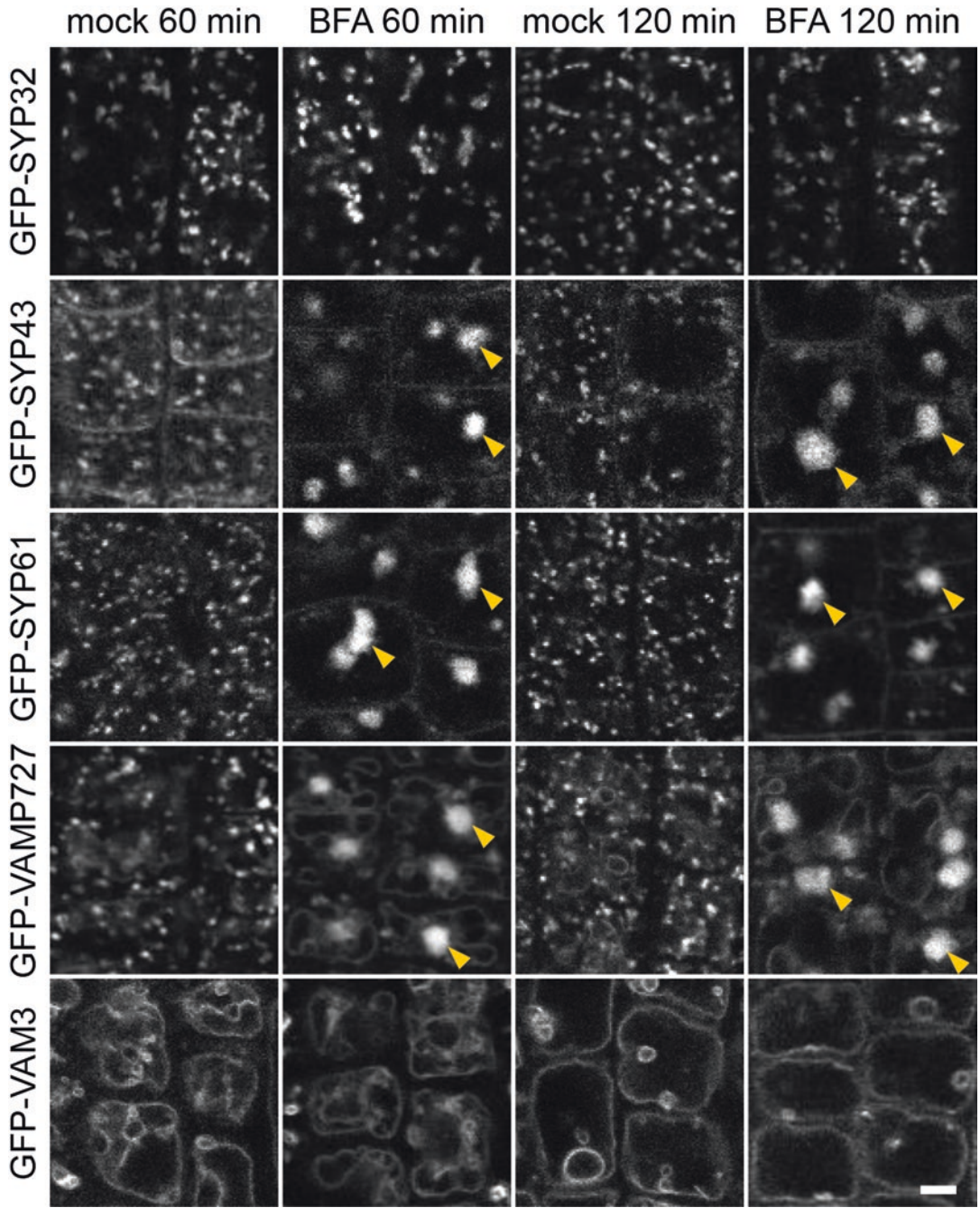

Fig. 1 BFA treatment causes TGN and endosomes to form aggregates termed "BFA compartments." Confocal images of root epidermal cells of 7-day-old seedlings expressing GFP-SYP32 (Golgi), GFP-SYP43 (TGN), GFP-SYP61 (TGN), GFP-VAMP727 (endosome), or GFP-VAM3 (vacuole), which were treated with either 50 μM BFA or DMSO (control). Arrowheads indicate BFA compartments. Bar = 5 μm

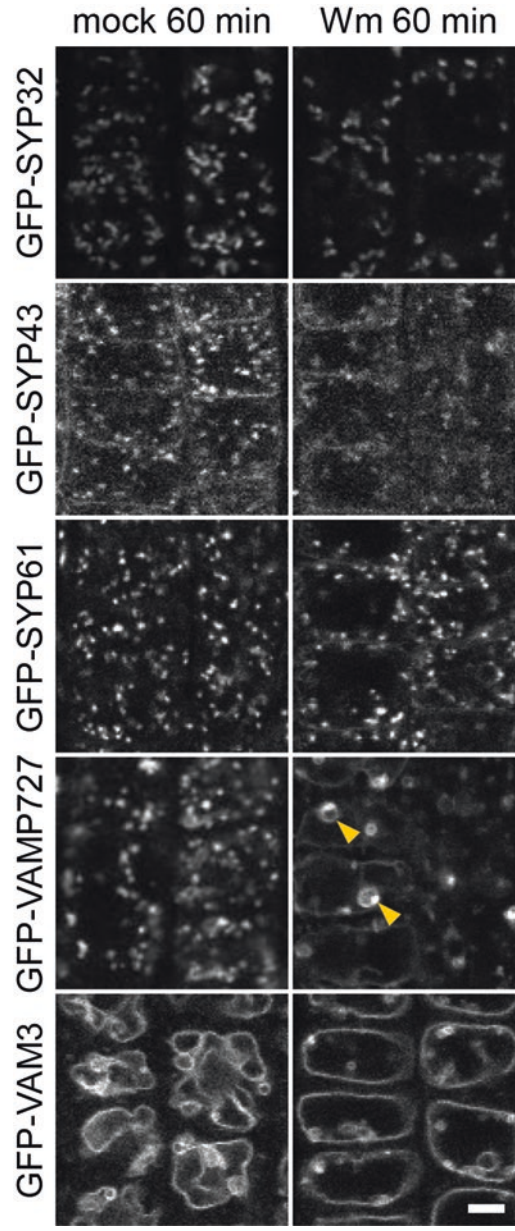

Fig. 2 Wm treatment causes endosome swelling. Confocal images of root epidermal cells of 7-day-old seedlings expressing GFP-SYP32 (Golgi), GFP-SYP43 (TGN), GFP-SYP61 (TGN), GFP-VAMP727 (endosome), and GFP-VAM3 (vacuole), which were treated with 33 μM Wm or DMSO (control). Arrowheads indicate enlarged endosomes. Bar = 5 μm

analysis using BFA and Wm in root cells of *Arabidopsis thaliana* expressing GFP-SYP32 (*cis*-Golgi) [35], GFP-SYP43 (TGN) [36], GFP-SYP61 (TGN) [37], GFP-VAMP727 (endosomes) [38], or GFP-VAM3/SYP22 (vacuole) [38].

2 Materials

2.1 Plant Materials

1. 7-day-old *Arabidopsis thaliana* seedlings stably expressing the protein of interest fused to a fluorescent protein. We used the following organelle marker lines: proSYP32:GFP-SYP32 (*cis*-Golgi) [35], proSYP43:GFP-SYP43 (TGN) [36], proSYP61:GFP-SYP61 (TGN) [37], proVAMP727:GFP-VAMP727 (endosome) [38], and proVAM3/SYP22:GFP-VAM3/SYP22 (vacuole) [38].

2.2 Culture Media and Stock Solutions

1. Murashige and Skoog (MS) plates: 1× MS, 1% (w/v) sucrose, 0.5% (w/v) gellan gum, 2.5 mM MES adjusted to pH 5.7 with KOH.
2. 50 mM BFA stock solution: 14.02 mg BFA dissolved in 1 ml dimethyl sulfoxide (DMSO). Store aliquots at −20 °C.
3. 10 mM Wm stock solution: 4.28 mg wortmannin dissolved in 1 ml DMSO. Store aliquots at −20 °C.

2.3 Other Reagents and Materials

1. 70% (v/v) ethanol.
2. 99.5% (v/v) ethanol.
3. Surgical tape.
4. Sterile distilled water.
5. Tweezers.
6. Microscope slides and coverslips.
7. Confocal laser scanning microscope.

3 Methods

3.1 Growth of Arabidopsis thaliana

1. Surface sterilize *Arabidopsis thaliana* seeds by incubation in 70% (v/v) ethanol for 10 min, and then rinse the seeds with 99.5% (v/v) ethanol. Remove the ethanol and let the seeds completely dry (*see* **Note 1**).
2. Sow the surface-sterilized seeds on MS plates, and then seal the plates using surgical tape.
3. Place the plates at 4 °C for 48 h to break dormancy.
4. Incubate the plates vertically at 23 °C for 9 days under continuous light.

3.2 BFA Treatment

1. Prepare 60-mm petri dishes with 50 μM BFA or DMSO (as a control) by adding 3 μl 50 mM BFA stock solution or 3 μl DMSO to 2.997 ml sterile distilled water (*see* **Note 2**).
2. Transfer seedlings into individual dishes using tweezers. Briefly shake the dishes and completely soak the root in the solution.

3. Incubate the seedlings for 1–2 h at 23 °C in the dark.
4. Mount the seedling in 50 μM BFA or DMSO on a microscope slide and cover with a coverslip.
5. Observe the root epidermal cells of the seedlings using confocal laser scanning microscopy.

3.3 Wortmannin Treatment

1. Prepare 60-mm petri dishes with 33 μM Wm or DMSO (control) by adding 9.9 μl 10 mM Wm stock solution or 9.9 μl DMSO to 2.99 ml of sterile distilled water (*see* **Note 2**).
2. Transfer seedlings into individual dishes with tweezers. Briefly shake the dishes, and completely soak the root in the solution.
3. Incubate the seedlings for 1 h at 23 °C in the dark.
4. Mount the seedling in 33 μM Wm or DMSO on a microscope slide and cover with a coverslip.
5. Observe the root epidermal cells of the seedlings using confocal laser scanning microscopy.

4 Notes

1. The sterilized seeds can be stored for about 2 weeks.
2. Liquid MS media or 1/2 MS media can be used instead of distilled water. However, note that this will slightly alter the drug effectiveness.

Acknowledgments

This work was supported by Grant-in-Aid for JSPS Research Fellow to J.T. (15J07657) and Grants-in-Aid for Scientific Research to T.U. (No. 15H04627) from the Japan Society for the Promotion of Science.

References

1. Griffing LR, Lin C, Perico C, White RR, Sparkes I (2017) Plant ER geometry and dynamics: biophysical and cytoskeletal control during growth and biotic response. Protoplasma 254(1):43–56. https://doi.org/10.1007/s00709-016-0945-3
2. Fuji K, Shirakawa M, Shimono Y, Kunieda T, Fukao Y, Koumoto Y, Takahashi H, Hara-Nishimura I, Shimada T (2016) The adaptor complex AP-4 regulates vacuolar protein sorting at the trans-Golgi network by interacting with VACUOLAR SORTING RECEPTOR1. Plant Physiol 170(1):211–219. https://doi.org/10.1104/pp.15.00869
3. Dettmer J, Hong-Hermesdorf A, Stierhof YD, Schumacher K (2006) Vacuolar H+-ATPase activity is required for endocytic and secretory trafficking in Arabidopsis. Plant Cell 18(3):715–730. https://doi.org/10.1105/tpc.105.037978
4. Reyes FC, Buono R, Otegui MS (2011) Plant endosomal trafficking pathways. Curr Opin Plant Biol 14(6):666–673. https://doi.org/10.1016/j.pbi.2011.07.009

5. Anders N, Jurgens G (2008) Large ARF guanine nucleotide exchange factors in membrane trafficking. Cellular and molecular life sciences: CMLS 65(21):3433–3445. https://doi.org/10.1007/s00018-008-8227-7
6. Jurgens G, Geldner N (2002) Protein secretion in plants: from the trans-Golgi network to the outer space. Traffic 3(9):605–613
7. Robinson DG, Langhans M, Saint-Jore-Dupas C, Hawes C (2008) BFA effects are tissue and not just plant specific. Trends Plant Sci 13(8):405–408. https://doi.org/10.1016/j.tplants.2008.05.010
8. Du W, Tamura K, Stefano G, Brandizzi F (2013) The integrity of the plant Golgi apparatus depends on cell growth-controlled activity of GNL1. Mol Plant 6(3):905–915. https://doi.org/10.1093/mp/sss124
9. Ito Y, Uemura T, Shoda K, Fujimoto M, Ueda T, Nakano A (2012) Cis-Golgi proteins accumulate near the ER exit sites and act as the scaffold for Golgi regeneration after brefeldin a treatment in tobacco BY-2 cells. Mol Biol Cell 23(16):3203–3214. https://doi.org/10.1091/mbc.E12-01-0034
10. Tse YC, Lo SW, Hillmer S, Dupree P, Jiang L (2006) Dynamic response of prevacuolar compartments to brefeldin a in plant cells. Plant Physiol 142(4):1442–1459. https://doi.org/10.1104/pp.106.090423
11. Ito Y, Toyooka K, Fujimoto M, Ueda T, Uemura T, Nakano A (2017) The trans-Golgi network and the Golgi stacks behave independently during regeneration after brefeldin a treatment in tobacco BY-2 cells. Plant Cell Physiol 58(4):811–821. https://doi.org/10.1093/pcp/pcx028
12. Geldner N, Anders N, Wolters H, Keicher J, Kornberger W, Muller P, Delbarre A, Ueda T, Nakano A, Jurgens G (2003) The Arabidopsis GNOM ARF-GEF mediates endosomal recycling, auxin transport, and auxin-dependent plant growth. Cell 112(2):219–230. doi:S0092867403000035 [pii]
13. Geldner N, Denervaud-Tendon V, Hyman DL, Mayer U, Stierhof YD, Chory J (2009) Rapid, combinatorial analysis of membrane compartments in intact plants with a multicolor marker set. Plant J 59(1):169–178. https://doi.org/10.1111/j.1365-313X.2009.03851.x. TPJ3851 [pii]
14. Teh OK, Moore I (2007) An ARF-GEF acting at the Golgi and in selective endocytosis in polarized plant cells. Nature 448(7152):493–496. https://doi.org/10.1038/nature06023
15. Munnik T, Nielsen E (2011) Green light for polyphosphoinositide signals in plants. Curr Opin Plant Biol 14(5):489–497. https://doi.org/10.1016/j.pbi.2011.06.007
16. Heilmann I (2016) Phosphoinositide signaling in plant development. Development 143(12):2044–2055. https://doi.org/10.1242/dev.136432
17. Simon ML, Platre MP, Assil S, van Wijk R, Chen WY, Chory J, Dreux M, Munnik T, Jaillais Y (2014) A multi-colour/multi-affinity marker set to visualize phosphoinositide dynamics in Arabidopsis. Plant J 77(2):322–337. https://doi.org/10.1111/tpj.12358
18. Thole JM, Nielsen E (2008) Phosphoinositides in plants: novel functions in membrane trafficking. Curr Opin Plant Biol 11(6):620–631. https://doi.org/10.1016/j.pbi.2008.10.010
19. Ischebeck T, Stenzel I, Heilmann I (2008) Type B phosphatidylinositol-4-phosphate 5-kinases mediate Arabidopsis and Nicotiana tabacum pollen tube growth by regulating apical pectin secretion. Plant Cell 20(12):3312–3330. https://doi.org/10.1105/tpc.108.059568
20. Kusano H, Testerink C, Vermeer JE, Tsuge T, Shimada H, Oka A, Munnik T, Aoyama T (2008) The Arabidopsis phosphatidylinositol phosphate 5-kinase PIP5K3 is a key regulator of root hair tip growth. Plant Cell 20(2):367–380. https://doi.org/10.1105/tpc.107.056119
21. Ischebeck T, Werner S, Krishnamoorthy P, Lerche J, Meijon M, Stenzel I, Lofke C, Wiessner T, Im YJ, Perera IY, Iven T, Feussner I, Busch W, Boss WF, Teichmann T, Hause B, Persson S, Heilmann I (2013) Phosphatidylinositol 4,5-bisphosphate influences PIN polarization by controlling clathrin-mediated membrane trafficking in Arabidopsis. Plant Cell 25(12):4894–4911. https://doi.org/10.1105/tpc.113.116582
22. Preuss ML, Schmitz AJ, Thole JM, Bonner HK, Otegui MS, Nielsen E (2006) A role for the RabA4b effector protein PI-4Kbeta1 in polarized expansion of root hair cells in Arabidopsis thaliana. J Cell Biol 172(7):991–998. https://doi.org/10.1083/jcb.200508116
23. Kang BH, Nielsen E, Preuss ML, Mastronarde D, Staehelin LA (2011) Electron tomography of RabA4b- and PI-4Kbeta1-labeled trans Golgi network compartments in Arabidopsis. Traffic 12(3):313–329. https://doi.org/10.1111/j.1600-0854.2010.01146.x
24. Kim DH, Eu YJ, Yoo CM, Kim YW, Pih KT, Jin JB, Kim SJ, Stenmark H, Hwang I (2001) Trafficking of phosphatidylinositol 3-phosphate from the trans-Golgi network to the lumen of the central vacuole in plant cells. Plant Cell 13(2):287–301
25. Phan NQ, Kim SJ, Bassham DC (2008) Overexpression of Arabidopsis sorting nexin AtSNX2b inhibits endocytic trafficking to the vacuole. Mol Plant 1(6):961–976. https://doi.org/10.1093/mp/ssn057

26. Jung JY, Kim YW, Kwak JM, Hwang JU, Young J, Schroeder JI, Hwang I, Lee Y (2002) Phosphatidylinositol 3- and 4-phosphate are required for normal stomatal movements. Plant Cell 14(10):2399–2412
27. Lee Y, Bak G, Choi Y, Chuang WI, Cho HT, Lee Y (2008) Roles of phosphatidylinositol 3-kinase in root hair growth. Plant Physiol 147(2):624–635. https://doi.org/10.1104/pp.108.117341
28. Aggarwal C, Labuz J, Gabrys H (2013) Phosphoinositides play differential roles in regulating phototropin1- and phototropin2-mediated chloroplast movements in Arabidopsis. PLoS One 8(2):e55393. https://doi.org/10.1371/journal.pone.0055393
29. Fujimoto M, Suda Y, Vernhettes S, Nakano A, Ueda T (2015) Phosphatidylinositol 3-kinase and 4-kinase have distinct roles in intracellular trafficking of cellulose synthase complexes in Arabidopsis thaliana. Plant Cell Physiol 56(2):287–298. https://doi.org/10.1093/pcp/pcu195
30. Vermeer JE, Thole JM, Goedhart J, Nielsen E, Munnik T, Gadella TW Jr (2009) Imaging phosphatidylinositol 4-phosphate dynamics in living plant cells. Plant J 57(2):356–372. https://doi.org/10.1111/j.1365-313X.2008.03679.x
31. Krinke O, Ruelland E, Valentova O, Vergnolle C, Renou JP, Taconnat L, Flemr M, Burketova L, Zachowski A (2007) Phosphatidylinositol 4-kinase activation is an early response to salicylic acid in Arabidopsis suspension cells. Plant Physiol 144(3):1347–1359. https://doi.org/10.1104/pp.107.100842
32. Takac T, Pechan T, Samajova O, Samaj J (2013) Vesicular trafficking and stress response coupled to PI3K inhibition by LY294002 as revealed by proteomic and cell biological analysis. J Proteome Res 12(10):4435–4448. https://doi.org/10.1021/pr400466x
33. Jaillais Y, Fobis-Loisy I, Miege C, Gaude T (2008) Evidence for a sorting endosome in Arabidopsis root cells. Plant J 53(2):237–247. https://doi.org/10.1111/j.1365-313X.2007.03338.x
34. Naramoto S, Otegui MS, Kutsuna N, de Rycke R, Dainobu T, Karampelias M, Fujimoto M, Feraru E, Miki D, Fukuda H, Nakano A, Friml J (2014) Insights into the localization and function of the membrane trafficking regulator GNOM ARF-GEF at the Golgi apparatus in Arabidopsis. Plant Cell 26(7):3062–3076. https://doi.org/10.1105/tpc.114.125880
35. Fujiwara M, Uemura T, Ebine K, Nishimori Y, Ueda T, Nakano A, Sato MH, Fukao Y (2014) Interactomics of Qa-SNARE in Arabidopsis thaliana. Plant Cell Physiol 55(4):781–789. https://doi.org/10.1093/pcp/pcu038
36. Uemura T, Kim H, Saito C, Ebine K, Ueda T, Schulze-Lefert P, Nakano A (2012) Qa-SNAREs localized to the trans-Golgi network regulate multiple transport pathways and extracellular disease resistance in plants. Proc Natl Acad Sci U S A 109(5):1784–1789. https://doi.org/10.1073/pnas.1115146109
37. Uemura T, Ueda T, Ohniwa RL, Nakano A, Takeyasu K, Sato MH (2004) Systematic analysis of SNARE molecules in Arabidopsis: dissection of the post-Golgi network in plant cells. Cell Struct Funct 29(2):49–65. doi:JST.JSTAGE/csf/29.49 [pii]
38. Ebine K, Okatani Y, Uemura T, Goh T, Shoda K, Niihama M, Morita MT, Spitzer C, Otegui MS, Nakano A, Ueda T (2008) A SNARE complex unique to seed plants is required for protein storage vacuole biogenesis and seed development of Arabidopsis thaliana. Plant Cell 20(11):3006–3021. https://doi.org/10.1105/tpc.107.057711
39. Nelson BK, Cai X, Nebenfuhr A (2007) A multicolored set of in vivo organelle markers for co-localization studies in Arabidopsis and other plants. Plant J 51(6):1126–1136. doi:TPJ3212 [pii]10.1111/j.1365-313X.2007.03212.x
40. Zheng H, Kunst L, Hawes C, Moore I (2004) A GFP-based assay reveals a role for RHD3 in transport between the endoplasmic reticulum and Golgi apparatus. Plant J 37(3):398–414
41. von der Fecht-Bartenbach J, Bogner M, Krebs M, Stierhof YD, Schumacher K, Ludewig U (2007) Function of the anion transporter AtCLC-d in the trans-Golgi network. Plant J 50(3):466–474. https://doi.org/10.1111/j.1365-313X.2007.03061.x
42. Shirakawa M, Ueda H, Koumoto Y, Fuji K, Nishiyama C, Kohchi T, Hara-Nishimura I, Shimada T (2014) CONTINUOUS VASCULAR RING (COV1) is a trans-Golgi network-localized membrane protein required for Golgi morphology and vacuolar protein sorting. Plant Cell Physiol 55(4):764–772. https://doi.org/10.1093/pcp/pct195
43. Gendre D, Oh J, Boutte Y, Best JG, Samuels L, Nilsson R, Uemura T, Marchant A, Bennett MJ, Grebe M, Bhalerao RP (2011) Conserved Arabidopsis ECHIDNA protein mediates trans-Golgi-network trafficking and cell elongation. Proc Natl Acad Sci U S A 108(19):8048–8053. https://doi.org/10.1073/pnas.1018371108
44. Inada N, Betsuyaku S, Shimada TL, Ebine K, Ito E, Kutsuna N, Hasezawa S, Takano Y, Fukuda H, Nakano A, Ueda T (2016) Modulation of plant RAB GTPase-mediated membrane traffick-

ing pathway at the Interface between plants and obligate Biotrophic pathogens. Plant Cell Physiol 57(9):1854–1864. https://doi.org/10.1093/pcp/pcw107

45. Jaillais Y, Fobis-Loisy I, Miege C, Rollin C, Gaude T (2006) AtSNX1 defines an endosome for auxin-carrier trafficking in Arabidopsis. Nature 443(7107):106–109. https://doi.org/10.1038/nature05046
46. Enami K, Ichikawa M, Uemura T, Kutsuna N, Hasezawa S, Nakagawa T, Nakano A, Sato MH (2009) Differential expression control and polarized distribution of plasma membrane-resident SYP1 SNAREs in Arabidopsis thaliana. Plant Cell Physiol 50(2):280–289. https://doi.org/10.1093/pcp/pcn197
47. Brux A, Liu TY, Krebs M, Stierhof YD, Lohmann JU, Miersch O, Wasternack C, Schumacher K (2008) Reduced V-ATPase activity in the trans-Golgi network causes oxylipin-dependent hypocotyl growth inhibition in Arabidopsis. Plant Cell 20(4):1088–1100. https://doi.org/10.1105/tpc.108.058362
48. Cutler SR, Ehrhardt DW, Griffitts JS, Somerville CR (2000) Random GFP::cDNA fusions enable visualization of subcellular structures in cells of Arabidopsis at a high frequency. Proc Natl Acad Sci U S A 97(7):3718–3723
49. Reichardt I, Stierhof YD, Mayer U, Richter S, Schwarz H, Schumacher K, Jurgens G (2007) Plant cytokinesis requires de novo secretory trafficking but not endocytosis. Curr Biol 17(23):2047–2053. doi:S0960-9822(07)02137-9 [pii]10.1016/j.cub.2007.10.040

Chapter 13

Use Endosidin2 to Study Plant Exocytosis and Vacuolar Trafficking

Lei Huang and Chunhua Zhang

Abstract

Membrane trafficking is essential for multiple aspects of plant growth and development. Some small molecules have been widely used to study the mechanisms of membrane trafficking in plants. For example, short-term treatment with small molecules combined with live cell imaging has been shown to be very useful in understanding the dynamic processes of membrane trafficking. Small molecule Endosidin2 (ES2) has been found to target Exo70 protein and inhibit exocytosis and promote vacuolar trafficking in plants. Here we describe the method of using short-term ES2 treatment combined with live cell imaging to study plant exocytosis and vacuolar trafficking in *Arabidopsis* seedlings expressing a cargo protein PIN2:GFP.

Key words Plant exocytosis, Vacuolar trafficking, Endosidin2 (ES2), PIN2:GFP, Brefeldine A (BFA)

1 Introduction

Plant cells are composed of multiple organelles with distinct morphology and functions. The transport of proteins and lipids among these organelles is through vesicles trafficking, which is essential for proper function of the cells. Vesicle trafficking between organelles is dynamic and bidirectional. Chemical genetic provides valuable tools in studying the process of vesicle trafficking because specific small molecule inhibitors allow transient manipulation of vesicle trafficking process without using genetic mutants. The combination of chemical treatment with live cell imaging of fluorescence-tagged protein has been widely used in plant cell biology research. Usually, the dosage of the small molecule inhibitors and the time length of treatment vary for different experiments, depending on the activity of the small molecules, the process that is being studied, and also the fluorescence-tagged marker protein that is being used. The inhibition by small molecules is often reversible upon removal of these molecules from the treatment media. This allows for better understanding on the mechanisms of the underling cellular process during cell recovery.

Cláudia Pereira (ed.), *Plant Vacuolar Trafficking: Methods and Protocols*, Methods in Molecular Biology, vol. 1789,
https://doi.org/10.1007/978-1-4939-7856-4_13,

Brefeldin A (BFA) is a fungal macrocyclic lactone that inhibits protein secretion and recycling by targeting the guanine nucleotide exchange factors for Arf GTPases [1–5]. Upon BFA treatment, proteins in Golgi, Trans-Golgi network (TGN) and some cargo proteins that constitutively recycle between the plasma membrane and early endosomes are found in large intracellular structures named BFA compartments [6–9]. When BFA is removed from short-term treatments, proteins in BFA compartments can recover from the inhibition and resume their trafficking process. BFA treatment in combination with live cell imaging has been widely used in plants to study vacuolar and endosomal trafficking pathways [10, 11].

Recently, another small molecule, Endosidin 2 (ES2) is shown to target the Exo70 subunit of the exocyst complex to inhibit exocytosis in plants [12]. Upon ES2 treatment, some proteins that are constitutively recycled between plasma membrane and early endosomes, such as PIN2 and BRI1, were affected. For example, in young *Arabidopsis* seedlings, after 2 h of 40 μM ES2 treatment, PIN2:GFP has reduced abundance at the plasma membrane and increased abundance in late endosome/prevacuolar compartments and vacuole. The recovery of proteins in BFA compartments is slowed down by ES2 as well. Thus, ES2 can serve as a valuable tool in studying the trafficking to the plasma membrane and vacuole. Because the processes of exocytosis and vacuolar trafficking are both very dynamic, the time length of ES2 treatment is important. Because GFP is quickly degraded by vacuolar papain-type cysteine proteinase under acidic condition [13], we usually perform ES2 treatment in the dark to observe its effect on vacuolar trafficking of GFP-tagged cargo proteins.

In this protocol, we describe the procedure for ES2 treatment of Arabidopsis seedlings in light and dark conditions. We also describe our procedure of performing ES2 treatment during BFA washout step.

2 Materials

1. 5–8-day-old *Arabidopsis thaliana* seedlings expressing fluorescence-tagged marker proteins, such as PIN2::PIN2:GFP (*see* **Note 1**).
2. Sterilized half strength Murashige and Skoog (MS) liquid medium with 1% (w/v) sucrose, adjusted to pH 5.8 with KOH.
3. Transparent, sterile 24-well tissue culture plate with lid. Usually the plates lay out as 6 wells (labeled 1–6) × 4 wells (labeled A–D).
4. Tweezers.

5. 1.7 or 2.0 mL microcentrifuge tubes.
6. Dimethyl sulfoxide (DMSO).
7. 8 mM ES2 stock solution in DMSO (*see* **Note 2**).
8. 40 mM BFA stock solution (*see* **Note 3**).
9. Glass slide and coverslip.
10. Timer.
11. Aluminum foil.
12. Laser scanning confocal microscope.

3 Method

3.1 Plant Sample Preparation

Arabidopsis seedlings express fluorescence-tagged proteins could be used to study their trafficking to the plasma membrane and vacuole using ES2 treatment. We found *Arabidopsis* roots are most efficient for ES2 uptake in compare with other tissues such as hypocotyls and cotyledons. We recommend observing the effects of ES2 on cargo protein trafficking using root system if the protein is present in roots. If protein of interest is not present in root cells, pollen tubes can be used instead. However, we recommend optimizing the concentration of ES2 first if pollen tubes will be used. Lower concentrations of ES2 (such as 4 μM) can efficiently inhibit exocytosis in pollen tubes [12]. In this protocol, we use *Arabidopsis* seedlings express PIN2::PIN2:GFP as the material.

1. Sterilize *Arabidopsis* PIN2::PIN2:GFP seeds and sow about 30 seeds evenly on one line of a 100 × 100 mm square petri dishes with ½ MS agar using a sterile pipette tip (*see* **Notes 1** and **4**).
2. Allow the petri dishes with seeds to dry in the sterile hood for 5 min and then seal them with micropore surgical tape.
3. Keep the petri dishes with sowed seeds at 4 °C for 2 days to break seed dormancy and then transfer them to the growth chamber and lay them in vertical orientation (*see* **Note 5**).
4. Keep the petri dishes with seeds vertically in the plant growth chamber with light intensity of 130 μmol/m^2/s and temperature at 22 °C for 5–7 days for ES2 treatment experiments.

3.2 ES2 Treatment

ES2 is an inhibitor of exocytosis and causes the accumulation of PIN2 and BRI1 in prevacuolar compartments (PVC) upon short-term treatment [12]. Usually, we can observe PIN2 localization in PVC after 2-h of ES2 treatment at 40 μM. PIN2 trafficking to the vacuole is also enhanced by ES2. However, we can only observe green fluorescence in the vacuole when we perform the treatment in the dark to prevent GFP from proteolysis.

3.2.1 ES2 Treatment in Light Condition

1. Take a new 24-well tissue culture plate and label one well as DMSO and one well as ES2.
2. Add 2 mL ½ MS liquid medium to each labeled well.
3. Take out an aliquot ES2 stock solution (8 mM) from −20 °C freezer and thaw it at room temperature.
4. Add 10 μL DMSO and 10 μL ES2 stock to the ½ MS media in the wells labeled with DMSO and ES2, respectively. Mix the solution with ½ MS media carefully by pipetting up and down (*see* **Note 6**).
5. Take out the petri dishes with 5–7 days old PIN2::PIN2:GFP seedlings from the growth chamber and remove the sealing tape.
6. Use a small tweezers, remove one seedling a time from the petri dish and immerse it in the ½ MS liquid medium containing DMSO or ES2. Repeat this process till we have three seedlings in DMSO well and three seedlings in ES2 well (*see* **Note 7**).
7. Cover the 24-well plate with the lid and transfer it into the growth chamber with light on.
8. After 2 h of treatment, mount the seedlings in a drop of water on glass slides, cover the root with coverslip and observe the PIN2 localization in the root transition zone using laser scanning confocal microscope (*see* **Note 8**). Example images of PIN2 localization after control and ES2 treatment in light condition are shown in Fig. 1A, B, respectively.
9. Quantify the number and size of intracellular compartments that are labeled by PIN2:GFP using ImageJ software.

3.2.2 ES2 Treatment in Dark Condition

To observe vacuolar trafficking of GFP-tagged proteins upon ES2 treatment, we need to completely avoid light during treatment and be very quick during imaging process. We usually perform ES2 dark treatment in individual microcentrifuge tubes instead of 24-well plates.

1. Take six 1.7 mL microcentrifuge tubes and label three tubes as DMSO and three tubes as ES2.
2. And 1 mL ½ MS media to each tube.
3. Add 5 μL DMSO to tubes labeled with DMSO and 5 μL 40 μM ES2 stock to tubes labeled with ES2. Mix by pipetting up and down.
4. Put one 5–7 days old PIN2::PIN2:GFP seedling to each tube and make sure the seedlings are submerged in the media.
5. Wrap each tube with aluminum foil to avoid light. Make sure the whole tube including the cap is covered.
6. Leave the tubes in the growth chamber for 2 h.

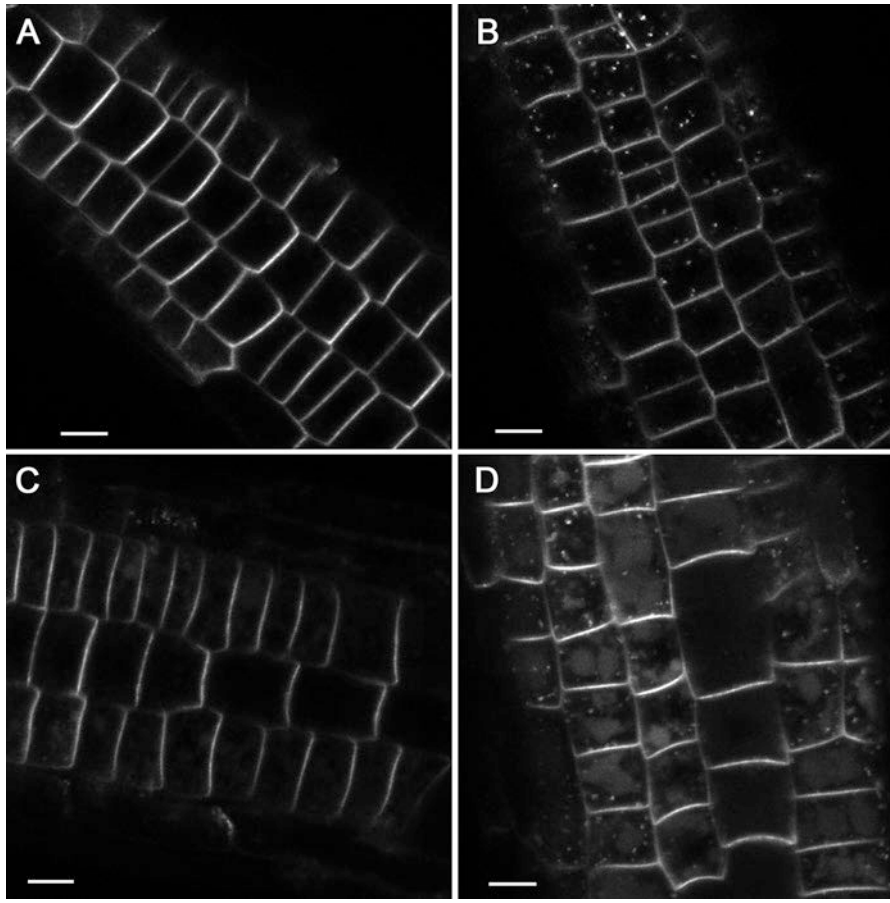

Fig. 1 ES2 reduces PIN2 trafficking to the plasma membrane and enhances PIN2 trafficking to the vacuole. (**A**) and (**B**) PIN2 localization in root epidermal cells after treated with 0.5% DMSO (**A**) or 40 μM ES2 (**B**) for 2 h under light condition. (**C**) and (**D**) PIN2 localization in root epidermal cells after treated with 0.5% DMSO (**C**) or 40 μM ES2 (**D**) for 2 h under dark condition. Scale bars: 10 μm

7. Unwrap one tube a time, mount the seedling to the glass slide with water, add the coverslip and examine PIN2:GFP localization in root transition zone (*see* **Note 9**). Example images of PIN2 localization in the vacuole after control and ES2 treatment is shown in Fig. 1C, D, respectively.
8. Quantify GFP fluorescence in the vacuole using ImageJ.

3.3 BFA Washout Experiment

BFA washout experiment consists of three steps. The first step is to treat seedlings with BFA solution. The second step is to wash the seedlings quickly with ½ MS liquid medium for three times and examine the localization of fluorescence protein upon BFA treatment. The third step is to put the seedling in ½ MS medium containing DMSO or ES2 to recover and examine fluorescence protein localization. The accuracy of BFA washout experiment depends on precise control of BFA treatment time, efficient washing and precise control of recovery time before imaging. We perform BFA

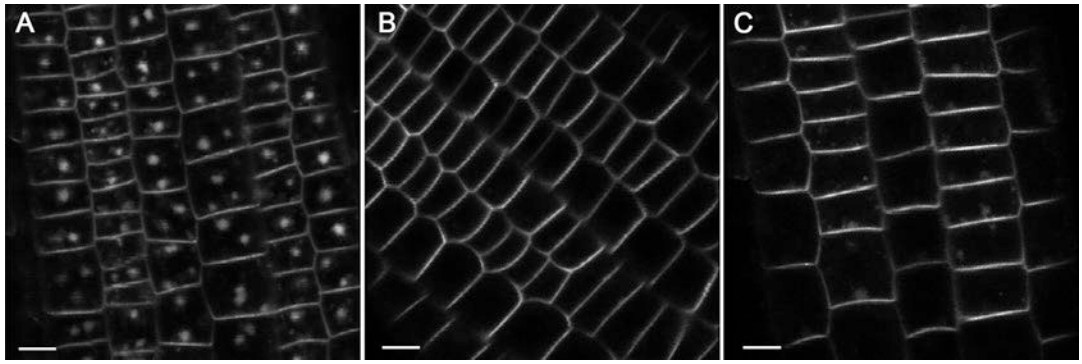

Fig. 2 ES2 reduces recycling efficiency of PIN2 from BFA compartments. (**A**) PIN2 localization after BFA treatment for 60 min. (**B**) PIN2 localization after 80 min of recovery from BFA treatment in ½ MS medium containing 0.5% DMSO. (**C**) PIN2 localization after 80 min of recovery in ½ MS medium containing 40 μM ES2. Scale bars: 10 μm

washout experiment by handling one seedling a time and strictly control the time and efficiency of each step (*see* **Note 10**). After BFA treatment for 60 min, PIN2:GFP is found to accumulate in large intracellular compartments named BFA compartments, as an example shown in Fig. 2A. After recovery for 80 min in 0.5% DMSO, most of the PIN2:GFP is not found in large intracellular compartments anymore (Fig. 2B). Whereas seedlings that have been recovered in ES2, PIN2:GFP is still found in large intracellular compartments (Fig. 2C). This method could be used to study trafficking dynamics of a specific cargo protein or the function of genes of interest in trafficking regulation.

3.3.1 BFA Treatment

1. Prepare two 24-well tissue culture plates and add 2 mL ½ MS liquid medium to all wells in plate 1 and wells A1–A6 on the second plate. At the same time, take out ES2 stock solution (8 mM) and BFA stock solution (40 mM) from −20 °C freezer and thaw at room temperature.
2. Add 2 μL BFA stock solution to wells A1–A6 of the first plate and mix by pipetting up and down.
3. Add 10 μL DMSO to wells A1–A3 of the second plate and add 10 μL ES2 to wells A4–A6 of the second plate. Mix by pipetting up and down.
4. Put one PIN2::PIN2:GFP seedling into A1 well of the first plate. Make sure the seedling is submerged in the solution. At the same time, start a timer as time 0 min.
5. Put one seedling to well A2, A3, A4, A5 and A6 of plate 1 at time 5 min, 10 min, 15 min, 20 min and 25 min, respectively.

3.3.2 Washout

1. At time 60 min, take out the seedling in well A1 on plate 1 using a tweezers. Hold the seedling with the tweezers and quickly rinse it in the ½ MS media in well B1, C1 and D1 of plate 1 sequentially (*see* **Note 11**).

2. Quickly mount the triple-rinsed seedling to the glass slide with a drop of water and examine the localization of PIN2:GFP in root transition zone under confocal microscope (*see* **Note 12**). Image collection step usually takes less than 3 min.
3. After collecting a Z-stack image from the transition zone, transfer the seedling to well A1 of plate 2 for recover.
4. At time 65 min, repeat similar washing step for the seedlings in well A2 of plate 1 using the washing media in wells B2, C2 and D2 of plate 1. Take a Z-stack image after rinsing and then let the seedling recover in well A2 of plate 2.
5. At time 70, 75, 80, and 85 min, repeat the washing steps and image collection for the seedlings in well A3 (rinse in B3, C3, and D3), A4 (rinse in B4, C4 and D4), A5 (rinse in B5, C5 and D5) and A6 (rinse in B6, C6 and D6) of plate 1. The seedlings will be recovered in wells A3, A4, A5 and A6 of plate 2, respectively.
6. At time 140 min, the seedling in well A1 of plate 2 has been recovered from BFA treatment for 80 min and is ready to be examined by confocal microscope again. Mount the seedling to glass slide with a drop of water and take the images from the transition zone of the root.
7. At time 145 min, 150 min, 155 min, 160 min and 165 min, collect images from seedlings in well A2, A3, A4, A5 and A6 of plate 2, respectively.
8. Quantify the number of BFA compartments per cell and measure the intensity of fluorescence intensity of BFA compartments using the ImageJ software.
9. Repeated BFA washout experiment for three independent times to generate triplicate data sets for quantitative image analysis (*see* **Note 13**).

4 Notes

1. Our laboratory grows sterilized Arabidopsis seeds on 0.8% (w/v) agar plates with half-strength Murashige and Skoog (MS) salts and 1% sucrose (w/v) at pH 5.8. We keep the seeds at 4 °C for 2 days before we transfer them to 22 °C to synchronize germination and let them grow for 5–7 days under continuous light at 22 °C [12]. The cargo proteins that have been found to be affected by ES2 include PIN2, PIN1, and BRI1. To study the mechanisms of exocytosis or vacuolar trafficking, these cargo proteins can be used. If a new protein will be used, we suggest to examine the cellular localization pattern of the candidate protein before test it with ES2.

2. We recommend to aliquot the ES2 stock to small volumes such as 100 μL and store at −20 °C to avoid freeze and thaw cycles.
3. We keep the BFA stock solution as 5 μL aliquots at −20 °C.
4. Different protocols for seeds sterilization can be used. We normally wash the seeds in 1.7 mL microcentrifuge tubes with 1 mL 50% bleach (with 0.05% tween-20) for 2 min, then wash the seeds with 1 mL 75% ethanol for 2 min and finally wash the seeds with 1 mL sterilized water for 5 times. When sow the seeds, make sure the seeds are separated with each other and not clustered together. Clustered seeds will result in tangled roots later and will make it difficult to separate them when perform the treatment. We prefer square petri dishes because they are more stable in compare with round dishes when we place them in vertical orientation.
5. By placing the petri dishes with sowed seeds in vertical orientation, the seedlings will grow on the surface of the ½ MS agar and will reduce the root damage when we pull the seedlings out of the petri dishes for treatment.
6. When mixing ES2 solution with ½ MS media, a white cloud of ES2 precipitation is usually seen. The precipitation usually disappears after pipetting up and down.
7. The roots of seedlings at 5–7 days old are soft. It is easier and will have less damage to the roots by taking the seedlings with the tweezers at the hypocotyl region. Make sure each seedling is submerged in the liquid media.
8. To make it easier for image collection, we usually cover the root region with the coverslip and leave the cotyledons out of the coverslip. We use 40× or 60× water objectives for image collection.
9. GFP is quickly degraded in the vacuole once the seedling is exposed to the light. To ensure detection of fluorescence, the sample mounting process and imaging process should be quick.
10. The interval time is reserved for operation the microscope of each seedling, including the time of mounting the seedling and image collection. The interval time varies depending on the degree of efficiency in operating the microscope. We recommend to use 5 min as the time interval between each sample for an experienced microscope operator.
11. The three rinsing steps should take less than 10 s.
12. The region that is chosen for imaging may vary depending on the purpose of the experiment. However, it needs to be consistent among different seedlings in the same experiment.
13. We usually grow seedlings in 3 consecutive days and perform BFA washout experiment in 3 consecutive days as well. This ensures that the seedlings are in the same growth stage.

Acknowledgments

This work was supported by Purdue University Provost start-up fund to C.Z.

References

1. Jackson CL, Casanova JE (2000) Turning on ARF: the Sec7 family of guanine-nucleotide-exchange factors. Trends Cell Biol 10:60–67
2. Mansour SJ, Skaug J, Zhao X-H, Giordano J, Scherer SW, Melançon P (1999) P 200 ARF-GEP1: a Golgi-localized guanine nucleotide exchange protein whose Sec7 domain is targeted by the drug brefeldin A. Proc Natl Acad Sci U S A 96:7968–7973
3. Morinaga N, Adamik R, Moss J, Vaughan M (1999) Brefeldin A inhibited activity of the sec7 domain of p200, a mammalian guanine nucleotide-exchange protein for ADP-ribosylation factors. J Biol Chem 274:17417–17423
4. Peyroche A, Paris S, Jackson CL (1996) Nucleotide exchange on ARF mediated by yeast Gea1 protein. Nature 384:479–481. https://doi.org/10.1038/384479a0
5. Steinmann T, Geldner N, Grebe M, Mangold S, Jackson CL, Paris S, Gälweiler L, Palme K, Jürgens G (1999) Coordinated polar localization of auxin efflux carrier PIN1 by GNOM ARF GEF. Science 286:316–318
6. Geldner N, Anders N, Wolters H, Keicher J, Kornberger W, Muller P, Delbarre A, Ueda T, Nakano A, Jürgens G (2003) The Arabidopsis GNOM ARF-GEF mediates endosomal recycling, auxin transport, and auxin-dependent plant growth. Cell 112:219–230
7. Grebe M, Xu J, Möbius W, Ueda T, Nakano A, Geuze HJ, Rook MB, Scheres B (2003) Arabidopsis sterol endocytosis involves actin-mediated trafficking via ARA6-positive early endosomes. Curr Biol 13:1378–1387
8. Lippincott-Schwartz J, Yuan L, Tipper C, Amherdt M, Orci L, Klausner RD (1991) Brefeldin A's effects on endosomes, lysosomes, and the TGN suggest a general mechanism for regulating organelle structure and membrane traffic. Cell 67:601–616
9. Paciorek T, Zazímalová E, Ruthardt N, Petrásek J, Stierhof YD, Kleine-Vehn J, Morris DA, Emans N, Jürgens G, Geldner N, Friml J (2005) Auxin inhibits endocytosis and promotes its own efflux from cells. Nature 435:1251–1256. https://doi.org/10.1038/nature03633
10. Pedrazzini E, Komarova NY, Rentsch D, Vitale A (2013) Traffic routes and signals for the tonoplast. Traffic 14:622–628. https://doi.org/10.1111/tra.12051
11. Robinson DG, Jiang L, Schumacher K (2008) The endosomal system of plants: charting new and familiar territories. Plant Physiol 147:1482–1492. https://doi.org/10.1104/pp.108.120105
12. Zhang C, Brown MQ, van de Ven W, Zhang ZM, Wu B, Young MC, Synek L, Borchardt D, Harrison R, Pan S, Luo N, Huang YM, Ghang YJ, Ung N, Li R, Isley J, Morikis D, Song J, Guo W, Hooley RJ, Chang CE, Yang Z, Zarsky V, Muday GK, Hicks GR, Raikhel NV (2016) Endosidin2 targets conserved exocyst complex subunit EXO70 to inhibit exocytosis. Proc Natl Acad Sci U S A 113:E41–E50. https://doi.org/10.1073/pnas.1521248112
13. Tamura K, Shimada T, Ono E, Tanaka Y, Nagatani A, Higashi SI, Watanabe M, Nishimura M, Hara-Nishimura I (2003) Why green fluorescent fusion proteins have not been observed in the vacuoles of higher plants. Plant J 35:545–555

Chapter 14

Visualization of RMRs (Receptor Membrane RING-H2) Dimerization in *Nicotiana benthamiana* Leaves Using a Bimolecular Fluorescence Complementation (BiFC) Assay

Alessandro Occhialini

Abstract

The bimolecular fluorescent complementation (BiFC) is a fluorescent complementation method largely used to investigate protein–protein interaction in living cells. This method is based on the ability of two nonfluorescent fragments to assemble forming a native fluorescent reporter with the same spectral properties of the native reporter. Such fragments are fused to putative protein partners that in case of interaction will bring the two halves in close proximity, allowing for the reconstitution of an active fluorescent reporter. The BiFC has been used to investigate protein–protein interaction in a number of different organisms, including plants. In plant cells, many essential pathways of protein trafficking and subcellular localization necessitate the intervention of several protein units organized in multisubunit complexes. It is well known that vacuolar sorting of many secretory soluble proteins require the intervention of specific transmembrane cargo receptors able to interact forming dimers. In this chapter we describe a BiFC method for the efficient visualization of RMR (Receptor Membrane RING-H2) type 2 dimerization in agro-infiltrated *Nicotiana benthamiana* leaves. Furthermore, this relatively simple method represents an optimal strategy to test protein–protein interaction using any other putative protein partners of interest in plant cells.

Key words Bimolecular fluorescent complementation, Yellow fluorescent protein, Protein–protein interaction, Dimerization, Receptor Membrane RING-H2, Protein trafficking, Endomembrane system, Confocal microscopy, *Nicotiana benthamiana*

1 Introduction

In plant cells, the biological function of many proteins depend on cellular context and interaction with others protein partners. Such protein units are assembled in large multisubunit complexes in which several factors act together allowing a specific cellular function. Protein–protein interaction occupy an essential role in cell life providing mechanisms involved in the integration of signals arose from different locations (the external environment and/or different subcellular compartments) and therefore allowing high-regulated processes of communication between different compartments [1, 2].

Cláudia Pereira (ed.), *Plant Vacuolar Trafficking: Methods and Protocols*, Methods in Molecular Biology, vol. 1789,
https://doi.org/10.1007/978-1-4939-7856-4_14,

Considering that many essential processes related to the regulation of protein trafficking between different subcellular compartments require the intervention of several protein units organized in complexes, the study of protein–protein interaction assume relevant interest in the study of endomembrane trafficking.

In plant cells, the mechanisms involved in vacuolar sorting of many soluble secretory proteins necessitate the intervention of transmembrane receptors able to bind particular amino acid sequences (VSDs: vacuolar sorting determinants) located in the precursors of vacuolar proteins [3–5]. So far, two different families of membrane receptors have been characterized in plant cells. The Vacuolar Sorting Receptors (VSRs) [5] encoded by seven genes in *Arabidopsis thaliana* (from *AtVSR1* to *AtVSR7*), and a second less-characterized family, the Receptor Membrane RING-H2 (RMRs) [6] which are encoded by six genes (from *AtRMR1* to *AtRMR6*). A significant feature of such vacuolar receptors is their ability to interact forming dimers (homo- and/or hetero-dimers) [7, 8], suggesting that this type protein–protein interaction is essential for their correct function during protein sorting to vacuoles.

In a recent investigation we have demonstrated by applying a bimolecular fluorescent complementation (BiFC) method that AtRMR2 forms homo-dimers and can also interact with AtRMR1 to form hetero-dimers [8]. Unlike the classical biochemical approaches which necessitate to remove the interacting proteins from their cellular environment, the BiFC is a noninvasive fluorescent method used to visualize protein interaction directly in living cells [9–11]. This technique is classified as a complementation method, which is based on the ability of two nonfluorescent fragments to interact and reconstitute a complete fluorescent protein reporter with the same spectral properties of the native protein [9–12]. Such nonfluorescent fragments are fused to either N- or C-terminus of different protein partners for which a possible interaction is investigated. If the protein partners are able to physically interact, the production of fluorescent signal is visualized by the reconstitution of a native fluorescent reporter (Fig. 1) [9, 11, 12]. Despite the fluorescent reporter originated from two nonfluorescent fragments has unchanged spectral properties, it has been estimated that the intensity of the fluorescent signal is reduced by the 10% compared to the native reporter [12].

The BiFC has been extensively used to investigate protein–protein interaction in a wide number of organisms, such as bacteria, yeast, plants, and mammals [10, 13–15]. Different reporters as well as different pairs of nonfluorescent fragments have found important applications in BiFC [9–11]. The most commonly used reporters belong to the family of GFP (green fluorescent protein) and derivatives (YFP: yellow fluorescent protein; and CFP: cyan fluorescent protein) [12, 13, 16, 17], but red fluorescent protein variants (mRFP: monomeric red fluorescent protein; and mCherry: monomeric Cherry), along with other reporters with different spectral properties

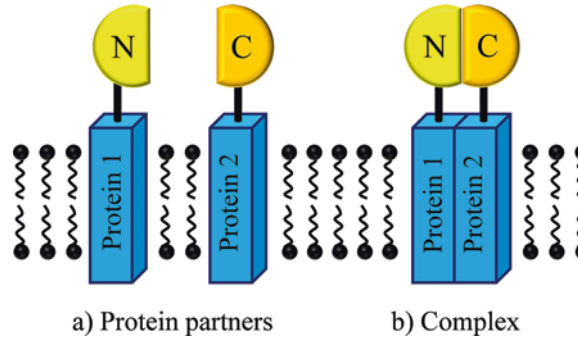

Fig. 1 Representation of BiFC assay to investigate protein–protein interaction between putative transmembrane protein partners. (**a**) The N-terminal (N: yellow) and C-terminal YFP (C: orange) nonfluorescent fragments, are fused to two putative protein–protein interaction partners (protein 1 and 2; blue). (**b**) If such transmembrane proteins are able to interact forming a complex, the two fragments are brought in close proximity reconstituting a native fluorescent reporter

have also been used [18–21]. YFP is one of the most important proteins for BiFC, as the nonfluorescent fragments originated from this reporter exhibit high association efficiency and very low background signal when they do not interact. The two pairs of YFP nonfluorescent fragments originated by truncation at the amino acidic positions 155 or 173 are largely used to investigate protein–protein interaction in both animal and plant cells. Possible drawbacks associated to the use of YFP are the sensitivity to pH and the low maturation time at 37 °C [9, 11–13], which however could be ameliorated by using an optimized YFP variant, known as Venus florescent reporter [22]. Furthermore, the high stability of YFP molecules originated by the assembly of two fragments prevents to visualize the kinetic of dissociation of protein partners [23].

The possibility to investigate protein–protein interaction using relatively simple equipment represents one of the major advantages associated with BiFC. In fact, the signal produced by the interacting proteins can be visualized using a common fluorescent microscope or a more sophisticated confocal microscope [9, 11]. Moreover, this technique does not require particular information about the structure of protein domains involved in the interaction. Possible steric constrains during the association have however to be considered for the success of the method. For instance, the efficient visualization of protein–protein interaction between transmembrane proteins necessitates the localization of nonfluorescent fragments in the same membrane site [9, 11, 17]. In addition, the fusion of the two fragments at either N- or C-terminal ends of protein partners could cover critical domains or prevent their correct folding. The presence of a protein linker between fragments and proteins of interest is important to guarantee the correct folding of fusion proteins [9, 11, 17].

The BiFC can be used in both transient and stable expression systems, and a wide number of different promoters can be used to obtain optimal expression levels. In general strong constitutive promoters such as the cauliflower mosaic virus (CaMV) 35S promoter and derivatives are used to guarantee high expression levels. Weak constitutive promoters and inducible promoters are preferred in case of excess of protein overexpression that in some cases could provoke mislocalization and nonspecific protein interactions [9, 11, 17]. Considering these drawbacks, the BiFC require to be validated using appropriate positive and negative controls. Optimal negative controls are represented by the co-expression of two non-interacting fusion proteins localized in the same subcellular compartments, or the introduction of specific point mutations preventing the interaction between protein partners. On the contrary, either natural or synthetic proteins able to interact forming complexes can be used as positive controls [12, 17, 24].

In the following chapter, the design of a BiFC assay for efficient visualization of AtRMR2 homo-dimers in agro-infiltrated *Nicotiana benthamiana* leaves is described. The simplicity of the method and possibility to be performed using relative simple equipment make this method applicable in the most laboratories of molecular biology. Furthermore, the pair of vectors for BiFC here described represents a valuable material for the investigation of protein–protein interaction of any other putative soluble or transmembrane protein partners in the plant secretory pathway.

2 Material

Prepare all solutions using ultrapure water (18 MΩ-cm resistivity at 25 °C). Sterilize all solutions by autoclaving (30 min at 121 °C and chamber pressure of ~16–20 psi), except the antibiotics which are filter-sterilized (0.2 μm filters).

2.1 Medium for Bacterial Culture

1. LB-liquid medium: 1% (w/v) Bacto tryptone, 0.5% (w/v) yeast extract, 1% (w/v) NaCl. For 1 L of medium, combine 10 g of Bacto tryptone, 5 g of yeast extract, and 10 g of NaCl. Add about 0.95 L of H_2O in a beaker and stir until components are completely dissolved. Adjust the pH to 7 using 1 M NaOH, and then adjust the final volume to 1 L using H_2O. Sterilize by autoclaving. Store at room temperature.
2. LB-agar medium: LB-liquid medium, 1.5% (w/v) agar. Prepare 1 L of LB-liquid medium and add 15 g of agar before autoclaving. Store at room temperature and use 20–25 mL of medium per petri dish.
3. Kanamycin stock-solution (50 mg/mL). Dissolve 500 mg of kanamycin in 10 mL of H_2O. Filter-sterilize, make aliquots of 1 mL and store at −20 °C (*see* **Note 1**).

4. Tetracycline stock-solution (5 mg/mL). Dissolve 50 mg of tetracycline in 10 mL absolute ethanol. Make aliquots of 1 mL and store at −20 °C (*see* **Note 2**).
5. Rifampicin stock-solution (50 mg/mL). Dissolve 500 mg of rifampicin in 10 mL of dimethyl sulfoxide (DMSO). Make aliquots of 1 mL and store at −20 °C (*see* **Note 3**).
6. LB-selective medium: LB-liquid or agar medium with appropriate selective agents as specified in the text. The final concentrations of selective agents are: 50 μg/mL kanamycin, 5 μg/mL tetracycline, and 50 μg/mL rifampicin. For 1 L of sterile LB medium, add 1 mL kanamycin stock-solution (50 mg/mL), 1 mL of tetracycline stock-solution (5 mg/mL), and 1 mL of rifampicin stock-solution (50 mg/mL). Before using, add antibiotics to precooled sterile LB medium at room temperature or ~50 °C for liquid and solid medium, respectively. Store at 4 °C (*see* **Note 4**).

2.2 Preparation of Electro-competent A. tumefaciens Cells

1. Washing solution: 10% (v/v) glycerol in H_2O. Add 100 mL of glycerol in a graduated cylinder and then adjust the volume to 1 L with H_2O. Mix well until glycerol is completed dissolved. Sterilize by autoclaving at store at 4 °C.

2.3 Transformation of A. tumefaciens by Electroporation

1. LB medium. *See* **items 1**, **2** and **6**, Subheading 2.1.
2. 5 M NaCl. Dissolve 292.20 g of NaCl in 1 L of H_2O. Sterilize by autoclaving and store at room temperature.
3. 1 M KCl. Dissolve 74.55 g of KCl in 1 L of H_2O. Sterilize by autoclaving and store at room temperature.
4. 1 M $MgCl_2 \cdot 6H_2O$. Dissolve 203.30 g of $MgCl_2$ in 1 L of H_2O. Sterilize by autoclaving and store at room temperature.
5. 1 M $MgSO_4$. Dissolve 120.37 g of $MgSO_4$ in 1 L of H_2O. Sterilize by autoclaving and store at room temperature.
6. 1 M glucose. Dissolve 180.15 g of glucose in 1 L of H_2O. Sterilize by autoclaving and store at room temperature (*see* **Note 5**).
7. SOC-medium: 2% (w/v) Bacto tryptone, 0.5% (w/v) yeast extract, 10 mM NaCl, 2.5 mM KCl, 10 mM $MgCl_2$, 10 mM $MgSO_4$, and 20 mM glucose. For 1 L of solution, add 20 g Bacto tryptone, 5 g yeast extract, 2 mL of 5 M NaCl, 2.5 mL of 1 M KCl, 10 mL of 1 M $MgCl_2$, 10 mL of 1 M $MgSO_4$, and 20 mL of 1 M glucose to ~0.9 L of H_2O. Stir until components are completely dissolved. Adjust the pH to 7 using 1 M NaOH, and then adjust the final volume to 1 L using H_2O. Sterilize by autoclaving, make aliquots and store at 4 °C (*see* **Note 6**).

2.4 Agro-Infiltration of N. benthamiana Leaves

1. 1 M MES. Dissolve 195.20 g of MES (2-(N-morpholino)-ethanesulfonic acid) in 1 L of H_2O. Sterilize by autoclaving and store at room temperature.
2. 1 M of Na_3PO_4. Dissolve 163.94 g of Na_3PO_4 in 1 L of H_2O. Sterilize by autoclaving and store at room temperature.
3. 1 M glucose. *See* **item 6**, Subheading 2.3.
4. Agro-infiltration buffer: 50 mM MES, 2 mM Na_3PO_4, 5 mM glucose. For 1 L of solution add 50 mL of 1 M MES, 2 mL of 1 M of Na_3PO_4, and 5 mL of 1 M glucose to ~0.9 L of H_2O. Adjust the pH to 5.6 using 1 M NaOH. Adjust the volume to 1 L and sterilize by autoclaving (*see* **Note 7**).
5. Acetosyringone stock-solution (100 mM). Dissolve 196.20 mg of acetosyringone in 10 mL of DMSO. Make 1 mL aliquots and store at −20 °C.
6. Agro-infiltration buffer, 100 μM acetosyringone. Add 1 mL of acetosyringone stock-solution (100 mM) in 1 L of agro-infiltration buffer (*see* **Note 8**).

2.5 Growth Condition for Nicotiana benthamiana

1. Grow *Nicotiana benthamiana* in controlled environment at light intensity of 120 μE/m²·s with a photoperiod of 16 h of light and 8 h of dark. Set the temperature at 22 °C during the day and 20 °C for the night, while keep the humidity constant at ~70%. Grow plants in 10 cm pots in nonsterile conditions using soil (45% sand; 10% perlite; 25% compost; 20% peat). Keep plants well-watered.

2.6 Equipment

1. Plant growth chamber.
2. Shaker and incubator at 28 °C and 37 °C.
3. Benchtop centrifuge.
4. Heating block equipped with temperature setting.
5. Thermocycler.
6. Electroporator.
7. Confocal microscope.

3 Methods

3.1 Constructions and Plasmids

1. Choose a suitable binary Ti vector for plant transformation via *Agrobacterium tumefaciens* (*see* **Note 9**). We use the Ti plasmid pGREEN0229 [25] equipped with cauliflower mosaic virus (CaMV) 35S promoter and the associated helper plasmid pSOUP. Such vector, that we named pGREEN-35S, has been obtained by cloning the 35S promoter and terminator from the pGY1 plant expression vector [26] into *Xho*I/*Sac*I restriction sites located in the multi cloning site (MCS) of pGREEN0229.

2. Generate DNA sequences encoding for an N-terminal YFP fragment (nYFP, aa 1–155) and a C-terminal YFP fragment (cYFP, aa 156–239) [13, 23]. Such DNA sequences can be obtained by performing two different sets of PCR, composed by two sequential PCR for each set. The primer pairs 1 and 7 (PCR 1), and 3 and 7 (PCR 2) are used to generate the *nYFP* fragment, while the primer pairs 2 and 6 (PCR 3) and, 3 and 6 (PCR 4) to generate the *cYFP* fragment (Table 1; *see* **Note 10**). Any plasmid equipped with the *YFP* cDNA can be use as substrate for PCR 1 and 3 (~50 ng of plasmid), while the PCR 2 and 4 are performed using the products of PCR 1 and 3 (~100 ng of PCR product), respectively. Such reactions produce the DNA sequences *MCS:Gly$_6$:HA:nYFP:Sal*I and *MCS:Gly$_6$:Myc:cYFP:Sal*I encoding for the N-terminal and C-terminal YFP fragments for BiFC, respectively. Both genes (*nYFP* and *cYFP*) are fused at their 5′ ends with a MCS (*Bam*HI, *Eco*RI, *Xba*I, *Hind*III, *Spe*I and *Nde*I), along with a sequence encoding a six-glycine spacer (*Gly$_6$*) and a protein tag, HA (*HA* for *nYFP*) or Myc (*Myc* for *cYFP*) (*see* **Note 11**). Both sequences are also generated with a 3′-*Sal*I restriction site.
3. Clone the *MCS:Gly$_6$:HA:nYFP:Sal*I and *MCS:Gly$_6$:Myc:cYFP:Sal*I fragments into pGREEN-35S, using *Bam*HI and *Sal*I restriction sites. By applying the aforementioned sequential PCR we add six extra basis at both 5′ and 3′ ends, allowing the fragments to be cut directly without subcloning into a suitable T/A cloning vector (*see* **Note 12**). In this step, the two empty vectors for BiFC, pGREEN-nYFP and pGREEN-cYFP, are generated (*see* **Note 13**).
4. Generate a DNA fragment encoding for AtRMR2 without the C-terminal RING-H2 and Ser-Rich domains (*AtRMR2ΔRingSer*, aa 1–207) (*see* **Note 14**). This DNA fragment is obtained by PCR using the primer 4 and 8 (Table 1), and a total cDNA preparation from *Arabidopsis thaliana* Col-0 as substrate [8]. This reaction produces an *AtRMR2ΔRingSer* fragment equipped with *Eco*RI and *Hind*III sites along with six extra basis at the 5′ and 3′ ends, respectively.
5. Generate a DNA fragment encoding for the positive control protein p6 from the Beet Yellow Virus (BYV) [27] (*see* **Note 15**). This fragment can be obtained by PCR, using the primer pair 5/9 (Table 1) and a cDNA encoding for p6. Using these primers, a *p6* fragment equipped with a 5′-*Eco*RI and 3′-*Spe*I sites along with six extra basis at both ends, is produced.
6. Clone the *AtRMR2ΔRingSer* fragment into *Eco*RI and *Hind*III sites of pGREEN-nYFP and pGREEN-cYFP, generating the two vectors for AtRMR2 BiFC, pGREEN AtRMR2ΔRingSer-nYFP and pGREEN AtRMR2ΔRingSer-cYFP, respectively. For the positive control, clone the *p6*

Table 1
List of oligonucleotides used in the construction of BiFC vectors

Primer number	Primer name	5′–3′ Sequence
1	Spacer-HA-YFP-n-fw	GGAGGAGGAGGAGGAGGATACCCATACGACGTCCCAGACTACGCTGTGAGCAAGGGCGAGGAGCTG
2	Spacer-Myc-YFP-c-fw	GGAGGAGGAGGAGGAGGAGAACAACAAAAACTTATTTCTGAAGAAGATCTGGACAAGCAGAAGAACGGCATC
3	MCS-spacer-fw	GCGCGCGGATCCGAATTCTCTAGAAAGCTTACTAGTCATATGGGAGGAGGAGGAGGAGGA
4	EcoRI-RMR2-fw	GCGCGCGAATTCATGAATCGTGCTTTGGTCC
5	EcoRI-p6-fw	GCGCGCGAATTCATGGACTGTGTACTCCGCTC
6	c-YFP-rev	GCGCGCGTCGACTTACTTGTACAGCTCGTC
7	n-YFP-rev	GCGCGCGTCGACTTAGGCCATGATATAGAC
8	DRS-RMR2-HindIII-rev	GGCCGGAAGCTTGCTCATACCGTGAAACTCA
9	p6-SpeI-rev	GCGCGCACTAGTCACGACCGTGGAACGGTTGA

The oligonucleotide sequences are named and numbered from 1 to 5 (forward primers) and 6 to 9 (reverse primers)

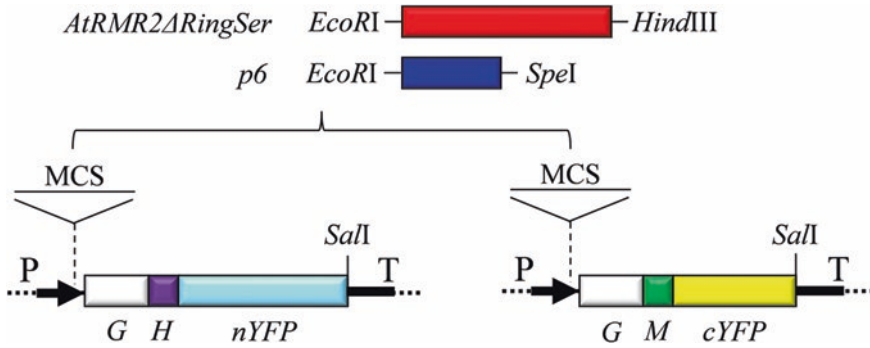

Fig. 2 Schematic representation of constructions for BiFC. DNA-sequences encoding the N-terminal (*nYFP*; cyan) and C-terminal (*cYFP*; yellow) YFP fragments are fused at their 5′ ends with sequences encoding for a six-glycine spacer (*G: Gly6*; white) along with an HA (*HA*: *H*; violet) or Myc (*Myc*: *M*; green) protein-tags. The cDNA encoding for AtRMR2 without the RING-H2 and Ser-Rich domains (*AtRMR2ΔRingSer*; red), and the positive control p6 (*p6*; blue) are cloned into the multi cloning site (MCS: *Bam*HI, *Eco*RI, *Xba*I, *Hind*III, *Spe*I and *Nde*I) of both vectors using *EcoR*I/*Hind*III and *EcoR*I/*Spe*I, respectively. The position of a *Sal*I restriction site at 3′ end of both *nYFP* and *cYFP* is also indicated. The expression of YFP fragments is under the control of the cauliflower mosaic virus (CaMV) 35S promoter (P) and terminator (T) of pGREEN-35S plasmid

fragment into the *Eco*RI and *Spe*I sites of pGREEN-nYFP and pGREEN-cYFP vectors, generating the two positive control vectors, pGREEN p6-nYFP and pGREEN p6-cYFP, respectively.

7. In Fig. 2 a schematic representation of the aforementioned constructions for BiFC is represented.

3.2 Preparation of Electro-Competent *A. tumefaciens* Cells

1. Strip *A. tumefaciens* strain GV3101 already transformed with the helper plasmid pSOUP (from glycerol stock stored at −80 °C) on a freshly made petri dish containing selective LB-agar medium (50 μg/mL rifampicin; 5 μg/mL tetracycline). Let the bacteria grow for ~48 h at 28 °C (*see* **Note 16**).
2. Inoculate a single bacterial colony from the previously made petri dish in selective LB-liquid medium (50 μg/mL rifampicin; 5 μg/mL tetracycline), and incubate for ~48 h at 28 °C in a shaker (200 rpm).
3. Inoculate 500 mL of fresh selective LB-liquid medium (50 μg/mL rifampicin; 5 μg/mL tetracycline) with 5 mL of bacterial preculture (1/100 dilution: 1 mL of preculture per each 100 mL of fresh medium). Incubate at 28 °C in a shaker (200 rpm) to an optical density (OD_{600}) of ~0.5–0.8 that represent the exponential phase of bacterial growth. Generally, *A. tumefaciens* reaches this OD value in ~8–10 h (*see* **Note 17**).
4. Transfer the bacterial culture in precooled ice-cold 50 mL falcon tubes and then centrifuge at 4000 × *g* for 15 min at 4 °C

(*see* **Note 18**). From this step, keep the cell cold on ice throughout all the remaining steps of the procedure.

5. Remove as much of the supernatant as possible, and then resuspend the bacterial pellet in ice-cold washing solution, keeping the bottles on ice (*see* **Note 19**). Centrifuge at 4000 × *g* for 15 min at 4 °C and then remove the supernatant. Wash the bacterial pellet for two more times.
6. At the end of the last wash, resuspend the cell in ~5 mL of ice-cold washing solution (1 mL of washing solution per each 100 mL of starting bacterial culture). Make 50 μL aliquots using prechilled 1.5 mL tubes on ice and then snap-freeze immediately in liquid nitrogen (LN_2). Store *A. tumefaciens* aliquots at −80 °C up to 10–12 months.

3.3 Transformation of A. tumefaciens by Electroporation

1. Remove an aliquot of electro-competent *A. tumefaciens* from −80 °C and thaw the cells on ice (use one aliquot per each transformation). When the cells are completely thawed, add 30 ng of plasmid (1 μL of 30 ng/μL plasmid solution in H_2O) and mix gently using the tip of the manual pipette (*see* **Note 20**).
2. Transfer the bacterial cells plus DNA to a prechilled 0.1 cm electroporation cuvette on ice. Gently tap the cuvette to eliminate air bubbles and remove any remaining residue of ice wiping the exterior of the cuvette. Place the cuvette in a correct orientation in the cell of the electroporator apparatus (preset at 2.2 kV of charging voltage, 200 Ohms of electrical resistance, and 25 μF of electrical capacitance) and immediately press the pulse button of the instrument until the acoustic signal will indicate the end of transformation. A time constant of electric field decay after electroporation of ~4–5 ms (shown in the screen of the instrument) indicate a good event of transformation (*see* **Note 21**).
3. After electroporation, gently resuspend the cells in 1 mL of SOC-medium (without antibiotics). Transfer the transformed *A. tumefaciens* in a clean 1.5 mL tube and incubate for 1–2 h at 28 °C under gentle agitation.
4. Pellet the transformed cells by centrifuging for 5 minutes at 4000 × *g* at room temperature. Discard the supernatant and resuspend the bacterial pellet in 200 μL of LB-medium (without antibiotics).
5. Plate 20 μL (1/10) and the remaining 180 μL (9/10) of transformed cells in two different petri dishes containing selective LB-agar medium (50 μg/mL kanamycin, 5 μg/mL tetracycline, and 50 μg/mL rifampicin) and incubate for ~48–72 h at 28 °C (*see* **Note 22**).

3.4 Agro-Infiltration of N. benthamiana Leaves and Visualization of YFP Signal

1. Inoculate a single bacterial colony from each previously transformed *A. tumefaciens* strains in 5 mL of selective LB-liquid medium (50 μg/mL kanamycin, 5 μg/mL tetracycline, and 50 μg/mL rifampicin) and grow at 28 °C for ~48 h under shaking (200 rpm).
2. Inoculate 1 mL of each preculture in 50 mL of fresh selective LB-liquid medium (50 μg/mL kanamycin, 5 μg/mL tetracycline, and 50 μg/mL rifampicin) and incubated at 28 °C under shaking (200 rpm) for ~24 h (*see* **Note 23**).
3. Transfer bacteria cultures in 50 mL tubes and centrifuge at 4000 × *g* for 10 min at room temperature. Remove as much of the supernatant as possible and then gently resuspend the pellet in 10 mL of agro-infiltration buffer using a manual pipette. Repeat this step two more times.
4. After the last wash, resuspend *A. tumefaciens* in agro-infiltration buffer containing 100 μM acetosyringone to an OD_{600} of about 0.5 (*see* **Note 24**). Thereafter, incubate the *A. tumefaciens* solutions for 1–2 h in the dark at room temperature gently agitating using a benchtop shaker.
5. Combine an equal volume of two *A. tumefaciens* solutions transformed with constructs encoding for N- and C-terminal YFP-fusion proteins for BiFC, respectively (e.g., pGREEN AtRMR2ΔRingSer-nYFP and pGREEN AtRMR2ΔRingSer-cYFP). Prepare an optimal amount of bacterial solution for your experiment, considering that 1–1.5 mL is enough to transform a fully expanded *N. benthamiana* leaf. To increase the expression of YFP fusion proteins, the bacterial solutions can be combined with an equal volume of an *A. tumefaciens* strain carrying a plasmid encoding the viral protein p19 [8, 28] (*see* **Note 25**).
6. By using a 1 mL syringe, infiltrate agrobacterial solution into 4–5-week-old *N. benthamiana* leaves, applying gentle pressure on the bottom leaf epidermis (*see* **Note 26**). Using a marker pen, circle the spot of infiltration to facilitate the following recognition of transformed area. Incubate the plants overnight in the dark (~12 h) at the growth conditions described before (Subheading 2.5).
7. Observe leaf material in proximity of the infiltration spot, 1 day (24 h), 2 days (48 h) and 3 days (72 h) post infiltration using a laser scanning confocal microscope (*see* **Note 27**). The excitation and emission wavelengths of YFP are 514 nm and 527 nm, respectively [29, 30]. Generally, this fluorescent reporter is imaged using an excitation argon laser (514 nm) and an appropriate emission filter (525LP). To guarantee reliability of the method, observe samples along with the positive and negative controls, the same day using the same setting

parameters of the microscope (laser power, gain, offset and magnification). In order to obtain representative results, take several pictures from several leaves of different transformed plants (at least three) of both samples and controls.

8. In Fig. 3 an experiment of BiFC to visualize AtRMR2ΔRingSer homo-dimerization is shown. A clear YFP fluorescent signal in leaves expressing AtRMR2ΔRingSer-nYFP/-cYFP indicates homo-dimerization (Fig. 3c, d). Both positive (Fig. 3a, b) and negative (Fig. 3e–n) controls support optimal functioning of this method to test protein–protein interaction. The surface plots (Fig. 4) of confocal images shown in Fig. 3 depict the different fluorescent intensities between positive (Fig. 4a, b) and negative (Fig. 4c–f) BiFC signals.

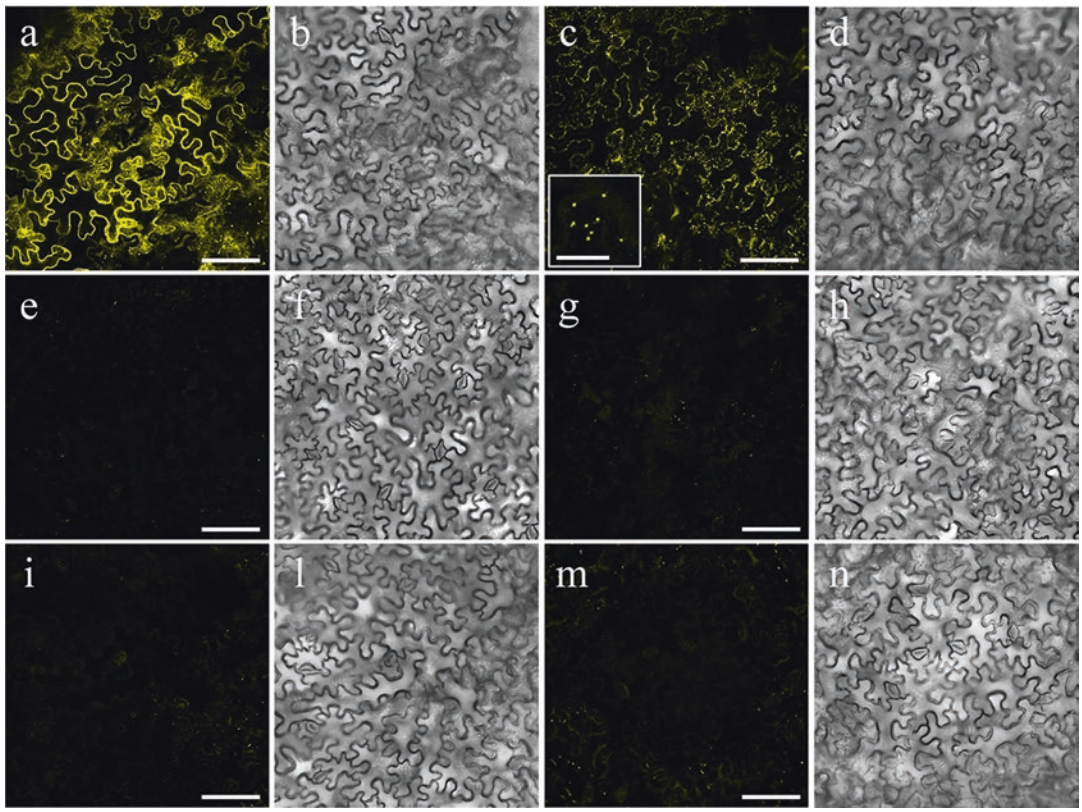

Fig. 3 Dimerization of AtRMR2ΔRingSer visualized by BiFC. Confocal images of agro-infiltrated *N. benthamiana* epidermal cells expressing BiFC constructs: (**a**, **b**) The positive control, p6-nYFP and p6-cYFP, showing a clear YFP signal; (**c**, **d**) AtRMR2ΔRingSer-nYFP and AtRMR2ΔRingSer-cYFP, showing a clear YFP signal indicating homo-dimerization; (**e**, **f**) negative control, AtRMR2ΔRingSer-nYFP alone; (**g**, **h**) negative control, AtRMR2ΔRingSer-cYFP alone; (**i**, **l**) negative control, AtRMR1ΔRing-nYFP and p6-cYFP; (**m**, **n**) negative control, p6-nYFP and AtRMR1ΔRing-cYFP. (**c**) Insert showing the subcellular localization of AtRMR2ΔRingSer homodimers in punctate structures. YFP signal (**a**, **c**, **e**, **g**, **i**, **m**); bright field (**b**, **d**, **f**, **h**, **l**, **n**). Scale bars = 100 μm (**a**–**n**); insert = 20 μm (**c**)

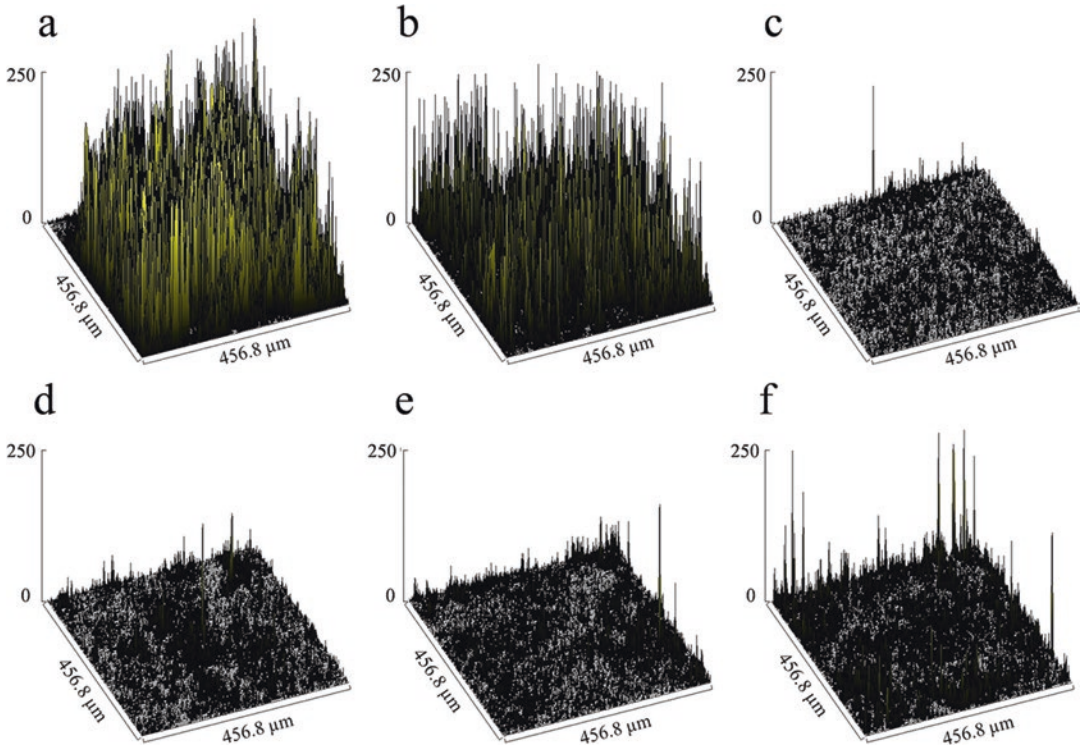

Fig. 4 Surface plots of confocal images. Three-dimensional graphs showing histograms of pixel intensities (z axis) of confocal images shown in Fig. 3. (**a**) The positive control, p6-nYFP and p6-cYFP; (**b**) AtRMR2ΔRingSer-nYFP and AtRMR2ΔRingSer-cYFP; (**c**) negative control, AtRMR2ΔRingSer-nYFP alone; (**d**) negative control, AtRMR2ΔRingSer-cYFP alone; (**e**) negative control, AtRMR1ΔRing-nYFP and p6-cYFP; (**f**) negative control, p6-nYFP and AtRMR1ΔRing-cYFP. The image sizes in μm are indicated in the x and y axis. Surface plots obtained using ImageJ 1.41o (National Institute of Health, Bethesda, MD, USA)

4 Notes

1. Filter-sterilize kanamycin using 0.2 μm filter devices with syringe adaptor. Perform all step under the fume hood in sterile conditions, using autoclaved tips and tubes. Make aliquots and store at −20 °C up to 12 months. Protect the antibiotic from direct light exposition, kanamycin is light-sensitive.
2. Tetracycline is difficult to solubilize and tend to precipitate in solution. For preparation of the stock solution mix thoroughly by vortexing and check the presence of insoluble precipitates before using. Tetracycline is resuspended in absolute ethanol and therefore do not necessitate to be filter-sterilized. Use sterile tips and tubes to make aliquots and store at −20 °C up to 12 months. Protect the antibiotic from direct light exposition, tetracycline is light-sensitive.

3. The rifampicin stock-solution in DMSO does not need to be filter-sterilized. Use sterile tips and tubes to make aliquots and store at −20 °C up to 12 months. As the previous two antibiotics, protect rifampicin from direct light exposition.
4. Antibiotics are temperature sensitive, do not add these selective agents to LB medium before autoclaving. The medium needs to be precooled before adding antibiotics: At room temperature for LB liquid; and ~50 °C for LB agar, preventing solidification of the medium.
5. 1 M glucose can get easily contaminated if used in nonsterile condition. Open the stock solution under the fume hood and store at room temperature or 4 °C after utilization.
6. SOC-medium can be stored in aliquots at −20 °C for a longer period of time (up to 12 months).
7. Agro-infiltration buffer contain glucose and can get contaminated if used in nonsterile condition. Make aliquots of 50 mL and use the necessary amount in nonsterile condition the day of transformation. Store at room temperature or 4 °C.
8. Acetosyringone stock solution do not necessitate to be filter-sterilized. Add fresh acetosyringone in agro-infiltration buffer immediately before plant transformation.
9. From the first efforts to generate a T-DNA vector for plant transformation [31, 32], over the past 30 years many sophisticated binary Ti vector systems for specialized purposes have been generated. A description of different features and a list of commonly used T-DNA binary vectors for plant transformation can be found in many complete review papers [33–35]. The most recent Ti binary vectors from pMDC series represent an optimal choice.
10. Perform gradient PCR to determine the optimum annealing temperature of primers used in the construction of BiFC vectors (Table 1). Such procedure is necessary to optimize PCR reactions using the long forward primers 1, 2, and 3 (66, 72 and 60 bp in length, respectively). We obtained good amount of PCR products using: Annealing temperature of ~60 °C for 30 s; 60 s of extension at 72 °C (~1 min/kb) catalyzed by a proofreading DNA polymerase; and 35 cycles of PCR. We suggest to check the accuracy of sequences before proceeding to the following steps of cloning.
11. The introduction of a six-glycine spacer (Gly6) in between YFP fragments and protein partners is necessary to space two different protein units along the same fusion protein and to guarantee their correct folding. The introduction of two different protein tags (HA and Myc) along with the N and C-terminal fragments, is useful to verify the expression of both BiFC fusion proteins by immunoblot.

12. The addition of six extra basis at both 5′ and 3′ ends of *MCS:Gly6:HA:nYFP:SalI* and *MCS:Gly6:Myc:cYFP:SalI* is necessary to give enough spacing and allow efficient annealing of restriction enzymes.
13. The two empty vectors for BiFC, pGREEN-nYFP and pGREEN-cYFP, can be used to test protein–protein interaction between any other protein partners of interest. These constructs are equipped with a MCS composed by six different restriction enzyme recognition sites that can be used for in-frame cloning with both *nYFP* and *cYFP* downstream genes.
14. The deletion mutant AtRMR2ΔRingSer lacking the C-terminal Ring-H2/Ser-Rich is more expressed (or more stable) facilitating efficient detection of BiFC signal. We demonstrated that the deletion of such C-terminal domains does not prevent correct protein–protein interaction, as the transmembrane domain and the neighboring sequences are the domains necessary for AtRMR2 homo-dimerization [8].
15. The positive control protein p6 (from the Beet Yellow Virus, BYV) is a 6-kDa nonstructural movement protein localized in the endoplasmic reticulum (ER) of infected plant cells. This protein is able to form homo-dimers by the formation of a disulfide bond between cysteine residues [27].
16. *A. tumefaciens* is characterized by lower growth rate comparing to *E. coli*. At 28 °C, untransformed *A. tumefaciens* takes ~24–48 h to grow in LB agar medium, whereas transformed bacteria inoculated in medium containing three selective agents (rifampicin, kanamycin, and tetracycline) grow in about 48–72 h. Both transformed and untransformed *A. tumefaciens* strains grow faster in liquid cultures when inoculated with freshly made precultures.
17. The preparation of electro-competent *A. tumefaciens* cells requires long time, therefore we suggest to start the culture early in the morning in order to have bacteria cells ready by the evening. It is also possible to start overnight culture, but it is necessary to make sure that the bacterial culture will not reach the stationary phase of growth (do not exceed OD_{600} ~1). Growing *A. tumefaciens* overnight at room temperature (~24–25 °C) will help to maintain bacteria in exponential growth phase for a longer period of time.
18. Regular bacterial pellet in the bottom of the tube can be obtained using a benchtop centrifuge equipped with a swing rotor.
19. Keep the tube on ice and gently resuspend the bacterial pellet using a manual pipette. It is important to do not warm up the bacterial pellet by holding the tube from the bottom. Prefer to hold the tube from the top.
20. It is also possible to transform simultaneously *A. tumefaciens* with both plasmid of interest and helper plasmid. In this case,

add an equal amount of each plasmid (30 ng) into the same cuvette for electroporation, and proceed with the transformation protocol described in Subheading 3.3.

21. During electroporation if you hear a popping sound, the transformation has failed. The presence of air bobbles and salts in the electroporation cuvette are the main factors causing arcing of the electric field and the failure of transformation. It is very important to gently tap the cuvette to eliminate any residual air bubbles, and use pure DNA preparation resuspended in ultrapure H_2O (this guarantee very low salt concentration). Commercial plasmid minipreps kits guarantee a good quality of DNA suitable for electroporation. In case enough funding for buying expensive kits are not available in the lab, perform a classical alkaline extraction followed by ethanol precipitation (do not use isopropanol). A time constant of the electric field decay of ~4–5 ms indicate a good event of transformation. In case the transformation has failed, discard the cuvette and try again adjusting the aforementioned variables.
22. It is important to get single bacterial colonies on the plate. In case you will obtain confluent colonies, increase the dilution of transformed bacteria per plates or decrease the amount of plasmid used for transformation.
23. Starting bacterial cultures early in the morning will allow to get bacteria ready to use the morning or afternoon of the day after. Do not overgrow *A. tumefaciens*, as the cell vitality could be affected if bacterial cultures are maintained too long at the stationary phase of bacteria growth.
24. Bacterial solution between an OD_{600} of 0.2 and 1 can be used for agro-infiltration. Low OD_{600} bacterial solutions are preferred in case of high protein expression, while increasing the OD_{600} up to 1 could be necessary for fusion proteins difficult to detect.
25. The optimization of protein expression of protein partners is necessary for optimal functioning of the BiFC method. Low protein expressions prevent a clear distinction of positive and negative signals, making results difficult to interpret. To increase protein expression, bacterial cultures transformed with BiFC constructs can be coinfiltrated with a second *A. tumefaciens* strain carrying a plasmid encoding for the viral protein p19 [8, 28].
26. Stomata close upon particular condition of stress (e.g., water, temperature), preventing efficient penetration of the bacterial solution. It is essential to avoid any types of environmental stress, keeping *N. benthamiana* plants at the optimal growth condition described in Subheading 2.5. Before transformation, acclimate plants on the bench for ~1 h, and keep them

constantly humid spraying water. Young and healthy (4–5-week-old) *N. benthamiana* guarantee optimal protein expressions comparing to old plants.

27. The observation at different times post transformation is necessary to get plant material at an optimal time of protein expression.

Acknowledgments

Alessandro Occhialini thanks prof. Jean-Marc Neuhaus (University of Neuchâtel, Switzerland) for helpful discussion and support.

References

1. Phizicky EM, Fields S (1995) Protein-protein interactions: methods for detection and analysis. Microbiol Rev 59(1):94–123
2. Braun P, Gingras AC (2012) History of protein-protein interactions: from egg-white to complex networks. Proteomics 12(10):1478–1498. https://doi.org/10.1002/pmic.201100563
3. Xiang L, Etxeberria E, Van den Ende W (2013) Vacuolar protein sorting mechanisms in plants. FEBS J 280(4):979–993. https://doi.org/10.1111/febs.12092
4. Kirsch T, Paris N, Butler JM, Beevers L, Rogers JC (1994) Purification and initial characterization of a potential plant vacuolar targeting receptor. Proc Natl Acad Sci U S A 91(8):3403–3407
5. Paris N, Rogers SW, Jiang L, Kirsch T, Beevers L, Phillips TE, Rogers JC (1997) Molecular cloning and further characterization of a probable plant vacuolar sorting receptor. Plant Physiol 115(1):29–39
6. Cao X, Rogers SW, Butler J, Beevers L, Rogers JC (2000) Structural requirements for ligand binding by a probable plant vacuolar sorting receptor. Plant Cell 12(4):493–506
7. Kim H, Kang H, Jang M, Chang JH, Miao Y, Jiang L, Hwang I (2010) Homomeric interaction of AtVSR1 is essential for its function as a vacuolar sorting receptor. Plant Physiol 154(1):134–148. https://doi.org/10.1104/pp.110.159814
8. Occhialini A, Gouzerh G, Di Sansebastiano GP, Neuhaus JM (2016) Dimerization of the vacuolar receptors AtRMR1 and −2 from *Arabidopsis thaliana* contributes to their localization in the trans-Golgi network. Int J Mol Sci 17(10):1661. https://doi.org/10.3390/ijms17101661
9. Kerppola TK (2008) Bimolecular fluorescence complementation: visualization of molecular interactions in living cells. Methods Cell Biol 85:431–470. https://doi.org/10.1016/s0091-679x(08)85019-4
10. Miller KE, Kim Y, Huh WK, Park HO (2015) Bimolecular fluorescence complementation (BiFC) analysis: advances and recent applications for genome-wide interaction studies. J Mol Biol 427(11):2039–2055. https://doi.org/10.1016/j.jmb.2015.03.005
11. Kerppola TK (2006) Visualization of molecular interactions by fluorescence complementation. Nat Rev Mol Cell Biol 7(6):449–456. https://doi.org/10.1038/nrm1929
12. Hu CD, Chinenov Y, Kerppola TK (2002) Visualization of interactions among bZIP and Rel family proteins in living cells using bimolecular fluorescence complementation. Mol Cell 9(4):789–798
13. Ghosh I, Hamilton AD, Regan L (2000) Antiparallel Leucine zipper-directed protein reassembly: application to the green fluorescent protein. J Am Chem Soc 122(23):5658–5659. https://doi.org/10.1021/ja994421w
14. Fang Y, Spector DL (2007) Identification of nuclear dicing bodies containing proteins for microRNA biogenesis in living Arabidopsis plants. Curr Biol 17(9):818–823. https://doi.org/10.1016/j.cub.2007.04.005
15. Tzfira T, Vaidya M, Citovsky V (2004) Involvement of targeted proteolysis in plant genetic transformation by agrobacterium. Nature 431(7004):87–92. https://doi.org/10.1038/nature02857
16. Miyawaki A, Griesbeck O, Heim R, Tsien RY (1999) Dynamic and quantitative Ca2+ measurements using improved cameleons. Proc Natl Acad Sci U S A 96(5):2135–2140
17. Hu CD, Kerppola TK (2003) Simultaneous visualization of multiple protein interactions in living

cells using multicolor fluorescence complementation analysis. Nat Biotechnol 21(5):539–545. https://doi.org/10.1038/nbt816

18. Jach G, Pesch M, Richter K, Frings S, Uhrig JF (2006) An improved mRFP1 adds red to bimolecular fluorescence complementation. Nat Methods 3(8):597–600. https://doi.org/10.1038/nmeth901
19. Shaner NC, Campbell RE, Steinbach PA, Giepmans BN, Palmer AE, Tsien RY (2004) Improved monomeric red, orange and yellow fluorescent proteins derived from Discosoma sp. red fluorescent protein. Nat Biotechnol 22(12):1567–1572. https://doi.org/10.1038/nbt1037
20. Chu J, Zhang Z, Zheng Y, Yang J, Qin L, Lu J, Huang ZL, Zeng S, Luo Q (2009) A novel far-red bimolecular fluorescence complementation system that allows for efficient visualization of protein interactions under physiological conditions. Biosens Bioelectron 25(1):234–239. https://doi.org/10.1016/j.bios.2009.06.008
21. Han Y, Wang S, Zhang Z, Ma X, Li W, Zhang X, Deng J, Wei H, Li Z, Zhang XE, Cui Z (2014) In vivo imaging of protein-protein and RNA-protein interactions using novel far-red fluorescence complementation systems. Nucleic Acids Res 42(13):e103. https://doi.org/10.1093/nar/gku408
22. Shyu YJ, Liu H, Deng X, Hu CD (2006) Identification of new fluorescent protein fragments for bimolecular fluorescence complementation analysis under physiological conditions. BioTechniques 40(1):61–66
23. Ohad N, Shichrur K, Yalovsky S (2007) The analysis of protein-protein interactions in plants by bimolecular fluorescence complementation. Plant Physiol 145(4):1090–1099. https://doi.org/10.1104/pp.107.107284
24. Grinberg AV, Hu CD, Kerppola TK (2004) Visualization of Myc/max/mad family dimers and the competition for dimerization in living cells. Mol Cell Biol 24(10):4294–4308
25. Hellens RP, Edwards EA, Leyland NR, Bean S, Mullineaux PM (2000) pGreen: a versatile and flexible binary Ti vector for agrobacterium-mediated plant transformation. Plant Mol Biol 42(6):819–832
26. Neuhaus JM, Ahl-Goy P, Hinz U, Flores S, Meins F Jr (1991) High-level expression of a tobacco chitinase gene in Nicotiana sylvestris. Susceptibility of transgenic plants to Cercospora nicotianae infection. Plant Mol Biol 16(1):141–151
27. Peremyslov VV, Pan YW, Dolja VV (2004) Movement protein of a closterovirus is a type III integral transmembrane protein localized to the endoplasmic reticulum. J Virol 78(7):3704–3709
28. Lin MT, Occhialini A, Andralojc PJ, Devonshire J, Hines KM, Parry MA, Hanson MR (2014) Beta-Carboxysomal proteins assemble into highly organized structures in Nicotiana chloroplasts. Plant J 79(1):1–12. https://doi.org/10.1111/tpj.12536
29. Day RN, Davidson MW (2009) The fluorescent protein palette: tools for cellular imaging. Chem Soc Rev 38(10):2887–2921. https://doi.org/10.1039/b901966a
30. Dixit R, Cyr R, Gilroy S (2006) Using intrinsically fluorescent proteins for plant cell imaging. Plant J 45(4):599–615. https://doi.org/10.1111/j.1365-313X.2006.02658.x
31. Hoekema A, Hirsch PR, Hooykaas PJJ, Schilperoort RA (1983) A binary plant vector strategy based on separation of vir- and T-region of the agrobacterium tumefaciens Ti-plasmid. Nature 303(5913):179–180
32. de Framond AJ, Barton KA, Chilton M-D (1983) Mini-Ti: a new vector strategy for plant genetic engineering. Nat Biotech 1(3):262–269
33. Lee LY, Gelvin SB (2008) T-DNA binary vectors and systems. Plant Physiol 146(2):325–332. https://doi.org/10.1104/pp.107.113001
34. Hellens R, Mullineaux P, Klee H (2000) Technical focus:a guide to agrobacterium binary Ti vectors. Trends Plant Sci 5(10):446–451
35. Komari T, Takakura Y, Ueki J, Kato N, Ishida Y, Hiei Y (2006) Binary vectors and super-binary vectors. In: Wang K (ed) Agrobacterium Protocols. Humana Press, Totowa, NJ, pp 15–42. https://doi.org/10.1385/1-59745-130-4:15

Chapter 15

Vacuole Dynamics in Rice Cells Invaded by the Blast Fungus *Magnaporthe oryzae*

Kiersun Jones and Chang Hyun Khang

Abstract

We describe a fluorescence imaging method to visualize the dynamics of the central vacuole in rice cells during invasion by the blast fungus *Magnaporthe oryzae*. This method utilizes the combination of confocal microscopy, rice sheath cells (optically transparent), fluorescently tagged *M. oryzae* (red fluorescence), and fluorescein diacetate staining (green fluorescence; visualizing vacuole dynamics). Using this method, we demonstrate that the vacuole undergoes progressive shrinkage and collapse during *M. oryzae* infection.

Key words Abiotic and biotic stress, Confocal imaging, Fluorescein diacetate, Plant cell death, *Magnaporthe oryzae*, *Oryza sativa*, Plant–pathogen interactions, Rice blast, Vacuolar dynamics, Vacuolar staining

1 Introduction

Plant cells contain a large central vacuole that plays essential roles in plant growth, development, and responses to biotic and abiotic stresses [1]. The vacuole contains various hydrolytic enzymes, and the collapse of the vacuole results in the release of these enzymes into the cytoplasm to degrade cellular organelles, leading to cell death [2, 3]. Increasing evidence suggests that the vacuole collapse contributes to either disease resistance or susceptibility depending on the pathogen's lifestyle and the timing of the collapse relative to infection stage [2, 4–6]. There is a need for cytological tools that allow the visualization of the vacuole dynamics in the context of pathogen development.

Fluorescein diacetate (FDA) is a commonly used viability dye. FDA is a nonfluorescent ester that freely penetrates the plasma membrane and is subsequently hydrolyzed by intracellular esterases to produce fluorescein, exhibiting green fluorescence, which is retained in the cytoplasm (Fig. 1A) [7]. Cytoplasmic accumulation of fluorescein and its exclusion from the vacuole offer a unique way to visualize plant vacuoles such as in epidermal cells of *Pisum*

Cláudia Pereira (ed.), *Plant Vacuolar Trafficking: Methods and Protocols*, Methods in Molecular Biology, vol. 1789,
https://doi.org/10.1007/978-1-4939-7856-4_15,

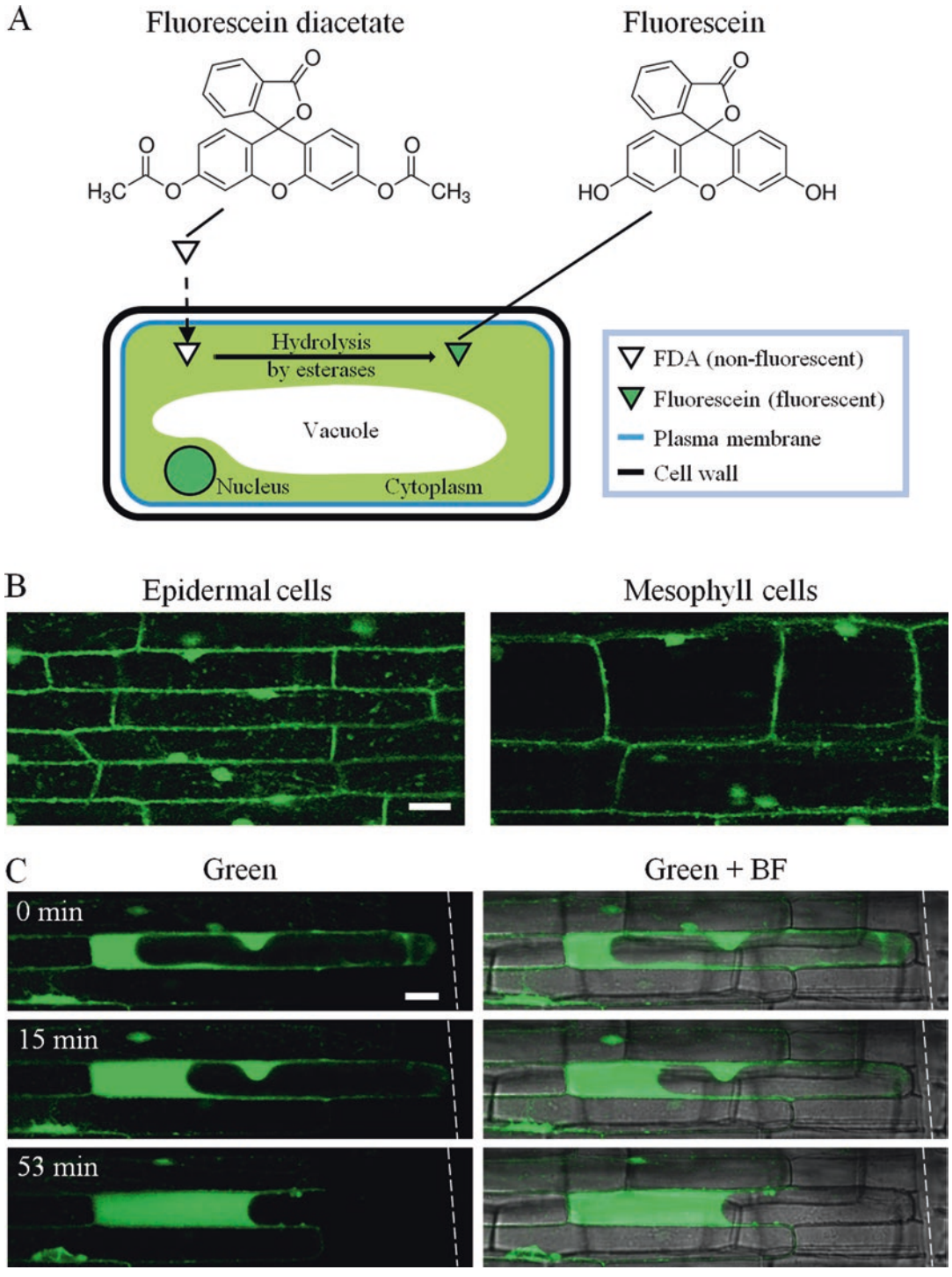

Fig. 1 Fluorescein diacetate staining to reveal the state of the vacuole in rice cells. (**A**) A schematic diagram demonstrating the process of nonfluorescent FDA molecules passing through the intact plasma membrane into the cytoplasm where they are then hydrolyzed by intracellular esterases to produce fluorescein. The membrane-impermeable fluorescein molecules then accumulate in the cytoplasm and exhibit

sativum [8], trichomes of *Arabidopsis thaliana* [9], guard cells of *Vicia faba* [10], and sheath epidermal cells of *Oryza sativa* [11].

Here, we describe a fluorescence imaging method to visualize vacuole dynamics in rice cells during intracellular invasion by the filamentous fungus *Magnaporthe oryzae* that causes the economically important rice blast disease. This method utilizes the combination of confocal microscopy, rice sheath cells (optically transparent), fluorescently tagged *M. oryzae* (red fluorescence), and FDA staining (green fluorescence). In particular, FDA is instrumental for time-lapse imaging not only for cell viability but also for the vacuole dynamics [11]. Using this method, we demonstrate the dynamics of the central vacuole in rice cells: (1) the vacuole occupies most of the cell volume (Fig. 1B), (2) upon mechanical wounding it progressively shrinks (Fig. 1C), and (3) it undergoes shrinkage and collapse during *M. oryzae* infection (Fig. 2). The vacuole dynamics observed in FDA-stained rice cells infected with *M. oryzae* are consistent with studies using a transgenic rice line expressing a GFP-tagged vacuolar membrane marker [6]. The method in this chapter can be used to compare and contrast plant vacuole dynamics associated with resistant and susceptible interactions between rice and *M. oryzae* as well as other plant–pathogen interactions.

2 Materials

2.1 Fluorescent Dye: Fluorescein Diacetate (FDA)

1. FDA stock solution (1 mg/mL in acetone): To make a 1 mL stock solution from the solid form, dissolve 1 mg FDA in acetone to a total volume of 1 mL in a 1.5 mL microcentrifuge tube. Dispense 20 μL aliquots of the stock solution in 1.5 mL tubes and store them at −20 °C, protected from light (e.g., covered in aluminum foil) (**Note 1**).
2. FDA working solution (2 μg/mL in 0.2% acetone): Dilute 2 μL of FDA stock solution in 998 μL deionized water to make a 1 mL working solution of 2 μg/ mL in 1.5 mL tube. Cover the tubes of working solution in aluminum foil and use at room temperature immediately or place on ice until use to ensure compound stability (**Note 2**).

Fig. 1 (continued) green fluorescence when excited at 488 nm. (**B**) Single plane confocal images showing typical fluorescein (green) patterns in rice sheath epidermal cells (left) and immediately underlying mesophyll cells (right). (**C**) Time-lapse confocal images showing increased fluorescein intensity with a progressively shrinking vacuole in a rice cell directly abutting a mechanically damaged cell. Shown are single plane confocal images of green fluorescence alone (left) and of a merge of green fluorescence and bright-field (right). The nick (dotted white line) was introduced just before imaging. Figure 1A, B are modified from [11] with permission from BioMed Central

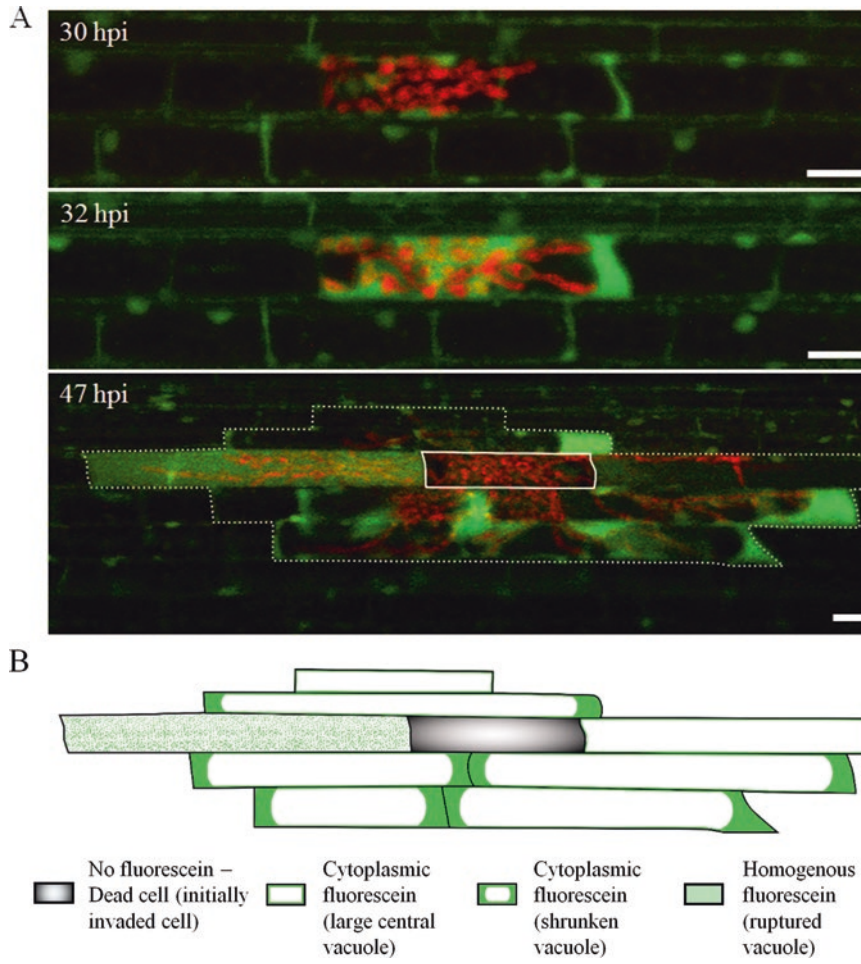

Fig. 2 Vacuole dynamics during rice blast invasion. (**A**) Time-lapse confocal images of *M. oryzae* (red) infecting susceptible rice cells from 30 to 47 h post inoculation (hpi). At 30 hpi, the invaded cell showed a typical cytoplasmic fluorescein pattern (green) excluded from the large central vacuole. At 32 hpi, hyphae had further colonized the first-invaded rice cell. The vacuole had shrunken and fragmented by this time. At 47 hpi, the sample was stained again with freshly prepared FDA to renew fluorescein intensity in the cytoplasm of viable cells. At this time, the initially colonized rice cell (solid white outline) lacked fluorescein signal, indicating host cell death. Subsequently invaded cells showed cytoplasmic fluorescein with a large central vacuole, cytoplasmic fluorescein with a shrunken vacuole, and fluorescein distributed throughout the rice cell lumen with a disrupted vacuole. Dotted white lines outline the rice cells invaded by hyphae. Bars = 20 μm. (**B**) Schematic representation of the infected cells in (**A**). Modified from [11] with permission from BioMed Central

2.2 Plant and Fungal Materials and Inoculation

1. Rice plants (16–19 days old): Grow rice in a growth chamber at 80% relative humidity on a 12/12 light/dark cycle at 28 °C during the day and 24 °C at night. Apply fertilizer (20-10-20 peatlite) once a week.
2. Transgenic *M. oryzae* expressing tdTomato (red fluorescent protein) under control of the constitutive promoter from the *M. oryzae* ribosomal protein 27 gene: Grow on oatmeal agar (OMA) media in an incubator under 24 h light at 24 °C.

3. Miracloth.
4. 1.5 mL microcentrifuge tubes.
5. Hemacytometer.
6. Light microscope.

2.3 Confocal Microscopy

1. Slide glass.
2. Coverslips 22 × 50 mm.
3. Forceps.
4. Razor blades (single edge).
5. Sterile water.
6. Transfer pipettes.
7. Humidity chamber (**Note 3**).
8. Confocal microscope system—we used a Zeiss LSM 510 Meta laser scanning confocal microscope and Zen software (Black edition) for image analysis (**Note 4**).

3 Methods

Perform all steps at room temperature, unless noted otherwise.

3.1 Determining Vacuole Morphology in Rice Leaf Sheath Cells

1. Prepare 1 mL tubes of FDA working solution: one for every two trimmed sheaths to be stained (**Note 5**).
2. Use a razor blade to trim a thin layer of cells from the interior of an excised inner leaf sheath from a 16–19-day-old rice plant (**Note 6**).
3. Immediately place trimmed sheaths in FDA working solution (**Note 7**).
4. Incubate for 15 min to allow for sufficient staining [11] (**Note 8**).
5. Mount stained sheaths on a microscope slide in the same FDA solution used for staining (**Note 9**).
6. Use a confocal microscope to image rice cells (Fig. 1B) (**Note 10**).

3.2 Vacuole Dynamics in Response to Wounding

1. Stain trimmed sheaths with FDA for 15 min as described in Subheading 3.1.
2. To cause mechanical wounding, introduce small nicks into the sheath with a razor blade before placing the coverslip over the sample (**Note 11**).
3. Image epidermal rice cells in the vicinity of the wounds.
4. Expected fluorescein patterns:
   (a) Healthy rice cells showing a typical cytoplasmic fluorescein pattern excluded from a large central vacuole (Fig. 1B).

(b) Perturbed rice cells showing significantly increased fluorescein intensity in the enlarged cytoplasm; excluded from the progressively shrinking vacuole (Fig. 1C) (**Note 12**).

(c) Nonviable cells showing no fluorescence.

3.3 Vacuole Dynamics During Invasion by the Rice Blast Fungus

1. Excise rice sheaths to about 8 cm in length and inoculate the inner epidermal cells by injecting a 5×10^4 spores/mL suspension of transgenic *M. oryzae* expressing cytoplasmic tdTomato into the hollow inner space of the sheath (**Note 13**).
2. Prepare 1 mL tubes of FDA working solution as in Subheading 3.1.
3. Trim inoculated rice sheaths with a razor blade at the desired infection stage time point (**Note 14**).
4. Immediately place trimmed sheaths into FDA working solution.
5. Mount stained sheaths on a microscope slide as in Subheading 3.1.
6. Use a confocal microscope to image infected cells. Optimize settings for the red channel to capture tdTomato fluorescence (**Note 15**). Be sure to image uninfected rice cells to compare the fluorescein pattern between invaded and noninvaded cells.
7. When collecting time-lapse images to track vacuole dynamics and hyphal growth, restain sheaths with fresh FDA working solution if the fluorescein signal becomes too weak. To restain, remove the previous FDA mounting solution and replace it with freshly prepared FDA working solution.
8. Perform image analysis in the Zen software (Black edition) to compare the fluorescein patterns between rice cells containing red fluorescent invasive hyphae and surrounding uninvaded cells. Compare these results to fluorescein patterns in both viable and wounded rice cells that were not infected by the fungus.

4 Notes

1. No sterilization process is needed for FDA (catalog No. F7378, 5 g; Sigma-Aldrich) dissolved in acetone as a stock solution. FDA stock solutions can be stored for at least 6 months protected from light at −20 °C. We found that a 2-year-old stock solution could be used without a noticeable decrease in efficiency of the dye. The stock solution does not freeze at −20 °C.
2. FDA is sensitive to both light and temperature in the stock solution, and even more so in the aqueous working solution. Therefore, prepare 1 mL tubes of FDA working solution just prior to use. If staining is not being performed immediately, place the tubes of FDA working solution on ice and use within a few hours.

3. Use any chamber which can both maintain high humidity and hold inoculated excised sheaths upright. We found it convenient to use a 10 cm glass petri dish with a wet 10 cm Whatman qualitative filter paper for the humidity chamber.
4. Use a confocal microscope equipped with an Argon/2 laser (458, 488, 514 nm) and a HeNe1 laser (543/561 nm). Use the 488 nm laser and a 505–530 nm bandpass filter for excitation and emission of fluorescein (Ex/Em maxima of 494 nm and 521 nm, respectively) and a 543-nm laser and a 560–615 nm bandpass filter for excitation and emission of tdTomato (Ex/Em maxima of 554 nm and 581 nm, respectively).
5. We found that placing more than two sheaths in a 1 mL tube of FDA working solution makes it difficult to remove one without causing damage to the others.
6. Cut a 2 cm segment from the middle of an excised sheath. Trim sheaths as previously described [12]. Briefly, hold the sheath segment gently at one end and trim the sides of the sheath off with a single edged razor blade. Trim the remaining side tissue, leaving the midvein. Finally, trim a thin layer from the midvein, including the inner epidermal layer. If trimmed too thin, the epidermal layer of cells can become damaged or be perturbed by damaged mesophyll cells directly beneath them.
7. It is important to immediately place trimmed sheaths into the FDA working solution, otherwise, trimmed sheaths will dry out. After removing the aluminum foil covering the staining tube and adding the trimmed sheath, gently invert the staining tube a few times to assist in homogenous staining. We found that sheaths sometimes float, therefore make sure that sheaths are submerged by tapping the tube gently with your finger before covering the tubes again with aluminum foil.
8. It was previously determined that fluorescein signal reached peak intensity in rice sheath epidermal cells after staining for 15 min (Fig. 1C in [11]).
9. Mount the sheath with the trimmed side (mesophyll) facing down on a slide glass. On the microscope, this can be confirmed by looking at the shape of the cells with rectangle-shaped cells being epidermal and square-shaped cells being mesophyll (Fig. 1B). Use care when applying the coverslip as not to introduce air bubbles or damage the sheath tissue. We find it best to first place the stained sheath on the slide glass, apply ~150 μL of FDA solution with a transfer pipette, contact the slide glass with the edge of the coverslip to one side of the sample, and then gently lower it at an angle onto the sample.
10. To determine the cytoplasmic fluorescein pattern in viable unperturbed rice cells, image epidermal cells toward the middle of the sheath that are not near any cut edges. To optimize image acquisi-

tion settings for fluorescein, stain a trimmed sheath with FDA and acquire images of unperturbed rice cells with settings such that there is sufficient fluorescence signal where expected (Fig. 1B). Make sure that there are no saturated regions of green fluorescence. As a control, prepare another sheath sample without FDA staining and acquire images using the same settings. There should be little to no green signal in the unstained sheath. If significant levels of plant autofluorescence or background noise are detected in the control sheath, adjust image acquisition such that the unstained sheath does not show significant levels of background noise while FDA stained samples still clearly show green fluorescence. For example, lowering the scan speed increases pixel dwell time, which reduces background noise. We found the following settings on an LSM 510 worked well for detecting specific fluorescein signal in trimmed FDA-stained rice leaf sheath cells: a Plan-Apochromat 20×/0.8 objective lens, low 488-nm laser power (actual laser power output varies based on age of laser, scope alignment, etc.), 1 airy unit, scan speed 8, and a zoom factor of 1 or 2.

11. To introduce nicks on the epidermal side of a trimmed sheath with a razor blade, we found it useful to place the sheath on the lid of the petri dish we used for the humidity chamber and hold one end of the trimmed sheath gently with forceps while holding the razor blade in the other hand to introduce the nicks by applying slight pressure.
12. We found fluorescein intensity to be significantly increased in the presence of a shrunken vacuole in damaged cells or cells abutting damaged cells. The cause of this increased fluorescein intensity is unknown, however it has been speculated that it may be due, at least in part, to increased esterase activity and/or a decrease in pH [11].
13. Sheath inoculation method [12, 13]: Harvest spores of the transgenic *M. oryzae* strain by pipetting 1 mL of water onto the OMA plate. Then, using the bottom of a microcentrifuge tube, gently dislodge spores from the outer edge of the mycelial colony into water. Pipette through miracloth into a 1.5 mL microcentrifuge tube. Determine spore concentration using a hemacytometer and a light microscope. Dilute spore suspension with water to obtain a concentration of 5×10^4 spores/mL. Mix the spore suspension to homogenize it just before injecting enough spore suspension into the hollow inner space of an excised rice sheath to completely fill it from end-to-end.
14. During highly susceptible interactions invasive hyphae typically colonize the first rice cell from 24 to 36 h post inoculation (hpi) and invade neighboring rice cells after 36 hpi [13].
15. When taking images of FDA-stained *M. oryzae*-infected rice cells, use settings previously determined for fluorescein detection

in the green channel. To image tdTomato along with fluorescein, set up a new acquisition channel using a 543-nm laser for excitation. We used these settings on an LSM 510 confocal microscope: a Plan-Apochromat 20×/0.8 objective lens, 80% 543-nm laser power, 1 airy unit, scan speed 8, and a zoom factor of 1 or 2. Note that some fluorescence bleed-through between channels can occur (detection of higher wavelengths of fluorescein emission in the red channel), however, hyphae should remain easily recognizable.

Acknowledgments

We thank Dong Won Kim, Jie Zhu, and Mariel Pfeifer in the Khang Lab (http://www.khanglab.org/) for their help and discussions. We acknowledge the assistance of the Biomedical Microscopy Core at the University of Georgia with imaging using a Zeiss LSM 510 confocal microscope. This work was supported by the Agriculture and Food Research Initiative competitive grants program, Award number 2014-67013-21717 from the USDA National Institute of Food and Agriculture.

References

1. Marty F (1999) Plant Vacuoles. Plant Cell 11:587–599
2. Hara-Nishimura I, Hatsugai N (2011) The role of vacuole in plant cell death. Cell Death Differ 18:1298–1304
3. Jones AM (2001) Programmed cell death in development and defense. Plant Physiol 125:94–97
4. Dickman MB, Fluhr R (2013) Centrality of host cell death in plant-microbe interactions. Annu Rev Phytopathol 51:543–570
5. Hatsugai N, Kuroyanagi M, Yamada K et al (2004) A plant vacuolar protease, VPE, mediates virus-induced hypersensitive cell death. Science 305:855–858
6. Mochizuki S, Minami E, Nishizawa Y (2015) Live-cell imaging of rice cytological changes reveals the importance of host vacuole maintenance for biotrophic invasion by blast fungus, *Magnaporthe oryzae*. Microbiology 4:952–966
7. Saruyama N, Sakakura Y, Yurina A et al (2013) Quantification of metabolic activity of cultured plant cells by vital staining with fluorescein diacetate. Anal Biochem 441:58–62
8. Mellersh DG, Heath MC (2001) Plasma membrane-cell wall adhesion is required for expression of plant defense responses during fungal penetration. Plant Cell 13:413–424
9. Mathur J, Mathur N, Kernebeck B et al (2003) Mutations in actin-related proteins 2 and 3 affect cell shape development in *Arabidopsis*. Plant Cell 15:1632
10. Gao X-Q, Li C-G, Wei P-C et al (2005) The dynamic changes of tonoplasts in guard cells are important for stomatal movement in *Vicia faba*. Plant Physiol 139:1207
11. Jones K, Kim DW, Park J et al (2016) Live-cell fluorescence imaging to investigate the dynamics of plant cell death during infection by the rice blast fungus *Magnaporthe oryzae*. BMC Plant Biol 16:1–8
12. Koga H, Dohi K, Nakayachi O et al (2004) A novel inoculation method of *Magnaporthe grisea* for cytological observation of the infection process using intact leaf sheaths of rice plants. Physiol Mol Plant Pathol 64:67–72
13. Kankanala P, Czymmek K, Valent B (2007) Roles for rice membrane dynamics and plasmodesmata during biotrophic invasion by the blast fungus. Plant Cell 19:706–724

Chapter 16

Characterization of Plant Glycoproteins: Analysis of Plant Glycopeptide Mass Spectrometry Data with plantGlycoMS, a Package in the R Statistical Computing Environment

Margaret R. Baker, Travers Ching, David L. Tabb, and Qing X. Li

Abstract

plantGlycoMS is a set of tools, implemented in R, which is used to assess and validate glycopeptide spectrum matches (gPSMs). Validity of gPSMs is based on characteristic fragmentation patterns of glycopeptides (*gPSMvalidator*), adherence of the glycan moiety to the known *N*-glycan biosynthesis pathway in plants (*pGlycoFilter*), and elution of the glycopeptide within the observed retention time window of other glycopeptides sharing the same peptide backbone (*rt.Restrict*). plantGlycoMS also contains a tool for relative quantitation of glycoforms based on selected ion chromatograms of glycopeptide ion precursors in the mass spectrometry level 1 data (*glycoRQ*). This protocol walks the user through this workflow with example mass spectrometry data obtained for a plant glycoprotein.

Key words Glycopeptide, Glycoprotein, Glycoproteomics, Mass spectrometry, *N*-glycosylation, Plant, R statistical computing environment

1 Introduction

N-Glycosylation is one of the most prevalent and complex cotranslational and posttranslational protein modifications, which can modulate protein structure and function and play key roles in events requiring self- or non-self-recognition [1]. In plants, *N*-glycosylation regulates growth, development, and defense [2–5]. Comprehensive characterization of protein *N*-glycosylation requires knowledge of the glycan profile at each glycosylation site as well as the relative abundance of those different glycans. Analysis of glycopeptides with mass spectrometry (MS) can provide this site-specific information.

We developed a suite of tools in R [6], plantGlycoMS, which is used in a workflow for analysis of plant glycopeptide MS data (Fig. 1) [7]. plantGlycoMS depends on the R package protViz [8, 9] and the workflow uses free and open-source software and tools. The workflow starts with processing of raw MS data files with tools in the ProteoWizard library [10]. Next, the target

Cláudia Pereira (ed.), *Plant Vacuolar Trafficking: Methods and Protocols*, Methods in Molecular Biology, vol. 1789,
https://doi.org/10.1007/978-1-4939-7856-4_16,

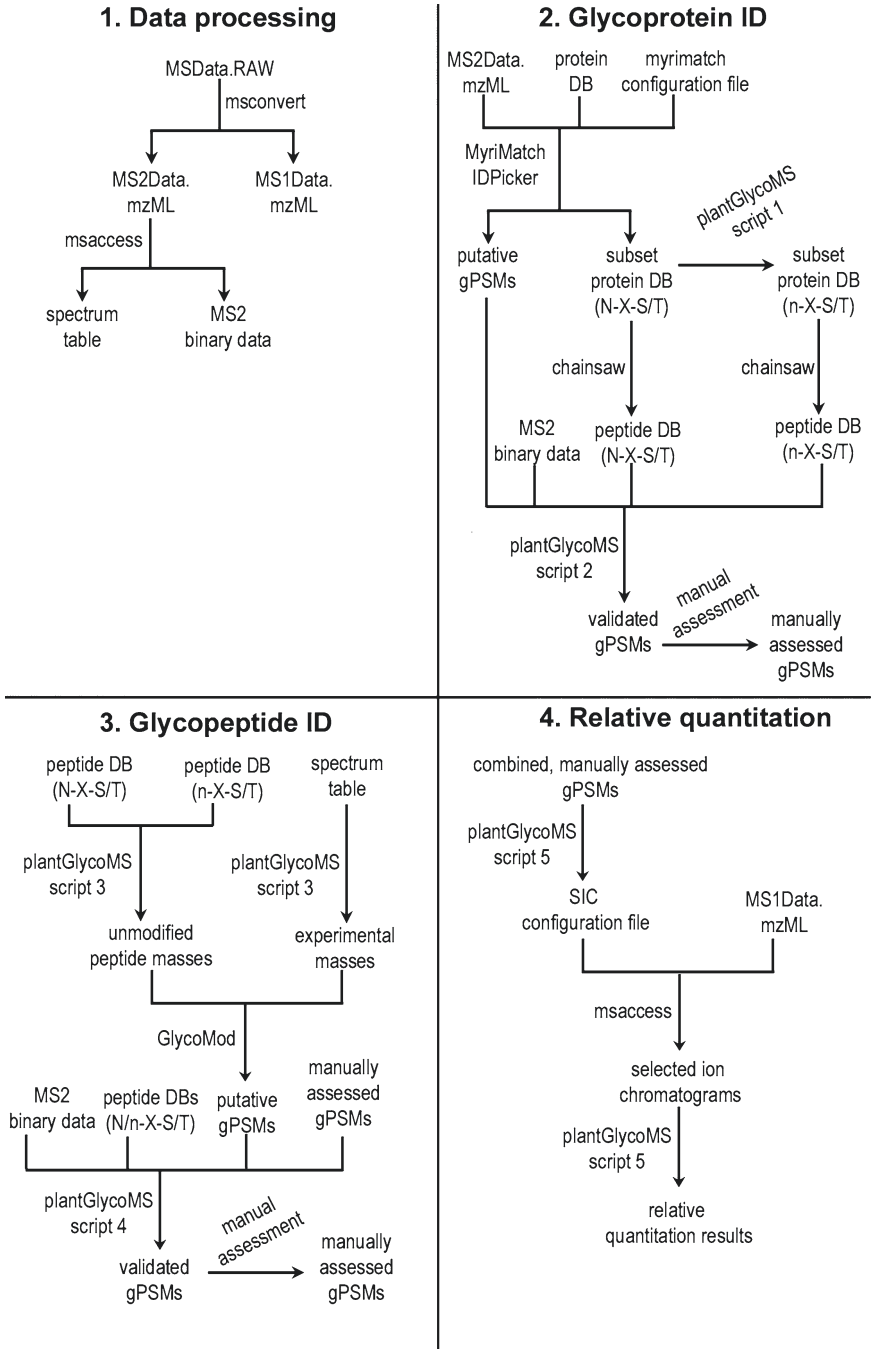

Fig. 1 A workflow for identification of plant glycopeptides from mass spectrometry data. Raw MS data are first processed with msconvert (ProteoWizard) [10]. Next, glycoproteins are identified with MyriMatch (Bumbershoot) [11] and IDPicker [12]. Glycopeptides are then identified with GlycoMod [13]. Validation of gPSMs is achieved with plantGlycoMS [7], which should be followed by manual validation. Finally, msaccess (ProteoWizard) and *glycoRQ* (plantGlycoMS) are used for relative quantitation of glycoforms

glycoproteins are identified with MyriMatch (Bumbershoot) [11] and IDPicker [12]. All possible glycopeptides are then identified with GlycoMod [13]. Various functions in plantGlycoMS are used to validate glycopeptide assignments, based on characteristic fragmentation patterns of glycopeptides (*gPSMvalidator*), adherence of the *N*-glycan moiety of glycopeptides to the known plant *N*-glycan biosynthesis pathway (*pGlycoFilter*), and the observed retention time of the peptide moiety of glycopeptides (*rt.Restrict*). Finally, selected ion chromatograms, extracted from mass spectrometry level 1 (MS1) data by msaccess (ProteoWizard), are assessed with *glycoRQ* (plantGlycoMS) to give estimates of the relative abundance of different glycans at each glycosylation site. This data analysis workflow enabled profiling of 13 sites for *N*-glycosylation on windmill palm tree peroxidase (WPTP) [7]. Glycan heterogeneity was observed at each site with up to 30 different glycans observed at one site.

2 Materials

1. A PC running Windows (*see* **Note 1**).
2. R, from The Comprehensive R Archive Network (cran.r-project.org/) (*see* **Note 2**).
3. R packages: devtools [14], seqinr [15], and protViz [8, 9] (*see* **Note 3**).
4. plantGlycoMS [7] (github.com/MargaretBaker/plantGlycoMS) (*see* **Note 4**).
5. ProteoWizard, IDPicker, and Bumbershoot (proteowizard.sourceforge.net/).
6. Mass spectrometry data (.RAW files) (*see* **Note 5**).
7. A protein database in FASTA format (*see* **Note 6**).
8. Optional: Example data on the ProteoSAFe server (massive.ucsd.edu/ProteoSAFe/static/massive.jsp, MassIVE ID: MSV000081440). Please check for updates which may include new raw MS data. Example data are for a plant glycoprotein, WPTP, and include raw MS data files (*see* **Note 5**), a protein database in FASTA format (proteinDatabase.fasta) (*see* **Note 6**), and other files generated in the workflow, which are referred to throughout the text.

3 Methods

3.1 Process Raw MS Data

1. Make a working directory (i.e., folder) called "<Drive>:/plantGlycoMS" and copy in the raw MS data and protein database.
2. Convert RAW data to mzML format with msconvert (ProteoWizard), a command line tool for converting raw MS files to open formats. Specify the raw MS data in the first argument (Data.RAW). Evaluate MS1 data to recalculate the precursor *m/z* and charge state with the "precursorRefine" filter. Additionally, use a filter to keep only MS2 data and name the resulting file to reflect that it contains only MS2 level data (*see* **Note 7**).
```
msconvert Data.RAW --filter precursorRefine --
filter "msLevel 2" --outfile MS2Data
```
3. Make a spectrum table of MS2 data using msaccess (ProteoWizard), a command line tool for extracting MS data and metadata. The table will contain summary information for each MS2 scan including the precursor *m/z* and charge state.
```
msaccess MS2Data.mzML --exec "spectrum_ta-
ble delimiter=comma"
```
4. Collect spectrum binary data (i.e., *m/z* vs. intensity data) for MS2 scans using msaccess (ProteoWizard). First, open the MS data file in seeMS, a spectrum viewer tool in ProteoWizard, and record the range of MS2 scans for which you want to collect data. Next, execute the binary command in msaccess and specify the range of scans. For example, "binary sn=1,20000" produces a text file for each scan (sn) from 1 to 20,000. The argument outdir creates an output directory in which created files are saved.
```
msaccess MS2Data.mzML --exec "binary
sn=1,20000" --outdir MS2Data
```
5. Convert RAW data to mzML format containing only MS1 level data. This mass spectrum file will be used for relative quantitation of glycoforms at each glycosylation site (Subheading 3.5).
```
msconvert Data.RAW --filter "msLevel 1"
--outfile MS1Data
```

3.2 Glycoprotein Identification

1. Use a text editor, such as Notepad++ (notepad-plus-plus.org/), to make a configuration file for the protein database search, conducted with MyriMatch (glycoProteinID.cfg). The configuration file specifies the name of the protein database, the amino acid residue(s) and the mass(es) of static or dynamic modifications, the maximum number of modifications allowed on a peptide, the minimal number of peptide termini which must adhere to the specificity of the defined protease, the protease used for sample preparation, and the

maximum number of cleavage sites allowed to be missed by the protease. It additionally specifies the precursor and fragment ion mass tolerances, as well as a suffix to be appended to the resulting files (*see* **Note 8**).

2. Perform the MyriMatch (Bumbershoot) search in the command line (*see* **Note 9**).

```
myrimatch MS2Data.mzML -cfg glycoProteinID.cfg
```

3. Open the MyriMatch results (MS2Data_MM.pepXML) in IDPicker. IDPicker assesses the putative peptide spectrum matches (PSMs), assembles a confident list of PSMs within a specified *q*-value, and produces a parsimonious list of proteins.
4. Export the peptide spectrum matches, which include putative gPSMs. In the "spectrum view," which is the lower left pane in the default arrangement, expand the "Group/Source/Spectrum" dropdown box. Go to "Export Options" and select "Export to File." Save the results as a tab delimited file (putative_gPSMs.tsv).
5. Export a subset protein database containing only the identified proteins. Under "File," go to "Export," and select "Export subset FASTA." When prompted to add a decoy for each target protein, select "No."
6. Using plantGlycoMS script 1 (*see* **Note 10**), make a subset protein database in which all glycosylation site Asn residues, defined as any Asn within the consensus sequence for glycosylation (N-X-S/T, where X is not P), are denoted with a lower case n (n) as opposed to an uppercase n (N).
7. Perform an in silico digest of the subset protein databases with chainsaw (ProteoWizard) (*see* **Note 7**). If using the example data, the cleavage enzyme (−c) should be set to chymotrypsin. In this example, other parameters are the number of missed cleavages (−n) and enzyme cleavage specificity (−s).

```
chainsaw MS2Data_MM.fasta -c Chymotrypsin
-n 2 -s fully
```

```
chainsaw MS2Data_MM_glyco.fasta -c
Chymotrypsin -n 2 -s fully
```

8. Assess the gPSMs from the MyriMatch search with plantGlycoMS script 2 (*see* **Note 11**). The inputs for this script are the peptide databases from the in silico digests (Subheading 3.2, **step 7**), the identification results from MyriMatch and IDPicker (putative gPSMs) (Subheading 3.2, **step 4**), and the MS2 binary data (Subheading 3.1, **step 4**). The validated gPSMs are reported in a set of annotated spectra (annotatedSpectra.pdf) and a table summarizing the identification information (infoTable.csv).

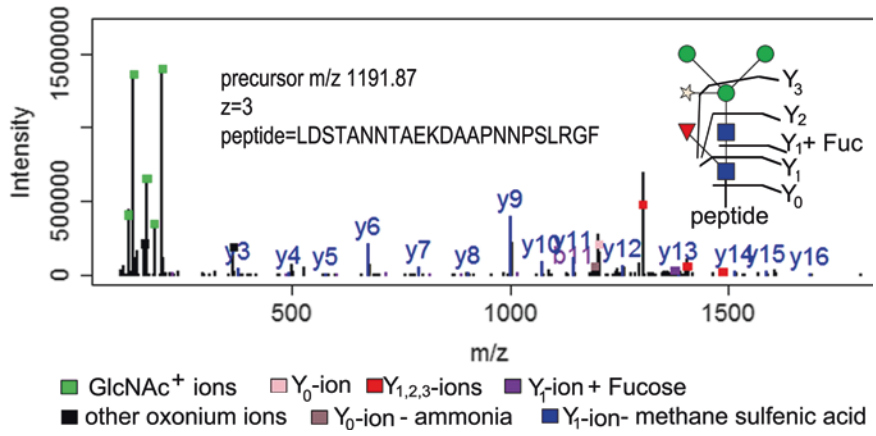

Fig. 2 Glycopeptide HCD fragmentation spectrum. Glycopeptide specific fragment ions are labeled according to the accompanying legend. Peptide backbone fragments are represented by blue (y-ions) and purple (b-ions) bars and y-ions and some b-ions are labeled above each relevant peak. The inset glycan structure (*N*-acetylglucosamine: blue square, mannose: green circle, xylose: white star, fucose: red triangle) was drawn with GlycanBuilder [25]. Adapted with permission from *J. Proteome Res.*, **2016**, *15*(6): 2026–2038. Copyright 2016, American Chemical Society

3.3 Manual Assessment of gPSMs

The R function *gPSMvalidator* validates and annotates gPSMs. Valid gPSMs have a minimum number of oxonium ions (default = 2), a minimum intensity ratio of oxonium ions to total signal (default = 2), and at least one Y_1- and one Y_0-ion. Peaks are chosen by *gPSMvalidator* as long as they are within a specified ion tolerance (default = 20 ppm), regardless of intensity or position in an isotope pattern. *gPSMvalidator* also annotates b- and y-ions, via functions from the R package protViz [8, 9], which are generated from fragmentation of the peptide backbone within a mass tolerance of 0.02 *m/z*.

1. Open the annotated gPSMs and the table summarizing the details of each gPSM (from Subheading 3.2, **step 8** or Subheading 3.4, **step 4**). Open the MS2 data (Subheading 3.1, **step 2**) in seeMS (ProteoWizard).
2. Assess the overall spectrum assignment (Fig. 2). Oxonium marker ions, including the *N*-acetylglucosamine (GlcNAc) oxonium ion and its internal fragments, should be abundant in the lower mass range. Peaks in the Y_1-/Y_0-ion pair, which differ by a GlcNAc residue (203 Da), should be prevalent in the mid to upper mass range, and are sometimes present in multiple charge states. The remainder of intense peaks should be annotated as b−/y-ions or glycan backbone fragments.
3. If the overall assessment of the spectrum assignment is ambiguous, consider alternate hypotheses for the spectrum by searching for duplicate scan values in the results summary table

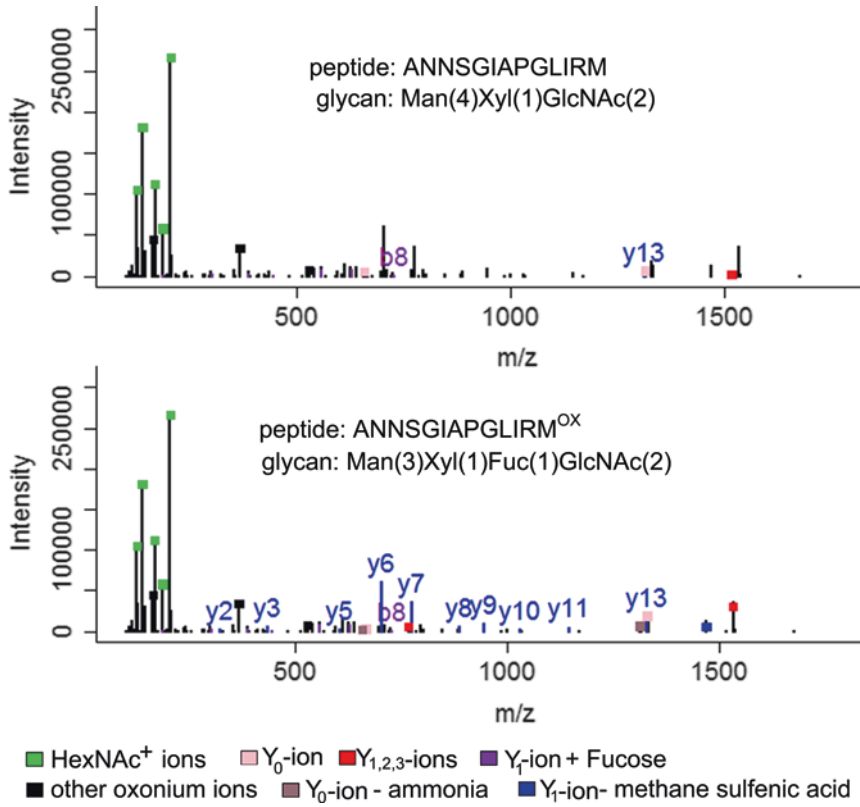

Fig. 3 Comparison between a false positive (top) and true positive result (bottom). Glycopeptide specific fragment ions are labeled according to the accompanying legend. Peptide backbone fragments are represented by blue (y-ions) and purple (b-ions) bars and y-ions and some b-ions are labeled above each relevant peak. Adapted with permission from *J. Proteome Res.*, **2016**, *15*(6): 2026–2038. Copyright 2016, American Chemical Society

(Fig. 3). The predominant glycan in plant *N*-linked glycoproteins is $Man_3XylFucGlcNAc_2$ (1170.417 Da) [16]. Is it possible that the spectrum can be explained by attachment of this predominant glycan and an artefact of sample preparation (e.g., methionine oxidation, nonspecific carbamidomethylation)? For glycopeptides with oxidized methionine, the Y_1-ion is often accompanied by a peak representing neutral loss of methane sulfenic acid (−64 Da) [17]. The Y_1-ion of carbamidomethylated glycopeptides is often accompanied by a peak representing neutral loss of 57 Da [18].

4. Further examine the Y_1-/Y_0-ion pair. The Y_0- and Y_1-ions are often accompanied by a peak representing the neutral loss of ammonia (−17 Da). For glycopeptides with core fucosylation the Y_1-ion is often accompanied by a peak representing addition of fucose (+146 Da).
5. Examine the isotope pattern of the Y_1-/Y_0-ion. Use the spectrum viewer seeMS to check if the monoisotopic peak was picked. The monoisotopic mass of the Y_1- and Y_0-ion are

given for each scan in the results summary table, which can be used to calculate the ions in different charge states (m/z = (mass + (1.007 * charge))/charge).

6. Check the retention time. Low abundance glycopeptides may only have the minimum number of ions identifying them. The retention time of the analyte can provide supporting evidence for the assignment. Glycoforms sharing the same amino acid sequence, but bearing a different glycan, will elute within a retention time window [19]. Those with larger, more hydrophilic glycans will elute earlier than those with smaller or truncated glycans.
7. Delete rows judged to be false positives and save the spreadsheet under a different name.

3.4 Glycopeptide Identification

1. Make a list of "unmodified peptide masses" for the GlycoMod search with plantGlycoMS script 3 (*see* **Note 12**). The inputs are the peptide databases (Subheading 3.2, **step 7**). The output is a text file containing a list of peptide masses for peptides containing glycosylation sites and with mass added for carbamidomethylation of cysteines and oxidation of methionines (unmodifiedPeptideMasses.txt).
2. Make a list of experimental masses for the GlycoMod search (*see* **Note 12**). The input is the spectrum table (Subheading 3.1, **step 3**) and the output is a list of experimental masses (experimentalMasses.txt).
3. Perform a GlycoMod search (web.expasy.org/glycomod/) to identify all possible gPSMs (*see* **Note 13**). Upload the experimental masses (Subheading 3.4, **step 2**). Select monoisotopic mass values in neutral mode [M]. Set the mass tolerance to an appropriate value, which depends on the mass spectrometer used. For example data, set the mass tolerance to 15 ppm. Under *N*-linked oligosaccharides, select glycopeptides with the motif N-X-S/T/C (X not P). Paste in the set of unmodified peptide masses (Subheading 3.4, **step 1**). Select "Yes" for the following monosaccharides which are underivatized: Hexose (0–9), HexNAc (1–4), Deoxyhexose (0–3), and Pentose (0–1). Select "No" for all other monosaccharides (*see* **Note 14**). Check the box "List compositions reported in UniCarbKB separately," so that the results are returned in a table format. Next, start the GlycoMod search. After the search is complete, copy the results (putative gPSMs) and paste them into a spreadsheet (gmodResults.csv).
4. Validate the gPSMs from the GlycoMod search with plantGlycoMS script 4 (*see* **Note 15**). The inputs for this script are the MS2 binary data (Subheading 3.1, **step 4**), the peptide databases (Subheading 3.2, **step 7**), the putative gPSMs from the GlycoMod search (Subheading 3.4, **step 3**), and the manually assessed gPSMs (Subheading 3.3, **step 7**). The plantGlycoMS

script filters for gPSMs with biologically probable glycan modifications (*pGlycoFilter*), falling into the observed retention time window (*rt.Restrict*), and containing oxonium and Y-ions (*gPSMvalidator*). The output is a set of annotated spectra (annotatedSpectra_gmod.pdf) and a table summarizing the identification information (infoTable_gmod.csv).

5. Manually assess the validated gPSMs using the procedure in Subheading 3.3.

3.5 Relative Quantitation of Glycoforms

1. In R, make a configuration file to obtain the selected ion chromatograms for identified glycopeptides (SICconfig.txt) (*see* **Note 16**).
2. Using MS1 data, obtain the selected ion chromatograms for each identified glycopeptide by running the "sic" command in msaccess (ProteoWizard) (*see* **Note 7**).
```
msaccess MS1Data.mzML --config SICconfig.txt
--outdir RQData
```
3. Run *glycoRQ* in R (*see* **Note 16**). In *glycoRQ*, the intensity of the monoisotopic peak of each glycoform (i.e., peptide and glycan pair) is summed over the retention time window for its respective glycoform series. The relative abundance of each glycoform is estimated by dividing its intensity by the sum intensity of all glycoforms in that particular series (*see* **Note 17**).

4 Notes

1. ProteoWizard, MyriMatch (Bumbershoot), and R can be downloaded for Windows, Macintosh, or Linux. A command line version of IDPicker is available for Linux; however, the IDPicker graphical user interface is only available for Windows.
2. The free version of RStudio (rstudio.com/) is a convenient tool for working in R.
3. Start a new session in RStudio and type the following command to install the necessary packages:
```
install.packages (c("devtools", "seqnr",
"protViz"))
```
4. First, install Rtools (cran.r-project.org/bin/windows/Rtools/). Next, start a new session in RStudio and type the following commands to install plantGlycoMS from GitHub:
```
library (devtools)
install_github ("MargaretBaker/plantGly-
coMS")
```
5. The data were obtained for glycopeptides derived from a chymotrypsin digest of WPTP, which were desalted or enriched for glycopeptides [7]. WPTP was purified to homogeneity;

however, we believe that this method is adaptable to a mixture of proteins. The glycopeptides were separated by nano-liquid chromatography on a reversed phase C_{18} column and analyzed on a Q Exactive mass spectrometer, which fragments ions with higher-energy collisional dissociation (HCD). Both MS1 and MS2 level data were collected in profile mode.

6. The example protein database contains the target protein sequence (WPTP, UniProtKB Entry A0A0A0Y4H8) and a set of protein contaminants frequently found in proteomics samples from The Global Proteome Machine (thegpm.org/) (ftp://ftp.thegpm.org/fasta/crap/crap.fasta). WPTP contains both *N*- and *C*-terminal signal peptides [20], which should be deleted manually from the FASTA file. SignalP [21] (cbs.dtu.dk/services/SignalP/) can be used to predict the *N*-terminal signal peptide, however, the *C*-terminal signal sequence was confirmed experimentally [20]. For WPTP, open the subset protein database FASTA file in NotePadd++ and trim the amino acid sequence so that it starts with "DLQ" and ends with "SAS".
7. For command-line tools in ProteoWizard, "tools tutorials" can be accessed on the ProteoWizard website (proteowizard.sourceforge.net/). Additionally, usage information for command-line tools in ProteoWizard can be obtained by running the individual commands with no arguments.
8. Example MyriMatch configuration:
```
ProteinDatabase = proteinDatabase.fasta
StaticMods = "C 57.021"
DynamicMods = "M ^ 15.9949 N!{P}[ST] *
1170.417"
MaxDynamicMods = 2
MinTerminiCleavages = 2
CleavageRules = "Chymotrypsin"
MaxMissedCleavages = 2
MonoPrecursorMzTolerance = 15 ppm
FragmentMzTolerance = 0.02 m/z
OutputSuffix = "_MM"
```
9. A benefit of MyriMatch and other search engines in Bumbershoot is the ability to search motif specific modifications. N!{P}[ST] means that the modification is added to Asn, given that the next residue is any residue besides Pro and it is followed by Ser or Thr. To search additional glycans in MyriMatch, simply add them to the DynamicMods parameter. For example, "`M ^ 15.9949 N!{P}[ST] * 1170.417 N!{P}[ST] * 1008.365`".
10. plantGlycoMS script1 is for modifying the subset protein database.
```
#1. prepare the environment
```

```
setwd ("<drive>:/plantGlycoMS")
library (plantGlycoMS)
library (seqinr)
#2. Change "N" to "n" in the subset protein
database FASTA file
fasta <- read.fasta (file="MS2Data_
MM.fasta", seqtype = "AA", as.string = T)
glycoFasta <- glycoChange (fasta=fasta)
write.fasta (sequences=glycoFasta,
names=names(glycoFasta), file.out="MS2Data_
MM_glyco.fasta", open="w", as.string=T)
```

11. plantGlycoMS script 2 is for assessing and validating gPSMs from a MyriMatch search.

```
#1. Prepare the R environment
setwd ("<drive>:/plantGlycoMS/")
library (plantGlycoMS)
#2. Make a data.frame containing in silico
digest data
N <- read.table (file="MS2Data_MM.fasta_di-
gestedPeptides.tsv", header=T, sep="\t")
n <- read.table (file="MS2Data_MM_glyco.
fasta_digestedPeptides.tsv", header=T,
sep="\t")
targetGps <- glycoChainSaw (digest.
N=N, digest.n=n, carbamidomethylation=T,
methionineOxidation=T, glycoOnly=T)
#3. Read in MyriMatch results and MS2 bi-
nary data
myrimatchResults <- read.table
(file="putative_gPSMs.tsv", sep="\t",
header=T, stringsAsFactors=F)
IDPdb <- Read.IDPdb
(IDPdb=myrimatchResults,
ChainSaw=targetGps, dir="MS2Data")
MS2Data <- Read.MS2Data (IDPdb=IDPdb,
dir="MS2Data")
#4. Calculate Y-ions
Ions <- calculateIons (IDPdb=IDPdb)
#5. Make a list to use in the "data" argu-
ment of gPSMvalidator and check the data
data <- compileData (analysis="myrimatch",
sampleName="results", IDPdb=IDPdb,
MS2Data=MS2Data, Ions=Ions)
str (data[[15]], nchar.max = 30)
#6. Prepare the data for the "modification"
argument of gPSMvalidator
ptm.0 <- cbind (AA="-", mono=0.0,
desc="unmodified")
```

```
ptm.1 <- cbind (AA="N", mono=0,
desc="glycanLoss")
ptm.2 <- cbind (AA="M", mono=15.994915,
desc="oxidation")
m <- as.data.frame (rbind(ptm.0, ptm.1,
ptm.2))
#7. Enter in the oxonium ion masses for the
"mZmarkerIons" argument of gPSMvalidator
otherOxonium <- c (528.1923, 366.1400,
163.0601, 325.11292)
HexNAc_markerIons <- c (126.05495,
138.05495, 168.06552, 186.07608, 204.08665)
markerIons <- c (HexNAc_markerIons)
#8. gPSM validation
pdf (file="annotatedSpectra.pdf", 11, 8.5)
s <- gPSMvalidator (data=data,
modification=m$mono, modificationName=m$desc,
mZmarkerIons=markerIons, minMarkerIons=2,
itol_ppm=20, minMarkerIntensityRatio=2,
peakplot02=T, validate=T)
dev.off ()
write.table (s, file="infoTable.csv",
sep=",", row.names=F, col.names=T, quote=F)
```

12. plantGlycoMS script 3 is used to prepare data needed for glycopeptide identification with GlycoMod.

```
#1. Prepare the R environment (see Note 11)
#2. Make a data.frame containing in silico
digest data (see Note 11)
#3. Write a list of unmodified peptide mass-
es for the GlycoMod search
write (targetGps$mass,
file="unmodifiedPeptideMasses.txt", sep="\n")
#4. Calculate experimental masses for the
GlycoMod search and write the results
MS2.dataTable <- spectrumTable
(input="MS2Data.mzML.spectrum_table.csv")
write (MS2.dataTable$MonoPrecursorMass,
file="experimentalMasses.txt", sep="\n")
```

13. In our experience, some web browsers tended to crash when large data sets were generated with GlycoMod. The example data were successfully searched using Mozilla Firefox.

14. The suggested glycan compositions are based on the plant *N*-glycosylation pathway [7, 22].

15. plantGlycoMS script 4 is for assessing and validating gPSMs from a GlycoMod search.

```
#1. Prepare the environment (see Note 11)
```

```
#2. Make a data.frame containing in silico
digest data (see Note 11)
#3. Run pGlycoFilter on GlycoMod results
input <- read.csv ("gmodResults.csv",
header=T, stringsAsFactors=F, check.
names=F)
structure <- input[,3]
output <- pGlycoFilter (structure, input)
IDPdb.ALL <- Read.GlycoMod (input=output,
spectrum.table="MS2Data.mzML.spec-
trum_table.csv", ChainSaw=targetGps,
dir="MS2Data")
#4. Restrict gPSMs by the retention time
rtTable <- read.csv ("infoTable_manually
Assessed.csv")
infoTable <- read.csv ("infoTable_manu-
allyAssessed.csv")
rtTable <- retentionTimeTable (infoTable)
IDPdb <- rt.restrict (IDPdb=IDPdb.ALL,
rtTable=rtTable, rt.min.minus=5, rt.min.
plus=5)
MS2Data <- Read.MS2Data (IDPdb=IDPdb,
dir="MS2Data")
#5. Calculate Y-ions (see Note 11)
#6. Make a list to use in the "data" argu-
ment and check the data
data <- compileData (analysis="glycoMod",
sampleName="results", IDPdb=IDPdb,
MS2Data=MS2Data, Ions=Ions)
str (data[[1]], nchar.max = 30)
#7. Prepare the data for the "modification"
argument (see Note 11)
#8. Enter in the oxonium ion masses for the
"mZmarkerIons" argument (see Note 11)
# 9. gPSM validation
pdf (file="annotatedSpectra_gmod.pdf", 11,
8.5)
s <- gPSMvalidator (data=data,
modification=m$mono, modificationName=m$desc,
mZmarkerIons=markerIons, minMarkerIons=2,
itol_ppm=20, minMarkerIntensityRatio=2,
peakplot02=T, validate=T)
dev.off()
write.table (s, file="infoTable_gmod.csv",
sep=",", row.names=F, col.names=T, quote=F)
```

16. plantGlycoMS script 5 is for relative quantitation analysis.

```
#1. Prepare the environment (see Note 11)
```

```
#2. Read in data and combine gPSMs from all
glycopeptide identification steps
myrimatch <- read.csv ("infoTable_manu-
allyAssessed.csv")
glycomod <- read.csv ("infoTable_gmod_manu-
allyAssessed.csv")
glycomod2 <- subset (glycomod, select = -c
(glycoform.mass, structure))
gPSMs.ALL <- rbind (myrimatch, glycomod2)
rtTable <- retentionTimeTable (gPSMs.ALL)
#3. Make a configuration file to collect se-
lected ion chromatograms with msaccess
RQ_input <- Read.RQinput (gPSMs.ALL)
RQ_config <- paste ("exec=sic mzCenter=",
RQ_input$exact.precursor.mz, " radius=5
radiusUnits=ppm delimiter=comma", sep="")
write (RQ_config, "SICconfig.txt", sep="/n")
#4. Run glycoRQ
RQ <- Read.RQ (input=RQ_input,
dir="RQData")
RQresults <- glycoRQ (RQ=RQ,
rtTable=rtTable, dir="RQData", rt.min.mi-
nus=3, rt.min.plus=3)
write.csv (RQresults, "RQresults.csv")
```

17. In *glycoRQ*, a glycoform series is defined by a set of glycoforms sharing the same peptide backbone and one charge state. Although a particular glycosylation site may be found on a number of different peptide backbones, relative quantitation of glycoforms using one peptide moiety has been found by others to be more reproducible than using multiple peptide moieties [23]. Minor glycoforms may not be detected in multiple different charge states; therefore, combining multiple charge states can discriminate against minor glycoforms [24].

Acknowledgments

This work was supported in part by the National Institutes of Health Research Centers in Minority Institutions Program (Grant 8G12 MD007601-28) and the Agriculture and Food Research Initiative Competitive Grants (Grant No. 2012-67011-19671 and Grant No. 2018-67012-28082) from the USDA National Institute of Food and Agriculture. DLT was funded in part by a Strategic Health Innovation Partnership (SHIP) grant from the South African (SA) Department of Science and Technology (DST) and SA Medical Research Council (SAMRC) to Gerhard Walzl.

References

1. Varki A (2017) Biological roles of glycans. Glycobiology 27:3–49. https://doi.org/10.1093/glycob/cww086
2. Fanata WID, Lee KH, Son BH, Yoo JY, Harmoko R, Ko KS, Ramasamy NK, Kim KH, Oh D-B, Jung HS, Kim J-Y, Lee SY, Lee KO (2013) *N*-glycan maturation is crucial for cytokinin-mediated development and cellulose synthesis in *Oryza sativa*. Plant J 73:966–979. https://doi.org/10.1111/tpj.12087
3. Harmoko R, Yoo JY, Ko KS, Ramasamy NK, Hwang BY, Lee EJ, Kim HS, Lee KJ, Oh D-B, Kim D-Y, Lee S, Li Y, Lee SY, Lee KO (2016) *N*-glycan containing a core α1,3-fucose residue is required for basipetal auxin transport and gravitropic response in rice (*Oryza sativa*). New Phytol 212:108–122. https://doi.org/10.1111/nph.14031
4. Takano S, Matsuda S, Funabiki A, Furukawa J, Yamauchi T, Tokuji Y, Nakazono M, Shinohara Y, Takamure I, Kato K (2015) The rice RCN11 gene encodes β1,2-xylosyltransferase and is required for plant responses to abiotic stresses and phytohormones. Plant Sci 236:75–88. https://doi.org/10.1016/j.plantsci.2015.03.022
5. Wang S, Xu Y, Li Z, Zhang S, Lim J-M, Lee KO, Li C, Qian Q, Jiang DA, Qi Y (2014) OsMOGS is required for *N* -glycan formation and auxin-mediated root development in rice (*Oryza sativa* L.) Plant J 78:632–645. https://doi.org/10.1111/tpj.12497
6. R Core Team (2016) R: a language and environment for statistical computing. R Foundation for Statistical Computing, Vienna, Austria. https://www.R-project.org
7. Baker MR, Tabb DL, Ching T, Zimmerman LJ, Sakharov IY, Li QX (2016) Site-specific *N* -glycosylation characterization of windmill palm tree peroxidase using novel tools for analysis of plant glycopeptide mass spectrometry data. J Proteome Res 15:2026–2038. https://doi.org/10.1021/acs.jproteome.6b00205
8. Nanni P, Panse C, Gehrig P, Mueller S, Grossmann J, Schlapbach R (2013) PTM MarkerFinder, a software tool to detect and validate spectra from peptides carrying post-translational modifications. Proteomics 13:2251–2255. https://doi.org/10.1002/pmic.201300036
9. Panse C, Trachsel C, Grossmann J, Schlapbach R (2015) specL—an R/Bioconductor package to prepare peptide spectrum matches for use in targeted proteomics. Bioinformatics 31:2228–2231. https://doi.org/10.1093/bioinformatics/btv105
10. Chambers MC, Maclean B, Burke R, Amodei D, Ruderman DL, Neumann S, Gatto L, Fischer B, Pratt B, Egertson J (2012) A cross-platform toolkit for mass spectrometry and proteomics. Nat Biotechnol 30:918–920. https://doi.org/10.1038/nbt.2377
11. Tabb DL, Fernando CG, Chambers MC (2007) MyriMatch: highly accurate tandem mass spectral peptide identification by multivariate hypergeometric analysis. J Proteome Res 6:654–661. https://doi.org/10.1021/pr0604054
12. Ma Z-Q, Dasari S, Chambers MC, Litton MD, Sobecki SM, Zimmerman LJ, Halvey PJ, Schilling B, Drake PM, Gibson BW, Tabb DL (2009) IDPicker 2.0: improved protein assembly with high discrimination peptide identification filtering. J Proteome Res 8:3872–3881. https://doi.org/10.1021/pr900360j
13. Cooper CA, Gasteiger E, Packer NH (2001) GlycoMod–a software tool for determining glycosylation compositions from mass spectrometric data. Proteomics 1:340–349. https://doi.org/10.1002/1615-9861(200102)1:2<340::AID-PROT340>3.0.CO;2-B
14. Wickham H, Chang W (2017) Devtools: tools to make developing R packages easier. R package version 1.13.3. https://CRAN.R-project.org/package=devtools
15. Charif D, Lobry JR (2007) SeqinR 1.0-2: a contributed package to the R project for statistical computing devoted to biological sequences retrieval and analysis. In: Structural approaches to sequence evolution. Springer Verlag, New York, pp 207–232. https://doi.org/10.1007/978-3-540-35306-5_10
16. Yoo JY, Ko KS, Seo H-K, Park S, Fanata WID, Harmoko R, Ramasamy NK, Thulasinathan T, Mengiste T, Lim J-M, Lee SY, Lee KO (2015) Limited addition of the 6-arm β1,2-linked *N* -acetylglucosamine (GlcNAc) residue facilitates the formation of the largest *N* -glycan in plants. J Biol Chem 290:16560–16572. https://doi.org/10.1074/jbc.M115.653162
17. Tabb DL, Friedman DB, Ham AJ (2006) Verification of automated peptide identifications from proteomic tandem mass spectra. Nat Protoc 1:2213–2222. https://doi.org/10.1038/nprot.2006.330
18. Darula Z, Medzihradszky KF (2015) Carbamidomethylation side reactions may lead to glycan misassignments in glycopeptide analysis. Anal Chem 87:6297–6302. https://doi.org/10.1021/acs.analchem.5b01121
19. Guzzetta AW, Basa LJ, Hancock WS, Keyt BA, Bennett WF (1993) Identification of carbohydrate structures in glycoprotein peptide maps by the use of LC/MS with selected ion extraction with special reference to tissue

plasminogen activator and a glycosylation variant produced by site directed mutagenesis. Anal Chem 65:2953–2962. https://doi.org/10.1021/ac00069a004

20. Baker MR, Zhao H, Sakharov IY, Li QX (2014) Amino acid sequence of anionic peroxidase from the windmill palm tree *Trachycarpus fortunei*. J Agric Food Chem 62:11941–11948. https://doi.org/10.1021/jf504511h
21. Petersen TN, Brunak S, von Heijne G, Nielsen H (2011) SignalP 4.0: discriminating signal peptides from transmembrane regions. Nat Methods 8:785–786. https://doi.org/10.1038/nmeth.1701
22. Strasser R (2016) Plant protein glycosylation. Glycobiology 26:926–939. https://doi.org/10.1093/glycob/cww023
23. Leymarie N, Griffin PJ, Jonscher K, Kolarich D, Orlando R, McComb M, Zaia J, Aguilan J, Alley WR, Altmann F (2013) Interlaboratory study on differential analysis of protein glycosylation by mass spectrometry: the ABRF glycoprotein research multi-institutional study 2012. Mol Cell Proteomics 12:2935–2951. https://doi.org/10.1074/mcp.M113.030643
24. Ozohanics O, Turiák L, Puerta A, Vékey K, Drahos L (2012) High-performance liquid chromatography coupled to mass spectrometry methodology for analyzing site-specific *N*-glycosylation patterns. J Chromatogr A 1259:200–212. https://doi.org/10.1016/j.chroma.2012.05.031
25. Damerell D, Ceroni A, Maass K, Ranzinger R, Dell A, Haslam SM (2012) The GlycanBuilder and GlycoWorkbench glycoinformatics tools: updates and new developments. Biol Chem 393:1357–1362. https://doi.org/10.1515/hsz-2012-0135

INDEX

Cláudia Pereira (ed.), *Plant Vacuolar Trafficking: Methods and Protocols*, Methods in Molecular Biology, vol. 1789, https://doi.org/10.1007/978-1-4939-7856-4, © Springer Science+Business Media, LLC, part of Springer Nature 2018

R

S

T

V

Y